AFOSR 66-1938

NATIONAL BUREAU OF STANDARDS REPORT

9389

Preliminary Report on the Thermodynamic Properties of Selected Light-Element and Some Related Compounds

(Supplement to NBS Reports 6297, 6484, 6645, 6928, 7093, 7192, 7437, 7587, 7796, 8033, 8186, 8504, 8628, 8919, and 9028)

1 July 1966

NBS

U.S. DEPARTMENT OF COMMERCE
NATIONAL BUREAU OF STANDARDS

THE NATIONAL BUREAU OF STANDARDS

The National Bureau of Standards[1] provides measurement and technical information services essential to the efficiency and effectiveness of the work of the Nation's scientists and engineers. The Bureau serves also as a focal point in the Federal Government for assuring maximum application of the physical and engineering sciences to the advancement of technology in industry and commerce. To accomplish this mission, the Bureau is organized into three institutes covering broad program areas of research and services:

THE INSTITUTE FOR BASIC STANDARDS . . . provides the central basis within the United States for a complete and consistent system of physical measurements, coordinates that system with the measurement systems of other nations, and furnishes essential services leading to accurate and uniform physical measurements throughout the Nation's scientific community, industry, and commerce. This Institute comprises a series of divisions, each serving a classical subject matter area:

—Applied Mathematics—Electricity—Metrology—Mechanics—Heat—Atomic Physics—Physical Chemistry—Radiation Physics—Laboratory Astrophysics[2]—Radio Standards Laboratory,[2] which includes Radio Standards Physics and Radio Standards Engineering—Office of Standard Reference Data.

THE INSTITUTE FOR MATERIALS RESEARCH . . . conducts materials research and provides associated materials services including mainly reference materials and data on the properties of materials. Beyond its direct interest to the Nation's scientists and engineers, this Institute yields services which are essential to the advancement of technology in industry and commerce. This Institute is organized primarily by technical fields:

—Analytical Chemistry—Metallurgy—Reactor Radiations—Polymers—Inorganic Materials—Cryogenics[2]—Materials Evaluation Laboratory—Office of Standard Reference Materials.

THE INSTITUTE FOR APPLIED TECHNOLOGY . . . provides technical services to promote the use of available technology and to facilitate technological innovation in industry and government. The principal elements of this Institute are:

—Building Research—Electronic Instrumentation—Textile and Apparel Technology Center—Technical Analysis—Center for Computer Sciences and Technology—Office of Weights and Measures—Office of Engineering Standards Services—Office of Invention and Innovation—Clearinghouse for Federal Scientific and Technical Information.[3]

---

[1] Headquarters and Laboratories at Gaithersburg, Maryland, unless otherwise noted; mailing address Washington, D. C., 20234.

[2] Located at Boulder, Colorado, 80302.

[3] Located at 5285 Port Royal Road, Springfield, Virginia, 22151.

AFOSR 66-1938

NATIONAL BUREAU OF STANDARDS REPORT

NBS PROJECT		NBS REPORT
221-0405	1 July 1966	9389
221-0426A		
221-0426B		
221-0426C		
221-0426D		
221-0441		
222-0423		
223-0513		
223-0442		
313-0430		

Preliminary Report on the Thermodynamic Properties of Selected Light-Element and Some Related Compounds

(Supplement to NBS Reports 6297, 6484, 6645, 6928, 7093, 7192, 7437, 7587, 7796, 8033, 8186, 8504, 8628, 8919, and 9028)

Technical Summary Report
on the Thermodynamic Properties
of Light-Element Compounds

Reference: U.S. Air Force Order No. ISSA 65-8 (ARPA),
Project No. 9713-02

IMPORTANT NOTICE

U.S. DEPARTMENT OF COMMERCE

NATIONAL BUREAU OF STANDARDS

ABSTRACT

Thermodynamic and related properties of substances important in current high-temperature research and development activities are being investigated under contract with the U. S. Air Force (USAF Order No. OAR ISSA 65-8) and the Advanced Research Projects Agency (ARPA Order No. 20). This research program is a direct contribution to the Interagency Chemical Rocket Propulsion Group: Working Group on Thermochemistry and, often simultaneously, to other organizations oriented toward acquiring the basic information needed to solve not only the technical problems in propulsion but also those associated with ballistics, reentry, and high-strength high-temperature materials. For given substances this needed basic information comprises an ensemble of closely related properties being determined by a rather extensive array of experimental and theoretical techniques. Some of these techniques, by relating thermodynamic properties to molecular or crystal structure, make it possible to tabulate these properties over far wider ranges of temperature and pressure than those actually employed in the basic investigations.

This report describes in detail a variety of recent NBS experimental results and their interpretation. The vibrational spectra of different isotopic varieties of MgF_2, $MgC\ell_2$, CaF_2, SrF_2, and BaF_2 molecules trapped in solid rare-gas matrices were determined and analyzed; this technique particularly defines the bending vibrations, heretofore unreliable but a major factor in the thermodynamic properties of such gases. Preliminary microwave studies of the CsOH molecule indicate it to be linear and with highly anharmonic bending vibrations; these pioneering results have important implications for the spectroscopically little-investigated hydroxides of all the elements of Groups I, II, and III. Further infrared studies of the borohydrides of aluminum and beryllium show, between the solid and gaseous forms of the beryllium compound, a great difference which is tentatively interpreted. Spectroscopic time histories of aluminum wires exploding in vacuum and controlled atmospheres of nitrogen and oxygen were obtained. Measured calorimetrically were the heats of formation of the perchlorates of hydrazine ($N_2H_4 \cdot 2HC\ell O_4$), sodium, potassium, and silver, as well as the high-temperature heat capacity, heat of transition, and transition temperature of crystalline $A\ell F_3$. The heats of combustion in fluorine of refractory substances (especially graphite, boron, boron carbide, and aluminum borides, measured for the Air Force Aero Propulsion Laboratory), are here summarized and analyzed. The heat of vaporization of liquid $A\ell_2O_3$ has been remeasured with more reliable

temperature determination, and new mass-spectrometric data on several compositions of the $BeO-Al_2O_3$ system give a consistent value for the heat of formation of the new high-temperature molecule BeOAl.

Several literature reviews with critical data analysis are included. The present status of the heats of formation of CF_4 and selected fluorides of nitrogen, carbon, chlorine, and oxygen is described, with a report of recent NBS flame calorimetry on OF_2. Thermochemical properties of compounds of cadmium, zinc, and copper (recently evaluated critically as part of a revision of NBS Circular 500) are tabulated. On the basis of a critical data analysis of published condensed-phase heat-capacity and enthalpy data on $BeSO_4$, SrF_2, $SrCl_2$, TiF_4, ZrF_4, ZrB_2, P_4O_{10}, KHF_2, and 13 mixed oxides, new tables of their thermodynamic properties are given. Analyses of the infrared spectra of fluorides of seven elements of Groups IV, V, and VI gave Coriolis zeta constants of the degenerate vibrational modes and certain unique harmonic force fields. The high-temperature thermodynamics of the $BeO-H_2O$ system was reviewed, with estimations of the possible effect of postulated higher hydrates on the volatility of BeO in water vapor up to 4000°K. The published data on the vaporization equilibria of the nitrides and carbides of aluminum, beryllium, magnesium, and titanium were reviewed and compared with the values calculated thermodynamically from the available up-to-date thermal data. A comprehensive review is presented of the theory of the equation of state of solid hydrogen and the calculation of properties of the as yet unobserved form metallic hydrogen. This form of hydrogen probably occurs on the planet Jupiter at pressures above one million atmospheres.

Thomas B. Douglas
Project Leader

Charles W. Beckett
Assistant Division Chief for Thermodynamics
Heat Division, Institute for Basic Standards

TABLE OF CONTENTS

TABLE OF CONTENTS (Continued)

TABLE OF CONTENTS (Continued)

TABLE OF CONTENTS (Continued)

TABLE OF CONTENTS (Continued)

TABLE OF CONTENTS (Continued)

TABLE OF CONTENTS (Continued)

TABLE OF CONTENTS (Continued)

TABLE OF CONTENTS (Continued)

TABLE OF CONTENTS (Continued)

TABLE OF CONTENTS (Continued)

Chapter 1

TIME-RESOLVED SPECTROSCOPIC STUDIES OF EXPLODING WIRES

Esther C. Cassidy and Stanley Abramowitz

1. ABSTRACT Electrically exploded wires in various controlled atmospheres were employed for production of atomic and molecular species. The spectrographic time histories of the various constituents (stable and unstable) of the explosion mixture were studied with the use of a rotating drum camera, focussed on the exit slit plane of a spectrograph. A rotating high-speed shutter was utilized to study (from more detailed photographic plates) the spectrum at selected times during the explosion. Results obtained with aluminum wires in various atmospheres are presented. Several considerations found to be important in the design of the explosion chamber are discussed.

2. INTRODUCTION Radiation from electrically exploded metal wires has been used as a spectral source[1,2] and as a flash source for producing photochemical reactions[3,4]. A few[5] have combined use of exploding wires with an ac arc to produce molecular absorption spectra. In general, results have been atomic lines and/or molecular bands against a strong background continuum. It now seems quite likely that weaker features may have been lost because the spectrographic plates were blackened by intense continuum radiation from the wire and high pressure metal vapor during the early stages of the explosion. The present experiments show that spectral results frequently depend not only upon the constituents of the explosion system (wire, electrode and vessel materials, and environment), but also upon the technique employed for observation.

To date, except for a few such as Bartels and Bortfeldt[6], Nagaoka _et al_[7], and Teeple[8], most workers have presented integrated spectra from the entire explosion. Because of the extreme intensity of the initial continuum radiation, such results could not reveal weaker or highly transient features of the explosion spectrum. This paper describes a procedure for more thorough spectral observations. A continuous, time-resolved spectrum of the explosion is taken with a high-speed drum camera in order to determine intervals most suitable for study of selected features of the spectrum. However, these results are limited by the camera's optical system; only a portion of the spectrum (at the focal plane of the spectrograph) is recorded, and the effective dispersion is reduced. More detailed information on the structure of the spectrum and broader wavelength coverage are then achieved by using a rotating shutter disc to limit photographic plate exposures of the spectrum to the selected (from the drum camera result) time intervals. The results obtained thus far suggest that this may be a promising method for detection of previously unobserved features from constituents of the explosion mixture present in low concentrations.

3. EXPERIMENTAL APPARATUS AND TECHNIQUES A capacitor discharge circuit (15 to 60 μF, 20 kV max, circuit inductance ~ 0.16 μH, and ringing frequency ~ 50 kHz) was employed for explosion of 99.999% pure aluminum wires (diam = 0.14 mm, length = 9.5 cm). The capacitors were connected in a parallel, flat-plate arrangement. The wire and current return path were coaxial in design. Whenever possible areas were minimized and symmetrical geometry was preserved in order to minimize circuit inductance. In order to contain the chemical reactions and products generated by the explosion, cylindrical vessels (I.D. = 7.6 cm, length = 9.5 cm), made from several different materials, (Plexiglass, Bakelite, Teflon, or Pyrex[9]) were used for enclosing the wire in controlled atmospheres (oxygen, hydrogen, argon, nitrogen or vacuum). Vessels with smaller diameters were less satisfactory because the interior walls suffered from increased burning and/or blackening, and because introduction of impurities from the walls was more pronounced.

A plane-grating spectrograph (dispersion 20 Å/mm in the first order) was used for the spectroscopic observations. The explosion was focussed on the entrance slit of the spectrograph by use of two quartz lenses. A corning ultraviolet absorbing filter (C.S. No. 0-52) was inserted before the slit to prevent overlapping of the second order features in the spectrum. An air-driven AVCO rotating drum camera was focussed on the focal plane of the spectrograph for photographic recording of the time history of the explosion spectrum in the region between 3000 and 6000 Å. The speed of the camera (600 rps max) was adjusted to give maximum time resolution over the 31.9 cm length of the film (70 mm Kodak Royal-X Pan). Diafine two-bath developer was used for processing the film.

Following the drum camera time survey, spectral plates were taken of selected intervals (of the explosion) in which intermediate species of interest were known (from the drum camera records) to exist. A rotating disc, similar to that described by Bartky[10], with slots for shuttering the spectrograph and for generating timing pulses, was used to prevent exposure of the plate except during the desired pre-selected interval of the explosion. The disc was driven by a synchronous motor (1800 rpm, 1/50 hp). The five degree shutter slot of the present disc (see Fig. 1) was designed to allow radiation from the explosion to pass into the spectrograph for an interval of 180 μsec. Synchronization of the slot's arrival at the entrance slit of the spectrograph with the interval of interest was achieved by use of a photomultiplier tube. The photomultiplier received light from a miniature six volt lamp through a small slit at a given time before the shutter slot reached the entrance slit. The photomultiplier signal was passed to the circuit shown in Fig. 1 for triggering of the explosion. This particular arrangement was convenient because it utilized on-hand general purpose equipment. A record of the timing (during the explosion) of the exposure was obtained by photographing a dual-beam oscilloscope display of the trigger signal from the photomultiplier tube and the voltage induced by the discharge in a small coil placed near the capacitor discharge circuit. Finer control (to ±50 μsec) of the delay time between the photomultiplier signal and firing of the discharge circuit was achieved by replacing the delay potentiometer of the Tektronix 161 Pulse Generator with a precision ten-turn potentiometer (IRC Type 8000, 100 kΩ). If necessary, more precise timing of the exposure may be achieved by using a more complicated shutter system with two rotating discs as described by Schneider[11], or by using ultra-high speed opening[12] and closing [13] shutters in combination.

4. RESULTS AND DISCUSSION The importance of time resolution in spectral studies of exploding wires is illustrated in Fig. 2, which shows the difference between an integrated plate (a) from the entire explosion, and plates (b) and (c) obtained using the rotating shutter technique. The latter plates were taken at an interval ($t \approx 1$ μsec) known from drum camera experiments to be favorable for observation of the AlO spectrum. A neutral density filter with approximately 5% transmission was used for (a) to permit approximately the same light exposure as in (b) and (c), where the shutter disc limited the exposure time to 180 μsec. The $\Delta v = 0$ through $+3$ sequences of the AlO spectrum are not distinguishable on the integrated plate. The intense continuum emitted at the very beginning of the explosion has washed out all but the most intense features. On plate (b) the $\Delta v = -3$ through $+3$ sequences are evident. On plate (c) the $\Delta v = -3$ and $+3$ sequences are barely visible, probably because the energy input was not sufficient. Without a complete time history of the spectrum one could not distinguish whether these features, observed in emission in (b), were overexposed by the continuum, or whether they were actually not excited (for experimental reasons) by the explosion.

A typical drum camera record from an explosion in vacuum (pressure about 3×10^{-4} torr) is shown in Fig. 3. The mercury line at 5461 Å was added for reference after the explosion. The record shows that radiation strong enough to expose the drum camera film was emitted for only about 100 μsec, and that no molecular bands appeared. The principal features of the spectrum are emission lines from the various impurities in the aluminum wire and in the electrodes used to clamp the wire. Since the stock from which the wire was drawn was certified by the manufacturer to be 99.99912% pure, the electrode material (Type 6061 aluminum) was assumed to be the source of the impurities. However, results obtained with electrodes made from 99.99% pure aluminum (Type 1199) still showed many lines from impurities, thus illustrating the method to be an extremely sensitive technique for detecting the constituents of a substance. It also seems quite clear that it is extremely difficult to construct an exploding wire apparatus for experiments with a selected system, free from the effects of impurities. This was found to be particularly true when the wires were exploded in gases (such as nitrogen or argon) which are not conducive to chemical reaction with the wire material.

The upper portion of Fig. 4 shows the first 300 μsec of a drum camera record from an explosion in nitrogen (Matheson Prepared Grade, pressure = 76 torr). Higher wavelength resolution and a broader range of wavelengths are given in the time-resolved spectrum shown under the drum camera result. The plate was taken, using the shutter disc, about 1 msec after initiation of the discharge. The spectrum from an iron arc in air is shown at the bottom for ready identification of the many FeI lines in the explosion spectrum. Though the discharge current lasted only about 90 μsec, atomic lines from the wire and electrode vapor endured well into the millisecond range.

In general, bands from molecular species were not observed (wavelength range studied: 3000 to 6000 Å) in the spectra from explosions in nitrogen, argon, or vacuum. However, early results from explosions in a nitrogen environment showed several band sequences. These were found to be caused by impurities from the vessel walls. Figure 5 was printed from a portion of drum camera film taken during one of these experiments. The experimental conditions were identical to those of Fig. 4, except that the explosion chamber was made from Teflon (rather than glass). Explosions in vacuum with a Teflon vessel gave essentially the same result. Radiation endured for more than 2 msec, and C_2 and CN bands from the vessel material were predominant. In spite of its desirable machining and high temperature characteristics, Teflon was therefore found not suitable for study of the spectral features from the wire and/or surrounding gas. Bakelite also proved unsatisfactory because the explosion caused the walls to burn freely, especially when the wire was exploded in an oxygen or hydrogen media. Glass vessels with flat quartz windows gave the best performance; impurities from the walls did not produce features in the spectrum, and it was possible to clean the entire vessel in hydrochloric acid. At the levels of energy applied, a wall thickness of about 4 mm was required to prevent explosion of the vessel.

Figure 6 illustrates another difficulty encountered when attempting to observe spectra from explosions in nitrogen, argon or vacuum. The first portion of the drum camera record (t = 0 to 300 μsec) is nearly identical to Fig. 4. The second portion (t = 1000 to 1200 μsec) shows several band sequences which are identified (from the AlO reference spectrum in the middle) as the $\Delta v = -1$ through $+1$ sequences of the AlO Blue-Green System. Investigation showed that the bands were due to a trace of oxygen from a small leak in the explosion chamber. It is interesting to see in this figure that the pulsations in intensity reported earlier[14], which are believed due to reflected shock waves, are evident for more than 300 μsec. The broadening of the NaI lines during the intervals of greater intensity suggests that the pressure of the radiating vapor is higher during these times.

Explosions in oxygen and hydrogen showed molecular bands from AlO and AlH, respectively. Figure 7, for example, is a portion of a drum camera record from an explosion in 0.5 atm oxygen. (Experience showed that the features were sharper, more enduring, and more intense at reduced pressures.) The film indicates that intervals later than t = 350 μsec yielded bands in emission. It is interesting to note, in this figure and in Figs. 5 and 6, that only the most intense atomic lines endure after chemical reaction occurs. In cases where there is no reaction or where the extent of reaction is small (e.g. Figs. 3 and 4), the atomic lines from the wire, the electrodes, and their impurities predominate the spectrum for the full duration of radiation (several milliseconds).

In conclusion, it is clear that spectral results from exploding wire experiments depend not only upon the conditions of the experiment (wire, electrode and vessel materials, etc.), but also upon the timing and interval of observation. It is hoped that the techniques described will be useful for obtaining time-resolved spectral measurements from exploding wire and other transient, detonation-type phenomena.

5. ACKNOWLEDGEMENTS The authors are grateful to Dr. I. R. Bartky for helpful discussions, and to Mr. W. A. Bagley for assistance in setting up the drum camera system.

REFERENCES AND FOOTNOTES

1. J. A. Anderson, Astrophys. J. 51, 37 (1920).

2. B. Rosen, Bull. Soc. Roy. Sci. Liege 13-14, 176 (1944).

3. G. K. Oster and R. A. Marcus, J. Chem. Phys. 27, 189 (1957).

4. Ibid, 472 (1957).

5. V. A. Loginov, Opt. Spectry. (USSR) VI, 67 (1959).

6. H. Bartels and J. Bortfeldt in Exploding Wires (Plenum Press, Inc. New York, 1964), Vol. III, p. 9.

7. H. Nagaoka, D. Nukiyama, and T. Futagami, Proc. Imp. Acad. (Japan) 3, 208-212, 258-264, 319-333, 392, 418, 499-502 (1927).

8. L. R. Teeple, Jr. in Proc. 6th International Congress on High Speed Photography, The Hague/Scheveningen (Netherlands), 1962, (J. G. A. De Graaf and P. Tegelaar eds. H. D. Tjeenk Willink and Zoon N. V., Haarlem, Netherlands, 1963), p. 605.

9. Certain commercial materials and equipment are identified in this paper in order to specify adequately the experimental procedure. In no case does such identification imply recommendation or endorsement by the National Bureau of Standards, nor does it imply that the material or equipment identified is necessarily the best available for the purpose.

10. I. R. Bartky and A. M. Bass, Appl. Opt. 4, 1354 (1965).

11. R. Schneider and M. Mailander, Z. Angew, Phys. 12, 521 (1960).

12. E. C. Cassidy and D. H. Tsai, J. Res. Natl. Bur. Std. 67C, 65 (1963).

13. R. S. Dike and E. L. Kemp, Rev. Sci. Instr. 36, 1256 (1965).

14. E. C. Cassidy and K. K. Neumann in Proc. 7th International Congress on High Speed Photography, Zurich, Switzerland, 1965, (in press).

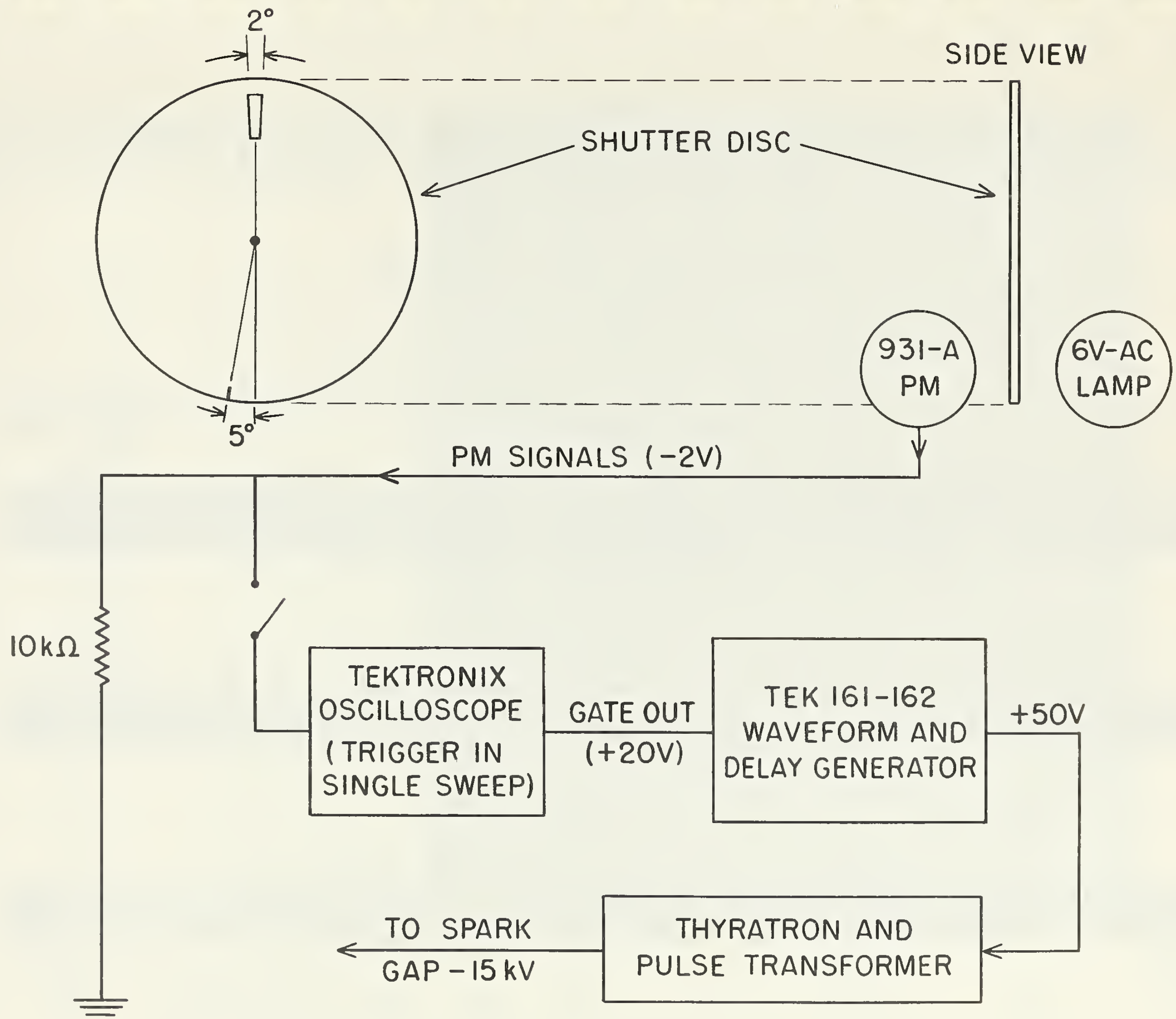

Fig. 1. **Block diagram of shutter disc and triggering circuit.**

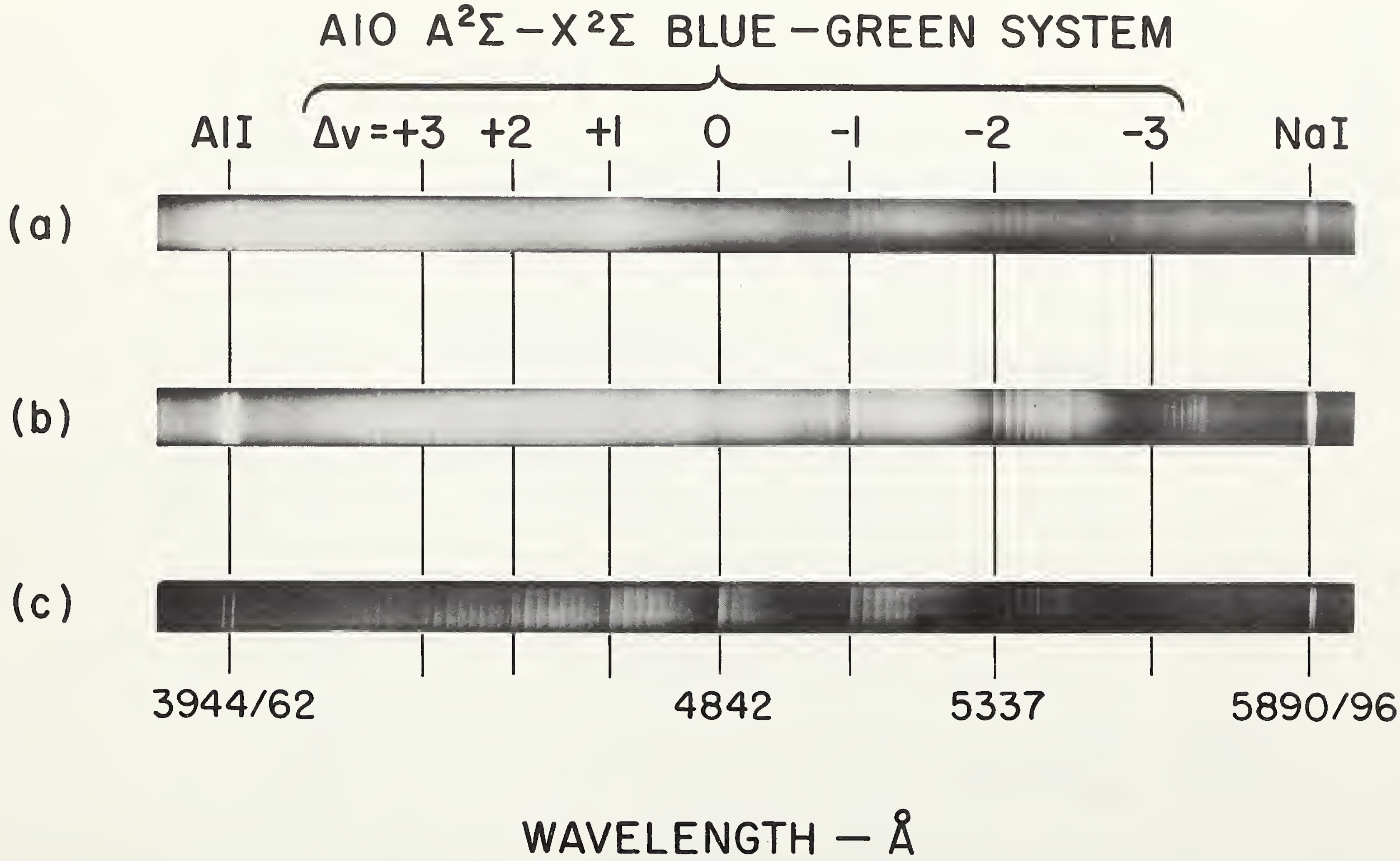

Fig. 2. The AlO A $^2\Sigma$ – X $^2\Sigma$ Blue-Green System from exploding wire experiments; (a) Integrated spectrum from entire explosion (60 μF at 14 kV); (b) Time-resolved spectrum at t ≈ 900 μsec, using rotating shutter (60 μF at 14 kV); (c) at t ≈ 1.1 msec with lower energy input (15 μF at 14 kV).

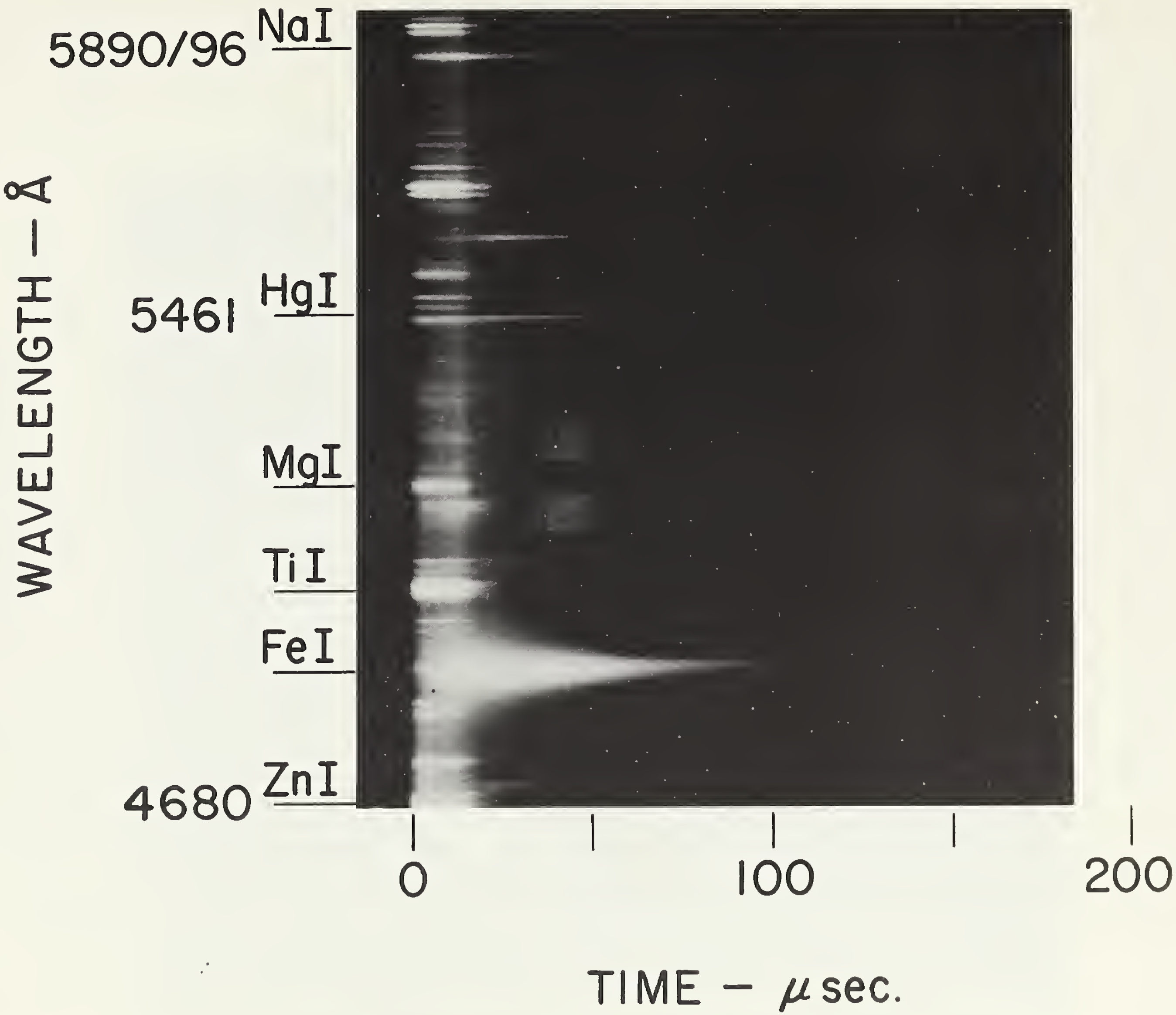

Fig. 3. Spectrum from aluminum wire exploded in vacuum as recorded by drum camera (15 μF at 14 kV).

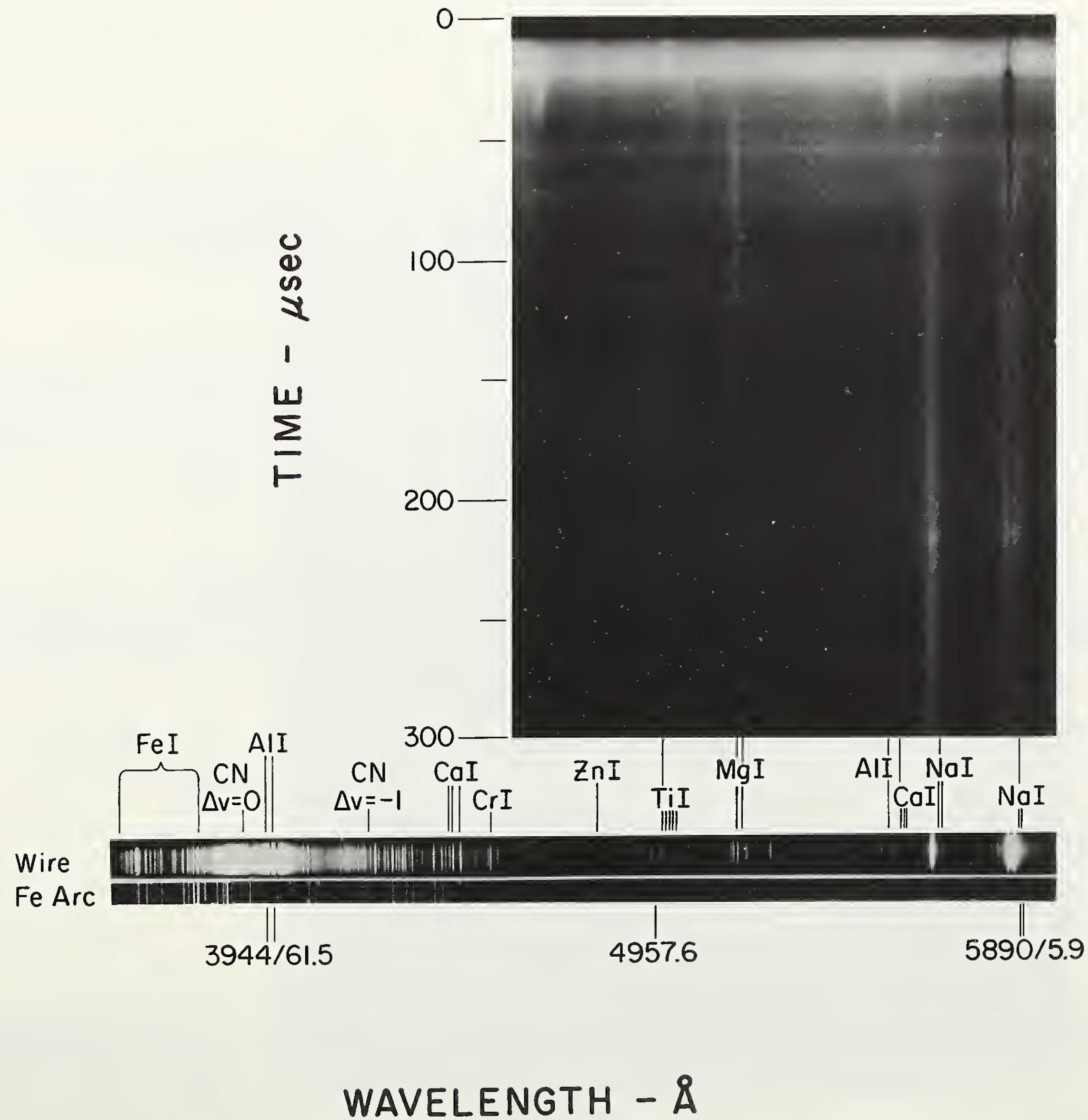

Fig. 4. Drum camera record and time-resolved spectrum (at $t \approx 1$ msec) from exploding aluminum wire in nitrogen (60 μF at 14 kV).

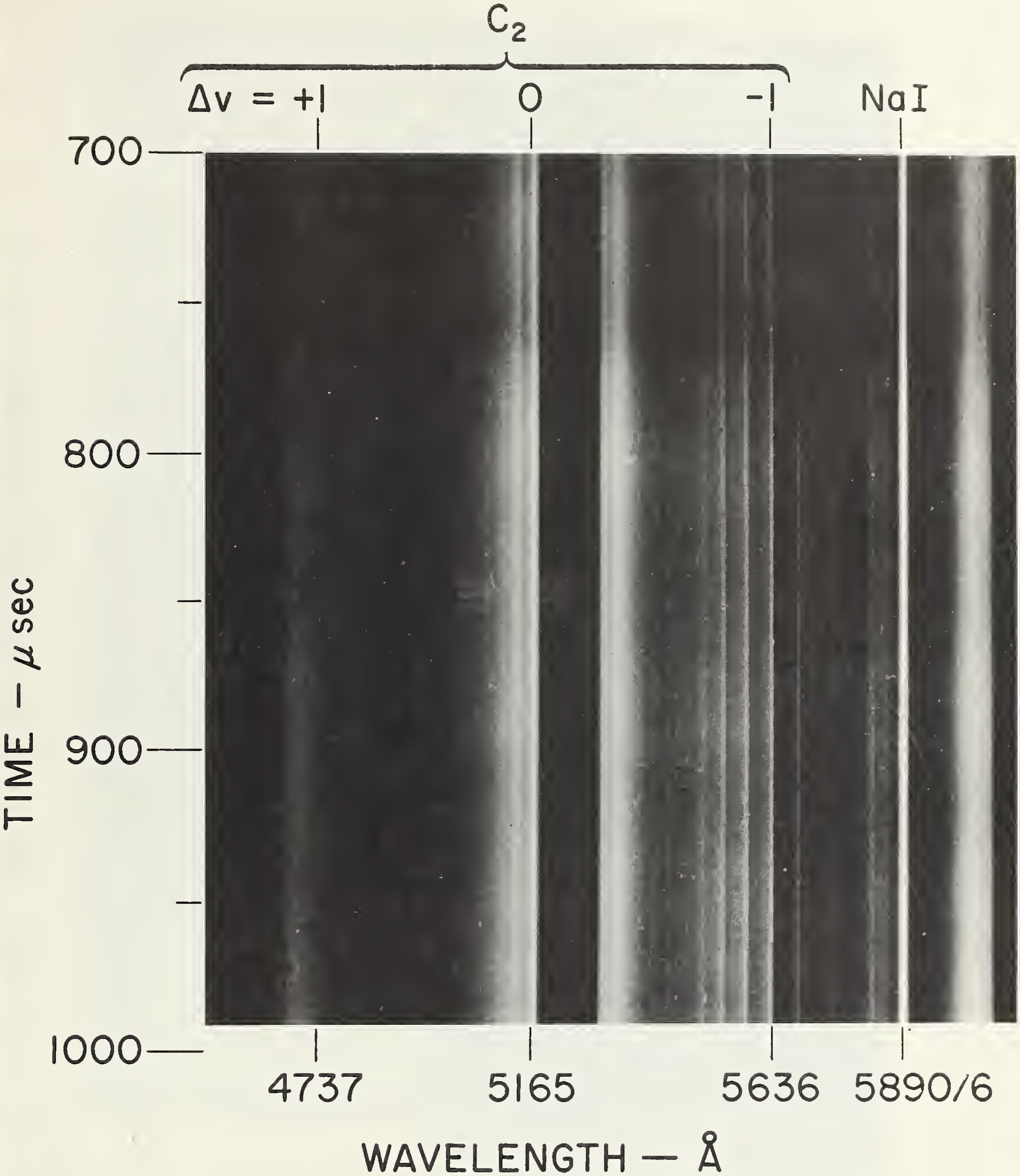

Fig. 5. Portion of drum camera record from exploding aluminum wire in nitrogen using a Teflon explosion chamber (15 μF at 14 kV).

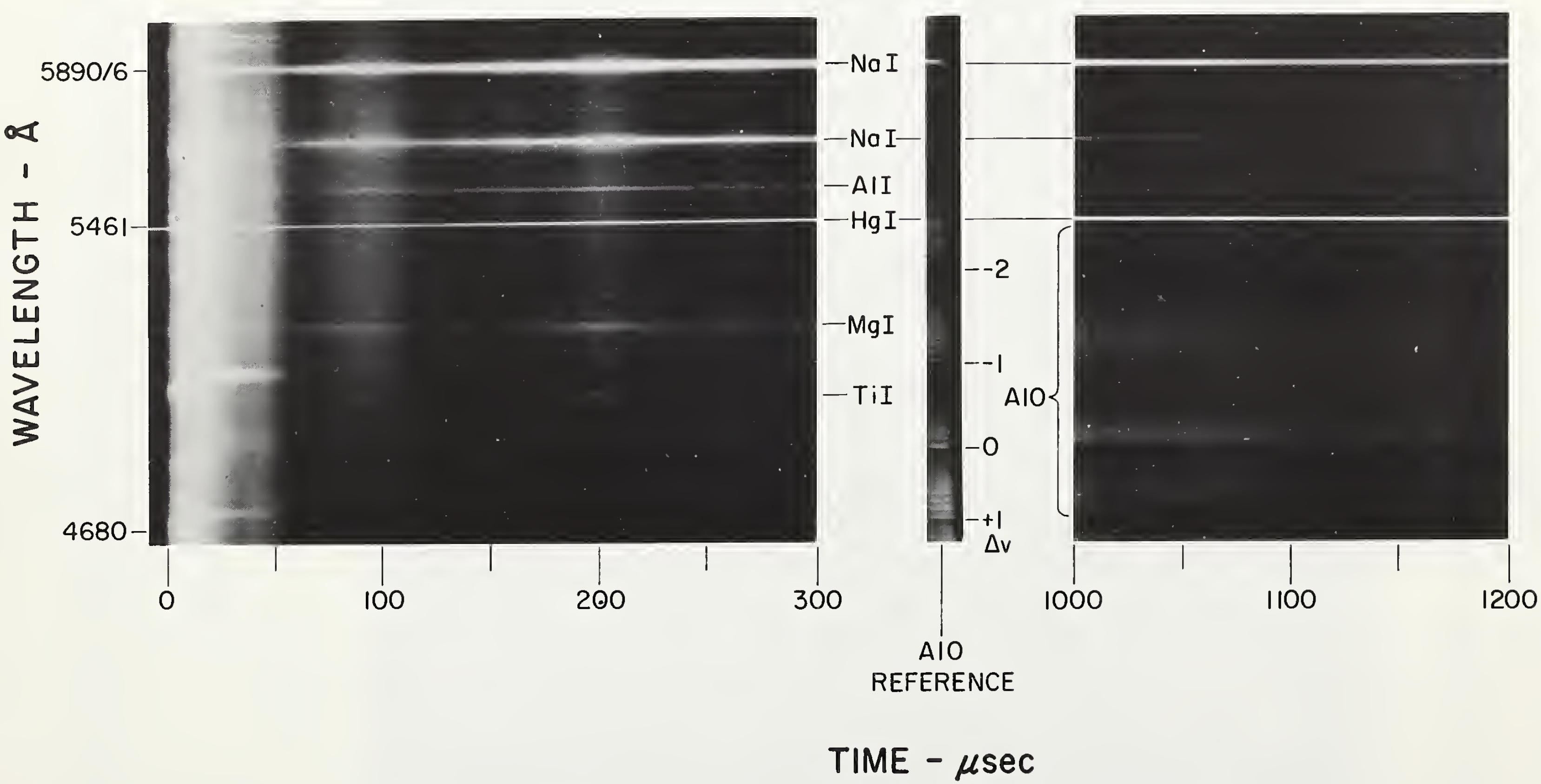

Fig. 6. Drum camera result from an explosion in nitrogen with trace of oxygen (60 μF at 14 kV).

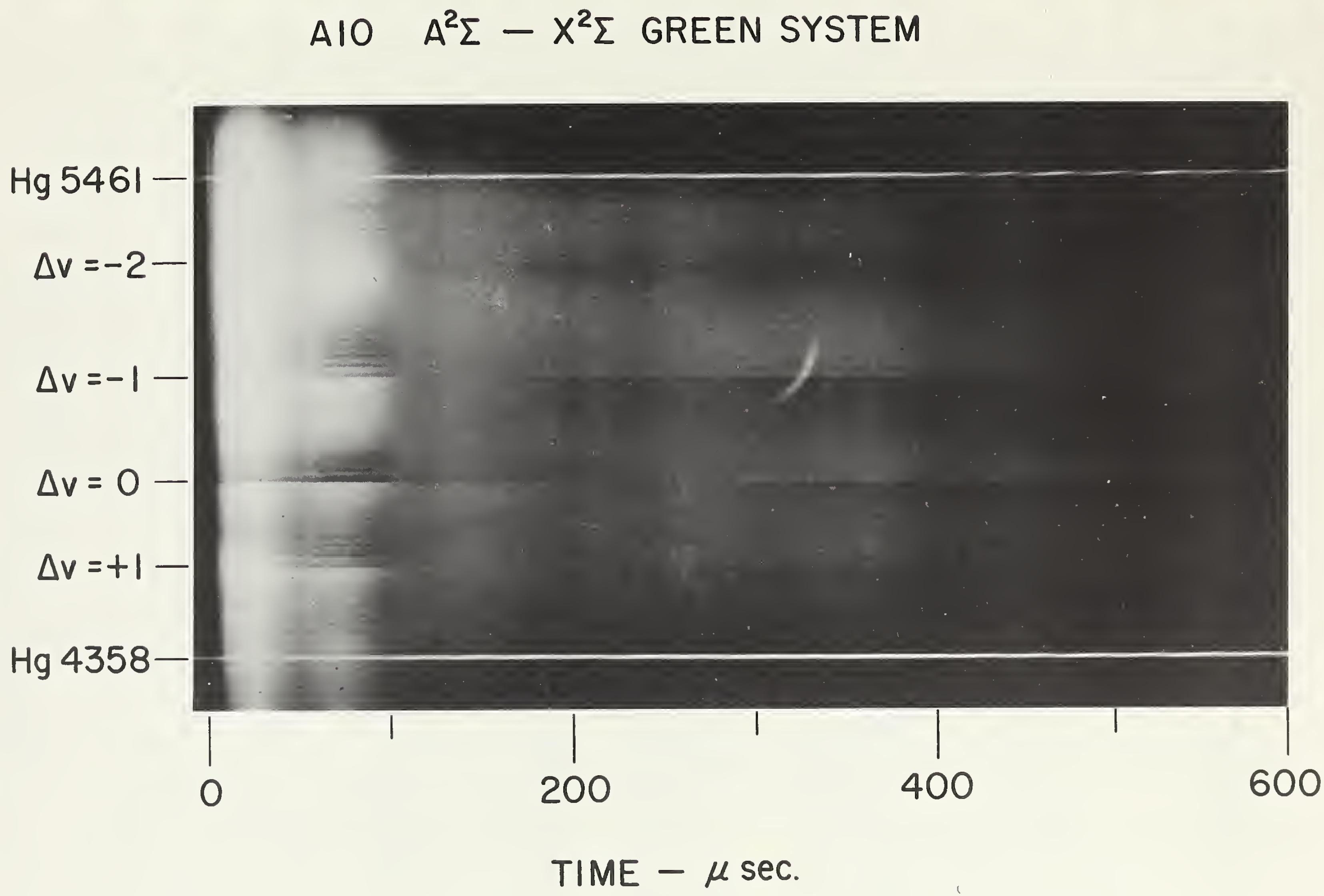

Fig. 7. Drum camera record of the AlO spectrum from exploding aluminum wire in oxygen (15 μF at 14 kV).

Chapter 2

EQUILIBRIUM VAPOR PRESSURES OF SOME CARBIDE AND NITRIDE SYSTEMS BASED ON RECENT CALORIMETRIC MEASUREMENT

R. F. Walker

Introduction

This chapter is essentially an up-dating of the discussion of the high temperature chemistry of the carbides and nitrides of the light elements which was given in Chapter A5 of NBS Report 6645, January 1, 1960. In general, data and discussion given in the earlier report is not repeated here.

Since that time new data has been reported on the heats of formation of several of the pertinent compounds, and new heat capacity data has resulted in revised tables of thermodynamic functions in other instances. With some systems additional insight has also been obtained of the condensed phases that exist.

The new calorimetric data have been used to predict the equilibrium vapor pressures of the condensed systems. The values given in the following tables may be compared for consistency with values obtained by direct measurement of equilibrium vapor pressures or evaporation rates. Experimental values were given in the previous report (NBS 6928) and reference to more recent experimental values are included in this chapter.

Even where no new calorimetric data have become available the opportunity has been taken to check the previous hand-calculated values and to extend them to cover wider ranges of temperature. The selected values for the heats of formation given in NBS Report 6928, July 1, 1960 have been used in all computations, except where more recent data indicates a revision is desirable. Likewise, the tabulated free energy functions given in this NBS ARPA-USAF series of semiannual reports have been used whenever possible. Where no NBS tables existed, the corresponding JANAF tables (with revisions up to December 31, 1965) were used.

In spite of the increased attention given to these systems during the past few years, scant information remains available on several of them. This is particularly true for systems containing lithium and magnesium. Furthermore, studies of compound formation among the condensed phases suggest that the phase diagrams are often more complex than previously suspected. This factor places a limitation on the reliability of some of the following predicted vapor pressures.

Aluminum Carbide

Although the phases of Al_3C [1] and $Al_2(C_2)_3$ [2] are reported in the literature, the compound Al_4C_3 is the only well-established and commonly encountered solid phase.

Since the preparation of NBS Report 6645, there have been two determinations of the heat of formation of Al_4C_3 by calorimetric methods [3,4] and further measurements of the decomposition pressure by the Knudsen method [5]. The values for $\Delta H_f^\circ(298)$ obtained calorimetrically were -53.4 ±2.0 kcal/mole and -49.7 ±1.2 kcal/mole, respectively, and these values compare with the value of -48.6 kcal/mole given in NBS Report 6645 and used in the previous calculations. Plante [5] derived the value of 366.4 kcal/mole for $\Delta H_s^\circ(Al_4C_3)(c)$ from his vapor pressure measurements. If $\Delta H_f^\circ(298)$ Al(g) is taken as 77.5 kcal/mole this leads to a value of $\Delta H_f^\circ(298)$ Al_4C_3 of -56.4 kcal/mole; however, $\Delta H_f^\circ(298)$ Al(g) is not known with sufficient accuracy other than to say that Plante's value is in better agreement with the lower of the recent calorimetric values.

Furukawa et al. [6] have measured the heat capacity of Al_4C_3, and they used their data to produce new tabulated free energy function for the compound. (See also NBS Report 7587, July 1, 1962.) These tables, together with the value of -52.2 kcal/mole for $\Delta H_f^\circ(298)$ Al_4C_3 (estimated by giving double weight to the above lower calorimetric value), were used to compute the decomposition pressures given in table I for the following reaction:

$$Al_4C_3(c) = 4Al(g) + 3C(c).$$

The computations ignore the possible formation of $C:C_2:C_3$ gaseous species at the highest temperatures and are lower-limiting values compared with those for which gaseous C but no C(c) is formed.

A comparison of the vapor pressures calculated from recent calorimetric data and published equilibrium measurements is given graphically by Furukawa et al. [6].

Reactions of Aluminum Carbide and Aluminum Nitride

An extensive discussion of the interpretation of measured and calculated pressures in the Al-C-N system, in terms of the condensed phases believed to exist, was given in NBS Report 6645. Furukawa et al. [6] brought the discussion up to date, using the more recent calorimetric data on Al_4C_3 mentioned above, and added further comments on the comparison between the calorimetric and equilibrium data. The discussions hinge on the extent of compound formation in this system and the presence or absence of the compound Al_5C_3N. However, Jeffrey and Wu [7] report the existence of three additional carbonitrides: $Al_6C_3N_2$, $Al_7C_3N_3$, and $Al_8C_3N_4$. The absence of calorimetric data on these compounds and the lack of information on their kinetics of formation at temperatures below 2000°C do not allow the comparisons between the calculated and measured pressures to be made with assurance. At low temperatures, where the kinetics of formation of the compounds is probably slow, pressures computed in terms of the reaction

$$4AlN(c) + 3C(c) = Al_4C_3(c) + 2N_2(g)$$

are in good agreement with measured pressures (NBS Report 6645). A comparison on this basis is also shown graphically by Furukawa et al. [6], using the more recent calorimetric results on Al_4C_3 and AlN (discussed below).

Reactions of Aluminum Oxide with Carbon

Furukawa et al. [6] have also used the recent calorimetric data on Al_4C_3 in making a graphical comparison between the calculated and measured pressures in the system Al-O-C. In their discussion they have also considered the recent measurements of Cox and Pidgeon [8] and the contribution of the phase diagram in this system made by Motzfeldt [9].

The lack of calorimetric data on the established compounds in this system, Al_4O_4C and Al_2OC, prevent reliable computations being made. At lower temperatures (1900°K and below) the rate of formation of the compounds is also not rapid, and equilibrium is probably not established during short-term experimental observations.

Table II gives the pressures calculated from calorimetric data, using the value of -52.2 kcal/mole for $\Delta H_f^\circ(298)$ Al_4C_3, and for the reaction

$$2Al_2O_3(c) + 9C(c) = Al_4C_3(d) + 6CO(g).$$

Aluminum Nitride

A value of -76.5 kcal/mole was used for $\Delta H_f^\circ(298)$ in the computed decomposition pressures of AlN that were given in NBS Report 6645. The selection of this value tended to be supported by the analysis of vapor pressure measurements, although calorimetric data gave values which varied from -57.4 to -76.5 kcal/mole. Since that time a further calorimetric determination has been made, yielding -75.6 kcal/mole, and this led to the selection of the value -76.0 kcal/mole in NBS Report 6928. This last value was used for the computations given below.

In addition to the calorimetric measurements there have also been four reports of measurements of the vapor pressure or evaporation rate of AlN [10-13]. In confirmation of the observations of Hoch and White discussed in NBS Report 6645, two of the studies [10,12] found that the sublimation coefficient of AlN is significantly less than unity. Thus, AlN behaves like several other nitrides, e.g., Be_3N_2, Mg_3N_2, GaN, and BN, in subliming at less than the maximum rate calculable from its equilibrium vapor pressure. Available evidence suggests that complex gaseous species are not significantly involved in the decomposition process [11]. Hildenbrand [12] corrected his observed pressures for the low value of the sublimation coefficient and obtained an average third law heat of sublimation at 298°K of 153.65 kcal/mole, a value which is consistent with a $\Delta H_f^\circ(298)$ of AlN of -76.15 kcal/mole. Blank [13] reports a value (seen only in abstract) of 153.2 kcal/mole for the third law heat of sublimation, and this yields a value of -75.7 kcal/mole for $\Delta H_f^\circ(298)$.

Table III presents the equilibrium decomposition pressures computed from the calorimetric data. Figure 1 compares the computed values with experimental values uncorrected for the low sublimation coefficient. Vaporization was presumed to occur in accordance with the reaction:

$$AlN(c) = Al(g) + \frac{1}{2}N_2(g).$$

Beryllium Carbide

No calorimetric measurements or vapor pressure measurements have been reported that provide a firm basis for modifying the computed pressures given for Be_2C in NBS Report 6645. H. L. Schick et al. [14] and the compilers of the JANAF tables have obtained estimates of $\Delta H_f^\circ(298)$ Be_2C from two sets of vapor pressure measurements not considered in NBS Report 6645 [15,16]. However, the computed values fall in the range -36.0 to +13.7 kcal/mole and thus provide no consistent basis for changing the previously selected value of -22.2 kcal/mole.

Table IV presents the results of computing the decomposition pressures for the reaction:

$$Be_2C(c) = 2Be(g) + C(c).$$

Beryllium Nitride

There have been several recent sets of measurements of the heat of formation of Be_3N_2 by calorimetric and vapor pressure methods. In addition, Douglas and Payne, NBS Report 7587, July 1, 1962, reported new heat capacity data from which a new NBS table of free energy functions was computed. Eckerlin and Rabernau [17] reported a new structural modification of Be_3N_2, which was formed by heating cubic α-Be_3N_2 in NH_3 at 1400-1650°, especially in the presence of Si. In the absence of thermodynamic data on the phase change and β-modification, the following discussion presumes the existence of only the well-known α-modification.

A value of -132 kcal/mole was previously selected for $\Delta H_f^\circ(298)$ $Be_3N_2(c)$ on the basis of calorimetric data. The JANAF value of -140.6 kcal/mole has been selected for the computations presented in table V. This value is the mean of the two values -140.8 and -140.4 kcal/mole, reported by Gross [18] to result from independent calorimetric determinations.

The sublimation coefficient of Be_3N_2 has been shown to have an upper limit of 0.001 -0.01 [19,20]. Recent evaporation measurements tend to support the selection of a higher value for $\Delta H_f^\circ(298)$. The data of Yates et al. [20], when corrected for a low sublimation coefficient, yield $\Delta H_f^\circ(298)$ $Be_3N_2(c)$ = -140.3 kcal/mole, or -141.35 kcal/mole if the $\Delta H_f^\circ(298)$ Be(g) given in NBS Report 6928 is used in the calculation. Hoenig [19] gives -136.0 ±5.0 kcal; however, the data have been seen only in an abstract, and it has not been ascertained what sources were used for the thermodynamic data used in the calculation of the value.

Table V shows the decomposition pressures calculated for the reactions:

$$Be_3N_2(c) = 3Be(g) + N_2(g)$$

$$Be_3N_2(l) = 3Be(g) + N_2(g).$$

The melting point was taken to be 2470°K and the $\Delta H_f^\circ(298)$ $Be_3N_2(l)$ = -113.54 kcal/mole. The heat of fusion of Be_3N_2 was estimated to be 30.9 kcal/mole.

Magnesium Nitride

Table VI gives the decomposition pressures for the reaction:

$$Mg_3N_2(c) = 3Mg(g) + N_2(g).$$

$\Delta H_f^\circ(298)$ Mg_3N_3 was taken as -110.2 kcal/mole, and the free energy functions given in NBS Report 6928 were used for these calculations. NBS Report 6645 (Chapter A2) gives a summary of the calorimetric determinations of $\Delta H_f^\circ(298)$ from which the foregoing value was selected.

Hildenbrand [21] confirmed the earlier observation of Soulen et al. (see Report 6645) that Mg_3N_2 has a low sublimation coefficient, but his value of -135 kcal/mole for $\Delta H_f^\circ(298)$ Mg_3N_2 is not in good agreement with the above accepted calorimetric value. Blank [13] (seen only in abstract) has studied the sublimation of Mg_3N_2 and gives the equation:

$$\text{LogKeq} = 4\log P_T - 0.9780 = \left(\frac{245.979 \pm 16.64}{45.76}\right) \frac{10^4}{T} + 28.733 \pm 3.162.$$

The heat of sublimation given in 242.3 kcal/mole (third law), which leads to $\Delta H_f^\circ(298)$ Mg_3N_2 = -135.5 kcal/mole using the value of $\Delta H_f^\circ(298)$ Mg(g) given in NBS Report 6928. Hildenbrand's and Blank's values are not inconsistent with one calorimetric determination of $\Delta H_f^\circ(298)$ (134.3 kcal/mole), but as discussed in NBS Report 6645 (Chapter A2) this has heretofore been considered to be a less reliable value. Further calorimetric determinations of $\Delta H_f^\circ(298)$ would seem to be indicated.

Titanium Carbide

The value for $\Delta H_f^\circ(298)$ TiC(c) used in the previously calculated decompositions pressures was -43.8 kcal/mole. This value has been retained for the computation of the pressures given in table VII, although several calorimetric and vapor pressure determinations of $\Delta H_f^\circ(298)$ have been made in the interim period [22-27]. The values obtained range from about -32.4 to -56.4 kcal/mole, with an average value within 300 to 700 kcal/mole of the selected value (depending on the tables of thermal functions used to treat the data) and show no obvious dependence on the experimental methods employed.

Table VII gives the computed decomposition pressures for the reactions:

$$TiC(c) = Ti(g) + C(c)(\text{graphite})$$

$$TiC(l) = Ti(g) + C(c)(\text{graphite}).$$

The melting point has been taken as 3410°K (as previously). A recent paper by Worrel [28], quoting Storms [29] gives the melting point as 3450°K, although Rudy [30] reports that the carbide melts congruently at 3340°K with a composition of $TiC_{0.88}$. The probable deviations from stoichiometry at high temperature have not been considered in making the computations. At the lower temperatures shown in table VII the rate of equilibration is probably slow, whereas at temperatures above about 2800°K the equilibrium is described more accurately by:

$$TiC(c) = Ti(g) + C(g)$$

$$2C(g) = C_2(g)$$

$$3C(g) = C_3(g), \text{ etc.}$$

and $P_C + 2P_{C_2} + 3P_{C_3} + \ldots\ldots = P_{Ti}$.

Thus, the pressures given in table VII tend to be too low in comparison with the true equilibrium pressures of TiC, but the true pressures of Ti will be lower than those in equilibrium with pure Ti. Likewise, at temperatures above 2800°K the pressures of carbon gas species will be lower than the pressures in equilibrium with pure graphite at the same temperatures.

Titanium Nitride

Holmberg [31] has reported the existence of a Ti_2N phase in the Ti-N system, but in the absence of any thermodynamic data on the compound its possible existence has been ignored for computational purposes.

Fesenko and Bolgar [25] give data on the rate of vaporization of TiN, and Akishin and Khodeev [32] have confirmed that vaporization occurs predominantly by dissociation to the gaseous elements.

The value of -80.5 kcal/mole for $\Delta H_f^\circ(298)$ TiN(c) was used to compute the decomposition pressures for the reactions:

$$TiN(c) = Ti(g) + \tfrac{1}{2}N_2(g)$$

$$TiN(l) = Ti(g) + \tfrac{1}{2}N_2(g).$$

This value for $\Delta H_f^\circ(298)$ and the melting point of 3200°K were the same as the values used in NBS Report 6645. However, the latest JANAF tables giving the free energy functions for Ti(g) were used to compute the pressures given in table VIII.

References

1. E. Baur and R. Brunner, Z. Elektrochem. 40, 154 (1934).
2. J. F. Durand, Bull. Soc. Chim. 35, 1141 (1924).
3. A. D. Mah, U. S. Bureau of Mines RI 6415 (1964).
4. R. C. King and G. T. Armstrong, J. Res. Nat. Bur. Stand. 68A, 661 (1964).
5. E. R. Plante and C. H. Schreyer, to be published, J. Res. Nat. Bur. Stand.
6. G. T. Furukawa, T. B. Douglas, W. G. Saba, and A. C. Victor, J. Res. Nat. Bur. Stand. 69A, 423 (1965).
7. G. A. Jeffrey and V. Y. Wu, Acta Cryst. 16, 559 (1963).
8. J. H. Cox and L. M. Pidgeon, Can. J. Chem. 41, 671 (1963).
9. K. Motzfeldt, Tek. Ukeblad. 109, 1137 (1962).
10. L. H. Dreger, V. V. Dadape, and J. L. Margrave, J. Phys. Chem. 66, 1556 (1962).
11. P. Schissel and W. Williams, Bull. Am. Phys. Soc. 4, 139 (1959).
12. D. L. Hildenbrand and W. F. Hall, J. Phys. Chem. 43, 888 (1963).
13. B. A. H. Blank, U. S. At. Energy Comm. UCRL-16018 (1965; Dissertation Abstr. 26, 3803 (1965-66).
14. H. L. Schick et al., Thermodynamics of Certain Refractory Compounds, 4th Quarterly Prog. Rept., 1 March 1963 to 31 May 1963. USAF Contract AF33(657)-8223, 15 June 1963.
15. J. Baboin, French Patents 1.193.790 (1959).
16. F. Muratov and A. Novoselova, Dokl. Akad. Nauk SSSR 129, 334 (1959).
17. P. Eckerlin and A. Rabernau, Z. anorg. u. allgem. Chem. 304, 218 (1960).
18. P. Gross, Admin. Rept. 14, Contract AF 61(052)-447, 30 September 1963 to 31 December 1963, Fulmer Research Inst. Stoke Poges, Bucks., England.
19. C. L. Hoenig (Univ. California, Berkeley), Dissertation Abstr. 25, 5549 (1964-65)
20. R. E. Yates, M. A. Greenbaum, and M. Farber, J. Phys. Chem. 68, 2682 (1964).
21. D. L. Hildenbrand, AD 258410(196). CA 58:7433d.
22. C. E. Lowell and W. S. Williams, Rev. Sci. Instr. 32, 1120 (1961).
23. M. P. Morozova, M. K. Khripun, S. M. Ariya, Zh. Obshch. Khim. 32,
24. G. L. Vidale, Measurement of Vapor Pressure of Atomic Species from Spectrometric Measurements of the Absorption of Resonance Lines. V. Free Energy of Formation of TiC and ZrC, Report No. R61D147, Missile and Space Vehicle Dept., General Electric Co., August 1961, AD 263336.
25. V. V. Fesenko and A. S. Bolgar, Poroshkovaya Met. Akad. Nauk Ukr. SSR 3 [1], 17-25 (1963).
26. S. Fujishiro and N. A. Gockcen, J. Phys. Chem. 65, 161 (1961).
27. J. A. Coffman, G. M. Kibler, T. F. Lyon, and B. D. Acchione, WADD-TR-60-646, Part II. Wright-Patterson Air Force Base (1963).
28. W. J. Worrel, J. Phys. Chem. 68, 954 (1964).
29. E. K. Storms, Los Alamos Sci. Lab. Rept. LAMS 2674 (1962).
30. E. Rudy, D. P. Harmon, and C. E. Brukl, AFML-TR-65-2, Part I, Vol. II. Wright-Patterson Air Force Base (1965).
31. B. Holmberg, Acta Chem. Scand. 16, 1255 (1962).
32. P. A. Akishin and Yu. S. Khodeev, Zh. Neorg. Khim 7, 941 (1962).

TABLE I

Decomposition Pressures for Aluminum Carbide

Temp °K	Log K	P(atm) Al
1000	-4.90×10^{1}	5.43×10^{-13}
1050	-4.53×10^{1}	4.64×10^{-12}
1100	-4.19×10^{1}	3.25×10^{-11}
1150	-3.88×10^{1}	1.92×10^{-10}
1200	-3.60×10^{1}	9.81×10^{-10}
1250	-3.34×10^{1}	4.37×10^{-9}
1300	-3.10×10^{1}	1.73×10^{-8}
1350	-2.88×10^{1}	6.22×10^{-8}
1400	-2.67×10^{1}	2.03×10^{-7}
1450	-2.48×10^{1}	6.11×10^{-7}
1500	-2.48×10^{1}	1.70×10^{-6}
1550	-2.14×10^{1}	4.45×10^{-6}
1600	-1.98×10^{1}	1.09×10^{-5}
1650	-1.83×10^{1}	2.54×10^{-5}
1700	-1.70×10^{1}	5.61×10^{-5}
1750	-1.57×10^{1}	1.18×10^{-4}
1800	-1.44×10^{1}	2.39×10^{-4}
1850	-1.33×10^{1}	4.67×10^{-4}
1900	-1.22×10^{1}	8.76×10^{-4}
1950	-1.11×10^{1}	1.59×10^{-3}
2000	-1.02×10^{1}	2.80×10^{-3}
2050	-9.26	4.81×10^{-3}
2100	-8.38	8.00×10^{-3}
2150	-7.53	1.30×10^{-2}
2200	-6.72	2.07×10^{-2}
2250	-5.95	3.23×10^{-2}
2300	-5.22	4.94×10^{-2}
2350	-4.51	7.42×10^{-2}
2400	-3.84	1.09×10^{-1}
2450	-3.19	1.59×10^{-1}
2500	-2.57	2.27×10^{-1}
2600	-1.41	4.42×10^{-1}
2700	-3.41×10^{-1}	8.21×10^{-1}
2800	6.53×10^{-1}	1.45
2900	1.57	2.48
3000	2.44	4.07

TABLE II

Reaction of Aluminum Oxide with Carbon

Temp °K	Log K	Log P(CO)	P(atm) CO
1000	-7.06×10^{1}	-1.17×10^{1}	1.69×10^{-12}
1050	-6.58×10^{1}	-1.09×10^{1}	1.06×10^{-11}
1100	-5.89×10^{1}	-9.83	1.47×10^{-10}
1150	-5.39×10^{1}	-8.99	1.01×10^{-9}
1200	-4.93×10^{1}	-8.22	5.98×10^{-9}
1250	-4.51×10^{1}	-7.51	3.04×10^{-8}
1300	-4.11×10^{1}	-6.86	1.36×10^{-7}
1350	-3.75×10^{1}	-6.26	5.45×10^{-7}
1400	-3.42×10^{1}	-5.70	1.97×10^{-6}
1450	-3.11×10^{1}	-5.18	6.50×10^{-6}
1500	-2.82×10^{1}	-4.70	1.98×10^{-5}
1550	-2.56×10^{1}	-4.27	5.32×10^{-5}
1600	-2.29×10^{1}	-3.82	1.48×10^{-4}
1650	-2.05×10^{1}	-3.43	3.69×10^{-4}
1700	-1.83×10^{1}	-3.05	8.72×10^{-4}
1750	-1.62×10^{1}	-2.70	1.95×10^{-3}
1800	-1.42×10^{1}	-2.37	4.17×10^{-3}
1850	-1.24×10^{1}	-2.06	8.53×10^{-3}
1900	-1.06×10^{1}	-1.77	1.69×10^{-2}
1950	-8.95	-1.49	3.22×10^{-2}
2000	-7.36	-1.22	5.93×10^{-2}
2050	-5.85	-9.76×10^{-1}	1.05×10^{-1}
2100	-4.40	-7.34×10^{-1}	1.84×10^{-1}
2150	-3.05	-5.08×10^{-1}	3.10×10^{-1}
2200	-1.73	-2.89×10^{-1}	5.13×10^{-1}
2250	-4.94×10^{-1}	-8.23×10^{-2}	8.27×10^{-1}
2300	6.95×10^{-1}	1.15×10^{-1}	1.30

TABLE III

Decomposition Pressures for Aluminum Nitride

Temp °K	Log K	P(atm) N_2	P(atm) Al	Total P
1000	-2.10×10^{1}	5.54×10^{-15}	1.10×10^{-14}	1.66×10^{-14}
1050	-1.94×10^{1}	6.31×10^{-14}	1.26×10^{-13}	1.89×10^{-13}
1100	-1.80×10^{1}	5.75×10^{-13}	1.15×10^{-12}	1.72×10^{-12}
1150	-1.67×10^{1}	4.31×10^{-12}	8.63×10^{-12}	1.29×10^{-11}
1200	-1.55×10^{1}	2.73×10^{-11}	5.46×10^{-11}	8.20×10^{-11}
1250	-1.44×10^{1}	1.49×10^{-10}	2.98×10^{-10}	4.47×10^{-10}
1300	-1.34×10^{1}	7.13×10^{-10}	1.42×10^{-9}	2.14×10^{-9}
1350	-1.24×10^{1}	3.03×10^{-9}	6.07×10^{-9}	9.10×10^{-9}
1400	-1.16×10^{1}	1.16×10^{-8}	2.32×10^{-8}	3.48×10^{-8}
1450	-1.07×10^{1}	4.05×10^{-8}	8.11×10^{-8}	1.21×10^{-7}
1500	-1.00×10^{1}	1.29×10^{-7}	2.59×10^{-7}	3.89×10^{-7}
1550	-9.31	3.85×10^{-7}	7.71×10^{-7}	1.15×10^{-6}
1600	-8.65	1.06×10^{-6}	2.13×10^{-6}	3.20×10^{-6}
1650	-8.03	2.78×10^{-6}	5.57×10^{-6}	8.35×10^{-6}
1700	-7.44	6.84×10^{-6}	1.36×10^{-5}	2.05×10^{-5}
1750	-6.89	1.59×10^{-5}	3.19×10^{-5}	4.79×10^{-5}
1800	-6.37	3.55×10^{-5}	7.11×10^{-5}	1.06×10^{-4}
1850	-5.87	7.58×10^{-5}	1.51×10^{-4}	2.27×10^{-4}
1900	-5.41	1.55×10^{-4}	3.10×10^{-4}	4.66×10^{-4}
1950	-4.96	3.06×10^{-4}	6.12×10^{-4}	9.19×10^{-4}
2000	-4.54	5.84×10^{-4}	1.16×10^{-3}	1.75×10^{-3}
2050	-4.15	1.07×10^{-3}	2.15×10^{-3}	3.23×10^{-3}
2100	-3.77	1.93×10^{-3}	3.86×10^{-3}	5.79×10^{-3}
2150	-3.40	3.36×10^{-3}	6.73×10^{-3}	1.00×10^{-2}
2200	-3.06	5.71×10^{-3}	1.14×10^{-2}	1.71×10^{-2}
2250	-2.73	9.47×10^{-3}	1.89×10^{-2}	2.84×10^{-2}
2300	-2.41	1.53×10^{-2}	3.07×10^{-2}	4.61×10^{-2}
2350	-2.11	2.44×10^{-2}	4.88×10^{-2}	7.32×10^{-2}
2400	-1.82	3.80×10^{-2}	7.60×10^{-2}	1.14×10^{-1}
2450	-1.55	5.80×10^{-2}	1.16×10^{-1}	1.74×10^{-1}
2500	-1.28	8.72×10^{-2}	1.74×10^{-1}	2.61×10^{-1}

TABLE IV

Decomposition Pressures for Beryllium Carbide

Temp °K	Log K	Log P (Be)	P(atm) Be
1200	-1.87×10^1	-9.36	4.30×10^{-10}
1250	-1.74×10^1	-8.72	1.90×10^{-9}
1300	-1.62×10^1	-8.12	7.49×10^{-9}
1350	-1.51×10^1	-7.57	2.65×10^{-8}
1400	-1.41×10^1	-7.06	8.60×10^{-8}
1450	-1.31×10^1	-6.59	2.56×10^{-7}
1500	-1.22×10^1	-6.14	7.09×10^{-7}
1550	-1.14×10^1	-5.73	1.83×10^{-6}
1600	-1.06×10^1	-5.34	4.48×10^{-6}
1650	-9.97	-4.98	1.03×10^{-5}
1700	-9.28	-4.64	2.26×10^{-5}
1750	-8.64	-4.32	4.74×10^{-5}
1800	-8.04	-4.02	9.53×10^{-5}
1850	-7.46	-3.73	1.84×10^{-4}
1900	-6.92	-3.46	3.43×10^{-4}
1950	-6.41	-3.20	6.20×10^{-4}
2000	-5.92	-2.96	1.08×10^{-3}
2050	-5.46	-2.73	1.84×10^{-3}
2100	-5.02	-2.51	3.05×10^{-3}
2150	-4.60	-2.30	4.95×10^{-3}
2200	-4.21	-2.10	7.82×10^{-3}
2250	-3.83	-1.91	1.21×10^{-2}
2300	-3.47	-1.73	1.83×10^{-2}
2350	-3.12	-1.56	2.74×10^{-2}
2400	-2.79	-1.39	4.02×10^{-2}

TABLE V

Decomposition Pressure of Beryllium Nitride

Temp °K	Log K	P(atm) N_2	P(atm) Be	Total P
1200	-3.95×10^{1}			
1300	-3.43×10^{1}	1.14×10^{-9}	3.42×10^{-9}	4.56×10^{-9}
1400	-2.99×10^{1}	1.46×10^{-8}	4.40×10^{-8}	5.87×10^{-8}
1500	-2.60×10^{1}	1.33×10^{-7}	4.01×10^{-7}	5.35×10^{-7}
1600	-2.27×10^{1}	9.19×10^{-7}	2.75×10^{-6}	3.67×10^{-6}
1700	-1.97×10^{1}	5.01×10^{-6}	1.50×10^{-5}	2.00×10^{-5}
1800	-1.71×10^{1}	2.25×10^{-5}	6.77×10^{-5}	9.02×10^{-5}
1900	-1.48×10^{1}	8.63×10^{-5}	2.59×10^{-4}	3.45×10^{-4}
2000	-1.27×10^{1}	2.87×10^{-4}	8.63×10^{-4}	1.15×10^{-3}
2100	-1.08×10^{1}	8.51×10^{-4}	2.55×10^{-3}	3.40×10^{-3}
2200	-9.14	2.27×10^{-3}	6.82×10^{-3}	9.10×10^{-3}
2300	-7.58	5.56×10^{-3}	1.67×10^{-2}	2.22×10^{-2}
2400	-6.16	1.26×10^{-2}	3.78×10^{-2}	5.04×10^{-2}
2470	-5.24	2.14×10^{-2}	6.42×10^{-2}	8.56×10^{-2}
2500	-2.53	1.01×10^{-1}	3.05×10^{-1}	4.07×10^{-1}
2600	-1.53	1.81×10^{-1}	5.43×10^{-1}	7.25×10^{-1}
2700	-6.13×10^{-1}	3.08×10^{-1}	9.24×10^{-1}	1.23
2800	2.38×10^{-1}	5.03×10^{-1}	1.50	2.01

TABLE VI

Decomposition Pressures of Magnesium Nitride

Temp °K	Log K	P(atm) N_2	P(atm) Mg	P(atm) Total
1100	-1.50×10^{1}	7.78×10^{-5}	2.33×10^{-4}	3.11×10^{-4}
1150	-1.31×10^{1}	2.23×10^{-4}	6.69×10^{-4}	8.92×10^{-4}
1200	-1.14×10^{1}	5.85×10^{-4}	1.75×10^{-3}	2.34×10^{-3}
1250	-9.95	1.41×10^{-3}	4.25×10^{-3}	5.67×10^{-3}
1300	-8.54	3.21×10^{-3}	9.63×10^{-3}	1.28×10^{-2}
1350	-7.23	6.83×10^{-3}	2.04×10^{-2}	2.73×10^{-2}
1400	-6.01	1.37×10^{-2}	4.13×10^{-2}	5.50×10^{-2}
1450	-4.88	2.63×10^{-2}	7.91×10^{-2}	1.05×10^{-1}
1500	-3.82	4.83×10^{-2}	1.45×10^{-1}	1.93×10^{-1}
1550	-2.84	8.52×10^{-2}	2.55×10^{-1}	3.40×10^{-1}
1600	-1.92	1.44×10^{-1}	4.34×10^{-1}	5.79×10^{-1}
1650	-1.06	2.37×10^{-1}	7.13×10^{-1}	9.51×10^{-1}
1700	-2.50×10^{-1}	3.79×10^{-1}	1.13	1.51
1750	5.13×10^{-1}	5.89×10^{-1}	1.76	2.35

TABLE VII

Decomposition Pressure of Titanium Carbide

Temp °K	Log K	P(atm) Ti
2000	-9.13	7.36×10^{-10}
2100	-8.33	4.66×10^{-9}
2200	-7.60	2.48×10^{-8}
2300	-6.94	1.14×10^{-7}
2400	-6.33	4.65×10^{-7}
2500	-5.77	1.68×10^{-6}
2600	-5.25	5.51×10^{-6}
2700	-4.78	1.64×10^{-5}
2800	-4.34	4.55×10^{-5}
2900	-3.92	1.17×10^{-4}
3000	-3.54	2.85×10^{-4}
3100	-3.18	6.48×10^{-4}
3200	-2.85	1.41×10^{-3}
3300	-2.53	2.91×10^{-3}
3400	-2.23	5.80×10^{-3}
3500	-1.01	9.71×10^{-2}
3600	-0.80	1.56×10^{-1}

TABLE VIII

Decomposition Pressures of Titanium Nitride

Temp °K	P(atm) N_2	P(atm) Ti	P(atm) Total
1400	8.84×10^{-13}	1.76×10^{-12}	2.65×10^{-12}
1500	1.85×10^{-11}	3.71×10^{-11}	5.56×10^{-11}
1600	2.64×10^{-10}	5.28×10^{-10}	7.92×10^{-10}
1700	2.74×10^{-9}	5.49×10^{-9}	8.24×10^{-9}
1800	2.18×10^{-8}	4.37×10^{-8}	6.56×10^{-8}
1900	1.39×10^{-7}	2.79×10^{-7}	4.18×10^{-7}
2000	7.29×10^{-7}	1.47×10^{-6}	2.21×10^{-6}
2100	3.31×10^{-6}	6.63×10^{-6}	9.95×10^{-6}
2200	1.30×10^{-5}	2.60×10^{-5}	3.90×10^{-5}
2300	4.50×10^{-5}	9.00×10^{-5}	1.35×10^{-4}
2400	1.40×10^{-4}	2.81×10^{-4}	4.22×10^{-4}
2500	4.00×10^{-4}	8.00×10^{-4}	1.20×10^{-3}
2600	1.04×10^{-3}	2.09×10^{-3}	3.14×10^{-3}
2700	2.55×10^{-3}	5.10×10^{-3}	7.65×10^{-3}
2800	5.81×10^{-3}	1.16×10^{-2}	1.74×10^{-2}
2900	1.25×10^{-2}	2.51×10^{-2}	3.76×10^{-2}
3000	2.55×10^{-2}	5.11×10^{-2}	7.67×10^{-2}
3100	4.99×10^{-2}	9.98×10^{-2}	1.49×10^{-1}
3200	9.33×10^{-2}	1.86×10^{-1}	2.80×10^{-1}
3300	7.29×10^{-1}	1.45	2.18
3400	1.15	2.30	3.45
3500	1.77	3.54	5.31

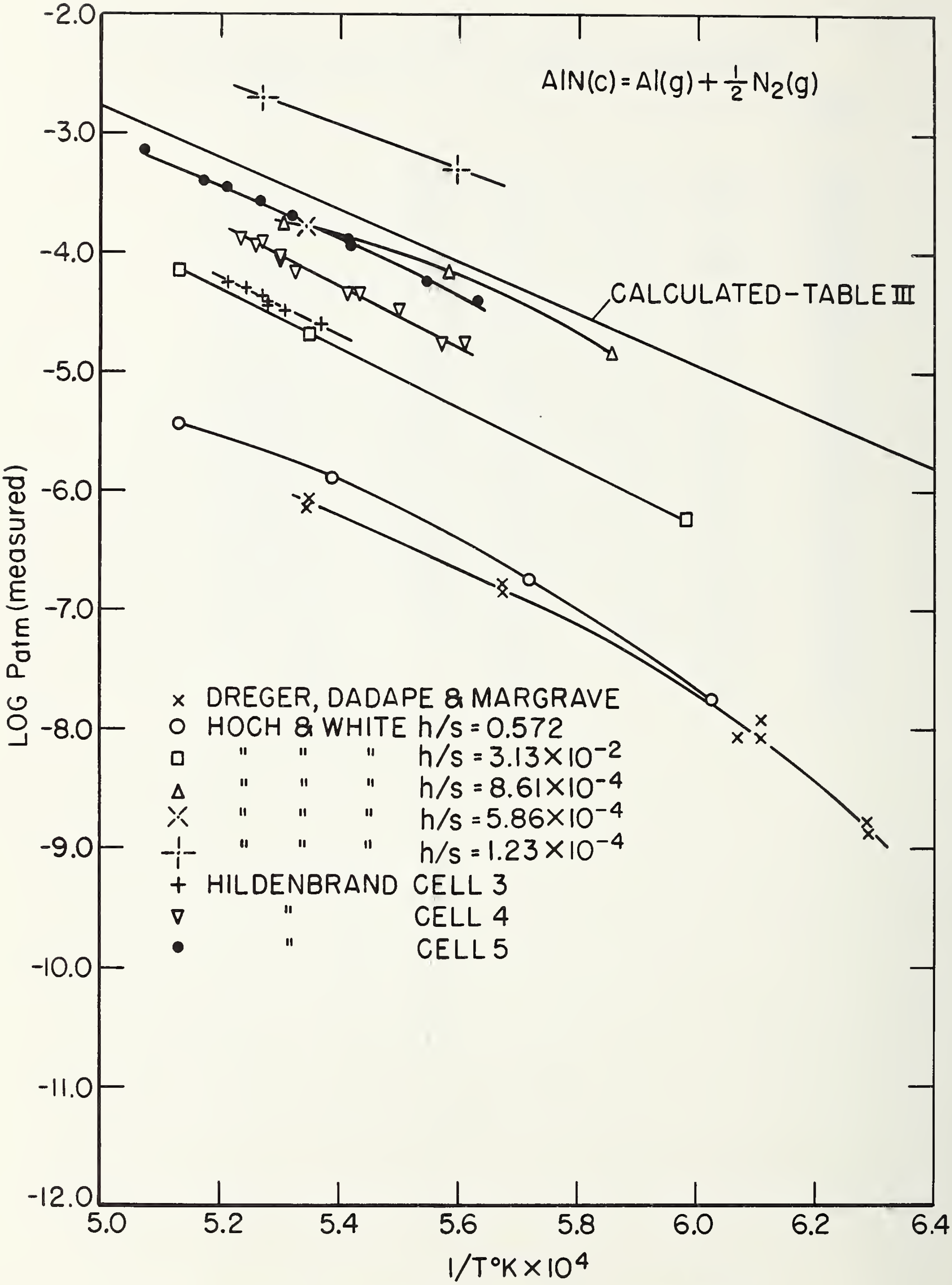

Figure 1: Decomposition Pressures of Aluminum Nitride

Chapter 3

VIBRATIONAL SPECTRA OF ALKALINE EARTH DIFLUORIDES

By. G. V. Calder

INTRODUCTION

The vibrational spectra of a number of Group IIA halides have been determined by the matrix-isolation technique. All of the spectra were measured by trapping the halide vapor species in a matrix of krypton or argon at 20°K. In addition to infrared absorptions of the triatomic monomeric species, absorptions specifically attributable to dimer symmetric with respect to the metal atoms were also observed. In one case absorptions believed to be due to a diatomic species MX were observed. The sorting out and selection of the proper fundamentals was made possible by the use of isotopically enriched samples of each of the metal halides where the isotope effect was large enough to be observed. Experimental work on $Mg^{24}F_2$, $Mg^{26}F_2$, $Ca^{40}F_2$, $Ca^{44}F_2$, $Sr^{86}F_2$, $Sr^{88}F_2$, $Ba^{n}F_2$, $Mg^{24}Cl^{n}_2$, $Mg^{26}Cl^{n}_2$ has been completed*. Analysis of the data on MgF_2 and CaF_2 has been completed, and the results on these two molecules will be reported here.

EXPERIMENTAL PROCEDURE

Detailed experimental procedure will not be presented here. However, a few words about the use of isotopically enriched samples is in order since they provide the most powerful tool available for interpretating the observed spectra.

Consider two pure isotopes M, M' in a triatomic molecule MX_2 and $M'X_2$. As is well known, the effect of the change in mass of M to M' has a calculable effect on the vibrational fundamentals, and this is useful in determining the force constants and structure (apex angle) of the molecule MX_2. A synthetically enriched sample of 50% MX_2 and 50% $M'X_2$ yields much information also. Any absorbing species containing only one metal atom M or M' will give rise to a doublet in the mixed isotope spectrum. Any absorbing species containing two equivalent metal atoms will give rise to three absorptions due to MM, MM' and M'M' species. For a 50% - 50% mixture the intensity ratio of the triplet will be 1:2:1,

---

* n = natural abundance

yielding an easily identifiable feature. In the experiments on MgF_2, absorptions in the region of 730 cm^{-1} were found which were shown to come from a species containing only one Mg atom. The isotope shift of the absorptions was consistent with the hypothesis that they were due to MgF. The spectra of CaF_2 yielded absorptions in the regions of 515 cm^{-1} and 360 cm^{-1} which were due to species containing two calcium atoms. It was found that the use of different matrix gases did not affect the isotopic frequency ratios (ν_3/ν_3') within the experimental error of ±.10 cm^{-1} despite the fact that in the case of MgF_2 the ν_3 frequency was a triplet in krypton and a quartet in argon matrices.

RESULTS ON MAGNESIUM FLUORIDE

The measurements on MgF_2 are summarized in the following table:

MgF_2 in Krypton (in cm^{-1})

	$Mg^{24}F_2$	$Mg^{25}F_2$	$Mg^{26}F_2$
ν_3 obs	833.06 834.54 837.41	822.98* 824.56* 827.24*	813.57 815.17 817.79
ν_3 calc	837.34**	827.24	817.87
ν_1 obs	478.04	477.31	476.61
ν_1 calc	478.28	477.21	476.25
ν_2 obs	241.8	not observed	237.9
ν_2 calc	242.5	240.1	237.8

Apex angle = 150°±10

MgF Bond Dist. (assumed) 1.77 Å

*Observed in natural abundance only (10%).
**Highest frequency chosen arbitrarily for calculation.

The following force constants were obtained from the analysis of the isotopic data:

Force Constants of MgF_2 in Krypton (Md/Å)

$F_r = 2.740$ $F_{rr} = -0.419$ $F_\alpha = .140$ $F_{r\alpha}$ $\frac{.03}{\sqrt{2}}$

The absorptions attributed to MgF are:

MgF in Krypton (in cm^{-1})

	$Mg^{24}F$	$Mg^{25}F$	$Mg^{26}F$
Mg Nat. Abundance	738.20	723.80	726.40
Mg^{26}	------	------	726.56
ν calc	738.20	732.12	726.56

The coincidence of the frequency observed in the Mg^{26} sample, 726.56 cm^{-1}, and that observed in the natural abundance sample, 726.40 cm^{-1}, proves that the absorbing species contains one and only one Mg atom. The magnitude of the shift from Mg^{24}, Mg^{25} and Mg^{26} is very nearly that expected for MgF. In the gas phase the fundamental of MgF is reported to be at 709 cm^{-1}.

RESULTS ON CALCIUM FLUORIDE

The study of the calcium fluoride spectrum yielded the following absoprtion frequencies:

$\underline{CaF_2 \text{ in Krypton}}$ (in cm^{-1})

	$Ca^{40}F_2$	50% Ca^{40}/50% Ca^{44}	$Ca^{44}F_2$
ν_3 obs	553.66	*	542.25
ν_3 calc	553.64		542.37
ν_1 obs	484.75	*	482.60
ν_1 calc	485.35		481.99
ν_2 obs	163.36	*	161.20
ν_2 calc	163.55		160.98
(Dimer)	522.70	517.27**	513.96
(Dimer)	365.08	362.46**	359.30

Apex angle 135±7°

CaF Bond Dist. (assumed) 2.10 Å

*Frequency of observed doublets identical to those of individual isotopes.

**These features were observed only in spectra of mixed samples of the isotopes.

The following force constants were obtained from the analysis of the isotopic data:

Force Constants of CaF_2 in Krypton (Md/Å)

$F_r = 2.31 \qquad F_{rr} = +0.39 \qquad F_\alpha = 0.075 \qquad F_{r\alpha} = \frac{.02}{\sqrt{2}}$

The thermodynamic properties of MgF_2 and CaF_2 have been calculated on the basis of the bent structures and vibrational frequencies determined in these experiments:

$$S^o_{1400°K} = 81.9 \text{ gibbs for } MgF_2 \text{ (g)}$$

$$S^o_{1600°K} = 87.8 \text{ gibbs for } CaF_2 \text{ (g)}$$

This is in agreement with the recent data of Hildenbrand (private communication) which reports $S^o_{1400°K}$ = 82.7 gibbs and $S^o_{1600°K}$ = 88.2 gibbs for MgF_2 (g) and CaF_2 (g) from thermal and vapor pressure data.

Chapter 4

PRELIMINARY REPORT ON THE MICROWAVE SPECTRUM AND STRUCTURE OF CESIUM HYDROXIDE

By D. R. Lide and R. L. Kuczkowski

INTRODUCTION

The structure of alkali hydroxide monomers raises a number of interesting questions. The overall geometry of these molecules cannot be predicted with any certainty. It is not clear whether the familiar bond angle of 100°-110° which is found for covalently-bonded oxygen compounds will apply to the hydroxides, where one bond is covalent and the other is presumably highly ionic. Indeed, there is a suggestion from somewhat indirect evidence on Li_2O[1,2] that the hydroxides might be linear rather than bent. The inter-atomic distances are also difficult to predict, since there are no reliable measurements on alkali-oxygen distances. The nature of the molecular vibrations is open to similar questions. There is little information available on alkali-oxygen stretching force constants, and the magnitude of the bending frequency in the hydroxides is entirely a matter of speculation.

There have been no experimental measurements on the gaseous hydroxides which provide any clues to these questions. Furthermore it should be emphasized that the structure and vibrational frequencies of the alkali hydroxides should be of great value in predicting the properties of compounds with OH groups attached to Group II or Group III metals, since such molecules clearly resemble alkali hydroxides much more closely than they do the familiar covalent hydroxyl compounds.

We have recently succeeded, after a considerable amount of effort, in detecting the microwave spectrum of cesium hydroxide, thereby providing the first direct experimental information on the structure of alkali metal hydroxides. Although the interpretation of the spectrum is not yet complete, a number of questions about these compounds can already be answered. A preliminary account of the spectrum and the results which may be drawn from it will be given here.

EXPERIMENTAL

The high-temperature microwave spectrometer developed under the Light-Elements Program[3] was used, after some modification, to observe the CsOH spectrum. In previous attempts to detect the spectra of NaOH and KOH a number of severe experimental difficulties were encountered. Decomposition of the hydroxide samples when heated resulted in excessively high ambient pressure in the microwave absorption cell, even with continuous pumping, and left considerable doubt about the presence of hydroxide vapors. After some experimentation with materials, it was found that silver seemed to produce the minimum amount of decomposition. The waveguide was therefore lined with thin silver sheet which had been formed to the correct shape, and the sample trays were also made of silver.

The tendency of the hydroxides to form solid deposits which bridged the gap between the Stark plates, and also to attack the ceramic spacers, led to very serious problems. During each run it was found that the conductivity between the Stark plates increased steadily until a point was reached where the Stark modulation field could not be sustained. Furthermore, modulation pick-up soon became prohibitive. This problem was alleviated to some extent by removing the ceramic spacers from the hot region of the waveguide and increasing the plate separation. In this way it was possible to achieve measuring times of 10-30 minutes under reasonably good conditions.

In spite of the above precautions the increase in conductivity eventually set in, even though no visible connection existed between the plates. This rather puzzling behavior has been traced to thermionic emission from metallic cesium deposited on the waveguide surface. When the Stark modulation field is applied, appreciable thermionic currents flow through the cell, and at high modulation fields this current completely precludes the observation of spectra. Attempts to poison or coat the waveguide surface have not been successful. However, some very promising results have been obtained by replacing Stark modulation with a form of saturation or "double-resonance" modulation. In this scheme a high-powered, amplitude modulated klystron is tuned to, say, the $J = 1 \rightarrow 2$ transition in a certain state. The waveguide cell is also fed by a klystron which is tuned to the $J = 2 \rightarrow 3$ transition, and the detector is arranged so that only the latter frequency is detected. When both klystrons are in resonance, the periodic disturbance of thermal equilibrium caused by the saturating (or pumping) klystron produces a modulation of the detected signal. This procedure has made it possible to measure a number of weak lines which could not be observed with the usual Stark modulation.

OBSERVED SPECTRUM AND INTERPRETATION

If the CsOH molecule were bent, the spectrum would show the characteristic pattern of a near-prolate asymmetric rotor with a-type selection rules (with the possibility of additional transitions from the b dipole component). The $J = 2 \rightarrow 3$ pattern, for example, would consist of a central $K = 0$ line ($1_{01} \rightarrow 2_{02}$), a pair of $K = 1$ lines of comparable intensity, and two $K = 2$ lines. Whatever the value of the CsOH angle, the asymmetry of the molecule will be so small that the $K = 0$ line will fall very near the mean frequency of the $K = 1$ pair, and the $K = 2$ lines will be essentially degenerate with $K = 0$. Similar patterns of lower intensity would be expected from excited vibrational states. A linear structure, on the other hand, would show a single strong ground-state line accompanied by weaker vibrational satellites. In particular, the π states resulting from excitation of the ν_2, the degenerate bending mode, would appear as characteristic ℓ-type doublets.

The principal features of the observed CsOH and CsOD spectra conform to the predictions of the linear rather than the bent structure. The features of the $J = 2 \rightarrow 3$ pattern which have been clearly identified are listed in Table I. The intensities of the lines assigned to excited vibrational states fall off quite rapidly, showing that these lines do arise from higher vibrational states rather than asymmetric rotor levels. Also, the spacing of the lines is completely incompatible with an asymmetric rotor assignment. We may therefore conclude that the cesium hydroxide molecule is linear.

The assignment of the satellite lines from excited vibrational states has been carried out in the following way. In a normal linear triatomic molecule, the effective rotational constant in a particular vibrational state is given by

$$B_{v_1 v_2 v_3} = B_e - \alpha_1 (v_1+\tfrac{1}{2}) - \alpha_2 (v_2+1) - \alpha_3 (v_3+\tfrac{1}{2}). \qquad (1)$$

For the π states ($\ell = \pm 1$), there is an additional term in the energy:

$$\pm \tfrac{1}{4} q (v_2+1) J(J+1). \qquad (2)$$

Thus it should be possible to recognize series of lines whose successive members have B values differing by α_1. A search for repeating intervals in the CsOH spectrum shows only one well-defined interval, about 200 Mc in the $J = 2 \rightarrow 3$ transition, which is equivalent to an α_1 of 33 Mc. When the symmetry of the observed states and the intensities of the lines are taken into account, it is found that the α_1 must be identified with ν_1, the Cs-O stretching mode. The value of α_1 = 33 Mc seems quite reasonable; in fact, it is practically identical with the α value found in CsF.[4]

The assignment of satellites of ν_2, the bending mode, presents more difficulty. A prominent set of ℓ-type doublets is readily assigned to the 010 π state, and there seems little question about the identification of the 020 Σ and Δ states given in Table I. However, no lines are observed at the frequencies where the 030 π and 040 Σ, Δ states would fall in a regular pattern. While some tentative assignments have been made for these higher states of the bending mode, the pattern is highly irregular, and there is not enough data at present to be certain of the interpretation. We can only conclude, then, that the bending mode is highly anharmonic; the elucidation of the detailed nature of the bending potential will require further data.

At the present time it is difficult to make a reliable estimate of the vibrational frequencies. No quantitative measurements of relative intensities have been achieved yet. However, rough estimates indicate that the Cs-O stretching frequency ω_1 is certainly greater than 300 cm^{-1} and could be as high as 600 cm^{-1}. It may be noted[4] that ω_e = 352 cm^{-1} in CsF. Since the intensities of the 100 and 020 Σ lines are roughly the same, it would appear that the bending fundamental ω_2 is about one-half of ω_1 - i.e., probably of the order of 150-300 cm^{-1}. Another estimate of ω_2 might be obtained from the splitting of the ℓ-doublets in the 010 π state. If the vibrations are assumed to be harmonic, this splitting leads to $\omega_2 \approx 250$ cm^{-1} in CsOH. However, it has been mentioned that the ν_2 mode appears to be quite anharmonic, so that this estimate is open to serious question. It is hoped that a study of higher states will provide better information on the bending levels.

The rotational constants of CsOH and CsOD permit the structural parameters of the molecule to be calculated. On the assumption of a rigid linear molecule, we obtain

$$r(OH) = 0.92 \text{ Å}$$

$$r(CsO) = 2.403 \text{ Å}$$

Again, it must be emphasized that the anomalous nature of the bending mode throws considerable doubt on the validity of the rigid rotor approximation. In particular, it seems unlikely that the OH distance is really as short as 0.92 Å. In all probability, the value obtained from this simple calculation represents, at least crudely, the average projection of the OH bond on the molecular axis and is therefore lower than the true bond distance. On the other hand, the calculation shows that the Cs-O distance is not at all sensitive to the value of r(OH), so that the value given here should be accurate to ±0.01 Å.

Quantitative Stark-effect measurements have not been made yet. However, the dipole moment of CsOH appears to be in the range of 8 to 10 Debye units. This result, along with the other evidence, indicates that the Cs-O bond is highly ionic and that CsOH may be regarded as a close analog of CsF with F^- replaced by OH^-.

REFERENCES

1. A. Buchler, J. L. Stauffer, W. Klemperer, and L. Wharton, J. Chem. Phys. 39, 2299 (1963).

2. D. White, K. S. Seshadri, D. F. Dever, D. E. Mann, and M. J. Linevsky, J. Chem. Phys. 39, 2463 (1963).

3. D. R. Lide, J. Chem. Phys. 42, 1013 (1965).

4. S. E. Veazey and W. Gordy, Phys. Rev. 138, A1303 (1965).

Table I. $J = 2 \rightarrow 3$ transition in CsOH and CsOD

$v_1 v_2 v_3$		ν (CsOH)	ν (CsOD)
0 0 0	Σ	33006.6 Mc	29981.0
0 1 0	Π	32928.1 32880.7	29991.6 29946.1
0 2 0	Σ	32834.6	29973.8
0 2 0	Δ	32795.8	29954.4
1 0 0	Σ	32807.0	
2 0 0	Σ	32607.5	
1 2 0	Σ	32630.1	

Chapter 5

INFRARED SPECTRA OF BERYLLIUM BOROHYDRIDE AND ALUMINUM BOROHYDRIDE

By A. G. Maki

INTRODUCTION

Aluminum borohydride, $Al(BH_4)_3$ and beryllium borohydride, $Be(BH_4)_2$, are expected to contain bridge hydrogen bonds of the type found in diborane (B_2H_6). One expects that $Be(BH_4)_2$ will have D_{2d} symmetry and that $Al(BH_4)_3$ will belong to either the D_{3h} or D_3 point group (see Ref. 1 for further details). The experimental evidence supporting these structures is, however, rather inconclusive. Electron diffraction work on $Al(BH_4)_3$ reported by Beach and Bauer[2] and by Silbiger and Bauer[3] can be interpreted in several different ways.

A rather thorough nuclear magnetic resonance study was carried out on $Al(BH_4)_3$ by Ogg and Ray using double resonance techniques.[4] Their results seem to favor a bridge structure. They found a barrier to the rotation of the BH_4 groups which is relatively high (estimated at 14 kcal/mole) although a related aluminum borohydride compound which they prepared has a low barrier to rotation of the BH_4 groups. Ogg and Ray did find, however, that there is an equivalence of the hydrogen atoms in the BH_4 groups which they interpret as being due to a slow tunnelling-type of exchange of the hydrogen atoms within each BH_4 group. A discussion of tunnelling or tautomerism in the borohydride compounds has been given by Williams.[5]

Banford and Coates[6] report that the B'' magnetic resonance spectrum of $Me_3P_3Be(BH_4)_2$ is similar to that of $Al(BH_4)_3$. Hence there is indirect evidence that in $Be(BH_4)_2$ there is either some type of exchange of the hydrogens within each BH_4 group, or else a rotation of the BH_4 groups.

The infrared spectrum of $Al(BH_4)_3$ and $Be(BH_4)_2$ was first measured by Price and others.[1,7] Since that time no other detailed spectral work has been done on $Be(BH_4)_2$. The Raman spectrum of $Al(BH_4)_3$ and $Al(BD_4)_3$ was subsequently studied by Emery and Taylor.[8] Although they favored the D_{3h} structure for these compounds, their work was by no means conclusive. Because of instrumental limitations neither $Be(BH_4)_2$ nor $Al(BH_4)_3$ has previously been studied in the far infrared region. Furthermore, the earlier gas phase spectra of these two compounds were obtained with such low resolution that it was not possible to use the shape of the rotational band envelopes as an aid to determining the symmetry classification of the transitions involved.

The work presented in this paper was undertaken with the intention of filling these gaps and with the additional hope that an improved vibrational assignment would then be possible. The shapes of the rotational band envelopes were not as helpful as had been expected. In the case of $Be(BH_4)_2$ this is rather surprising; presumably the bands are badly overlapped by hot band lines from some very low frequency vibrations. A hindered rotation of the BH_4 groups may also cause complications which obscure the characteristic shape expected for the band envelope.

In this paper we will also show that there is a great difference between the infrared spectrum of solid and gaseous $Be(BH_4)_2$. This is tentatively interpreted as being due to a transition from a weak, covalent bridge-hydrogen structure in the gas phase to a more ionic structure in the solid. The latter would contain BH_4 groups which are very similar to BH_4 ions.

EXPERIMENTAL

The spectra in the region from 250 cm^{-1} to 4000 cm^{-1} were obtained using a Beckman IR-7 foreprism-grating spectrometer. The far infrared spectra (from 80 to 300 cm^{-1}) were obtained with a Grubb Parsons interferometric spectrometer similar in design and operation to that described in Ref. 9. Gas phase spectra were obtained using a 9 cm long glass absorption cell fitted with either KBr, Irtran-2, or polyethylene windows. Solid phase spectra were obtained by freezing the gas onto either a silicon window or a KBr window. To be certain that there was no reaction with the substrate, some experiments were performed in which the cold surface was completely covered with a thin sheet of a terephthalate plastic material (mylar). Since the spectrum of solid $Be(BH_4)_2$ was different from that of the gas, the same sample was taken through several solid-gas transitions and the spectrum of each phase was studied in turn. In all cases the solid phase spectra were identical and the gas phase spectra were identical although the two phases had quite different spectra.

Both the beryllium and the aluminum compounds contained small amounts of diborane (B_2H_6) which was largely eliminated by two trap to trap distillations. The weak features at 1600 cm^{-1} in Figs. 1 and 2 are due to diborane impurity. Some weak absorption bands in the CH stretching vibration region may be due to small amounts of organic impurities, but such small amounts of impurities cannot account for any of the strong absorption features with which this paper is concerned.

The compounds used in this study contained the natural abundance of boron isotopes. Hence, the beryllium borohydride spectra are for a mixture of approximately 66% $Be(^{11}BH_4)_2$, 31% $Be(^{10}BH_4)(^{11}BH_4)$, and 4% $Be(^{10}BH_4)_2$ and the aluminum borohydride spectra for a mixture of 54% $Al(^{11}BH_4)_3$, 37% $Al(^{10}BH_4)(^{11}BH_4)_2$, and 9% $Al(^{10}BH_4)_2(^{11}BH_4)$. Such a mixture of isotopic species will destroy to some extent the usefulness of the band contours for making vibrational assignments. Since diborane gives useful band contour information without using isotopically enriched samples, we expected that the band contours for beryllium borohydride would be similarly useful.

ASSIGNMENTS FOR ALUMINUM BOROHYDRIDE

General

In Table 1 we have listed the observed infrared absorption bands in aluminum borohydride. Figure 1 shows the spectrum for both the gas and solid phases from 500 cm^{-1} to 3000 cm^{-1}. Table 2 summarizes the numbering of the vibrations used in this paper assuming that the $Al(BH_4)_3$ molecule belongs to the D_{3h} point group. While we cannot claim that there is strong physical evidence favoring this point group, it does seem to be the most reasonable symmetry from several points of view. In this paper we will only consider the assignments for a D_{3h} point group. Both the infrared and Raman spectrum favor the D_{3h} point group in terms of the total number of strong transitions, but there are enough difficulties in the assignments and enough unassigned weak spectral features to prevent us from drawing any firm conclusions.

In the following selections we will treat each symmetry species separately in making the assignments. For the assignments we have relied rather heavily on the similarity with the structures of the diborane (see Ref. 10) and the boron trifluoride (see Ref. 11) molecules. The similarity in structure of the bridge hydrogens and the end hydrogens in $Al(BH_4)_3$ with those of diborane is obvious. The similarity of the heavy atom motions with those of boron trifluoride is not so obvious. Nevertheless if one makes crude allowance for the existence of the bridge hydrogens and consequently assumes that the bending and stretching of the heavy atom skeleton is much weaker in $Al(BH_4)_3$ than in BF_3, the analogy with BF_3 is very helpful.

Table 1. Infrared and Raman spectra for aluminum borohydride. Spectral measurements are reported in cm^{-1}

Raman (liquid)* (see Ref. 8)	Infrared* (solid at 100°K)	Infrared* (gas)	Assignment
2549	2544 (s)	2556 (s)	ν_{15} (e')
2473 (polarized)	----	----	ν_{1} (a_1')
----	2474 (s)	2491 (s)	ν_{16} (e')
2226 (v.w.)	2235 (m)	2220 (w)	?
----	2140 (w)	shoulder	ν_{11} (a_2'')
2969 (polarized)	----	----	ν_{2} (a_1')
----	2065 (m)	----	?
2010	2030 (s)	2031 (s)	ν_{17} (e')
1925	1920 (w)	1930 (w)	?
1885 (v.w.)	----	----	?
1521 (w)	1523 (s)	1504 (s)	ν_{18} (e')
1495 (polarized)	----	----	ν_{3} (a_1')
----	1455 (s)	overlapped	ν_{12} (a_2'')
----	1415 (s)	1420 (s)	? e'
1392	----	----	ν_{25} (e'')
----	----	1354	?
1149	----	----	ν_{26} (e'')
1116 (polarized)	----	----	ν_{4} (a_1')
1116	1104 (s)	1112 (s)	ν_{19} (e')
976	970 (m)	984 (m)	ν_{20} (e')
----	774 (m)	764 (w)	ν_{13} (a_2'')
602	600 (s)	607 (s)	ν_{21} (e')
510 (polarized)	----	----	ν_{5} (a_1')
318	334 (m)	326 (w)	ν_{22} (e')
----	221 (m)	----	ν_{14} (a_2'')
----	135 (w)	----	ν_{23} (e')

*Intensity designations are given in parenthesis - s = strong, m = medium, w = weak.

Table 2. Identification of the fundamental vibrations with symmetry species and type of vibration for aluminum borohydride. This table assumes that $Al(BH_4)_3$ belongs to the D_{3h} point group. For the D_3 point group the primes and double primes should be dropped.

	a_1' (Raman active)	a_1''	a_2'	a_2'' (infrared active)	e' (infrared and Raman active)	e'' (Raman active)
B-H stretch	ν_1	--	ν_8	---	ν_{15}, ν_{16}	---
B-H' stretch*	ν_2	--	---	ν_{11}	ν_{17}	ν_{24}
B-Al stretch	ν_5	--	---	---	ν_{21}	---
$\angle$B-H_2' deformation*	ν_3	--	---	---	ν_{18}	---
$\angle$B-H_2 deformation	ν_4	---	---	---	ν_{19}	---
$\angle$B-Al-B deformation	--	---	---	---	ν_{23}	---
B-H'-Al bridge shear*	--	---	---	ν_{12}	---	ν_{25}
B-H_2 rock	--	---	ν_9	---	ν_{20}	---
B-H_2 wag	--	---	---	ν_{13}	---	ν_{28}
Bridge wag or pucker	--	---	ν_{10}	---	ν_{22}	---
Bridge torsion	--	ν_6	---	---	---	ν_{26}
End torsion	--	ν_7	---	---	---	ν_{27}
Out-of-plane bend (B_3Al)	--	---	---	ν_{14}	---	---

*The prime above the H indicates a bridge hydrogen is involved.

The a_1' Species

Emery and Taylor[8] have shown that there are five polarized Raman transitions for $Al(BH_4)_3$ which must be the five a_1' species vibrations. The frequencies of all the B-H stretching vibrations are found to be approximately where one would predict if the analogy with the diborane molecule is valid. The Al-B stretching motion is expected to be somewhat below 600 cm^{-1} so that the polarized Raman line at 510 cm^{-1} must be assigned to that vibration. The remaining polarized Raman lines at 1495 cm^{-1} and at 1116 cm^{-1} must then be assigned respectively to the bridge deformation, ν_3, (alternatively called the symmetric bridge stretch) and the terminal BH_2 deformation, ν_4.

The a_2'' Species

Vibrations belonging to the a_2'' species are infrared active but do not appear in the Raman effect. In the vapor phase these transitions will correspond to parallel transitions for a symmetric top. If there are no complications due to hot bands, isotopic mixtures, etc. these bands should have band contours with widths of about 20 cm^{-1} in the vapor phase.

The bridge B-H stretching vibration (ν_{11}) is expected to be around 2200 to 2000 cm^{-1}. The band at 2235 cm^{-1} would be the obvious choice for this vibration except for the fact that there is a weak Raman line at the same frequency. Presumably this is an indication that this is an overtone or combination band (most likely $2\nu_4 = 2 \times 1116$ cm^{-1}). In the infrared spectrum there is a weak shoulder at about 2140 cm^{-1} for which there is no corresponding Raman line. In the solid this is seen as a well defined absorption maximum. We have assigned this as ν_{11}.

The out-of-plane vibration of the AlB_3 skeleton (ν_{14}) is expected to be the lowest frequency member of this symmetry species. This is probably the 221 cm^{-1} band observed in the infrared spectrum of the solid.

The band at 764 cm^{-1}, which for some reason is much stronger in the spectrum of the solid, is assigned to the BH_2 wagging motion (ν_{13}) although it is at a frequency somewhat lower than the corresponding vibrations in diborane.

The bridge shearing vibration, ν_{12}, will be somewhere around 1400 to 1500 cm^{-1}. It is rather arbitrarily assigned to the feature at 1455 cm^{-1} observed in the solid spectrum. None of these transitions corresponds to any feature reported for the Raman spectrum.

The e' Fundamentals

The e' species vibrations will be both infrared and Raman active. They will correspond to perpendicular bands in a symmetric top, consequently they will in general have broader band contours in the infrared spectrum of the vapor than was the case with the a_2'' vibrations.

The two-BH stretching vibrations are easily identified as the two strong infrared bands at 2556 cm^{-1} and 2491 cm^{-1} in the vapor. The strong, broad band observed at 2031 cm^{-1} in the infrared spectrum must be the bridge B'H' stretching vibration. The Raman transition at 2010 cm^{-1} in the liquid probably corresponds to this transition. The infrared and Raman bands at 607 cm^{-1} probably correspond to the B-Al stretching vibration (ν_{21}) in agreement with the assignment of the corresponding a_1' vibration at 510 cm^{-1}. The bridge BH_2' deformation or symmetric bridge stretching vibration, ν_{18}, is assigned to the strong and broad infrared band at 1504 cm^{-1} for which there is a corresponding weak Raman line at 1521 cm^{-1}. The terminal BH_2 deformation and rocking vibrations are assigned to the 1112 cm^{-1} and 984 cm^{-1} bands, respectively, by analogy with the corresponding vibrations in diborane.

Both the B-H'-Al puckering vibration (ν_{22}) and the B-Al-B deformation vibration (ν_{23}) are expected to be at very low frequencies. Only one low frequency Raman band remains (at 318 cm^{-1}). This probably corresponds to the infrared absorption at 334 cm^{-1} and is assigned to ν_{22}. The broad, weak feature observed in the infrared spectrum of the solid at about 135 cm^{-1} is assigned to ν_{23}. This would be too close to the exciting line to be observed in the Raman spectra.

The e" Species

The remaining intense Raman shifts which are not present in the infrared spectrum must be due to e" vibrations. The bridge shearing vibration is probably the band at 1392 cm^{-1}. The band at 1149 cm^{-1} is either a torsion or else the BH_2 wagging vibration, probably the former. The remaining torsion and the BH_2 wag are then unknown. The bridge B-H' stretch ν_{24} should be near 2000 cm^{-1} but we are unable to assign it.

Final Summary

Since they are inactive in both the Raman and infrared effects, neither the three a_2' vibrations nor the two a_1'' vibrations can be assigned on the basis of our present knowledge. We have also been unable to assign three of the e" vibrations. The remaining assignments are all compatible with the observed spectra with one exception. The infrared spectrum of the gas indicates that there is a broad absorption around 1400 cm^{-1}. The solid spectrum clearly shows three very strong absorptions between 1550 cm^{-1} and 1400 cm^{-1}. We can only assign two of these. The extra absorption seems to be much too high for assignment to anything but a bridge hydrogen motion. If the molecule had D_3 symmetry, this absorption would be assigned to ν_{25}. In the gas phase spectrum a Coriolis interaction between ν_{25} and ν_{18} is allowed according to Jahn's rule. Such a Coriolis interaction would cause ν_{25} to become infrared active at high rotational levels, but that will not explain the intensity in the solid state. A more satisfactory explanation would be that the extra peak is due to a combination or overtone which has a high intensity due to intensity borrowing through Fermi resonance.

In Table 3 we have given some of the fundamentals for $Al(BH_4)_3$ and $Al(BD_4)_3$ using the Raman measurements of Emery and Taylor in conjunction with our own infrared measurements on $Al(BH_4)_3$. The observation of six polarized Raman lines for $Al(BD_4)_3$ has been explained by Emery and Taylor as due to the appearance of an overtone through Fermi resonance with a fundamental. We would also like to point out that neither the D_{3h} nor the D_3 point group would predict two polarized Raman lines near 1500 cm^{-1} for $Al(BD_4)_3$ hence this observation gives absolutely no support to the D_3 model.

There are still a number of weaker absorption bands in the infrared spectrum. These are probably either overtone and combination bands, or else they are due to impurities. We have made no attempt to assign the overtone and combination bands since there are enough assigned and unassigned fundamentals to account for most of the features in several different ways.

Table 3. Infrared and Raman active fundamentals of aluminum borohydride and aluminum borodeuteride*.

Symmetry	Fundamental	$Al(BH_4)_3$ (cm^{-1})	$Al(BD_4)_3$ (cm^{-1})
a_1'	ν_1	2473	1810
	ν_2	2069	{1511, 1455}
	ν_3	1495	1092
	ν_4	1116	829
	ν_5	510	463
a_2''	ν_{11}	2140	----
	ν_{12}	1455	----
	ν_{13}	774	----
	ν_{14}	221	----
e'	ν_{15}	2549	1928
	ν_{16}	2474	----
	ν_{17}	2030	----
	ν_{18}	1523	----
	ν_{19}	1104	829
	ν_{20}	970	743
	ν_{21}	600	569
	ν_{22}	334	267
	ν_{23}	135	----
e"	ν_{24}	----	----
	ν_{25}	1392	----
	ν_{26}	1149	829?
	ν_{27}	----	----
	ν_{28}	----	----

*Data are for solid or liquid state; data on $Al(BD_4)_3$ are entirely due to Emery and Taylor (Ref. 8).

ASSIGNMENT FOR BERYLLIUM BOROHYDRIDE

General

The observed absorption frequencies and the assignments for beryllium borohydride are given in Table 4. Table 5 identifies the type of vibration corresponding to each fundamental. It should be remembered, of course, that no fundamental is purely of one type of vibration but is really a linear combination of many types of vibration with one type usually predominating. The infrared absorption spectrum is shown in Fig. 2. We have assumed that the molecule belongs to the D_{2d} point group. The individual assignments for that point group are discussed below. As an aid in making the assignments we have made use of the similarity between beryllium borohydride and both allene (H_2CCCH_2)[12] and diborane.[10]

Since the spectrum of the solid is quite different from that of the gas, the assignments for the gas phase will be discussed first. In the last part of this section we will discuss the implications of the solid state spectra.

As yet there seem to be no Raman measurements reported for $Be(BH_4)_2$. Consequently, we will only concern ourselves with the infrared active fundamentals which are of species b_2 and e.

b_2 Species Fundamentals

The fundamentals of the b_2 symmetry species will be parallel type bands in infrared absorption. That is, they will have a single Q branch flanked by P and R branches. A band contour calculation shows that for beryllium borohydride the parallel bands will be about 30 cm^{-1} in breadth. Similar calculations show that the perpendicular bands will generally be much broader, of the order of 100 cm^{-1}. The exact shape of the perpendicular bands is dependent on the value of ζ, but since ζ is almost never greater than 0.8, it is easy to show that the perpendicular bands will almost always be broader than the parallel bands. None of the bands in the spectrum of $Be(BH_4)_2$ show any trace of a Q-branch. This may be due to the presence of many hot bands due to very low vibrational frequencies. Such hot bands will have the effect of smearing out the spectrum to some extent.

There will be one B-H stretching vibration of b_2 species expected around 2600 cm^{-1}. The narrowest band in that region is at 2625 cm^{-1} and is attributed to this vibration. Similarly the

Table 4. Infrared absorption and assignments for gaseous beryllium borohydride.

Wavenumber* (cm^{-1})	Assignment
2625 (m)	ν_9 (b_2)
2530 (m)	ν_{14} (e)
2180 (m)	?
2130 (s)	ν_{15} (e)
2075 (m)	ν_{10} (b_2)
1997 (w)	?
1600 (m)	?
1550 (vs)	ν_{16} (e)
1242 (m)	ν_{12} (b_2)
1130 (w)	?
1020 (vs)	ν_{18} (e)
282 (w)	ν_{19} (e)

*Intensity is indicated as

vs = very strong, s = strong,

m = medium, w = weak.

Table 5. Identification of the fundamental vibrations with symmetry species and type of vibration for beryllium borohydride. This table assumes that the molecule belongs to the D_{2d} point group.

	a_1 (Raman active)	a_2	b_1 (Raman active)	b_2 (infrared and Raman active)	e (infrared and Raman active)
B-H stretch	ν_1	--	--	ν_9	ν_{14}
B-H' stretch	ν_2	--	--	ν_{10}	ν_{15}
B-Be stretch	ν_5	--	--	ν_{13}	---
$\angle BH'_2$ deformation	ν_3	--	--	ν_{11}	---
$\angle BH_2$ deformation	ν_4	--	--	ν_{12}	---
$\angle$B-Be-B bend	--	--	--	---	ν_{20}
bridge shear	--	--	--	---	ν_{16}
BH_2 rock	--	--	--	---	ν_{17}
BH_2 wag	--	--	--	---	ν_{18}
bridge wag or pucker	--	--	--	---	ν_{19}
bridge torsion	--	--	ν_7	---	---
end torsion	--	ν_6	ν_8	---	---

bridge B-H stretching fundamental is attributed to the relatively sharp feature at 2075 cm^{-1}. One BH_2 bridge deformation vibration is expected at about 1600 cm^{-1}. This is evidently hidden by the strong, broad features in that region which must be perpendicular vibrations. The terminal BH_2 deformation (ν_{12}) is probably the band at 1242 cm^{-1}. The Be-B stretching vibration is probably between 800 and 500 cm^{-1} but in the gas phase we have been unable to locate any absorption in that region. There is a strong band at 734 cm^{-1} in the solid phase spectrum, but it may be due to another vibration which has shifted downward in frequency in going from the gas phase structure to the solid phase structure.

The e Species Fundamentals

As mentioned in the previous section these vibrations will give rise to broad perpendicular type infrared absorption bands. The two B-H stretching vibrations are probably the broad features centered at about 2530 cm^{-1} and 2130 cm^{-1}. The bridge shearing vibration (ν_{16}) may be the sharper, but still very broad, absorption at 1550 cm^{-1}. The BH_2 wagging vibration (ν_{18}) by analogy with the allene molecule is probably the broad band centered at 1020 cm^{-1}.

The two remaining e fundamentals would be expected to occur at relatively long wavelengths. By analogy with diborane the bridge puckering vibration will probably be somewhat below 360 cm^{-1}. We would expect the B-Be-B bending vibration to be at an even lower frequency. Since none of the perpendicular bands show a trace of fine structure, there must be one or more vibrations of very low frequency. If sufficiently numerous, the hot bands will obscure the fine structure. For this reason we expect that there will be at least two fundamental vibrations below 300 cm^{-1}. The 282 cm^{-1} band is one of them, probably the puckering vibration, ν_{19}. The existence of a very weak absorption close to 180 cm^{-1} in the solid suggests that there may be another low vibration in the gas phase, but it is too weak to observe with a 10 cm pathlength. This would be the B-Be-B bending vibration, ν_{20}.

Solid Phase Spectra

In Fig. 2 the gas phase spectrum of beryllium borohydride can be compared with that of the solid phase. Table 6 gives the positions of the principal absorption features in the solid phase. The spectra in the solid and gas phases are so different that one is tempted to believe that they do not belong to the same molecular species. It was for that reason that experiments were made to be certain that the molecule has not undergone an irreversible change.

Table 6. Principal absorption features observed in the infrared spectrum of solid beryllium borohydride at about 100°K.

Wavenumber (cm^{-1})	Intensity
2514	medium
2456	medium
2340	strong
2120	strong
1997	weak
1552	strong
1457	very strong
1325	very strong
1131	medium
1010	weak
734	strong
408	medium
320	medium
180	very weak

As mentioned in the experimental section of this paper, experiments show that any change in the $Be(BH_4)_2$ molecule on condensation or sublimation is a reversible change since the same spectra are always obtained regardless of the past history of the sample. By way of contrast, the spectrum of $Al(BH_4)_3$ (shown in Fig. 1) was the same for both the solid and the gas phase (after allowing for the rotational transitions present in the gas phase).

In the solid phase the four B-H stretching vibrations seem to be merging. The lower frequency vibrations are shifted to higher frequencies in the solid while the high frequency vibrations are shifted to lower frequencies. This suggests that the BH_4 group is approaching the structure of the BH_4^- ion for which $Be(BH_4)_2$ might have two triply degenerate vibrations at nearly the same frequency. Such a supposition is supported by the fact that most of the other vibrations seem to be at lower wave numbers in the solid state although definite correlations are not yet possible. As the BH_4 group goes over to the ionic structure many of the internal vibrations of the covalent $Be(BH_4)_2$ molecule will become the lattice vibrations and librations of the ionic compound. Such motions would usually be expected to be at lower frequencies than the internal vibrations.

Although the change from a covalent form for $Be(BH_4)_2$ in the gas phase to a more nearly ionic form in the solid phase is quite unexpected, there are examples of even greater changes. For example, N_2O_5 has been shown to be covalent in the gas phase while the solid consists of NO_2^+ ions and NO_3^- ions.

It would be of particular interest to investigate the spectrum of $Be(BH_4)_2$ frozen in an inert matrix at very low temperatures. Under such conditions one would expect the molecule to retain the gas phase bonding, hence the gas phase spectrum should be obtained (without the rotational transitions, of course). Such matrix isolated spectra would probably have quite sharp absorption bands so that it might be possible to see individual peaks due to the absorption of both $Be(^{11}BH_4)_2$ and $Be(^{10}BH_4)(^{11}BH_4)$. By measuring the isotope shift, the assignments could be made with more confidence. Such an experiment is planned for the near future. The compound magnesium borohydride ($Mg(BH_4)_2$) may also show very similar behavior and should be studied.

BIBLIOGRAPHY

1. W. C. Price, J. Chem. Phys. 17, 1044 (1949).

2. J. Y. Beach and S. H. Bauer, J. Am. Chem. Soc. 62, 3440 (1940).

3. G. Silbiger and S. H. Bauer, J. Am. Chem. Soc. 68, 312 (1946).

4. R. A. Ogg, Jr. and J. D. Ray, Discussions Faraday Soc. 19, 239 (1955).

5. R. E. Williams, J. Inorg. and Nuclear Chem. 20, 198 (1961).

6. L. Banford and G. E. Coates, J. Chem. (1964) 5591.

7. Price, Longuet-Higgins, Young, and Rice, J. Chem. Phys. 17, 217 (1949).

8. A. R. Emery and R. C. Taylor, Spectrochimica Acta 16, 1455 (1960).

9. H. A. Gebbie and N. W. B. Stone, Infrared Physics 4, 85 (1964).

10. W. L. Smith and I. M. Mills, J. Chem. Phys. 41, 1479 (1964).

11. G. Herzberg, Infrared and Raman Spectra (D. Van Nostrand Co., New York, 1945).

12. J. Blanc, C. Brecher, and R. S. Halford, J. Chem. Phys. 36, 2654 (1962).

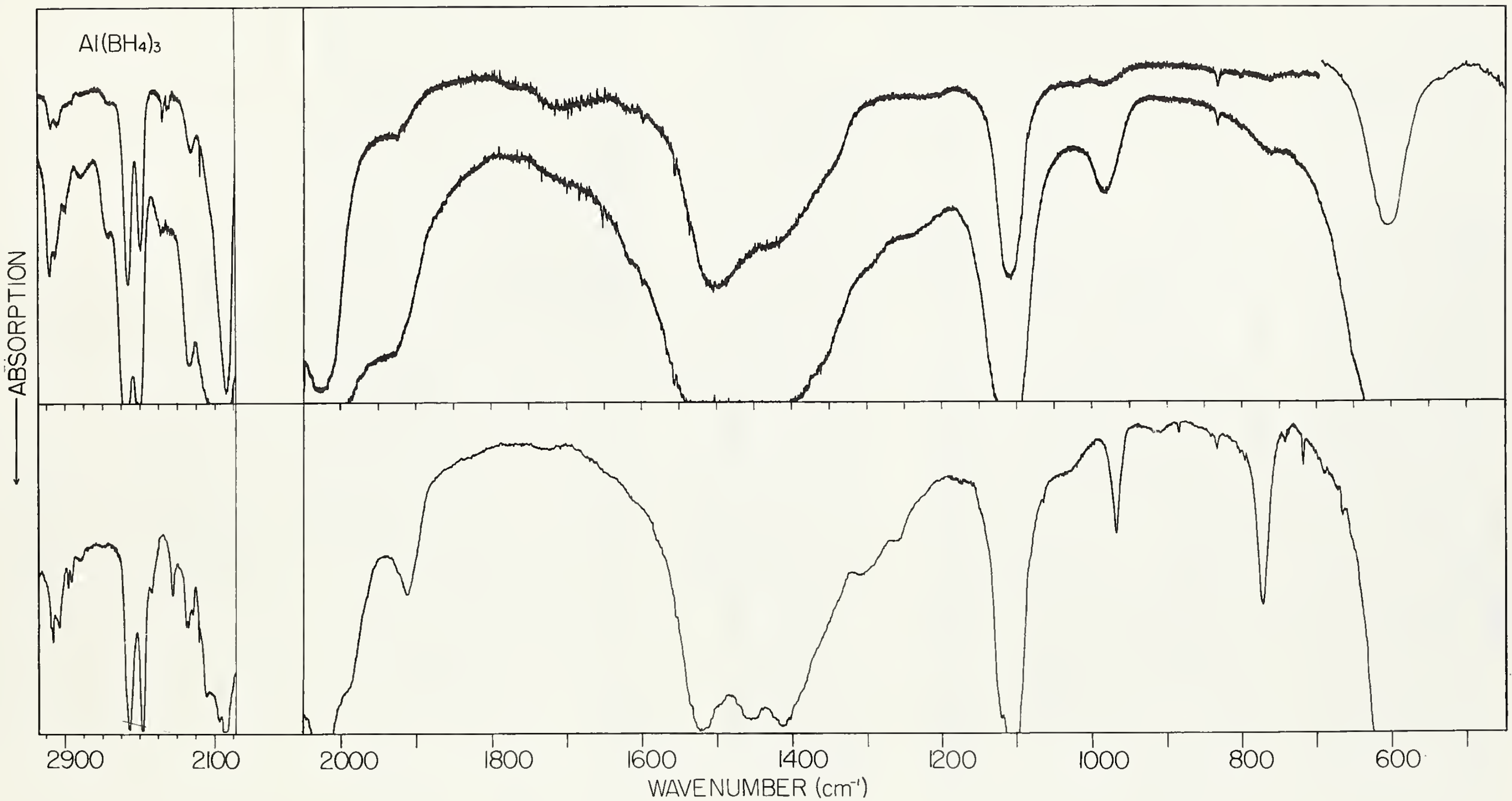

Figure 1 - The infrared spectrum of aluminum borohydride. The upper curve shows the gas phase spectrum with a pathlength of 10 cm and pressures of about 5 Torr and 30 Torr. The lower panel shows the solid phase spectrum at about 100°K.

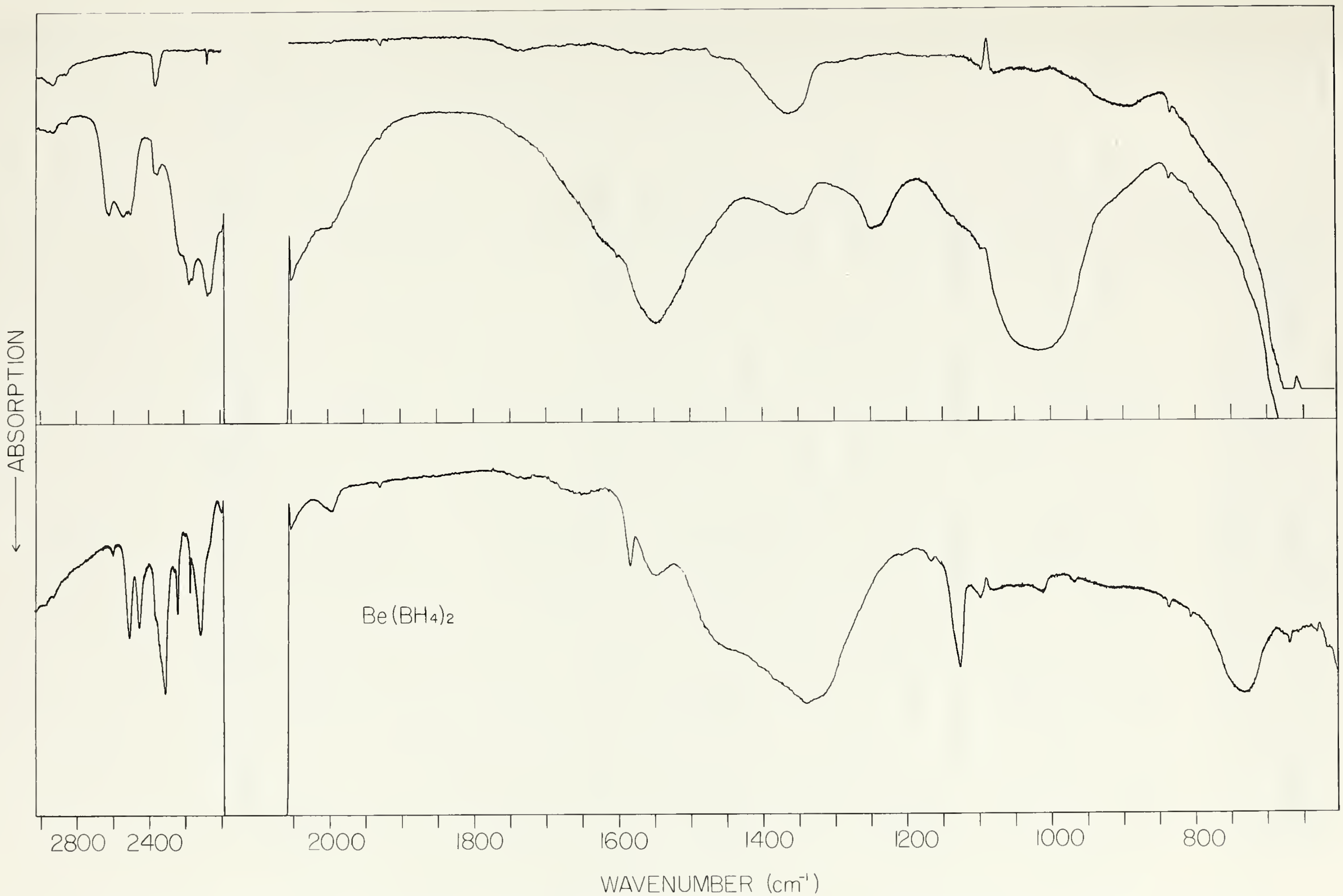

Figure 2 - The infrared spectrum of beryllium borohydride. The top curve is the background absorption of the gas cell. The middle curve is the absorption in the gas phase with a 9 cm pathlength and a pressure equal to the vapor pressure at 40°C. The lowest curve is the absorption of the solid at about 100°K.

Chapter 6

FORCE FIELDS FOR SOME SIMPLE INORGANIC FLUORIDES

S. Abramowitz and I. W. Levin

The Coriolis zeta constants of the degenerate modes of SiF_4, GeF_4, NF_3, PF_3, AsF_3, SF_6, and TeF_6 were determined from gas phase infrared band contour measurements. These Coriolis coupling data provided the necessary constraints for the unique determination of the harmonic force fields for the F_2, E, and F_{1u} symmetry species of the Group IV, V, and VI fluorides studied. The rotational distortion data which are functions of both the A and E symmetry species of the XF_3 molecules were found to be useful only in the case of NF_3. Experimental details and discussion of the results of these studies may be found elsewhere (1, 2, 3). The results of the studies together with the data used for computation may be found in Tables 1 – 5.

Table 1. The observed data for the Group IV tetrafluorides and the Group V trifluorides. $\Delta\nu_{P-R}$ represents the P-R separation in cm^{-1}. The frequencies are in cm^{-1}; the ζ_i are dimensionless. Values for the zeta sum rules are given.

	Observed frequency (cm^{-1})	$\Delta\nu_{P-R}$	ζ_i	$\Sigma\zeta_i$	Sum Rule
SiF_4					
ν_3	1030	11[a]	0.49		
ν_4	390	24[a]	-0.12	0.37	0.50
GeF_4					
ν_3	821.6	16	0.20		
ν_4	271	13	0.35	0.55	0.50
NF_3					
ν_1	1032				
ν_2	647				
ν_3	907	3	0.91		
ν_4	492	40	-0.96	-0.05	-0.09
PF_3					
ν_1	892				
ν_2	487				
ν_3	860	14	0.47		
ν_4	344	32	-0.65	-0.18	-0.15
AsF_3					
ν_1	740				
ν_2	336				
ν_3	702	14	0.31		
ν_4	262	26.7	-0.44	-0.13	-0.18

[a] S. Abramowitz, "Intermolecular Forces in Condensed Phases," Ph.D. thesis, Polytechnic Institute of Brooklyn, 1963.

Table 2. Structural data for the tetrafluorides and the trifluorides

Molecule	Bond length (Å)	Bond angle
SiF_4	1.55[a]	109°28′
GeF_4	1.67[b]	109°28′
NF_3	1.371[c]	102.1°
PF_3	1.52[d]	102°[f]
AsF_3	1.712[e]	102°

[a] H. Braune and P. Pinnow, Z. Physik. Chem. B35, 239 (1937).

[b] A. D. Gaunt, H. Mackle, and L. E. Sutton, Trans. Faraday Soc. 47, 943 (1951).

[c] J. Sheridan and W. Gordy, Phys. Rev. 79, 513 (1950).

[d] L. Pauling and L. O. Brockway, J. Am. Chem. Soc. 57, 2684 (1935).

[e] P. Kisliuk and S. Geschwind, J. Chem. Phys. 21, 828 (1953).

[f] Assumed.

Table 3. Force constants for the XF_3 and XF_4 molecules. The units are expressed in millidynes per angstrom.

Species	Force constant	NF_3	PF_3	AsF_3
A_1				
	$F_{11}=f_r+2f_{rr'}$	4.80±0.10		
	$F_{12}=2f_{\alpha r}+f_{\alpha r'}$	0.54±0.05		
	$F_{22}=f_\alpha+2f_{\alpha\alpha'}$	1.59±0.05		
E				
	$F_{33}=f_r-f_{rr'}$	2.92±0.12	4.74±0.06	4.20±0.05
	$F_{34}=f_{\alpha r}-f_{\alpha r'}$	0.17±0.04	0.12±0.03	0.00±0.05
	$F_{44}=f_\alpha-f_{\alpha\alpha'}$	1.02±0.06	0.46±0.01	0.30±0.02

Species	Force constant	CF_4 [a]	SiF_4	GeF_4
F_2				
	$F_{33}=f_r-f_{rr}$	6.22±0.25	6.58±0.10	5.79±0.05
	$F_{34}=-\sqrt{2}(f_{r\alpha}-f_{r\alpha'})$	-0.84±0.05	-0.38±0.05	-0.24±0.04
	$F_{44}=f_\alpha-f_{\alpha\alpha'}$	1.01±0.03	0.44±0.01	0.27±0.01

[a] Data for CF_4 taken from J. L. Duncan and I. M. Mills, Spectrochim. Acta 20, 1089 (1964).

Table 4. The observed data for the Group VI hexafluorides. $\Delta\nu_{P-R}$ represents the P-R separation in cm^{-1}. The frequencies are in cm^{-1}; the ζ_i are dimensionless. Values for the zeta sum rules and bond lengths are given.

	Observed Frequency cm^{-1}	$\Delta\nu_{P-R}$	ζ_i	$\Sigma\zeta_i$	Sum Rule	Bond Length Å
SF_6						
ν_3	947.5	2.9	-0.33			
ν_4	615.5	23.0	0.83			
				0.50	0.50	1.56[a]
TeF_6						
ν_3	751.0	12.5	0.18			
ν_4	326.5	11.0	0.28			
				0.46	0.50	1.84[a]

[a] L. O. Brockway and L. Pauling, Proc. Nat. Acad. Sci. 19, 68 (1933).

Table 5. Force constants for the XF_6 series. The values are expressed in millidynes/Å.

Species	Force Constant	SF_6	TeF_6
A_{1g}	$F_{11} = f_r + 4f_{rr} + f_{rr'}$	6.72	5.50
E_g	$F_{22} = f_r - 2f_{rr} + f_{rr'}$	4.64	5.08
F_{1u}	$F_{33} = f_r - f_{rr'}$	4.75 ± 0.15	4.98 ± 0.10
	$F_{34} = -2(f_{r\alpha} - f_{r\alpha''})$	-0.74 ± 0.03	-0.24 ± 0.05
	$F_{44} = f_\alpha + 2f_{\alpha\alpha} - 2f_{\alpha\alpha''} - f_{\alpha'''}$	1.10 ± 0.03	0.40 ± 0.05
F_{2g}	$F_{55} = f_\alpha + f_{\alpha\alpha'''} - 2f_{\alpha\alpha'}$	0.77	0.27
F_{2u}	$F_{66} = f_\alpha - 2f_{\alpha\alpha} + 2f_{\alpha\alpha''} - f_{\alpha\alpha'''}$	0.66	0.22

References

1. I. W. Levin and S. Abramowitz, J. Chem. Phys. 44, 2562 (1966).

2. S. Abramowitz and I. W. Levin, J. Chem. Phys., In Press.

3. I. W. Levin and S. Abramowitz, J. Chem. Phys. 43, 4213 (1965).

Chapter 7

MEASURED RELATIVE ENTHALPY AND DERIVED THERMODYNAMIC PROPERTIES OF ANHYDROUS CRYSTALLINE ALUMINUM TRIFLUORIDE, $A\ell F_3$, FROM 273 TO 1173 °K*

*This work was sponsored by the U.S. Air Force, Office of Scientific Research, under Order No. OAR ISSA 65-8.

Thomas B. Douglas and David A. Ditmars
Institute for Basic Standards, National Bureau of Standards
Washington, D. C.

(Abstract)

Using an ice calorimeter and a "drop" method, the enthalpy of a high-purity sample of anhydrous crystalline aluminum trifluoride, $A\ell F_3$, relative to that at 0°C (273.15 °K), was precisely measured at 18 temperatures starting at 50 °C and proceeding in 50-deg steps to 900 °C (1173.15 °K). Thirty additional enthalpy measurements between 450 and 453 °C revealed in this temperature interval a gradual transition. A simple general relation for the progress of transition when impurity is in solid solution is derived which fits the observed transition data and indicates a first-order transition temperature of 455 °C (728 °K). X-ray powder patterns on the sample, measured in the Crystallography Section of the NBS, established the existence of a phase transition by showing not only the known hexagonal structure at room temperature (even after violent quenching from above the transition temperature region) but a new, simple-cubic structure at 570 °C (843 °K). The smooth heat-capacity curve formulated from the data merges very smoothly with that representing published precise low-temperature data. The common thermodynamic properties were derived, and are tabulated at and above 298.15 °K, with extrapolation up to 1600 °K.

I. Introduction

During the past several years the National Bureau of Standards has conducted a comprehensive program of research to determine accurately the thermodynamic properties of substances that are important in high-temperature applications, such as chemical propulsion, yet for which accurate data have been lacking. Aluminum trifluoride, $A\ell F_3$, is a key example of prime importance in this area, as well as being one of the simplest of inorganic substances. In this research program its heat of formation at room temperature [1][1] and its vapor pressures at elevated temperatures [2] have been accurately measured, and a current thermodynamic study of the $A\ell F_3$-$A\ell C\ell_3$ system involving vaporization equilibrium is in progress. Reliable thermodynamic properties of the solid up to high temperatures are needed, not only to afford its heat of formation and reaction at such temperatures but also to interpret accurately such vaporization data as those just referred to.

---

[1] Numbers in brackets refer to literature references at the end of this paper.

Low-temperature heat-capacity measurements on $A\ell F_3$ (from 54 to 298 °K), believed to be accurate, have been reported by King [3]. Lyashenko [4] measured the high-temperature enthalpy from 290 to 1305 °K, but the results of O'Brien and Kelley [5] (298-1401 °K), while not differing seriously, have been regarded as somewhat more reliable.[2] However, Frank [6] noted systematic differences between the results of O'Brien and Kelley and those of others for two other substances measured at the same time as the aluminum fluoride, and, concluding that O'Brien and Kelley's recorded temperatures were too high by amounts up to 20° at 1373 °K, made an adjustment of their smoothed data on $A\ell F_3$ which leads to corrected heat capacities in poor agreement with King's.

Because of the need for accurate high-temperature enthalpies of $A\ell F_3$ and the uncertainties in the existing data, the measurements reported in the present paper were undertaken.

II. Sample

The sample of aluminum fluoride was supplied by the Alcoa Research Laboratories of the Aluminum Company of America, New Kensington, Pa., who had purified it by sublimation at 1050 °C in a nickel retort. It was in the form of a fine white crystalline powder.

---

[2] For one thing, Lyashenko failed to detect the transition found by O'Brien and Kelley.

Specimens were analyzed chemically for aluminum and fluorine in the Applied Analytical Research Section of the NBS, and spectrochemically for a number of heavier chemical elements by a general qualitative method in the Spectrochemistry Section of the NBS. The results of these analyses are given in table 1. Although the supplier thought that the sample would contain "a small amount of aluminum oxide and a spectroscopic amount of nickel," and no analysis for oxygen was made, the percentages of aluminum and fluorine in table 1 agree with the theoretical composition within the precision of analysis, and hence no corrections for impurity were made other than adjustment of the enthalpy near the transition temperature as described in Section IV.

III. Calorimetric Procedure and Thermal Data

The enthalpy measurements were made by a "drop" method employing a silver-core furnace and a precision ice calorimeter. The temperature of the furnace core, held constant to ±0.01 deg during a measurement, was measured up to 500 °C by a platinum resistance thermometer (ice-point resistance, about 25 ohms) that had been calibrated at the NBS and whose ice-point resistance was frequently rechecked. Above 500 °C the furnace temperatures were measured by two Pt--Pt-10% Rh thermocouples whose independent NBS calibrations were slightly adjusted to make them exactly concordant with the resistance thermometer below 500 °C when compared with it in the furnace of the enthalpy-measuring apparatus. The mass of the sample-plus-container was periodically checked for constancy during the series of measurements. Other details of the method and apparatus are discussed in extensive detail in an earlier publication [7].

All the enthalpy measurements were made on a single specimen ("sample") of aluminum fluoride weighing about 5 g. The cylindrical sample container (wall thickness, about 0.015 in.) was fabricated from annealed 99.9%-pure silver. One end was drawn down to a narrow neck, and, after introduction of the sample in the air atmosphere of a dry box at room temperature, was evacuated and filled with helium to a few torr pressure before pinching the neck and sealing it off with a torch.

The individual enthalpy measurements on the sample-plus-container, the mean corresponding net relative enthalpy of the sample at each temperature, and the deviations of these means from the empirical equations derived to represent them (Section V), are given in table 2 for the various furnace temperatures arranged in increasing order. Although the enthalpy measurements at a given furnace temperature are listed in chronological order, the temperatures themselves (particularly from 720 to 726 °K) are not. (The details of the empty-container measurements that were used to complete these calculations are given in another paper [8].) The tabulated values are those after correction for small unavoidable differences in parts of the sample and of the empty container. The vapor pressure of aluminum fluoride at the highest furnace temperature involved, 900 °C, is only about 1 torr, and it can be shown that at this temperature the heat of evaporation to saturate the 3 cm^3 of gas space in the sample container was negligible (about 0.003 cal).

The enthalpy values of table 2 are further treated in Sections IV and V.

IV. Phase Transition

It is known that $A\ell F_3$ undergoes a solid-state transition, though the authors are unaware that anyone has previously investigated the nature of the structural change. O'Brien and Kelley's [5] enthalpy measurements showed a small but definite enthalpy increment (150 cal/mole), and over so small a temperature interval that it was attributed to a first-order transition reported to occur at 727 °K.

The present investigation likewise shows a transition, and with a heat and temperature approximately in agreement with the above values; so, in addition to a series of enthalpy measurements at furnace temperatures every 50 deg from 273 to 1173 °K, a special series of enthalpy values was determined at closely spaced temperatures between 722 and 727 °K, in an effort to distinguish between a first- and second-order transition and also to define as closely as possible the true (equilibrium) transition temperature (or temperature range).

The individual unsmoothed enthalpy values obtained in this small range are shown in figure 1. The frame of reference which gives these points significance with regard to the transition is afforded by the two solid curves, calculated from the empirical equations derived later (Section V). The lower curve is part of that fitting closely all the values at and below 723 °K (except three values approached from higher temperatures, presently to be discussed), and the upper curve similarly fits closely the values from 773° to 1173 °K. Associating these two curves with, respectively, the low-temperature (α) and high-temperature (β) forms of $A\ell F_3$, it is natural to take the vertical position of any point between as a linear measure (within the experimental precision) of the fraction of the sample which has converted from α to β, provided the sample can be assumed to have always reverted to the same state when cooled in the calorimeter to 273.15 °K.

On this basis the intermediate points approached from lower temperatures ("by heating") indicate a gradual transition between 723 and 726 °K, and it is believed that these represent approximately true equilibrium because two pairs of points involved times at furnace temperature which differed by factors of 4 and 10, respectively, without appreciably changing the enthalpy found. On the other hand the points approached by cooling after first heating above 726 °K (i.e., "by cooling") lie along the upper curve. It is believed that in these latter cases the sample completely converted to the $\underline{\beta}$ form but failed to revert partially to $\underline{\alpha}$ (until cooled in the calorimeter). These points would then not correspond to phase equilibrium, and will not be discussed further.

It may be noted that the sharp upturn in the enthalpy between 723 and 726 °K, which would correspond to a hump in the heat-capacity curve, is in strong contrast to the gradual upward curvature of the heat-capacity curve over some 200 deg below 723 °K (fig. 3), so that the two phenomena appear to be of different origin. In order to throw light on the nature of the 3-deg upturn, X-ray powder patterns were taken in the Crystallography Section of the NBS on three specimens of the same aluminum-fluoride sample. These specimens were, respectively, one not used in the enthalpy measurements, one that had been heated well above 726 °K and then cooled slowly over two days to room temperature, and one that, after similar heating, had then been quenched in liquid nitrogen (i.e., much more drastically quenched than in the ice calorimeter). All three specimens gave at room temperature the same known pattern associated with the room-temperature hexagonal structure of $A\ell F_3$ [9]; it was therefore concluded that in all the enthalpy measurements the sample probably returned to this same form in the calorimeter, and consequently that the points in figure 1 are true measures of the relative enthalpy under the furnace conditions.

Additional X-ray patterns, however, were taken on one of the specimens while at approximately 840 °K, well above the transition region. In these cases the hexagonal pattern was missing, but was replaced by a new pattern interpreted as due to a primitive (simple) cubic structure having a cell dimension of 3.580 Å (or possibly some multiple thereof). (TaF_3 is said to show a similar structure at certain temperatures.) From this result it is concluded that the transition in $A\ell F_3$ at about 726 °K involves a change in crystal structure. And since a true second-order transition is compatible with only a continuous change in structure not readily conceivable for most pairs of well-defined structures, the conclusion is that pure $A\ell F_3$ exhibits a true first-order transition. A quantitative explanation of the observed 3-deg transition is offered below after postulating the presence of impurity soluble in both forms of $A\ell F_3$ and then treating the sample as a two-component system.

Two-component systems combining appreciable solid solubility with a first-order transition of one component are very common, and enthalpy data on some such systems have been interpreted in accordance with these characteristics with as much care as the very common treatment of premelting. However, no one treatment is equally appropriate in every case, as in each one approximations must be made that are consistent with the amount and quality of the information available. With this fact in mind, the following very simple treatment was developed for application to the present case, but obviously is more generally useful.

The situation tentatively assumed to exist is illustrated by the type of phase diagram shown in figure 2 (whose specific details are those subsequently derived for the present sample). For simplicity the principal component is assumed to be contaminated with a single component (which may be a combination of impurities in fixed ratio) whose overall mol fraction, N_2, is so small that the temperature-composition phase boundaries may be taken as straight lines in this region. Also for simplicity, maintenance of complete phase equilibrium is assumed. In the example illustrated, the impurity depresses the transition temperature of the pure substance, T_{tr}, to a finite temperature interval T_1 to T_2, the sample at any intermediate temperature T consisting of α and β phases of compositions N_2' and N_2'' respectively. Though in most known cases of this type the impurity does depress the transition temperature (as in fig. 2), some cases are known where this is elevated, but the following equations are equally applicable to both situations.

The two phase boundaries may be defined by

$$N_2' = A(T - T_{tr}); \tag{1}$$

$$N_2'' = B(T - T_{tr}) , \tag{2}$$

where $\underline{A}$ and $\underline{B}$ are constants. The limits of the two-phase temperature region are then obviously given by

$$T_1 = T_{tr} + N_2/A \;; \tag{3}$$

$$T_2 = T_{tr} + N_2/B \,. \tag{4}$$

If at temperature $\underline{T}$ each mol of the principal component is distributed with $\underline{n}'$ mol in the $\underline{\alpha}$ solid solution and $\underline{n}''$ mol in the $\underline{\beta}$ solid solution, the overall mol balance of each component gives the well-known "lever" relations; on assuming that $\underline{N_2}$, $\underline{N_2}'$, and $\underline{N_2}''$ are negligible compared to unity, these relations are

$$n' = \frac{N_2 - N_2''}{N_2' - N_2''} \;; \tag{5}$$

$$n'' = \frac{N_2' - N_2}{N_2' - N_2''} \,. \tag{6}$$

It is convenient to define a constant parameter $\underline{k}$ by

$$B/A = k. \tag{7}$$

From these equations then follow the two relations

$$n'' = \left[\left(\frac{T_2 - T}{T - T_1} \right) k + 1 \right]^{-1} \;; \tag{8}$$

$$T_{tr} = T_2 + \frac{T_2 - T_1}{k - 1} \,. \tag{9}$$

If ΔH_{tr} is the molal heat of transition, the molal enthalpy of the sample $n''\Delta H_{tr}$ at T in excess of that of the pure α phase may be calculated from eq (8), and eq (9) gives the transition temperature corrected for the impurity. A well-known relation[3] applicable to dilute solutions exhibiting

[3] See, for example, reference [10].

miscibility in both phases is, in the present notation (and with R as the gas constant),

$$\frac{N_2{}' - N_2{}''}{T - T_{tr}} = \frac{\Delta H_{tr}}{R T_{tr}{}^2} , \qquad (10)$$

and this may be combined with previous equations to give the amount of impurity in the sample, N_2, causing the transition over the interval T_1 to T_2:

$$N_2 = \frac{k(T_2 - T_1)\,\Delta H_{tr}}{(1-k)^2\, R T_{tr}{}^2} . \qquad (11)$$

If T_1, T_2, k, and ΔH_{tr} can be evaluated from the thermal data such as that shown in figure 1, eq (9) and (11) may be readily solved.

Close examination of eq (8) shows, however, that some measure of the curvature of the "excess enthalpy" curve in the transition region ($n''\Delta H_{tr}$ vs. T) is essential to assigning a value to k and hence using eq (9) and (11) significantly. If the impurity elevates the transition temperature ($T_{tr} < T_1$), then $k < 1$ and this curve is concave downward; but if the transition temperature is depressed ($T_{tr} > T_2$), then $k > 1$ and the curve is concave upward. In either event the curve begins (at T_1) and ends (at T_2) with finite positive slope.

The enthalpy values of figure 1 (excluding the points "by cooling"), though subject to apparently considerable scatter which is a result of the unusually small magnitude of the heat of transition and the correspondingly expanded scale of this plot[4], were deemed sufficiently numerous and

[4]Note that in figure 1 the total ordinate distance between the two solid curves is equivalent to only about 1.5 percent of the measured relative enthalpy which determines any one point.

interconsistent to apply the above relations. An approximation to the best fit to the data gave

$$\left.\begin{aligned} T_1 &= 723.2\ ^\circ K \\ T_2 &= 725.85\ ^\circ K \\ k &= 2.5 \end{aligned}\right\} , \qquad (12)$$

from which were calculated

$$\left.\begin{aligned} T_{tr} &= 727.6\ ^\circ K \\ N_2 &= 0.0004 \end{aligned}\right\} \qquad (13)$$

and the dashed curve drawn through the transition region in figure 1. This curve fits the points within their precision, and it may be added that a value $N_2 = 0.0004$ is plausible (e.g., if due to MgF_2, this would correspond to 0.01 weight % of Mg, which is consistent with table 1). This explanation of the observed transition data is thus regarded as acceptable, with the transition temperature of pure $A\ell F_3$ lying above 726 °K. Since the value derived above for the transition temperature must be considered uncertain by the order of one degree, it will be rounded to 728 °K for calculations on pure $A\ell F_3$.

V. Data-Smoothing; Derived Thermodynamic Functions

Pure aluminum fluoride was assumed to have a first-order transition at 728 °K, as derived in Section IV, and two separate empirical equations were derived by the method of least squares to fit the observed enthalpy values as functions of temperature below and above this transition temperature. In this fitting, only the mean enthalpy values (given equal weight) at temperatures exactly 50 degrees apart, from 323.15° to 1173.15 °K, were used[5]. After so trying several forms of equation to obtain the closest smooth fits, the equations selected were as follows (with the enthalpy in cal mol^{-1} deg^{-1} at *T* °K, relative to that of the *α* form at 273.15 °K).

[5] Except for 723.15 °K, in place of which the mean of the measurements at 721.89 and 722.13 °K was used.

α-$A\ell F_3$ (273-728 °K):

$$H_T - H_{273.15} = -6.34206T + 7.075295\,(10^{-2})\,T^2 - 8.28056\,(10^{-5})T^3 + 3.949522\,(10^{-8})\,T^4 - 2078.89 \quad (14)$$

β-$A\ell F_3$ (728-1173.15 °K):

$$H_T(\beta) - H_{273.15}(\alpha) = 22.13869T + 1.08571\,(10^{-3})\,T^2 + 2.1078\,(10^5)\,T^{-1} - 6899.86 \quad (15)$$

Smooth high-temperature thermodynamic functions of sluminum trifluoride that represent the present work and merge smoothly with those given by King's low-temperature heat capacities [3] are given in table 3 in terms of defined calories, and in the table in the Appendix in joules. As a step in generating this table (and particularly to evaluate $(H^\circ_{298.15}-H^\circ_0)$), a set of smooth thermodynamic functions was first evaluated from King's results alone, using a computer code which employs four-point Lagrangian interpolation and employing King's combination of Debye and Einstein functions[6] for temperatures below his range of measurement (below 51 °K).

[6] King states that this function fits his heat capacities to within 0.8 percent from 51 to 298 °K.

This procedure gave a Third-Law value for $\underline{S^\circ_{298.15}}$ of 15.893 cal deg^{-1} mol^{-1} (King gave 15.89 ±0.08) and $C^\circ_{p(298.15)}$ = 17.958 cal deg^{-1} mol^{-1} (King's value is 17.95). Since eq (14) gives a virtually identical value for $C^\circ_{p(298.15)}$, 17.952, and nearly the same temperature derivative of heat capacity at this temperature[7], this equation was used without adjustment

[7] This excellent agreement is somewhat fortuitous, as may be noted from the slight trend of deviations from eq (14) shown for the first two temperatures in the last column of table 2.

to generate the thermodynamic functions from 298.15 °K to the transition temperature. Above the transition temperature eq (15) was used, the necessary integration constants being required to be consistent with the heat of transition, 135.2 cal mol^{-1}, given by the difference of eq (14) and (15) at the transition temperature, 728 °K.

VI. Discussion

The heat capacities of α- and β-$A\ell F_3$ above 250 °K are shown as functions of temperature in figure 3. For each form the solid curve, which represents the smoothed results of the present work (eq (14) or (15), or table 3), lies between that for O'Brien and Kelley's original work [5] and that for their results as adjusted by Frank [6]. King's [3] values merge very smoothly with the authors' curve and nearly as well with O'Brien and Kelley's, but definitely not with Frank's. Furthermore, the authors' curve for the β form is closer to O'Brien and Kelley's than to Frank's. A conclusion from the present work is, therefore, that Frank's corrections are completely invalid near room temperature and of doubtful value at the higher temperatures. (Lyashenko's [4] values were not available for inclusion in figure 3, but O'Brien and Kelley [5] state that his enthalpies are in fair agreement with theirs, with an average deviation of about 0.8 percent from 298 to 1100 °K.)

Just previous to the authors' measurements on $A\ell F_3$ they made checks on the calorimetric apparatus by repeating measurements of the enthalpy of Calorimetry-Conference standard-sample synthetic sapphire ($A\ell_2O_3$) at 373, 773, and 1173 °K relative to 273 °K. At all these temperatures the agreement with earlier work at the NBS using the same sample and the same apparatus was within 0.2 percent, which is within the present precision at 373 and 773 °K but slightly outside it at 1173 °K. Because the calorimetric apparatus used to measure $A\ell F_3$ was very recently used also to measure $BeO \cdot A\ell_2O_3$ and $BeO \cdot 3A\ell_2O_3$ over the same temperature range and with the same high precision, the authors feel that their general discussion of accuracy for the latter two substances [8,11] are equally applicable to $A\ell F_3$. The actually observed enthalpy of the sample very near the transition temperature is, of course, subject to additional uncertainty owing to the possibility of incomplete phase equilibrium, but for other temperatures this introduces no uncertainty into the enthalpy and very little into the entropy.

The gradual upturn of the heat-capacity curve for about 200 deg below the transition temperature is interesting (figure 3). Many solids show this behavior below their melting points or transition temperatures, and it is usually attributed to some type of disorder (of which lattice vacancies form a special case). Despite the X-ray diffraction results summarized in Section IV, not enough structural data are presently available on $\underline{\beta}$-$A\ell F_3$ to suggest how the lattice may tend to rearrange near the transition temperature.

The authors wish to acknowledge the particularly helpful contributions of the following persons. George Long, of the Alcoa Research Laboratories, Aluminum Company of America, furnished the sample. It was analyzed by members of the National Bureau of Standards: for aluminum by E. June Maienthal, for fluorine by Rolf A. Paulson, and spectrochemically by Elizabeth K. Hubbard. Howard E. Swanson, also of the NBS, carried out the X-ray examinations and made the structural interpretations of them.

VII. References

[1] E. S. Domalski and G. T. Armstrong, J. Research NBS 69A (Physics and Chemistry), 137 (1965).

[2] R. F. Krause, Jr., T. B. Douglas, and A. C. Victor, unpublished work.

[3] E. G. King, J. Amer. Chem. Soc. 79, 2056 (1957).

[4] V. S. Lyashenko, Metallurg. (USSR) 10, 85 (1935).

[5] C. J. O'Brien and K. K. Kelley, J. Amer. Chem. Soc. 79, 5616 (1957).

[6] W. B. Frank, J. Phys. Chem. 65, 2081 (1961).

[7] G. T. Furukawa, T. B. Douglas, R. E. McCoskey, and D. C. Ginnings, J. Research NBS 57, 67 (1956) RP2694.

[8] D. A. Ditmars and T. B. Douglas, publication pending.

[9] F. Hanic, K. Matiasovsky, D. Stempelova, and M. Malinovsky, Acta Chim. Acad. Sci. Hung. 32, (No. 3), 309 (1962).

[10] S. Glasstone, Textbook of Physical Chemistry, 2nd ed., D. Van Nostrand Co., Inc., New York, 1944 (p. 650, eq (45)).

[11] D. A. Ditmars and T. B. Douglas, publication pending.

Table 1. Chemical composition of the sample of aluminum trifluoride as determined by chemical and qualitative spectrochemical analysis.

Element	Percentage by weight		
	Found		Theoretical
	Individual analysis	Mean	
Al	32.13 32.15 32.17	32.15	32.13
F	68.00 67.66 67.61	67.76	67.87
Mg	0.01 - 0.1		0
Ca, Cu, Fe, Mn, Ni, Si	0.001 - 0.01[a]		0
Cr, V	0.0001 - 0.001[a]		0
Ag, As, Au, B, Ba, Be, Bi, Cd, Ce, Co, Ga, Ge, Hf, Hg, In, Ir, La, Mo, Nb, Os, P, Pb, Pd, Pt, Rh, Ru, Sb, Sc, Sn, Sr, Ta, Te, Th, Ti, Tl, U, W, Y, Zn, Zr	Undetected		0

[a] For each of the elements listed.

Table 2. High-temperature enthalpy measurements on aluminum trifluoride, $A\ell F_3$.

Furnace temperature $\underline{T}$[a]	Measured heat (net for sample)[b,c,e]	$H_T - H_{273.15}$ of $A\ell F_3$[c,d] Individual measurement[e]	Mean observed	Mean observed — smoothed[f]
°K	cal	cal mol^{-1}	cal mol^{-1}	cal mol^{-1}
323.15	53.77	898.7	899.7	+ 3.2
	53.91	901.0		
	53.81	899.4		
373.15	112.10	1873.5	1871.8	+ 2.2
	112.03	1872.3		
	111.87	1869.7		
423.15	173.34	2896.9	2894.4	- 4.1
	173.08	2892.7		
	173.15	2893.7		
473.15	237.16	3963.5	3965.0	- 3.2
	237.29	3965.7		
	237.30	3965.9		
523.15	303.13	5066.1	5069.6	- 0.1
	303.48	5071.9		
	303.41	5070.7		
573.15	371.40	6207.0	6206.8	+ 6.8
	371.37	6206.5		
623.15	440.35	7359.4	7363.2	+ 1.3
	440.66	7364.5		
	440.72	7365.6		
673.15	511.86	8554.4	8556.7	- 7.3
	511.98	8556.4		
	512.15	8559.2		
719.78	591.90[g]	9892.2[g]	- - -	
721.89	585.72	9788.9	- - -	+ 2.9
722.13	586.43	9800.8	- - -	
722.16	595.94[g]	9959.6[g]	- - -	See figure 1.
723.06	597.59[g]	9987.1[g]	- - -	
723.59	588.48	9834.9	- - -	
723.76	597.57[g]	9986.9[g]	- - -	
723.77	588.79	9840.1	- - -	
723.84	590.02	9860.6	- - -	
723.90	589.89	9858.6	- - -	
723.91	596.93[g]	9976.1[g]	- - -	
724.04	590.38	9866.8	- - -	
724.30	590.97	9876.5	- - -	
724.33	592.02	9894.1	- - -	
724.40	597.30[g]	9982.3[g]	- - -	
724.52	591.50	9885.4	- - -	
724.80	592.67	9904.9	- - -	
724.98	593.95	9926.4	- - -	
725.18	596.09	9962.2	- - -	
725.20	595.39	9950.5	- - -	
725.24	596.21	9964.1	- - -	
725.27	595.94	9959.6	- - -	
725.31	599.75[g]	10023.3[g]	- - -	
725.31	596.55	9969.7	- - -	
725.38	596.45	9968.1	- - -	

Table 2 (continued) (HEADINGS RESPECTIVELY AS ON PREVIOUS PAGE)

725.44	597.47	9985.2	- - -	See figure 1.
725.54	597.92	9992.6	- - -	
725.60	598.86	10008.4	- - -	
725.70	599.24	10014.8	- - -	
725.89	599.79	10024.0	- - -	
726.08	600.65	10038.3	- - -	
726.64	601.43	10051.4	- - -	
733.00	610.24	10198.7	- - -	(0.0)
742.00	622.96	10411.2	- - -	(+2.3)
763.06	652.70	10908.2	- - -	(+6.5)
	666.46	11138.1		
773.15	666.78	11143.5	11140.4	+ 2.2
	666.55	11139.7		
783.22	680.10	11366.2	- - -	(−8.5)
793.31	694.46	11606.2	- - -	(−5.8)
803.50	707.81	11829.2	- - -	(−22.7)
812.99	722.20	12069.8	- - -	(− 5.7)
818.07	729.56	12192.7	- - -	(− 2.7)
820.84	732.37	12239.6	- - -	(−21.2)
	737.07	12318.3		
823.15	736.68	12311.8	12315.0	- 0.3
	736.88	12315.0		
873.15	807.44	13494.3	13494.0	- 5.7
	807.40	13493.6		
	879.00	14690.2		
923.15	879.06	14691.2	14691.8	+ 0.8
	879.23	14694.1		
	950.92	15892.3		
973.15	950.74	15889.2	15891.1	+ 1.9
	950.90	15891.8		
	1023.49	17105.0		
1023.15	1023.11	17098.7	17099.9	+ 6.0
	1022.96	17096.1		
	1094.81	18296.9		
1073.15	1095.07	18301.3	18300.6	- 4.5
	1095.21	18303.6		
	1168.19	19523.4		
1123.15	1167.89	19518.3	19521.1	- 1.4
	1168.09	19521.7		
	1241.33	20745.6		
1173.15	1241.58	20749.8	20747.1	+ 1.0
	1241.34	20745.8		

[a] International Temperature Scale of 1948, as modified in 1954. 0°C = 273.15 °K.

[b] Sample mass = 5.0248g.

[c] cal (defined) = 4.1840 J.

[d] Molecular weight = 83.9767.

[e] In calculating the net heat due to the sample, the gross heat was decreased by the smoothed empty-container heat calculated from the equation

$$H_T - H_{273.15} = 0.76152\ (T-273.15) + 2.3649(10^{-5})(T-273.15)^2 + 0.42246(10^{-7})(T-273.15)^3 - 8.9987\ [(T-273.15)/T]$$

cal at t °K.

The observed values which this equation represents are given in table 3 of reference [8].

[f] The smoothed values below 728 °K were calculated from eq (14), and those above 728 °K, from eq (15).

[g] In determining the enthalpy values so indicated in columns 2 and 3, the final sample temperature (column 1) was approached by cooling after first heating above 726 °K. In determining all other enthalpy values in this table, the final sample temperature was approached by heating only.

Table 3. Thermodynamic functions for aluminum trifluoride, AlF_3, solid phases

(in terms of defined calories per mol)

(1 cal = 4.1840 J; T°K = t°C + 273.15; 1 mol = 83.9767g.)

T	C_p^o	$(H^o-H_0^o)$	$(H^o-H_0^o)/T$	S^o	$-(G^o-H_0^o)$	$-(G^o-H^o)/T$
°K	cal deg^{-1} mol^{-1}	cal mol^{-1}	cal deg^{-1} mol^{-1}	cal deg^{-1} mol^{-1}	cal mol^{-1}	cal deg^{-1} mol^{-1}
			Alpha Phase			
298.15	17.958	2778.9	9.320	15.893	1959.5	6.573
300	18.018	2812.2	9.374	16.004	1989.1	6.630
325	18.832	3273.0	10.071	17.479	2407.8	7.408
350	19.527	3752.8	10.722	18.901	2862.6	8.179
375	20.120	4248.6	11.329	20.269	3352.4	8.940
400	20.624	4758.0	11.895	21.584	3875.6	9.689
425	21.055	5279.2	12.422	22.848	4431.1	10.426
450	21.427	5810.3	12.912	24.062	5017.6	11.150
475	21.755	6350.2	13.369	25.230	5633.9	11.861
500	22.054	6897.8	13.796	26.353	6278.7	12.557
550	22.624	8014.8	14.572	28.482	7650.3	13.910
600	23.255	9161.2	15.269	30.476	9124.6	15.207
650	24.066	10343.	15.913	32.368	10696.	16.455
700	25.175	11573.	16.533	34.190	12360.	17.657
728	25.971	12289.	16.880	35.193	13332.	18.314
			Beta Phase			
728	23.322	12424.	17.066	35.378	13332.	18.314
750	23.392	12938.	17.250	36.074	14118.	18.824
800	23.546	14111.	17.639	37.588	15959.	19.949
850	23.693	15292.	17.991	39.020	17875.	21.029
900	23.833	16480.	18.312	40.379	19860.	22.067
950	23.968	17675.	18.606	41.671	21912.	23.065
1000	24.099	18877.	18.877	42.904	24027.	24.027
1050	24.227	20085.	19.129	44.082	26201.	24.953
1100	24.353	21300.	19.363	45.212	28434.	25.849
1150	24.476	22520.	19.583	46.298	30722.	26.715
1200	24.598	23747.	19.790	47.342	33062.	27.552
1250	24.718	24980.	19.985	48.349	35455.	28.364
1300	24.837	26219.	20.169	49.320	37896.	29.151
1350	24.954	27464.	20.344	50.260	40387.	29.916
1400	25.071	28715.	20.511	51.170	42923.	30.659
1450	25.187	29971.	20.670	52.051	45502.	31.381
1500	25.302	31233.	20.822	52.907	48128.	32.085
1550	25.417	32501.	20.968	53.739	50795.	32.771
1600	25.531	33775.	21.109	54.547	53501.	33.438

H_0^o is the enthalpy of the α form at 0°K (and 1 atm pressure). Values for temperatures higher than 1150 °K are by extrapolation beyond the measuring range.

Appendix. Thermodynamic functions for aluminum trifluoride, $A\ell F_3$, solid phases

(in terms of joules per mol)

($T°K = t°C + 273.15$; 1 mol = 83.9767g.)

T	C_p^o	$(H^o-H_0^o)$	$(H^o-H_0^o)/T$	S^o	$-(G^o-H_0^o)$	$-(G^o-H_0^o)/T$
°K	J deg^{-1} mol^{-1}	J mol^{-1}	J deg^{-1} mol^{-1}	J deg^{-1} mol^{-1}	J mol^{-1}	J deg^{-1} mol^{-1}
			Alpha Phase			
298.15	75.136	11627.	38.996	66.495	8198.5	27.498
300	75.387	11766.	39.221	66.961	8322.4	27.740
325	78.793	13694.	42.137	73.132	10074.	30.995
350	81.701	15702.	44.861	79.082	11977.	34.221
375	84.182	17776.	47.401	84.805	14026.	37.405
400	86.291	19907.	49.769	90.307	16216.	40.539
425	88.094	22088.	51.974	95.596	18540.	43.622
450	89.651	24310.	54.024	100.68	20994.	46.652
475	91.023	26569.	55.936	105.56	23572.	49.626
500	92.274	28860.	57.722	110.26	26270.	52.538
550	94.659	33534.	60.969	119.17	32009.	58.199
600	97.299	38330.	63.885	127.51	38177.	63.626
650	100.69	43275.	66.580	135.43	44752.	68.848
700	105.33	48421.	69.174	143.05	51714.	73.877
728	108.66	51417.	70.626	147.25	55781.	76.626
			Beta Phase			
728	97.579	51982.	71.404	148.02	55781.	76.626
750	97.874	54133.	72.174	150.93	59070.	78.760
800	98.519	59040.	73.802	157.27	66772.	83.467
850	99.130	63982.	75.274	163.26	74789.	87.985
900	99.716	68952.	76.617	168.95	83094.	92.328
950	100.28	73952.	77.848	174.35	91680.	96.504
1000	100.83	78981.	78.981	179.51	100530.	100.53
1050	101.37	84036.	80.036	184.44	109620.	104.40
1100	101.89	89119.	81.015	189.17	118970.	108.15
1150	102.41	94224.	81.935	193.71	128540.	111.78
1200	102.92	99357.	82.801	198.08	138330.	115.28
1250	103.42	104520.	83.617	202.29	148340.	118.67
1300	103.92	109700.	84.387	206.35	158560.	121.97
1350	104.41	114910.	85.119	210.29	168980.	125.17
1400	104.90	120140.	85.818	214.10	179590.	128.28
1450	105.38	125400.	86.483	217.78	190380.	131.30
1500	105.86	130680.	87.119	221.36	201370.	134.24
1550	106.34	135980.	87.730	224.84	212530.	137.11
1600	106.82	141310.	88.320	228.22	223850.	139.90

H_0^o is the enthalpy of the $\underline{\alpha}$ form at 0°K (1 atm pressure). Values for temperatures higher than 1150 °K are by extrapolation beyond the measuring range.

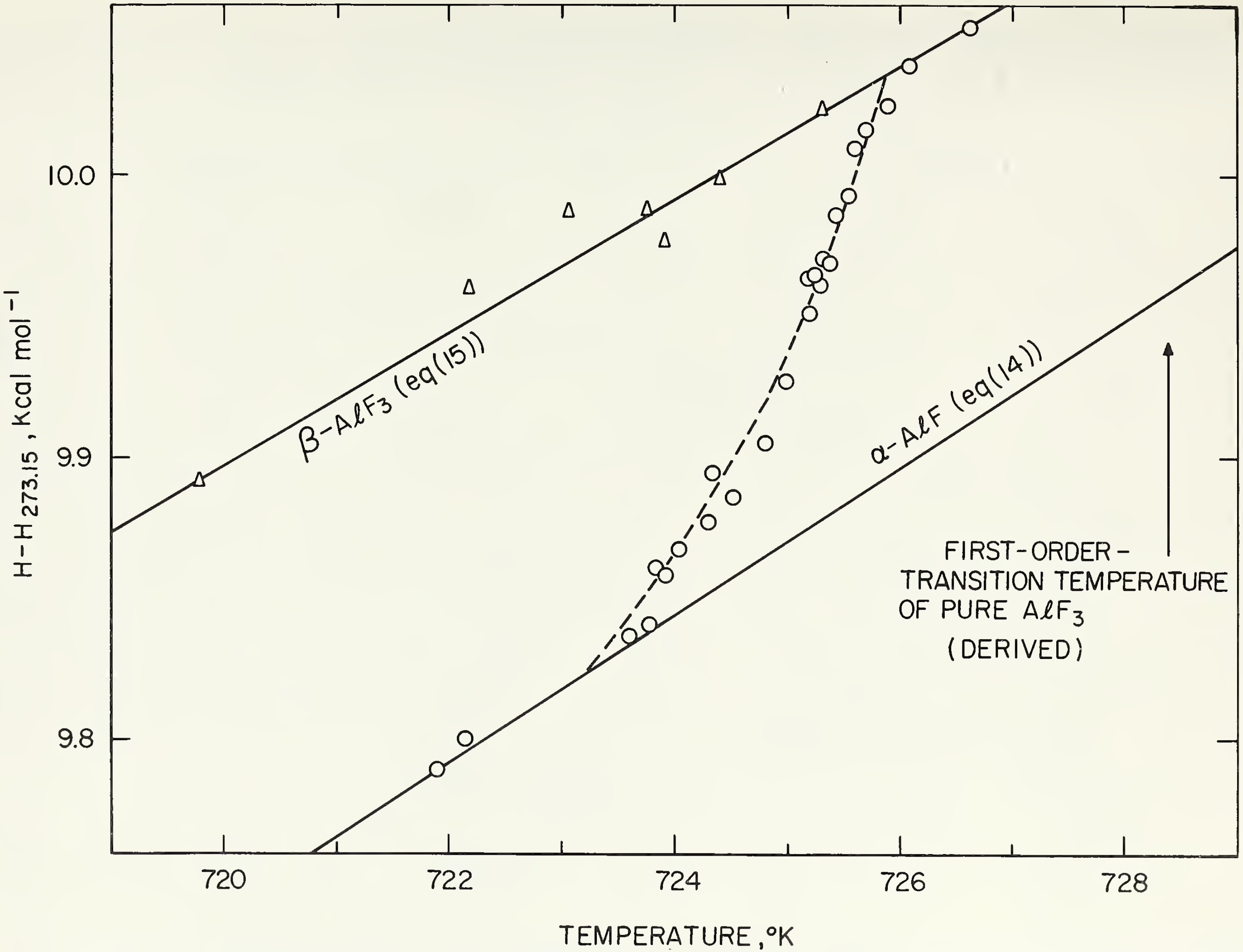

Figure 1. Observed enthalpy of the sample of aluminum fluoride near the transition temperature. (O, temperature approached by heating only; Δ, temperature approached by cooling after first heating above 726°K. For the derivation of the dotted curve, see text.)

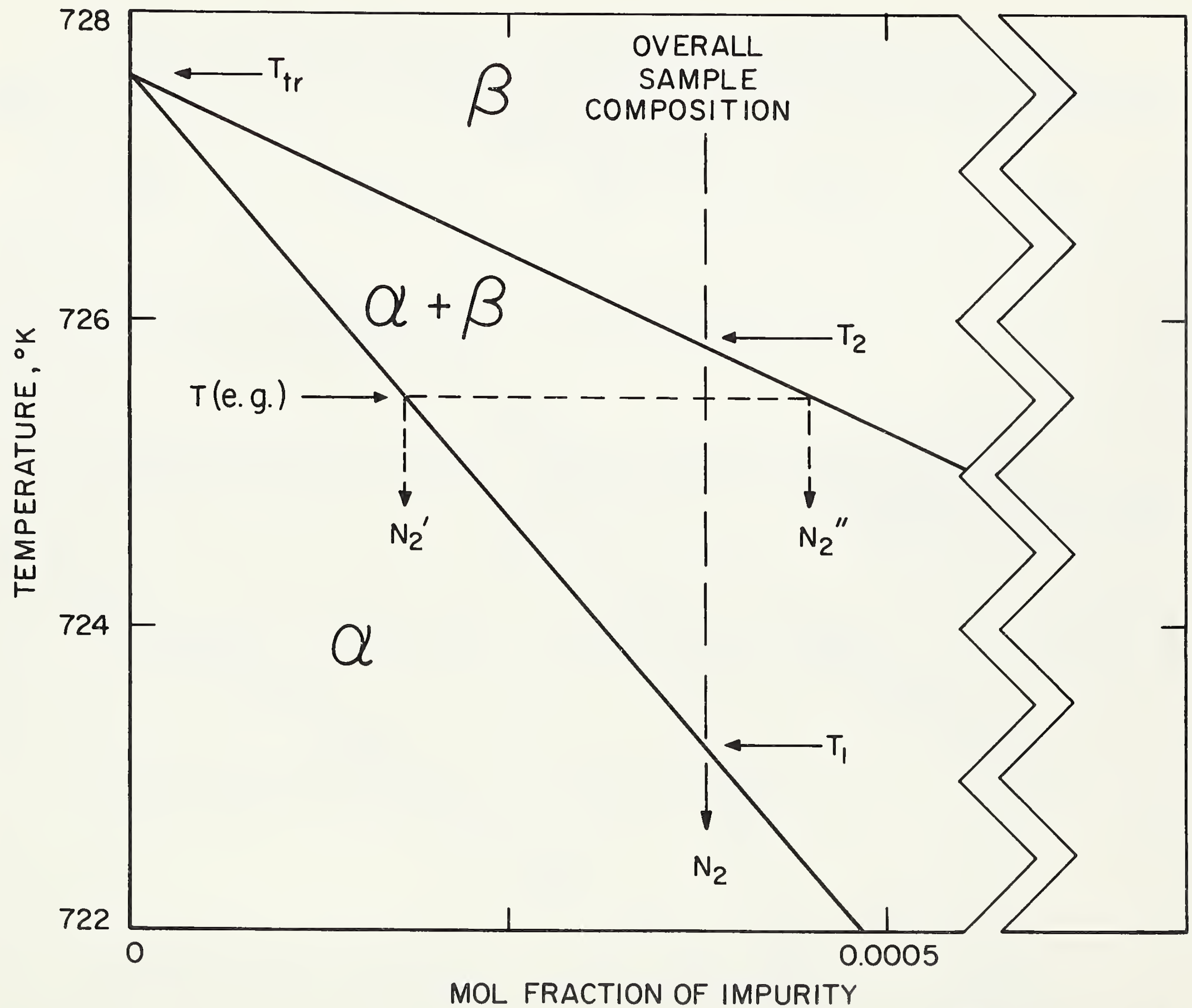

Figure 2. Phase-diagram representation of the transition of the sample of aluminum fluoride as affected by impurity. (See text for definitions of symbols.)

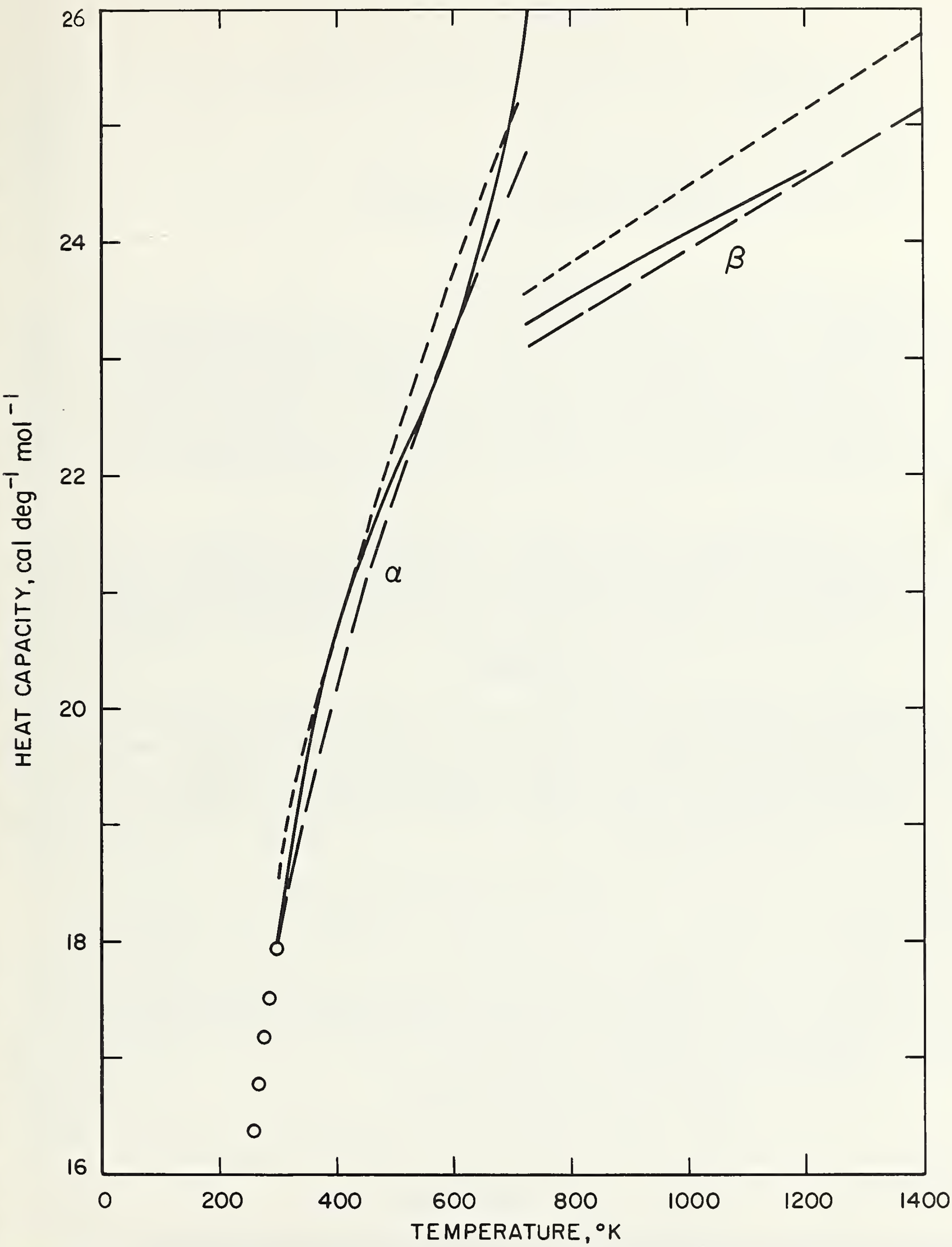

Figure 3. Heat capacity of α- and β-AℓF$_3$. (The curves represent smoothed values. O, King [3]; —, this work; — —, O'Brien and Kelley [5]; ----, O'Brien and Kelley as adjusted by Frank [6].)

Chapter 8

THE HEATS OF DECOMPOSITION OF $NaClO_4$ AND $AgClO_4$

by

A. A. Gilliland and D. D. Wagman
National Bureau of Standards
Washington, D.C. 20234

I. INTRODUCTION

The values for the heats of formation of most inorganic perchlorates have been based on values obtained for $KClO_4$(c) by thermal decomposition to KCl(c) and O_2(g). Vorob'ev et al [1] have reported a value of -2.55 ±0.18 kcal/mol for the heat of decomposition of $KClO_4$(c), whereas the value obtained in this laboratory was -0.96±0.08 kcal/mol [2]. Vorob'ev also reported a value of -7.70±0.28 kcal/mol for the heat of decomposition for $NaClO_4$(c). This value leads to a difference in the heats of formation between $KClO_4$ and $NaClO_4$ which agrees with that reported in [3].

Because of the interest in the data on perchlorates we have now measured the heats of thermal decomposition of $NaClO_4$(c) and $AgClO_4$(c) and have also used heat of solution calorimetry to measure the differences in the heats of formation of the three perchlorates $KClO_4$, $NaClO_4$, and $AgClO_4$.

II. MATERIALS

$AgClO_4$(c) was prepared by the addition of a slight excess of Ag_2O(c) to aqueous $HClO_4$. After filtering off the excess oxide, the solution was evaporated to dryness at 140°C, the residue ground up and dried in a vacuum dessicator under an infrared lamp. Analysis by precipitation of silver as AgCl corresponded to 99.64% of the theoretical yield. The principal impurity is assumed to be H_2O.

$NaClO_4$(c) was prepared by the addition of aqueous perchloric acid to Na_2CO_3 followed by intensive drying at 350-380°C. Analysis by the Analytical Chemistry Division indicated 0.15% water and 0.01% of chloride and chlorate.

The NaCl(c) and KCl(c) were recrystallized from reagent-grade materials and dried at 140°C. All materials were stored over anhydrous $Mg(ClO_4)_2$, and a large dry-box was used to transfer samples of $AgClO_4$ and $NaClO_4$ to avoid additional absorption of atmospheric water vapor.

III. UNITS AND CONSTANTS

All values are reported in both joules and calories; the defining relation is:

$$1 \text{ calorie(cal)} = 4.1840 \text{ joules (J)}.$$

Molecular weights are calculated on the basis of the 1961 International Table of Atomic Weights, based on $C^{12} = 12$.

IV. THERMAL DECOMPOSITION

The thermal decomposition of $NaClO_4$ and $AgClO_4$ was measured using apparatus and procedures similar to that described in [4]. The upper crucible, containing the perchlorate, was covered with a piece of platinum gauze supported on a platinum wire loop. This cover effectively prevented splattering of the crucible contents during the decomposition. The samples of perchlorates ranged from 1 to 3 grams; the benzoic acid pellets, placed in the lower crucible, were approximately 0.5 g for the $AgClO_4$ experiments, and about 1.0 g for the $NaClO_4$ decompositions.

The calorimeter system was calibrated with benzoic acid Standard Sample 39h, the same material that was used for the auxiliary combustion pellets. Because of the deliquescent nature of the perchlorates, no liquid water was added to the bomb for the calibration or the decomposition experiments. Appropriate corrections were applied. The amount of CO_2 produced by the combustion of the benzoic acid was determined by absorption in Ascarite. The ratio of the mass of CO_2 collected to that calculated from the amount of acid burned was generally greater than 0.9995. The results of the calibration experiments are given in Table I.

In each decomposition experiment the solid reaction product was analyzed to determine the completeness of reaction and to make the necessary corrections. In the $NaClO_4$ experiments, analysis for chloride indicated that decomposition was complete in all cases. The $AgClO_4$ decomposition products usually showed presence of small amounts of metallic silver and unreacted $AgClO_4$. The bomb residue was extracted with H_2O and the dissolved Ag^+ from the unreacted perchlorate was titrated with aqueous potassium thiocyanate. The water-insoluble portion, consisting of Ag and AgCl, was extracted with aqueous ammonia, filtered and the silver chloride reprecipitated with dilute HNO_3. The amount of reaction was calculated from the mass of AgCl formed, and corrected for the decomposition to metallic Ag. No difference was found by X-ray analysis between the AgCl formed in the bomb and that produced by precipitation from aqueous solution. The results of the decomposition experiments are given in Tables II and III.

V. SOLUTION CALORIMETRY

The reactions measured were the heats of solution of KCl(c) and NaCl(c) in aqueous $AgClO_4$ solution. The apparatus and procedure were similar to that described in [3]. Only a slight excess of $AgClO_4$ was used, so that the final solution was 0.017 molal with respect to alkali perchlorate and only about 0.001 molal with respect to $AgClO_4$. The calorimetric system was calibrated electrically and for the heats of solution of $KClO_4$ and $AgClO_4$ electrical energy was added during the solution reaction to provide a slight over-all temperature rise. The results of the three heat of solution reactions are summarized in Tables IV - VII.

VI. RESULTS

The results of Tables IV and VII may be combined with the heat of solution of $NaClO_4$(c) from NSRDS-NBS 2 [5] as follows:

$NaCl(c) + AgClO_4(0.017\ m) \rightarrow AgCl(c) + NaClO_4(0.017)\ m)$

$\Delta H° = -14.71 \pm 0.06$ kcal

$AgClO_4(c) \rightarrow AgClO_4(0.017\ m)$

$\Delta H° = 1.79 \pm 0.14$ kcal

$NaClO_4(c) \rightarrow NaClO_4(0.017\ m)$

$\Delta H° = 3.36 \pm 0.01$ kcal

$NaCl(c) + AgClO_4(c) \rightarrow AgCl(c) + NaClO_4(c)$

$\Delta H° = -16.28 \pm 0.14$ kcal

From Table II

$AgClO_4(c) \rightarrow AgCl(c) + 2\ O_2(g)$

$\Delta H° = -23.29 \pm 0.13$ kcal

Hence

$NaClO_4(c) \rightarrow NaCl(c) + 2\ O_2(g)$

$\Delta H° = 16.28 - 23.29 = -7.01 \pm 0.19$ kcal/mol

This is to be compared with the result given in Table III, $\Delta H° = -7.03 \pm 0.07$ kcal/mol.

If the results of Tables V, VI, VII and II are combined we obtain:

$KClO_4(c) \rightarrow KCl(c) + 2\ O_2(g)$

$\Delta H° = -1.41 \pm 0.20$ kcal/mol

which compares with the result obtained from [2], $\Delta H° = -0.96 \pm 0.08$ kcal/mol.

The solution data given in reference [4] may also be used for comparison with the present results. From equation (11) of that reference we have:

$NaClO_4(c) + KCl(c) \rightarrow NaCl(c) + KClO_4(c)$

$\Delta H° = -5.794 \pm 0.064$ kcal/mol

The results given in Table III may be combined with the decomposition data of reference [2] on $KClO_4(c)$ to obtain $\Delta H = -6.07 \pm 0.11$ kcal/mol.

REFERENCES

[1] A. F. Vorob'ev, N. M. Privalova, A. S. Monaenkova, and S. M. Skuratov, Dokl. Akad. Nauk S.S.S.R. 135, 1388 (1960).

[2] W. H. Johnson and A. A. Gilliland, J. Research NBS 65A, 63 (1961).

[3] A. A. Gilliland and W. H. Johnson, J. Research NBS 65A, 67 (1961).

[4] A. A. Gilliland and D. D. Wagman, J. Research NBS 69A, 1 (1965).

[5] V. B. Parker "Thermal Properties of Aqueous Uni-univalent Electrolytes" NSRDS-NBS 2, U.S. Dept. of Commerce (1965).

TABLE I. CALIBRATION OF DRY BOMB

ΔRc ohm	q_{BA} J	q_i J	q_N J	W.C. J	E_s J/ohm
0.100985	13,565.6	35.2	0.9	-11.2	134579
.101197	13,611.6	34.9	0.8	-11.2	134521
.101273	13,631.2	34.7	0.5	-11.2	134603
.101484	13,658.1	35.6	0.9	-11.2	134599
.101562	13,667.3	34.9	0.5	-11.2	134586
Mean					134578 J/ohm
2 Standard deviation of the mean					±32

TABLE II. $AgClO_4$ DECOMPOSITION EXPERIMENTS

$AgClO_4$ g	q_{BA} J	Δe J/ohm	q_{corr} J	W.C. J	ΔRc ohm	AgCl m x 10^3	-ΔE° kJ/mole
1.71261	13589.9	13.2	36.1	-8.1	0.105707	5.9847	101.81
1.87682	13580.1	18.1	35.9	-5.7	.107995	8.9544	103.34
2.87421	13658.8	25.8	32.8	-1.9	.111757	13.4641	101.99
2.39005	13638.8	22.1	34.1	-3.6	.109984	11.3729	102.64
3.05016	13621.9	27.2	35.8	-0.9	.112540	14.5979	102.18
1.21350	13658.8	13.0	33.1	-10.1	.104306	3.3281	107.21*

-ΔE°(25°C) = 102.39 kJ/mol = 24.47 kcal/mol

2 Standard deviation of the mean = ±0.55 kJ/mol = ±0.13 kcal/mol

-ΔH°(25°C) = 23.29±0.13 kcal/mol

*Not included in mean.

TABLE III. $NaClO_4$ DECOMPOSITION

$NaClO_4$ g	q_{BA} J	Δe J/ohm	q_{corr} J	W.C. J	ΔRc ohm	-ΔE° kJ/mol
16.8181	27503.6	23.2	36.3	12.1	0.208984	34.332
18.1227	26265.4	24.0	35.5	12.5	.200050	33.864
20.6210	26172.0	26.4	36.4	14.6	.200185	35.047
18.1864	26547.0	24.2	34.2	12.6	.202212	34.328
17.8356	26348.9	23.6	36.8	12.1	.200670	34.358
14.7329	26133.3	20.5	34.9	9.0	.198230	34.223

Mean -ΔE°(25°C) = 34.36 kJ/mol = 8.212 kcal/mol

2 Standard deviation of the mean = ±0.28 kJ/mol = 0.066 kcal/mol

-ΔH°(25°C) = 7.03±0.07 kcal/mol

TABLE IV. REACTION OF NaCl + $AgClO_4$

NaCl moles	Δe J/ohm	E_a J/ohm	ΔRc ohm	q J	$-\Delta H$ kJ/mol
0.0161291	8.0	22,938.0	.043417	995.90	61.745
.0161417	8.1	22,938.1	.043380	995.06	61.645
.0162543	8.2	22,869.2	.043503	994.88	61.207
.0154015	7.8	22,937.8	.041379	949.14	61.627

$-\Delta H$ = 61.56±0.24 kJ/mol

= 14.71±0.06 kcal/mol

TABLE V. REACTION OF KCl + $AgClO_4$

KCl moles	Δe J/ohm	E_a J/ohm	ΔRc ohm	q J	$-\Delta H$ kJ/mol
0.0164539	6.1	22,936.1	.034072	781.48	47.495
.0161045	6.0	22,936.0	.034066	781.34	48.517
.0163399	6.1	22,867.1	.034456	787.91	48.220
.0161546	6.0	22,936.0	.034210	784.64	48.571

$-\Delta H$ = 48.20±0.35 kJ/mol

= 11.52±0.08 kcal/mol

TABLE VI. SOLUTION OF $KClO_4$ IN KCl SOLUTION

ΔRc ohm	Δe J/ohm	E_a J/ohm	$q_1 = \Delta Rc(E_a)$ J	q_2 = eit J	$KClO_4$ moles	ΔH kJ/mol
0.085376	7.3	20,706.5	1767.84	2137.34	.00721862	51.256
.085026	7.9	20,707.1	1760.64	2131.31	.00724951	51.130
.085639	7.6	20,706.8	1773.31	2133.93	.00709975	50.793
.085968	7.4	20,706.6	1780.10	2138.57	.00709751	50.506
.090226	8.1	20,707.3	1868.34	2239.47	.00734175	50.551

ΔH = 50.847±0.30 kJ/mol

= 12.15±0.07 kcal/mol

TABLE VII. HEAT OF SOLUTION OF $AgClO_4$

No.	ΔRc ohm	Δe J/ohm	$q_1=\Delta Rc(Ea)$ J	$q_2=eit$ J	$AgClO_4$ moles	ΔH kJ/mol
1	0.088315	196.9	1845.44	1895.48	.00692974	7.221
2	.093790	201.5	1960.28	2029.34	.00970432	7.117
3	.094300	198.9	1970.69	2028.17	.00810564	7.091
4	.093695	201.0	1958.24	2026.98	.00940107	7.312
5	-0.002238	194.4	-46.76	-	.0053052	8.81

Mean = 7.51 kJ/mol = 1.79 kcal/mole

2 Standard deviation of the mean = 0.60 kJ/mol = ±.14 kcal/mole

Chapter 9

HEAT OF FORMATION OF HYDRAZINE DIPERCHLORATE

by

Alexis A. Gilliland and Donald D. Wagman
National Bureau of Standards
Washington, D.C.

ABSTRACT

The heat of formation of hydrazine diperchlorate ($N_2H_4 \cdot 2HClO_4(c)$) was carried out by reacting hydrazine dihydrochloride ($N_2H_4 \cdot 2HCl(c)$) with aqueous silver perchlorate in a solution calorimeter. This process may be represented by the equation:

$$N_2H_4 \cdot 2HCl(c) + 2AgClO_4(c) \rightarrow N_2H_4 \cdot 2HClO_4(c) + 2AgCl(c)$$

$$\Delta H°(25°C) = -116.85 \pm 1.34 \text{ kJ/mole}$$

$$= -27.93 \pm 0.32 \text{ kcal/mole}$$

Using the values of $N_2H_4 \cdot 2HCl(c)$ and AgCl from Technical Note 270-1, and the value of $AgClO_4(c)$ measured in this laboratory, we obtain:

$$\Delta H° \; N_2H_4 \cdot 2HClO_4 = -289.5 \text{ kj/mole}$$

$$= -69.2 \text{ kcal/mole}$$

I. INTRODUCTION

In continuation of our work on the heats of formation of inorganic perchlorates we have measured the heat of formation of hydrazine diperchlorate. Because of the problems associated with HCl as a possible decomposition product, solution calorimetry involving the reaction between hydrazine dichloride and silver perchlorate was used, following the procedures described in the preceding paper.

II. MATERIALS

The hydrazine diperchlorate was furnished by the Thiokol Chemical Co. The seven gram sample was dated April 30, 1963 and designated No. 9. An analysis furnished by the company indicated that:

hydrazine diperchlorate	99.47 ± 0.13%
perchloric acid	0.21 ± 0.04%

The hydrazine dihydrochloride was prepared by making a slush of the commercial material and concentrated HCl. The slush was permitted to stand overnight in a vacuum dessicator and was then dried by pumping the dessicator down for several hours. The hydrazine dihydrochloride was analyzed by the gravimetric silver chloride method, and the sample used in this work contained 99.92% of the theoretical chloride.

The silver perchlorate was prepared by adding a slight excess of silver oxide to a solution of perchloric acid. The excess silver oxide was then filtered off, and the solution was evaporated to dryness at 140°C. The crystalline mass was then broken up and dried under an infrared lamp in a vacuum dessicator under continuous pumping. Silver perchlorate is strongly deliquescent, and the sample used in this work contained 99.64% of the theoretical silver, based on analysis by the gravimetric silver chloride method. The principal impurity was presumed to be water.

For the work involving a silver perchlorate solution, a stock solution was prepared by the method described above, and a standard volume was added to the calorimeter solution in each experiment.

III. UNITS OF ENERGY AND MOLECULAR WEIGHTS

The unit of energy is the joule; for conversion into the conventional thermochemical calorie, one calorie is taken as 4.1840 J.

All atomic weights were taken from the 1961 International Table of Atomic Weights [1][1].

IV. APPARATUS AND PROCEDURE

The glass calorimeter, thermometric system, apparatus for measurement of electrical energy and general calorimetric procedure have been described [2, 3, 4]. In the measurement of electrical energy however, time was measured on a Beckman/Berkeley 7060 C/R Electronic Counter, by means of a 10,000 cps frequency which was triggered when the current was switched from the spill coil to the heater and stopped when the current was switched back to the spill coil.

Three sets of measurements and calibrations were made. In the first, silver perchlorate, $AgClO_4(c)$, was loaded into soft glass bulbs in a dry box and sealed under vacuum. These samples, approximately 0.008 M, were in the crushing device of the calorimeter, into which had been weighed 447 g, 24.82 moles, of distilled water. The calorimeter was then assembled, a platinum resistance thermometer was inserted, and the calorimeter was immersed in a thermostatically controlled water bath maintained at 25.0°C. After an initial rating period, the bulb was broken while a measured quantity of electrical energy was passed through the heater. The amount of heat absorbed by the endothermic reaction was calculated as the difference between the amount of heat required to produce the temperature rise and the amount of heat actually put in. The calorimeter stirrer, operating at 900 rpm, provided sufficient agitation to afford thermal equilibrium in 20 min. Temperatures were observed at 1-min. intervals during the reaction period and at 2-min. intervals during the initial and final rating periods.

The calibrations were carried out using an empty bulb and duplicating the initial condition of the system. However, the system was modified slightly in the interval between calibration and reaction experiments, and a correction has been applied to make the calibrations comparable with the reaction experiments. A different calorimeter of the same type was used in the rest of the work described in this paper.

---

[1]The figures in brackets indicate the literature references at the end of this paper.

The procedure followed with $N_2H_4 \cdot 2HClO_4(c)$ was identical with that used for the $AgClO_4(c)$, except that in the new calorimeter samples of approximately .004 moles were broken in 500 g, 27.75 moles, of distilled water, and the calibrated system was identical with the initial state of the reaction experiments.

In the final set of experiments, soft glass bulbs containing $N_2H_4 \cdot 2HCl(c)$ were loaded in air and sealed under vacuum. These samples of approximately .006 moles were broken in a solution containing 0.0175 moles of $AgClO_4$. $AgCl(c)$ was precipitated and the final solution contained $N_2H_4 \cdot 2HClO_4$ with a small amount of excess $AgClO_4$. Here a reaction period of 30 min. was required to attain thermal equilibrium, owing to the slowness with which the chemical reaction came to completion.

Calibrations were carried out with a solution of $AgClO_4$ of the same concentration as that used in the reaction experiments.

V. RESULTS AND CALCULATIONS

The results of the calibration experiments on the calorimetric system used to measure the heat of solution of $AgClO_4(c)$ are given in Table I. ΔRc corresponds to the corrected temperature rise of the system. The energy equivalent, ΔE_s, of this system was obtained as the ratio of the quantity of electrical energy, E, to ΔRc, the corresponding rise in temperature. Δe represents the correction made for a change in the system in the final measurement.

The results of the solution experiments are given in Table II. Here, Δe is the change in the energy equivalent from that of the calibrated system due to the heat capacity of the sample, and to deviations in the mass of the glass bulb from that of the reference bulb, (0.299 g). The energy evolved, q_1, is the product of ΔRc, and the energy equivalent of the actual calorimetric system, $E_s + \Delta e$ or E_a. The amount of electrical energy put into the system, q_2, is the product of current, potential and time. The heat of solution of $AgClO_4$ is q, the difference between q_1 and q_2, and the ratio of q to moles of $AgClO_4(c)$ gives the heat of solution per mole.

The results of the calibration experiments on the calorimetric system used to measure the heat of solution of $N_2H_4 \cdot 2HCl(c)$ are given in Table III; the heat of solution experiments are given in Table IV.

The results of the calibration and measurement experiments for the heat of reaction of $N_2H_4 \cdot 2HCl(c)$ with aqueous $AgClO_4$ are given in Tables V and VI.

By combining the results of Tables II, IV and VI in the relation (VI) + 2(II) - (IV) we obtain:

$$N_2H_4 \cdot 2HCl(c) + 2AgClO_4(c) \rightarrow 2AgCl(c) + N_2H_4 \cdot 2HClO_4(c)$$

$$\Delta H = -116.85 \pm 1.34 \text{ kJ/mol}$$

$$= -27.93 \pm 0.32 \text{ kcal/mol.}$$

This may now be combined with the known heats of formation of $N_2H_4 \cdot 2HCl(c)$ and AgCl(c) from TN 270-1 [5] and the heat of decomposition of $AgClO_4(c)$ from the preceding paper to obtain:

$$N_2H_4 \cdot 2HClO_4(c);\ \Delta Hf°(25°C) = -69.2\ kcal/mol$$

with an over-all estimated uncertainty of about ±0.5 kcal.

REFERENCES

[1] A. E. Cameron and E. Wichers, J. Am. Chem. Soc. 84, 4175 (1962).

[2] W. H. Johnson, A. A. Gilliland and E. J. Prosen, J. Research NBS 63A, 161 (1959).

[3] E. J. Prosen, W. H. Johnson, and F. Y. Pergiel, J. Research NBS 62, 43 (1959), RP2927.

[4] E. J. Prosen, F. W. Maron and F. D. Rossini, J. Research NBS 46, 106 (1951), RP2181.

[5] National Bureau of Standards Technical Note 270-1, October 1, 1965.

TABLE I. CALIBRATION FOR $AgClO_4$(c) SOLUTION

No.	ΔRc ohm	E, J	Δe	ΔE_s J/ohm
1	.092368	1914.40	-	20725.7
2	.087768	1814.69	-	20676.0
3	.090201	1867.65	-	20705.5
4	.092773	1920.35	-	20699.4
5	.092808	1919.42	7.9	20689.5
Mean				20699.2
2 Standard deviation of the mean				±16.6

TABLE II. HEAT OF SOLUTION OF $AgClO_4$

No.	ΔRc ohm	Δe J/ohm	q_1 J	q_2 J	$AgClO_4$ moles	ΔH kJ/mol
1	.088315	196.9	1845.44	1895.48	.00692974	7.221
2	.093790	201.5	1960.28	2029.34	.00970432	7.117
3	.094300	198.9	1970.69	2028.17	.00810564	7.091
4	.093695	201.0	1958.24	2026.98	.00940107	7.312
5	-.002238	194.4	-46.76	-	.0053052	8.81

Mean ΔH = 7.51 kJ/mol = 1.79 kcal/mol

2 Standard deviation of the mean = 0.60 kJ/mol = ±.14 kcal/mol

TABLE III. CALIBRATION FOR $N_2H_4 \cdot 2HClO_4$ SOLUTION EXPERIMENTS

No.	ΔRc ohm	E, J	E_s J/ohm
1	.105560	2434.3	23,060.8
2	.105670	2435.92	23,052.0
3	.094049	2169.5	23,067.8
4	.099658	2301.06	23,089.5
5	.099822	2302.65	23,104.0
Mean			23,072.4
2 Standard deviation of the mean			±19.5

TABLE IV. $N_2H_4 \cdot 2HClO_4$(c) SOLUTION EXPERIMENTS

No.	ΔRc ohm	Δe J/ohm	$q_1 = \Delta Rc(E_a)$ J	q_2 = eit J	HDP moles	$+\Delta H(25)$ kJ/mol
1	.113031	10.5	2609.08	2710.52	.0038218	26.54
2	.113793	9.2	2626.52	2712.50	.0033590	25.60
3	.105641	13.8	2438.85	2572.36	.0050473	26.45
4	.114200	7.8	2635.76	2711.87	.0028478	26.73
Mean					26.33 kJ/mol 6.29 kcal/mol	
2 Standard deviation of the mean					±0.50 kJ/mol ±0.12 kcal/mol	

TABLE V. CALIBRATION FOR $N_2H_4 \cdot 2HCl$ REACTION EXPERIMENTS

No.	ΔRc ohm	E, J	E_s J/ohm
1	.100268	2300.00	22,938.5
2	.106443	2439.76	22,920.8
3	.106369	2438.38	22,923.8
4	.107891	2473.70	22,927.8
5	.112232	2574.40	22,938.2
Mean			22,929.8
2 Standard deviation of the mean			±7.3

TABLE VI. REACTION OF $N_2H_4 \cdot 2HCl$ WITH $AgClO_4$

No.	ΔRc ohm	Δe J/ohm	E_a J	$q = \Delta Rc(E_a)$ J	HDH moles	$-\Delta H$ kJ/mol
1	.030798	4.2	22,934.2	706.33	.0066837	105.68
2	.028706	3.9	22,933.9	658.34	.0062123	105.97
3	.027183	3.5	22,933.5	623.40	.0059440	104.88
4	.033054	4.4	22,934.4	758.07	.0072111	105.12
5	.028366	3.7	22,933.7	650.54	.0061354	106.03
Mean					105.54 kJ/mol 25.22 kcal/mol	
2 Standard deviation of the mean					± .11 kcal/mol	

Chapter 10

STATUS OF LIGHT-ELEMENT HEAT-CAPACITY CALORIMETRY AT THE NATIONAL BUREAU OF STANDARDS; A REVIEW OF THE HIGH-TEMPERATURE THERMODYNAMICS OF THE $BeO-H_2O$ SYSTEM

Thomas B. Douglas
National Bureau of Standards, Washington, D. C.

ABSTRACT

Heat-capacity calorimetry recently completed and in progress at the National Bureau of Standards is reviewed briefly. After a critical review of the thermodynamic properties of the $BeO-H_2O$ system, it is concluded that the product of the reaction between BeO(c) and $H_2O(g)$ below 1850°K is probably largely $Be(OH)_2(g)$, but that higher hydrates may be sufficiently stable to hold considerable amounts of BeO in the gas phase at much higher temperatures.

NBS HEAT-CAPACITY CALORIMETRY

Table I summarizes the current status of heat-capacity calorimetry at the National Bureau of Standards, from 0° to 2500°K, on compounds of importance as combustion products in chemical propulsion.

TABLE I. CURRENT NBS HEAT-CAPACITY CALORIMETRY†

Completed	In Progress	Planned
$A\ell_2O_3$(1200°-2500°K)[1]	W(to 2500°K)	BeO (through M.P.)
Be_3N_2(273°-1200°K)[2]	Be_3N_2(15°-400°K)	Be_2C or mixed oxides
$Li_3A\ell F_6$(273°-1000°K)[3]	$Li_3A\ell F_6$(15°-400°K)	$Li_3A\ell F_6$(1000°-1200°K)
$BeO\cdot A\ell_2O_3$(15°-1200°K)[4,5]	$A\ell F_3$(273°-1200°K)	
$BeO\cdot(A\ell_2O_3)_3$(15°-1200°K)[5,6]	BeO(10-100μ)(15°-400°K)	

$A\ell_2O_3$ has recently been measured to about 200 degrees above its melting point. Final results for the heat of fusion and liquid heat capacity await the completion of current measurements on the container material, tungsten. However, the heat of fusion found may not differ by more than 1 kcal/mole from the value adopted in the latest JANAF table for this substance [7]. Then an attempt will be made to measure accurately the heat of fusion of BeO. $A\ell F_3$ is currently being measured above room temperature because of uncertainties in the existing data, and large-particle BeO is being measured at low temperatures to eliminate possible surface effects on the existing entropy values.

---

* This paper reports work sponsored by the U. S. Air Force Office of Scientific Research, Propulsion Division, Order No. OAR ISSA 65-8.

† Numbers in brackets refer to literature and report references at the end of this paper.

THE $BeO-H_2O$ SYSTEM AT HIGH TEMPERATURES

Several of us at the National Bureau of Standards recently undertook to examine critically the available data bearing on the thermodynamic properties of gaseous hydrates of BeO. We felt that the interpretation of these data may be subject to some ambiguity, particularly in their extrapolation to represent the important $BeO-H_2O$ system at much higher temperatures.

The pertinent quantitative experimental studies of which we are aware are as follows. Hildenbrand, Theard, and Ju [8] observed the species BeOH and $Be(OH)_2$ mass-spectrometrically at 2327°K, but because of unusually large background assigned only upper limits to their abundance, which, however, are not inconsistent with the transpiration data discussed below. Following several earlier studies, three quantitative investigations of the transpiration by water vapor of BeO from the solid have been published by Grossweiner and Seifert (1470°-1820°K) [9], Young (1580°-1850°K) [10], and Stuart and Price (1340°-1650°K) [11]. All this work except that of Stuart and Price was critically reviewed by Altman [12], and was made the basis of a JANAF table of the thermodynamic properties of $Be(OH)_2(g)$ [13].

The three transpiration studies cited above cover a total range of 500 degrees, are fairly interconsistent, and are therefore considered together in some detail below.

<u>The Reaction Occurring in the Transpiration Studies</u>. -- The reaction taking place was assumed in all three investigations to be

$$BeO(c) + H_2O(g) = Be(OH)_2(g). \qquad (1)$$

In two of the studies the partial pressure of steam was varied over a wide range at constant temperature: the results of Grossweiner and Seifert were open to some question, apparently owing to the limitations of experimental accuracy; but Stuart and Price found an approximate proportionality to the concentration of the evaporated BeO. (The partial pressures of pure BeO and $A\ell_2O_3$ are negligible at these temperatures.) Because of this evidence and because of the impossibility of formulating a molecule of a hydrate of BeO formed from more than one molecule of H_2O and still obeying the saturated covalences, we assume that the ratio 1:1 of H_2O to the hydrate species in reaction (1) is established.

However, no one has demonstrated that one mole of H_2O evaporates only one gram-formula-weight of BeO, and in view of the ease of formulating the general structures of higher hydrates of BeO, we replaced reaction (1) by the more general reaction

$$nBeO(c) + H_2O(g) = (BeO)_n \cdot H_2O(g) , \qquad (2)$$

and then proceeded to look for evidence as to the probable value of <u>n</u> (which may be effectively non-integral if more than one reaction of type (2) occur simultaneously). It should be noted that the ratio of BeO to H_2O reacting at any temperature in the range of these studies has been determined and hence cannot be assumed to depend on <u>n</u>, because it was this ratio that was measured. But we think we can show that if $\underline{n}$ was not exactly unity, there may be serious practical consequences at temperatures much higher than 1850°K.

When, as in this case, the gaseous product is identified only by inference and not by direct spectroscopic observation, two alternative oft-used methods for evaluating $\underline{n}$ suggest themselves, and will be discussed in turn. The first method is the one which indicated a 1:1 ratio for H_2O and the hydrate in reaction (2), is straightforward when the necessary accurate data are available, and should be more often applied to the condensed phases of transpiration reactions. The coefficients in the chemical reaction such as (2) are, of course, the powers of the respective thermodynamic activities in the equilibrium constant. Consequently, if in this case the transpiration measurement is repeated at the same temperature and partial pressure of steam but with a different activity (free energy) of the condensed BeO, what is equivalent to a log-log plot should determine $\underline{n}$.

In principle, the necessary data are available in the present case. Young [10] transpired BeO by water vapor not only from pure solid BeO but also from two solid beryllium aluminates, and reported evidence that the ad tional reactions occurring were

$$3BeO\cdot Al_2O_3(c) + 2H_2O(g) = BeO\cdot(Al_2O_3)_3(c) + 2Be(OH)_2(g) \quad (3)$$

and

$$BeO\cdot(Al_2O_3)_3(c) + H_2O(g) = 3Al_2O_3(c) + Be(OH)_2(g) \;. \quad (4)$$

These beryllium aluminates may be considered to be solutions of BeO in an inert solvent, Al_2O_3, but cannot be assumed to be <u>ideal</u> solutions, so that ascertaining the activity of the BeO (relative to pure BeO) in each compound is not simple. Kleppa [14] has recently measured calorimetrically the heats of formation of these two beryllium aluminates from their component oxides, and we have recently measured their Third-Law entropies [4,5,6]. However, our application of these data to determine $\underline{n}$ led to inconclusive results, probably for one or more of the following reasons:

1. Kleppa's data are presently preliminary, lacking final corrections;

2. There are reasons for thinking that our samples of the beryllium aluminates may have possessed appreciable frozen-in disorder not reflected in the heat-capacity data; and

3. The transpiration data are not sufficiently precise to give small differences accurately.

The second method is to compare the experimental (Second-Law) entropy change ΔS of the reaction with what is predicted using estimates of the molecular constants (or parameters) of each of the postulated hydrate molecules. We made such estimates, by analogy, for the three molecules $(BeO)_n\cdot H_2O$ with n=1, 2, and 3, for $(BeO)_3\cdot H_2O$ including three sets of frequency fundamentals designed to cover the likely range. (The entropies of BeO(c) and $H_2O(g)$ are by comparison very well established [15].) The results for 1700°K are shown in Table II, where ranges are given corresponding to the three sets of estimates for n=3 and the three independent transpiration investigations.*

TABLE II. COMPARISON OF EXPERIMENTAL AND ESTIMATED ΔS°_{1700} FOR REACTION (2)

	ΔS°_{1700} (e.u.)†		
n	Experimental [9-11]	Estimated	Source for S° of $(BeO)_n \cdot H_2O$
1	7-9	15	NBS
2	6-7	29	NBS
3	5-7	24-54	NBS

†All values are positive.

It is seen that the estimated values of ΔS° are all higher than the corresponding experimental values, a consistent discrepancy which may reflect systematic error in the experimental results, in the estimates, or both. (The JANAF table for $Be(OH)_2(g)$ [13] leads to $\Delta S^\circ_{1700} = +7$, but in its formulation it was required to fit some of the transpiration data.) Nevertheless, the discrepancies with n > 1 are large, and suggest that under the conditions of the transpiration measurements the hydrate product is all or predominantly $Be(OH)_2$.

Other Expected Properties of Higher Gaseous Hydrates of Beryllia. -- Even if the product of the transpiration reaction is largely $Be(OH)_2$ below 1850°K, it would be premature to dismiss the possibility of small amounts of higher hydrates being formed at these temperatures. Such hydrates would undoubtedly have much larger molal heats of formation from BeO(c) and $H_2O(g)$, and hence their abundance would increase with temperature much faster than that of $Be(OH)_2$. Actually, the question is not whether these are highly stable molecules in themselves, but rather, under what conditions their stabilities are comparable to those of others, such as $Be(OH)_2$, with which they must compete.

Chupka, Berkowitz, and Giese [16] have observed gaseous polymers of BeO up to the hexamer, which may be considered to be related to the postulated beryllia hydrates. The following drawing illustrates how one such polymer of BeO, which has been postulated to be a ring, may be converted by H_2O into the corresponding "beryllia hydrate" molecule.

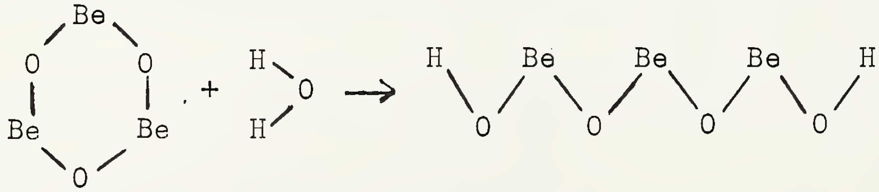

The shape of such a hydrate molecule is debatable, but a more important question is whether there is any basis for estimating its dissociation energy. The simplest approach to this question is to test for approximate additivity of bond energies in known molecules containing Be-O and/or O-H

* The estimated molecular parameters are deliberately not listed here in order to avoid implying a reliability which we think they do not have.

bonds. Within the uncertainties of the available information this is done in Table III, where the Be-F and O-H bond energies have been assumed to be the same as their mean values in $BeF_2(g)$ and $H_2O(g)$, respectively, and all data are taken from JANAF tables except for $Be_2OF_2(g)$ [17].

TABLE III. APPARENT Be-O BOND ENERGIES (KCAL/MOLE), FROM ΔHf°_{298}

$(BeO)_2$	94
$(BeO)_3$	111
$(BeO)_4$	116
$(BeO)_5$	120
$(BeO)_6$	122
Be_2OF_2	120
$Be(OH)_2$	119

With the exception of the smaller rings, where some strain may be operative, all values are near 120 kcal/mole, and may be supposed to be so also in the hydrate chains.

Some Postulated Gas Compositions to 4000°K. -- On the basis of the foregoing discussion we made exemplary calculations designed to show whether the higher hydrates may be important species at high temperatures. The calculations were limited to the polymers of BeO; monoberyllia hydrate, $Be(OH)_2$ or $BeO{\cdot}H_2O$; and triberyllia hydrate, $(BeO)_3{\cdot}H_2O$. The partial pressures of these in equilibrium with condensed BeO (solid at 2000°, and liquid at 3000° and 4000°K) were calculated. (If the total available BeO is not sufficient to produce these pressures, the condensed BeO would of course disappear or not form.) The available JANAF tables were used except that the molecular parameters of the unobserved $(BeO)_3{\cdot}H_2O$ were assumed to be those estimated as "most likely", and its bond energies were assumed to be the same as in H_2O and $Be(OH)_2$. The results are shown in Table IV.

TABLE IV. CALCULATED PARTIAL PRESSURES OF SOME NEUTRAL GASEOUS SPECIES IN EQUILIBRIUM WITH CONDENSED BeO

(in atm. of equivalent BeO)

Species	2000°	3000°	4000°K	
BeO to $(BeO)_6$	6×10^{-9}	0.003	0.3	
$BeO{\cdot}H_2O$	1×10^{-3}	0.03	0.07	per atm. of H_2O
$(BeO)_3{\cdot}H_2O$	1×10^{-4}	3.	50.	per atm. of H_2O

The various polymers of BeO, as well as Be (not shown because it depends in a complicated way on the amounts of oxygen, hydrogen, and water) account for some of the evaporated BeO. But the most significant thing in Table IV is shown by a comparison of the last two lines. These indicate that, compared with $BeO{\cdot}H_2O$, $(BeO)_3{\cdot}H_2O$ accounts for only 10% as much evaporated BeO at 2000°, but 100 times as much at 3000° and 700 times as much at 4000°. According to these figures, above about

2500°K much more BeO would be in the vapor state than predicted by the existing JANAF tables.

It should be emphasized that Table IV cannot be taken as a docisive picture of the actual situation because of the uncertainties in calculating the last line. For example, if we had used not the "most likely" but the "highest likely" set of estimated frequencies, the entropies of $(BeO)_3 \cdot H_2O$ would have been calculated lower by about 20 e.u. and hence the abundance of this species would have been calculated lower by a factor of about 10^4 at every temperature. However, we feel that the basis of Table IV is within the plausible range, and hence that serious experimental investigation of higher hydrates of beryllia is needed. This is merely one case among many where the failure to observe molecular species is no guarantee of their lack of importance at much higher temperatures.

Some Comments on Experimental Approaches. -- How might one best hunt experimentally for these hydrates and measure their properties? Mass spectrometry, matrix spectrometry, and transpiration studies at higher temperatures are obvious possible approaches. But unless the temperature is rather high, the minimum water-vapor pressures required to produce measurable or even detectable amounts of the higher-hydrate species seem to present formidable practical difficulties.

The current research program at the National Bureau of Standards on the thermodynamic properties of rocket combustion products includes plans for work on the $BeO-H_2O$ and $A\ell_2O_3-H_2O$ systems in the near future, but whether these results will represent the conditions at the high temperatures of practical interest remains an open question. We believe that other laboratories should be encouraged to investigate this area more intensively than heretofore.

ACKNOWLEDGEMENTS

The NBS heat-capacity calorimetry summarized is the work of G. T. Furukawa, E. D. West, the author, and their associates. Several participated actively with the author in reviewing and discussing the $BeO-H_2O$ thermodynamics: C. W. Beckett, D. R. Lide, Jr., J. Efimenko, and G. V. Calder of the National Bureau of Standards, and O. J. Kleppa of the University of Chicago. C. W. Beckett and D. R. Lide, Jr., made the estimates of molecular constants of spectroscopically unobserved species.

REFERENCES

[1] E. D. West and S. Ishihara, NBS Report 9028, National Bureau of Standards, Washington, D. C., 1 January 1966, pp. 71-79.

[2] T. B. Douglas and W. H. Payne, NBS Report 7587, National Bureau of Standards, Washington, D. C., 1 July 1962, pp. 44-54.

[3] T. B. Douglas and J. E. Neufer, NBS Report 8186, National Bureau of Standards, Washington, D. C., 1 January 1964, pp. 68-74.

[4] G. T. Furukawa and W. G. Saba, J. Research Natl. Bur. Standards 69A, 13-18 (1965).

[5] D. A. Ditmars and T. B. Douglas, NBS Report 9028, National Bureau of Standards, Washington, D. C., pp. 80-94.

[6] G. T. Furukawa and W. G. Saba, NBS Report 9028, National Bureau of Standards, Washington, D. C., pp. 45-58.

[7] JANAF Thermochemical Tables, The Dow Chemical Co., Midland, Mich. (table for alpha Al_2O_3(crystal), Mar. 31, 1964).

[8] D. L. Hildenbrand, L. P. Theard, and F. Ju, Publication No. U-2231 (Third Quarterly Technical Report: Investigation of Thermodynamic Properties of Rocket Combustion Products), Ford Motor Co., Aeronutronic Division, Newport Beach, Calif., 31 July 1963, pp. 8-18.

[9] L. I. Grossweiner and R. L. Seifert, J. Amer. Chem. Soc. 74, 2701-2704 (1952).

[10] W. A. Young, J. Phys. Chem. 64, 1003-1006 (1960).

[11] W. I. Stuart and G. H. Price, J. Nucl. Materials 14, 417-424 (1964).

[12] R. L. Altman, J. Chem. Engg. Data 8, 534-536 (1963).

[13] JANAF Thermochemical Tables, The Dow Chemical Co., Midland, Mich. (table for $Be(OH)_2$(g), Sept. 30, 1963).

[14] O. J. Kleppa, University of Chicago (private communication).

[15] JANAF Thermochemical Tables, The Dow Chemical Co., Midland, Mich. (table for BeO(c), Sept. 30, 1963; table for H_2O(g), Mar. 31, 1961).

[16] W. A. Chupka, J. Berkowitz, and C. F. Giese, J. Chem. Phys. 30, 827 ff (1959).

[17] J. Efimenko, NBS Report 8186, National Bureau of Standards, Washington, D. C., 1 January 1964, pp. 103-112.

Chapter 11

VAPORIZATION OF REFRACTORY MATERIALS: ARC-IMAGE FURNACE

by

J. J. Diamond and A. L. Dragoo

Further comparisons between the automatic and visual optical pyrometers have been carried out since the previous report (NBS Report 9028).

A critical examination was made of two sets of data on the heat of vaporization of molten alumina, one based on temperatures measured with the L&N visual pyrometer and the other based on the L&N automatic pyrometer. On the basis of the data presented in Table 1 we concluded that the visual pyrometer data are valid, but that the automatic pyrometer data are not.

From the second law heats, the standard deviation of the mean and range of the third law heats, and the range of temperatures, it is evident that the scatter of data is very much greater for the automatic pyrometer data. This conclusion is strengthened and explained by the rank-correlation coefficients. For the visual pyrometer, the only significant correlation is between the rate of vaporization and temperature. For the automatic pyrometer, the situation is exactly reversed: Rate of vaporization is <u>not</u> a function of temperature, while there is a very strong correlation between ΔH_v and T and a weak, though significant, negative correlation between ΔH_v and rate of evaporation. One must conclude there is a random factor in temperature measurement with the automatic pyrometer which complicates its use with the arc-image furnace; this is in spite of the fact that mean third law heats are quite comparable using the two pyrometers, corresponding to a difference in mean temperature of only 15°C.

Further comparison of the applications of the visual and automatic pyrometers to temperature measurements in the arc-image furnace have begun.

The effective wavelengths of the automatic pyrometer for a range of temperatures from 2300 to 2750°K were calculated from data supplied by Leeds and Northrup for that instrument. The effective wavelengths of the visual and automatic pyrometers are nearly the same (e.g., at 2500°K, λ_e = 0.6511 μ for the visual pyrometer and 0.6465 μ for the automatic pyrometer).

The possibility that the surface of the liquid cools perceptibly when the cross-over point chopper is interposed between the arc and the sample was discussed briefly in the previous report. Further consideration has been given to this effect which is illustrated in Figure 1. During one complete revolution of the choppers a sawtooth-shaped fluctuation of temperature must be somewhat as illustrated. This type of variation would result in a temperature measured with synchronized choppers which would be less than the true average temperature of the sample. This suggests that the 2° difference found between the temperature of infinitely-thick alumina drops as measured with the visual pyrometer synchronized and unsynchronized is due to this variation and not to a reflection error as previously advanced. It leads to the conclusion that the best temperature measurement is obtained by focussing on the non-glare area with the visual pyrometer, without using a chopper and sector disc.

This view also serves to explain current results obtained by simultaneously measuring the temperature of liquid alumina drops with the automatic and visual pyrometers. The automatic pyrometer measured only synchronized temperatures. Since a sector disc could not be used, the visual pyrometer was sighted on the non-glare central portion of the drop, and the average temperature was measured. Above 2060°C (apparent temperature), where the drop became infinitely thick, the automatic pyrometer read 25° below the visual pyrometer. This difference is greater than that observed when the visual pyrometer is synchronized and unsynchronized and suggests that there is an additional effect present with the automatic pyrometer which accentuates the observed cooling of the drop.

TABLE 1

Vaporization Data

	Visual Pyrometer	Automatic Pyrometer
Mean third law $\Delta H_V^\circ(298)$	729.0 kcal mol^{-1}	724.6 kcal mol^{-1}
Standard deviation of mean $\Delta H_V^\circ(298)$	0.9 kcal mol^{-1}	3.4 kcal mol^{-1}
Range of $\Delta H_V^\circ(298)$	9.1 kcal mol^{-1}	56.9 kcal mol^{-1}
Second law $\Delta H_V^\circ(2550°K)$	794.4 kcal mol^{-1}	- 16.8 kcal mol^{-1}
Standard deviation $\Delta H_V^\circ(2550°K)$	77.4 kcal mol^{-1}	66.4 kcal mol^{-1}
Range of temperatures	113°K	195°K
Rank Correlation Coefficients		
Rate of Vaporization and T°K	+ .93	- .04
$\Delta H_V^\circ(298)$ and T°K	- .30	+ .91
$\Delta H_V^\circ(298)$ and rate of vaporization	- .49	- .40
Critical coefficient (10% level)	.558 (n = 10)	.377 (n = 20)

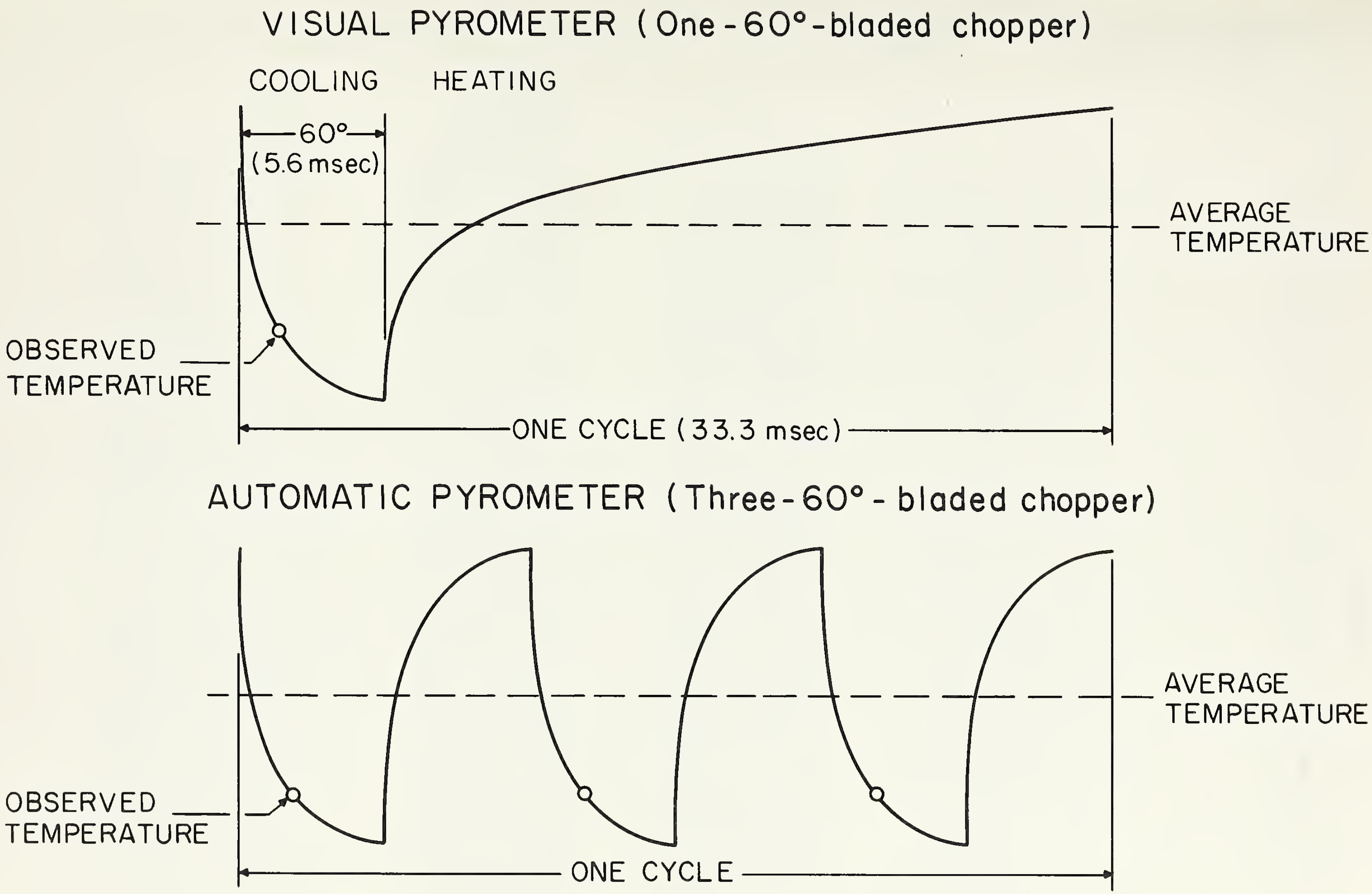

Figure 1: Illustration of temperature fluctuation of sample due to periodic interruption of arc radiation by a chopper.

Chapter 12

HIGH TEMPERATURE MASS SPECTROMETRY, ALUMINA-BERYLLIA SYSTEM

by

J. Efimenko

Introduction

Data on vapor species at high temperatures have been obtained starting with four specific compositions of the alumina-beryllia system. The compositions studied correspond to the compounds $BeO \cdot Al_2O_3$, $BeO \cdot 3Al_2O_3$ and the eutectics $57BeO:43Al_2O_3$ (75 wgt%), $40BeO:60Al_2O_3$ (86 wgt%). These mixtures were prepared by fusion in an arc-image furnace.

Experimental

A more efficient ionization source containing a magnetically collimated electron beam, has been installed in the mass spectrometer. The source produces a maximum in the ionization efficiency curve at 18 ev. The maximum is broad enough to allow stable operating conditions. All the samples were contained in tungsten cups, inside a tungsten effusion cell. The present data should show less electron impact fragmentation than previous data taken with electrons of 70 ev.

Discussion

The results reported here are for the eutectic mixture $3Al_2O_3:2BeO$, melting point 1850° ± 10°C, obtained with the low electron energies. The ion intensities are presented in Table 1. Except for the gaseous molecule at mass position 52, AlOBe, no new specie was observed over the mixtures studied. Since fragmentation was considered to be less in this experiment, one reaction was selected to compare with previously obtained results.

$$Al_2O(g) + Be(g) \rightleftarrows AlOBe(g) + Al(g)$$

The equilibrium constant for this reaction involves terms to the first power only. Since the ionization cross sections have not been evaluated yet for 18 ev electrons, an approximate equilibrium constant can be computed from the ion intensities alone. The experimental data were treated by a van't Hoff plot and from the slope the enthalpy change was obtained, $\Delta H°(2330°K) = 14.05$ kcal/mol and reduced to absolute zero reference state temperature, $\Delta H_0° = 13.3$ kcal/mol. This compares much better with the value based on free energy functions, $\Delta H_0° = 17.1$ kcal/mol, Report 9028, p. 64.

Changes that occur during the volatilization of the alumina-beryllia mixtures can be followed by comparing the concentrations of the various species over a mixture to those over pure alumina. Since the product of the ion intensity and temperature is proportional to the partial pressure of a specie, these values are compared at the same temperatures. Table 2 contains some previously obtained intensity data on pure alumina. From the data of Tables 1 and 2, curves of $\ell n\ I^+T$ vs. 1/T were plotted for the species O^+, Al^+, AlO^+, and Al_2O^+. From these curves, $\ell n\ I^+T$ values were read off at the same temperature and the values are listed in Table 3. It is apparent that the ease of forming a specie from a mixture is less than from pure alumina. Further treatment will be attempted in order to show other quantitative relationships. The results from the other mixtures will be correlated also.

Due to the use of 18 ev electrons, additional instrument calibrations were carried out with weighed samples of aluminum and beryllium. This will allow conversion to partial pressures with less error than with the relation often used to correct ionization cross sections for the effect of a different electron energy.

TABLE 1

Mass Spectrometric Intensities for $40BeO:60Al_2O_3$, liquid
(Intensities in units of volts)

T °K	$I_9^+ \times 10^3$	$I_{16}^+ \times 10^4$	$I_{27}^+ \times 10^2$	$I_{43}^+ \times 10^4$	$I_{52}^+ \times 10^4$	$I_{70}^+ \times 10^4$	$I_{75}^+ \times 10^4$
2550	500.	1125.	340.	2400.	410.	3400.	147.
2518	390.	850.	261.	1770.	295.	2550.	120.
2476	231.	490.	141.	960.	151.5	1320.	76.5
2428	151.5	295.	86.	575.	81.	730.	50.
2370	79.0	142.5	38.5	246.	35.	310.	28.5
2290	36.5	54.0	15.3	93.	11.	99.	12.
2417	174.0	370.	114.	785.	120.	1050.	63.
2370	90.0	174.	48.	305.	46.	400.	33.5
2327	58.0	102.	29.	178.5	23.5	223.5	21.5
2412	180.0	340.	109.	710.	108.	975.	63.
2375	126.0	237.	69.	430.	67.	580.	43.
2338	84.0	142.5	42.	243.	37.	325.	27.
2295	55.0	79.5	26.1	148.	22.	198.	19.
2243	18.7	28.0	6.5	35.	4.8	40.	
2243	23.4	34.0	8.2	47.	6.45	58.5	
2243	25.9	30.5	9.1	53.	7.	56.	
2190	12.4	18.5	4.5	24.	3.15	24.	
2227	26.5	41.0	1.15	55.	8.5	63.	
2259	30.0	27.0	11.7	16.5	8.0	81.	
2201	17.4	23.5	6.6	32.	7.0	36.5	
2153	3.2	13.5	3.2	15.	5.0	17.0	
2106	4.1	8.0	1.1	240.	8.0	44.	
2158	9.75	12.0	2.9	13.5		15.5	
2127	6.0	6.0	1.83	8.0			
2148	7.8	7.5	2.34			2.25	
2259		45.0	12.6	63.0	11.0	72.0	

TABLE 2

Mass Spectrometric Intensities for Al_2O_3, Liquid
(Intensities in units of volts)

T °K	$I^+_{16} \times 10^2$	$I^+_{27} \times 10^2$	$I^+_{32} \times 10^3$	$I^+_{43} \times 10^3$	$I^+_{70} \times 10^3$
2354	250.0	1260.	150.	96.0	1200.
2401	171.0	895.	78.	60.0	660.
2372	160.5	755.	66.	52.5	480.
2353	117.0	550.	60.	37.0	340.
2296	42.0	207.	21.	15.0	144.
2317	57.0	192.	51.	23.0	162.
2285	42.0	129.	33.	10.0	96.
2232	21.0	60.	9.	10.0	48.
2232	25.0	54.	14.	1.1	33.
2127	5.4	9.3	3.3	3.6	9.
2132	25.0	63.0	21.	20.0	75.
2237	4.5	12.3	2.7	2.4	
2174	10.2	24.3		3.0	25.
2179	25.0	30.0		16.0	45.

TABLE 3

Comparison of Vapor Specie Concentrations for Pure Alumina with Alumina-Beryllia Eutectic

$10^3/T$	Al_2O_3 $\ell n\ I_{16}^+T$	eutectic $\ell n\ I_{16}^+T$	Al_2O_3 $\ell n\ I_{27}^+T$	eutectic $\ell n\ I_{27}^+T$	Al_2O_3 $\ell n\ I_{43}^+T$	eutectic $\ell n\ I_{43}^+T$	Al_2O_3 $\ell n\ I_{70}^+T$	eutectic $\ell n\ I_{70}^+T$
0.39	10.90	5.80	12.72	9.55	9.57	6.67	9.61	7.07
0.40	9.70	5.14	11.48	8.58	8.77	5.91	8.78	6.27
0.41	8.97	4.48	10.62	7.86	7.97	5.14	7.96	5.50
0.42	8.24	3.82	9.73	7.14	7.17	4.38	7.14	4.70
0.43	7.52	3.17	8.85	6.43	6.37	3.62	6.32	3.92
0.44	6.82	2.50	7.96	5.70	5.58	2.85	5.50	3.14
0.45	6.10	1.84	7.07	5.00	4.79	2.07	4.68	2.35
0.46	5.40	1.20	6.20	4.27	4.00	1.33	3.87	1.56
0.47	4.69	0.53	5.33	3.57	3.20	0.57	3.05	0.78
0.48	3.97	-0.12	4.45	2.84	2.40	- .15	2.23	0.0

Chapter 13

ANALYSIS OF HEAT-CAPACITY DATA ON SOME SELECTED COMPOUNDS

George T. Furukawa and Martin L. Reilly

Literature survey and analysis of heat-capacity and relative-enthalpy data on substances of interest to the program have been continued and the thermodynamic properties calculated wherever the data were found suitable. High-speed computer techniques were used for analyzing the heat data. Briefly, the method involved, wherever the high-temperature enthalpy data were available, the evaluation of heat capacities at closely spaced intervals using the authors' enthalpy equation. These values were smoothly joined whenever possible with the low-temperature values. The joining process consisted of smoothing the apparent Debye θ's obtained from the heat capacities after suitable scaling. The extrapolation to 0°K below the lowest observed value was done in terms of the θ's. Whenever the low and high temperature data were inconsistent, the tables of thermodynamic properties were terminated around 300°K. The enthalpy equations were found to be inconsistent with the low-temperature measurements in most of the cases since the equations are intended to fit the enthalpy data over a broad range of temperatures. The first and second derivatives of the equation in the region of room temperature were not considered when they were formulated.

The low-temperature heat-capacity measurements reported from the Berkeley Bureau of Mines did not go below about 50°K. The Debye-Einstein heat-capacity equations used in their extrapolation to 0°K were evaluated at closely spaced temperature intervals and joined smoothly to the observed values above 50°K by the method described above.

In the following section the sources of data analyzed in obtaining the thermodynamic properties are described. Many of the substances that have been examined for this report are difficult to obtain in high purity. The method of preparation and analysis for characterizing the sample are given wherever the authors described them.

The tabular values of thermodynamic properties given are in calories defined by 1 calorie = 4.1840 joules. The 1961 atomic weights based on C-12 adopted by IUPAC were used.

Beryllium Sulfate, $BeSO_4$, 105.0738

A. R. Taylor, Jr., T. E. Gardner, and D. F. Smith (Bureau of Mines RI 6240, 1963) measured the heat capacity of $BeSO_4$ from 10 to 301°K and the enthalpy relative to 273.15°K up to 864°K. The sample was prepared from the tetrahydrate by heating first at 1000°F for several hours, then ground and reheated overnight at 1000°F. Spectrochemical analysis showed 0.01 to 0.1 per cent Mg, 0.001 to 0.01 per cent Al and Fe, and 0.0001 to 0.001 per cent Mn. Tables of thermodynamic properties from 0 to 900°K were prepared from the data.

Strontium Fluoride, SrF_2, 125.6168

Low-temperature heat capacities of SrF_2 were measured by D. F. Smith, T. E. Gardner, B. B. Letson and A. R. Taylor, Jr. (Bureau of Mines RI 6316, 1963) from 11 to 300°K. The sample was prepared by precipitation, obtained by reacting $SrCl_2$ and KF in aqueous solution. The precipitate was washed with water and dried at 600°C. Spectrochemical analysis of the product showed 0.001 to 0.01 per cent Ca and K with traces of Cu, Fe and Mg. The x-ray diffraction patterns corresponded to 1962 ASTM powder data and the petrographic examination showed the amount of foreign phases to be small. The experimental heat-capacity data varied smoothly with temperature, showing no phase transitions. No high-temperature data were found. Thermodynamic properties from 0 to 300°K were calculated from the data.

Strontium Chloride, $SrCl_2$, 158.526

D. F. Smith, T. E. Gardner, B. B. Letson, and A. R. Taylor, Jr. (Bureau of Mines RI 6316, 1963) reported low-temperature heat capacities of $SrCl_2$ in the range 7 to 300°K. The sample was prepared by recrystallizing a reagent-grade material from water and drying at 600°C for 3 hours. Spectrochemical analysis showed 0.0002 to 0.002 per cent of Ca, Al, and Ba; 0.0005 to 0.005 per cent Na, and traces of Cu, Mg, and Mn. Petrographic examination indicated the refractive index to be in agreement with established values.

A. S. Dworkin and M. A. Bredig (J. Chem. Eng. Data 8, 416 (1963)) measured the enthalpy relative to 298°K up to 1204°K. Their sample was prepared by dehydrating the hydrate over P_2O_5 and by heating under vacuum for several days at 100° below the melting point (1146°K). The material was finally melted under dry HCl gas, purged with argon, and filtered through sintered quartz.

The relative enthalpy equation derived by Dworkin and Bredig was found to be unreasonably low compared with the low-temperature heat capacities. Examination of the experimental data at the lower temperatures showed their enthalpy equation to deviate negatively from their experimental relative enthalpy values. Since further intensive analysis of the high-temperature data is needed, the thermodynamic properties up to 300°K are given at this time.

Titanium Tetrafluoride, TiF_4, 123.8936

R. D. Euler and E. F. Westrum, Jr. (J. Phys. Chem. 65, 132 (1961)) measured the heat capacity of TiF_4 from 6 to 300°K. The sample was prepared by the reaction of F_2 on pure TiO_2 and subsequent sublimation of the fluoride in a nickel vessel. Chemical analysis of the product indicated it to be 99.9 per cent TiF_4. The heat-capacity values vary smoothly with temperature. No transitions were observed. Thermodynamic properties were calculated from 0 to 300°K.

Zirconium Tetrafluoride, ZrF_4, 167.2136

E. F. Westrum, Jr. (J. Chem. Eng. Data 10, 140 (1965)) reported low-temperature heat-capacity measurements on ZrF_4 from 7 to 302°K. The sample was prepared by hydrofluorination of pure ZrO_2 in a platinum vessel at 700°C until constant weight was obtained. The fluoride was further purified by vacuum sublimation. Spectrochemical analysis showed $<$ 2 ppm of Ag, Ba, Co, Li, Be, Mg, V, Mn, Ca, Cu, Ti, B, Cd, and Na; 7 ppm of Cr; 25 ppm of Ni, Al, and Sn; 35 ppm of Pb; 70 ppm of HF; $<$ 100 ppm of P and Zn; 175 ppm of Fe; and 600 ppm of Si. Chemical analysis yielded 54.9 ± 1.0 per cent Zr and 45.2 ± 1.0 per cent F (weighed as PbClF), the theoretical being 54.55 and 45.45 per cent, respectively. X-ray and petrographic examinations showed no oxide or oxyfluoride. The sample was taken to be 99.7 per cent or better in purity.

R. A. McDonald, G. C. Sinke, and D. R. Stull (J. Chem. Eng. Data 7, 83 (1962)) determined the enthalpy relative to 298.15°K up to 1205°K. Their sample was prepared by dissolving HF-free Zirconium in 48 per cent aqueous hydrofluoric acid and evaporating the solution to dryness. The product was heated at 500°C in a platinum boat in a stream of anhydrous HF gas. Chemical analysis yielded 54.6 per cent Zr and 44.9 per cent F.

The two data were combined to obtain thermodynamic properties from 0 to 1205°K.

Zirconium Diboride, ZrB_2, 112.842

Low-temperature heat-capacity measurements were reported for ZrB_2 by E. F. Westrum, Jr. and G. Feick (J. Chem. Eng. Data 8, 193 (1963)) in the range 5 to 345°K. The authors estimated the composition of the sample used, from chemical analysis, x-ray diffraction measurements, and metallographic examination, to be ZrB_2 100 - 97 per cent, ZrB 0 - 3 per cent, ZrC 0.2 per cent, ZrN 0.1 per cent, and ZrO_2 0.02 per cent. No corrections were made for the impurities since estimates indicated that the impurities would cause insignificant errors.

R. H. Valentine, T. F. Jambois, and J. L. Margrave (J. Chem. Eng. Data 9, 182 (1964)) reported measurements of the enthalpy relative to 298.15°K up to 1125°K on a sample of ZrB_2 from the same batch used by Westrum and Feick. The enthalpy equation obtained by Valentine et al. was found to be inconsistent with the heat-capacity data of Westrum and Feick. The lowest measurement by Valentine et al. was at 410°K. For this report thermodynamic properties of ZrB_2 up to 350°K based on the measurements of Westrum and Feick are given.

<u>Strontium 1:1 - Silicate, $SrO \cdot SiO_2$, 163.7042</u>

W. W. Weller and K. K. Kelley (Bureau of Mines RI 6556, 1964) measured the heat capacity of $SrSiO_3$ from 52 to 296°K. The sample was prepared by heating between 1000 and 1350°K a stoichiometric mixture of $SrCO_3$ and pure quartz. The material was repeatedly ground, analyzed and adjusted for composition, and reheated. The total heating time was 246 hours, of which 32 hours were above 1200°C. X-ray diffraction patterns agreed with existing data and the chemical analysis yielded 63.26 per cent SrO, 36.66 per cent SiO_2, and 0.12 per cent of the oxides of Fe and Al the theoretical being 63.30 and 36.70 per cent SrO and SiO_2, respectively.

The heat-capacity values below 52°K were obtained from the Debye-Einstein function:

$$C = D(192/T) + 2E(348/T) + 2E(1026/T)$$

given by Weller and Kelley.

<u>Strontium 2:1 - Silicate, $2SrO \cdot SiO_2$, 267.3236</u>

W. W. Weller and K. K. Kelley (Bureau of Mines RI 6556, 1964) reported heat-capacity measurements on Sr_2SiO_4 from 52 to 296°K. The sample was prepared by heating between 1200 and 1300°C a stoichiometric mixture of $SrCO_3$ and pure quartz. Four cycles of grinding, analyzing and adjusting for composition, and heating were performed, the total heating time being 35 hours. X-ray patterns disagreed with existing data which may be on a different crystalline form. No uncombined oxides were detected. Chemical analysis yielded 77.51 per cent SrO, 22.47 per cent SiO_2, and 0.03 per cent Na_2O, the theoretical being 77.52 and 22.48 per cent SrO and SiO_2, respectively.

The Debye-Einstein heat capacity function:

$$C = D(179/T) + 2E(221/T) + 2E(448/T) + 2E(1024/T)$$

given by Weller and Kelley was used for values below 52°K.

<u>Barium 1:1 - Silicate, $BaO \cdot SiO_2$, 213.4242</u>

W. W. Weller and K. K. Kelley (Bureau of Mines RI 6556, 1964) determined the heat capacity of $BaSiO_3$ from 52 to 296°K. The sample was prepared by heating between 1000 and 1410°C a stoichiometric mixture of reagent-grade $BaCO_3$ and pure quartz. The material was ground, analyzed and adjusted for composition, pelletized, and reheated. This process was repeated nine times with a total heating time of 247 hours. The x-ray diffraction patterns did not agree with existing data, but did not show any uncombined oxides. Chemical analysis yielded 71.95 per cent BaO and 28.17 per cent SiO_2, the theoretical being 71.85 and 28.15 per cent, respectively.

The Debye-Einstein heat-capacity function:

$$C = D(151/T) + E(213/T) + E(450/T) + 2E(973/T)$$

given by Weller and Kelley was used below 52°K.

<u>Barium 1:2 - Silicate, $BaO \cdot 2SiO_2$, 273.509</u>

W. W. Weller and K. K. Kelley (Bureau of Mines RI 6556, 1964) reported heat-capacity measurements on $BaSi_2O_5$ between 52 and 296°K. The sample was prepared by heating a stoichiometric mixture of $BaCO_3$ and pure quartz at temperatures ranging from 950 to 1350°C. Prolonged heating at 1350°C was done to stabilize the compound. [R. Barany, E. G. King, and S. S. Todd (J. Am. Chem. Soc. <u>79</u>, 3639 (1957)) reported a slow change in x-ray patterns at room temperature for a sample prepared in a similar manner but with insufficient heating]. X-ray examination of the sample before and after the heat-capacity measurements showed no significant changes in the pattern. Chemical analysis yielded 55.85 per cent BaO and 43.77 per cent SiO_2 with 0.32 per cent Al_2O_3, the theoretical being 56.06 and 43.94 per cent BaO and SiO_2, respectively.

The Debye-Einstein heat-capacity function:

$$C = D(120/T) + 2E(235/T) + 3E(632/T) + 2E(1415/T)$$

given by Weller and Kelley was used below 52°K.

Barium 2:3 - Silicate, $2BaO \cdot 3SiO_2$, 486.9332

W. W. Weller and K. K. Kelley (Bureau of Mines RI 6556, 1964) reported heat-capacity measurements on $Ba_2Si_3O_8$ from 52 to 296°K. The sample was prepared by repeated heating, grinding, analyzing and adjusting for composition, and pelletizing at high pressures prior to the heating. The total heating times were 11 days at 1050°C, 78 hours at 1200°C, 24 hours at 1250°C, and 6 hours at 1300°C. X-ray patterns agreed with existing data and chemical analysis yielded 63.00 per cent BaO, 37.05 per cent SiO_2, and 0.01 per cent Fe_2O_3 and Al_2O_3, the theoretical being 62.98 and 37.02 per cent BaO and SiO_2 respectively.

The Debye-Einstein heat-capacity function:

$$C = D(105/T) + 3E(176/T) + 3E(443/T) + 2E(603/T) + 4E(1240/T)$$

given by Weller and Kelley was used below 52°K.

Barium 2:1 - Silicate, $2BaO \cdot SiO_2$, 366.7636

W. W. Weller and K. K. Kelley (Bureau of Mines RI 6556, 1964) measured the heat capacity of Ba_2SiO_4 from 52 to 296°K. The sample was prepared by heating a stoichiometric mixture of $BaCO_3$ and pure quartz, between 1000 and 1300°C. The material was ground, analyzed and adjusted for composition and reheated. This process was repeated five times with total heating times of 10 days at 1000 - 1150°C and 16 hours at 1150 - 1300°C. X-ray patterns agreed with existing data and the chemical analysis yielded 83.78 per cent BaO and 16.37 per cent SiO_2, the theoretical being 83.62 and 16.38 per cent, respectively.

The Debye-Einstein heat-capacity function:

$$C = D(115/T) + 2E(185/T) + 2E(405/T) + 2E(1080/T)$$

given by Weller and Kelley was used below 52°K.

Calcium 1:1 - Zirconate, $CaO \cdot ZrO_2$, 179.2982

E. G. King and W. W. Weller (Bureau of Mines RI 5571, 1960) reported heat-capacity measurements of $CaZrO_3$ from 53 to 296°K. The sample was prepared by heating between 1200 and 1500°C a stoichiometric mixture of $CaCO_3$ and ZrO_2. Seven cycles of grinding, analyzing and adjusting for composition, and heating were performed. The total heating times were 30 hours between 1200 and 1300°C and 32 hours between 1400 and 1500°C. Chemical analysis of the final product was 31.19 per cent CaO and 68.16 per cent ZrO_2, the theoretical being 31.28 and 68.72 per cent respectively.

The Debye-Einstein heat-capacity function:

$$C = D(233/T) + 2E(355/T) + 2E(722/T)$$

given by King and Weller was used below 53°K.

Strontium 1:1 - Zirconate, $SrO \cdot ZrO_2$, 226.8382

E. G. King and W. W. Weller (Bureau of Mines RI 5571, 1960) reported heat-capacity measurements on $SrZrO_3$ from 53 to 296°K. The sample was prepared by heating a stoichiometric mixture of $SrCO_3$ and ZrO_2. The heating times were as follows: 24 hours at 1000°C, 6 hours between 1350 and 1400°C, 8 hours between 1350 and 1470°C, 12 hours between 1350 and 1450°C, and 12 hours between 1300 and 1350°C. The material was ground and thoroughly mixed between the heats. Chemical analysis yielded 45.56 per cent SrO and 54.42 per cent ZrO_2, the theoretical being 45.68 and 54.32 per cent, respectively. X-ray diffraction patterns were in agreement with existing data and no unreacted oxides were observed.

The Debye-Einstein heat-capacity equation:

$$C = D(177/T) + 2E(308/T) + 2E(678/T)$$

given by King and Weller was used below 53°K.

Barium 1:1 - Zirconate, $BaO \cdot ZrO_2$, 276.5582

E. G. King and W. W. Weller (Bureau of Mines RI 5571, 1963) measured the heat capacity of $BaZrO_3$ from 54 to 296°K. The sample was prepared by heating a stoichiometric mixture of $BaCO_3$ and ZrO_2. The heating times were as follows: 24 hours at 1000°C, 6 hours at 1350 - 1400°C, 20 hours at 1350 - 1470°C, and 12 hours at 1300 - 1350°C, the sample being ground and thoroughly mixed between heats. Chemical analysis of the final product yielded 55.40 per cent BaO and 44.63 per cent ZrO_2, the theoretical being 55.45 and 44.55 per cent, respectively. The x-ray diffraction pattern was in agreement with the ASTM catalog.

The Debye-Einstein heat-capacity equation:

$$C = D(144/T) + 2E(273/T) + 2E(692/T)$$

given by King and Weller was used below 54°K.

Sodium 1:1 - Tungstate, $Na_2O \cdot WO_3$, 293.8272

E. G. King and Weller (Bureau of Mines RI 5791, 1961) measured the heat capacity of Na_2WO_4 from 52 to 300°K. The sample was prepared by heating a stoichiometric mixture of Na_2CO_3 and H_2WO_4. The mixture was melted twice in platinum and heated four times for a total of 4.5 days at 460 to 600°C. After each melting and heating process, the material was ground, analyzed and adjusted for composition. Chemical analysis of the final product yielded 78.95 per cent WO_3, the theoretical being 78.91 per cent. The x-ray diffraction pattern was in agreement with that given in the ASTM catalog.

The Debye-Einstein heat-capacity function:

$$C = D(168/T) + 2E(225/T) + 2E(456/T) + E(531/T) + E(1288/T)$$

given by King and Weller was used below 52°K.

Sodium 1:2 - Tungstate, $Na_2O \cdot 2WO_3$, 525.6754

W. W. Weller and K. K. Kelley (Bureau of Mines RI 6191, 1963) measured the heat capacity of $Na_2W_2O_7$ from 53 to 296°K. The sample was prepared by heating a stoichiometric mixture of Na_2CO_3 and H_2WO_4. Chemical analysis of the product yielded 87.78 per cent WO_3, the theoretical being 88.21 per cent. Impurities were 0.24 per cent Al_2O_3 and 0.24 per cent SiO_2. X-ray diffraction patterns agreed with existing data.

The Debye-Einstein heat-capacity function:

$$C = D(123/T) + 4E(210/T) + 4E(501/T) + 2E(1229/T)$$

given by Weller and Kelley was used below 53°K.

Magnesium 1:1 - Tungstate, $MgO \cdot WO_3$, 272.1596

E. G. King and W. W. Weller (Bureau of Mines RI 5791, 1961) measured the heat capacity of $MgWO_4$ from 53 to 296°K. The sample was prepared by heating a stoichiometric mixture of MgO and H_2WO_4 at 900°C. The process of grinding, chemical analysis, adjusting of composition, and heating was repeated eight times. The total heating time was five days. Chemical analysis of the final product yielded 14.79 per cent MgO and 85.24 per cent WO_3, the theoretical being 14.81 and 85.19 per cent, respectively. X-ray diffraction patterns agreed with existing data.

The Debye-Einstein heat-capacity function:

$$C = D(233/T) + E(319/T) + 3E(487/T) + E(1270/T)$$

given by King and Weller was used below 53°K.

Calcium 1:1 - Tungstate, $CaO \cdot WO_3$, 287.9276

E. G. King and W. W. Weller (Bureau of Mines RI 5791, 1961) determined the heat capacity of $CaWO_4$ from 52 to 296°K. The sample was prepared by heating a stoichiometric mixture of $CaCO_3$ and H_2WO_4 at temperatures between 680 and 800°C. The grinding, chemical analysis, adjusting of composition, and heating procedure was repeated seven times. The total heating times were two days at 680°C and ten days at 800°C. The final product was 19.49 per cent CaO and 80.59 per cent WO_3, the theoretical being 19.48 and 80.52 per cent, respectively. The x-ray diffraction pattern agreed with existing data.

The Debye-Einstein heat-capacity function:

$$C = D(180/T) + E(220/T) + E(387/T) + 2E(558/T) + E(1350/T)$$

given by King and Weller was used below 52°K.

Potassium Hydrogen Fluoride, KHF_2, 78.10677

E. F. Westrum, Jr. and K. S. Pitzer (J. Am. Chem. Soc. 71, 1940 (1949)) reported heat-capacity measurements from 16 to 316°K and enthalpy measurements relative to 298.15°K up to 523°K. The sample was prepared by reacting "chemically pure" K_2CO_3 and aqueous hydrofluoric acid. The solution, containing several per cent excess of HF, was concentrated by boiling and KHF_2 precipitated by controlled cooling. To obtain higher yields the mother liquor was further concentrated with an excess of HF and ethyl alcohol used as precipitant. Ethyl alcohol was used also to wash the KHF_2 crystals. The alcohol and water, if any, were removed by vacuum drying at 40°C. Chemical analysis of the sample yielded 48.5 ± 0.2 per cent F, the theoretical being 48.65 per cent. Titration of the acid hydrogen yielded 100.03 ± 0.06 per cent of the theoretical. The data were used to obtain the table of thermodynamic properties from 0° to 530°K.

Phosphorus Pentoxide, P_4O_{10}, 283.8892

R. J. L. Andow, J. F. Counsell, H. McKerrell, and J. F. Martin (Trans. Far. Soc. 59, 2702 (1963)) reported heat-capacity measurements on hexagonal P_4O_{10} from 12 to 325°K. The sample was of commercial source that was further purified by two vacuum sublimations. Chemical analysis showed the material to be 99.8 per cent and x-ray diffraction pattern was in agreement with the hexagonal form. Thermodynamic properties from 0 to 330°K were calculated from the data.

Chapter 14

THE DETERMINATION OF HEATS OF FORMATION OF REFRACTORY COMPOUNDS

George T. Armstrong and Eugene S. Domalski

1. INTRODUCTION

Refractory compounds have an application in propellants as possible ingredients of air breathing engines. This chapter reviews some of the results of a study [6] of the heats of formation of refractory borides, of which the experimental part was carried out for the Air Force Aero Propulsion Laboratory, Wright Patterson Air Force Base (A. Zengel, technical advisor). A recalculation and reappraisal of the data and some new analyses of the samples studied were carried out in this program, leading to revisions of some of the conclusions drawn in the earlier report. This work was presented at the 4th Meeting of the Working Group in Thermochemistry [7]. The heats of combustion in fluorine of several boron compounds were measured. To determine auxiliary data for calculating the heats of formation of the compounds, the heats of combustion in fluorine of polytetrafluoroethylene (Teflon), graphite, and boron were determined also. Analysis of the compounds becomes a major problem in deriving heats of formation from the observed calorimetric data. The effects of analysis in the interpretation of the data are discussed. The presentation is in the nature of a summary. Details will be presented in projected publications.

2. SAMPLE PREPARATION

Because boron, graphite and some borides react spontaneously on exposure to fluorine, the samples were protected from pre-ignition reaction by a covering of Teflon. In order to sustain combustion until the sample was essentially completely consumed, the samples were mixed with powdered Teflon. The sample preparation technique was developed for these experiments. Figure 1 shows a schematic cross section of the sample pellet. A pelleted mixture of powdered Teflon with the powdered refractory material forms the core. This is enclosed in a Teflon film bag and then further protected with a thin outer layer of compressed powdered Teflon. With this method of sample preparation combustions were essentially complete.

Figure 1. SAMPLE CONFIGURATION FOR REACTIVE SAMPLES FOR FLUORINE BOMB CALORIMETRY

Cylindrical Pellet

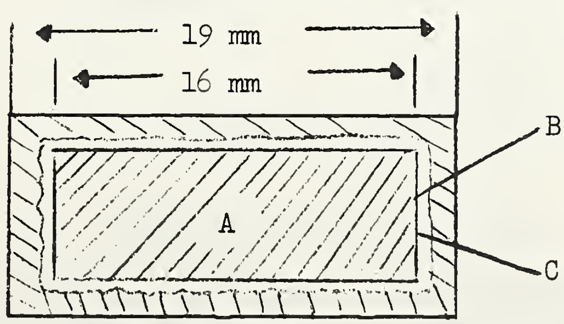

A. Mixture of sample (0.15-0.25 g) and Teflon 7 (1.3-2.0 g).
B. Teflon film bag (0.3 g).
C. Teflon 7 (0.7-0.8 g).

3. COMBUSTION OF TEFLON

Because there is Teflon present in each of the combustion experiments with a refractory material, the energy of combustion of the Teflon used in the mixtures was determined. The data from a typical combustion experiment with Teflon are shown in Table I. Seven experiments of this type were carried out, and are summarized in Table II. The experiments were reproducible and led to a mean value of -10372.8 J g^{-1} with a standard deviation of the mean of 0.77 J g^{-1} for ΔE^{o}_{303}. Because of differences in preparation the energy of combustion of Teflon may not be the same from batch to batch. The energy of combustion must therefore be determined for each batch that is to be used.

TABLE I. TEFLON COMBUSTION EXPERIMENT (TYPICAL)

Experiment No.	4
Mass Teflon, g	4.44373
P_{F_2}, atm.	22.3
ε, J deg^{-1}	14,802.21
Δt_c, deg	3.11615
$-\varepsilon \cdot \Delta t_c$, J	-46,125.9
ΔE fuse, J	17.5
ΔE gas, J	21.3
$\Delta E^{o}_{303^{o}K}$ J g^{-1}	-10,371.3

TABLE II. TEFLON COMBUSTION EXPERIMENTS (SUMMARY)

Experiment No.	ΔE^{o}_{303}, J g^{-1}
1	-10372.7
2	-10376.3
3	-10374.1
4	-10371.3
5	-10372.4
6	-10373.2
7	-10369.9
Mean	-10372.8
σ	0.77

$\Delta H^{o}_{298} = -10369.4$ J g^{-1}

C_2F_4 (polymer) + $2F_2(g) = 2CF_4(g)$

4. COMBUSTION OF GRAPHITE

To provide auxiliary data for calculating the heat of formation of boron carbide, the heat of combustion of carbon (graphite) is needed. Combustion measurements on graphite were carried out to provide this data.

Table III shows the characteristics of the sample that was used.

TABLE III. ELEMENTAL CARBON

Crystal form	- graphite crystals of -35 on 100 mesh
a = 2.460A°; C = 6.721 A°	
spectroscopic grade	
ash	< 10 ppm
Metals	insignificant
O (neutron activation	< 86 ppm
N (neutron activation)	< 204 ppm
C by difference	> 99.97 percent

Table IV gives the results of a typical experiment. A series of seven experiments of this type was carried out which is summarized in Table V.

TABLE IV. GRAPHITE - TEFLON COMBUSTION EXPERIMENT (TYPICAL)

Experiment No.	1
Mass graphite, g	0.243088
Mass Teflon, g	2.419090
P_{F_2}, atm.	21.1
ε, J deg^{-1}	14,758.06
Δt_c, deg.	2.97695
$-\varepsilon \cdot \Delta t_c$, J	-43,934.0
ΔE fuse, J	17.2
ΔE gas, J	8.4
ΔE° (Teflon), J	25,092.7
ΔE°_{303}, graphite sample, J g^{-1}	-77,402.8

TABLE V. GRAPHITE - TEFLON COMBUSTION EXPERIMENTS (SUMMARY)

Experiment	$-\Delta E^\circ_{303}$, J g^{-1}
1	77,402.8
2	77,462.3
3	77,424.4
4	77,398.1
5	77,437.5
6	77,383.0
7	77,335.7
Mean	77,406.3
σ	15.5

The measurements had a small dispersion, giving a standard deviation of the mean of about 0.02 percent. The energy of combustion observed for the sample was adjusted as shown in Table VI to obtain the standard enthalpy of formation of $CF_4(g)$. The value obtained is more negative than most values reported for carbon tetrafluoride and tends to substantiate the more negative values suggested for the heat of formation of HF, though it is not as negative as was calculated by Cox et al. [1].

TABLE VI. CARBON TETRAFLUORIDE - HEAT OF FORMATION

	$J\ g^{-1}$	
$-\Delta E^{\circ}_{303}$ (per gram of graphite sample)	77,406.3	
Energy of combustion of impurities	0.0	(0.029% impurities)
$\Delta E^{\circ}_{303} - \Delta E^{\circ}_{298}$	- 4.2	
$-\Delta E^{\circ}_{f\,298}$ (per gram of pure carbon)	77,424.6	
$-\Delta nRT$	209.8	
$-\Delta H^{\circ}_{f\,298}$ $(CF_4)(g)$	77,634.4	(222.87 kcal mol^{-1})
Uncertainty		0.38 kcal mol^{-1}

C (graphite) + $2F_2(g) = CF_4(g)$

5. COMBUSTION OF BORON

Because boron is a component of all the refractory compounds later described here, a knowledge of its heat of combustion is necessary to calculate their heats of formation. Although the heat of combustion of boron in fluorine has recently been accurately determined, the heats of formation of the refractory borides are so sensitive to its value that a redetermination in the same calorimeter in which the rest of the experiments were being carried out was deemed advisable. A series of combustion measurements was made on elemental boron to provide the required data. Table VII lists the characteristics of the boron sample that was burned.

TABLE VII. ELEMENTAL BORON

β-rhombohedral crystals of -100 mesh
prepared by hydrogen reduction of BBr_3
on a substrate of zone refined boron.

		percent		
Analysis =	Metals	0.120	(a)	(Fe = 0.079) (b)
	C	0.11	(a)	
	N	$<$ 0.005	(c)	
	O	0.161	(d)	
	B (by difference)	99.604		

(a) by chemical analysis
(b) Spectroscopic analysis showed $<$ 0.01% Fe
(c) Kjeldahl
(d) Neutron activation analysis. C, N, and O were assumed to be present as B_4C, BN, and B_2O_3, respectively.

Table VIII lists the data obtained from a typical calorimetric experiment with boron. Ten experiments of this type were carried out, which are summarized in Table IX. The experiments were in good agreement with each other, giving a standard deviation of the mean of about 0.05 percent. Table X shows the reduction of the observed energy of combustion to the standard enthalpy of combustion, which is the enthalpy of formation of $BF_3(g)$. The observed average, -271.21 kcal mol^{-1}, for the enthalpy of formation of $BF_3(g)$ is in good agreement with a value (-271.65 ±0.22 kcal mol^{-1}) by Johnson, Feder and Hubbard [2].

TABLE VIII. BORON - TEFLON COMBUSTION EXPERIMENT (TYPICAL)

Experiment No.	1
Mass boron sample, g	0.157445
Mass Teflon, g	2.767867
P_{F_2}, atm.	21.2
ε, J deg^{-1}	14,798.95
Δt_c, deg	3.05494
$-\varepsilon \cdot \Delta t_c$, J	-45,209.9
ΔE fuse, J	20.2
ΔE gas, J	13.2
$-\Delta E^{\circ}$ Teflon, J	28,710.5
ΔE°_{303} boron sample, J g^{-1}	-104,583

TABLE IX. BORON - TEFLON COMBUSTION EXPERIMENTS (SUMMARY)

Experiment No.	$-\Delta E^{\circ}_{303}$ boron sample, J g^{-1}
1	104,583
2	104,389
3	104,129
4	104,362
5	104,519
6	104,751
7	104,450
8	104,501
9	104,717
10	104,470
Mean	104,487
σ	57

TABLE X. BORON TRIFLUORIDE HEAT OF FORMATION

	$J\ g^{-1}$	
$-\Delta^{o}_{303}$ (per gram of sample)	104,487	
Energy of combustion of impurities	-556	(0.869% impurities)*
$\Delta E^{o}_{303} - \Delta E^{o}_{298}$	- 4	
$-\Delta E^{o}_{298}$ (per gram of pure boron)	104,838*	
-nRT	115	
$-\Delta H^{o}_{298}$ (boron)	104,953	(271.21 kcal mol^{-1})*
Uncertainty		0.38 kcal mol^{-1})

(The chemical atomic weight of the boron in the sample was measured and found to be 10.812 ±0.005 (based on C^{12} = 12).

$B(C,\beta) + 3/2\ F_2(g) = BF_3(g)$

*Values listed in this table are subject to small revision on the basis of reanalysis of the sample which is now in progress.

6. COMBUSTION OF BORON CARBIDE AND ALUMINUM BORIDES

The combustion measurements on the refractory compounds showed good reproducibility and in some cases the precision was comparable to that of the combustion of boron and graphite in fluorine. A series of eight combustion measurements on boron carbide is summarized in Table XI. The standard error is 0.04 percent. The standard errors of $A\ell B_2$, α-$A\ell B_{12}$, and γ-$A\ell B_{12}$ were 0.08, 0.05, and 0.09 percent, respectively.

TABLE XI. BORON CARBIDE COMBUSTION (SUMMARY)

Experiment	$-\Delta E^{o}_{303}$ B_4C sample, $J\ g^{-1}$
1	96,995.3
2	97,019.7
3	96,977.1
4	97,241.4
5	97,106.2
6	97,082.6
7	97,197.7
8	97,279.6
Mean	97,112.5
σ	40.8

Boron carbide burned to form $BF_3(g)$ and $CF_4(g)$. The aluminum borides burned to form $A\ell F_3(c)$ and $BF_3(g)$. Observed energies of combustion were used to calculate the standard enthalpies of combustion of the pure compounds as shown in Table XII. Note, however, that in order to make this calculation detailed information on the make-up of the samples is required. Table XII is based on a hypothetical composition for each sample, obtained by normalizing the composition determined by analysis. In normalizing the composition the presumption is made that the total error of the analysis (deviation from 100 percent) is divided among the observed constituents in proportion to their abundance. The limits imposed by assumptions of this type upon the determination of the heat of formation of the compound are discussed in section 7.

TABLE XII. HEATS OF REACTION - ALUMINUM BORIDES AND BORON CARBIDE

$$AlB_{2.215}(c) + \frac{9.645}{2} F_2(g) = AlF_3(c) + 2.215\ BF_3(g)$$

$$AlB_{12}(c) + 39/2\ F_2(g) = AlF_3(c) + 12\ BF_3(g)$$

$$B_4C(c) + 8F_2(g) = 4BF_3(g) + CF_4(g)$$

(Molecular weights)		$AlB_{2.215}$ (50.9279)	α-AlB_{12} (156.7135)	γ-AlB_{12} (156.7135)	B_4C (55.25515)
(1) No. of Experiments		6	11	2	8
(2) $-\Delta E^\circ_{303}$ (sample),	J g^{-1}	76,182.3	92,926.5	95,354.0	97,112.5
(3) σ	J g^{-1}	59.7	45.8	85.2	40.8
(4) Impurity (%)		2.768	3.210	4.766	0.700*
(5) Impurity contribution,	J g^{-1}	-731.7	-1027.7	-4365.2	-196.4*
(6) $\Delta E^\circ_{303} - \Delta E^\circ_{298}$,	J g^{-1}	+2.7	+0.5	+0.5	-3.6
(7) $-\Delta E^\circ_{298}$ (compound)	J g^{-1}	77,601.2	94,944.4	95,542.8	97,595.7*
(8) $-\Delta nRT$ (compound)	J g^{-1}	139.7	120.6	120.6	136.8
(9) $-\Delta H^\circ_{298}$ (compound)	J g^{-1}	77,740.9	95,065.0	95,663.4	97,732.5*
(10) $-\Delta H^\circ_{298}$ (compound)	kcal mol^{-1}	946.27	3560.7	3583.1	1290.7*

*A reanalysis of some samples is being undertaken, which may cause modification of some values listed.

NOTE: The above table is based upon sample compositions normalized to total 1.0000 on the basis that the error in each element is proportional to its amount present. Items 1, 2, 3 are unaffected by any manner of treating the composition, but the remaining items are affected.

7. ANALYSIS OF COMPOSITION AND THE INTERPRETATION OF COMBUSTION-CALORIMETRIC DATA OF REFRACTORY BORIDES

The samples of boron compounds used in the study described here were analyzed chemically, spectroscopically, by neutron activation, and by X-radiation as indicated in Table XIII. The results are summarized in Table XIV. The stoichiometric proportions of the principal elements are shown at the bottom of the table. Deviations of the ratios of the principal elements from the stoichiometric ratios are large, and deviations of the sum of all substances from 1.00 (100 percent) are also large. The oxygen contents range from 0.002 to 0.013 and thus form a significant amount. The validity of the neutron activation analysis for these samples is now questionable because it has been found that boron interferes [3]. Deviations of the total composition from 1.00, amounting to .0226, 0.0160, 0.0041, and 0.0271 cannot be accounted for solely on the basis of errors in the oxygen analysis. Appreciable errors in the analyses for boron, aluminum and carbon are suggested by this fact. Because of this the validity of the observed deviation from stoichiometry is also brought into question. This class of compounds cannot be presumed to be stoichiometric. Thus, an analysis which might be quite adequate to assign a formula to a stoichiometric compound is quite inadequate to assign a composition to a non-stoichiometric compound.

TABLE XIII. METHOD OF ANALYSIS OF BORIDES

Aℓ	Carbonate fusion, precipitation as hydroxide and roasting to $A\ell_2O_3$.
B	Carbonate fusion followed by boric acid determination - titration using mannitol.
C	CO_2 determination.
N	Kjeldahl
O	Neutron activation analysis.
Si, Metal	Chemical tests approximately verified by spectroscopic analysis.

Also determined: crystal unit cell dimensions by X-ray diffraction.

TABLE XIV. ANALYSES OF SOME BORIDES

Element \ Compound	B_4C	$A\ell B_2$	α-$A\ell B_{12}$	γ-$A\ell B_{12}$
Aℓ	-	0.5300	0.1701	0.1603
B	0.777	.4704	.8150	.8071
C	.196	.0008	.0011	.0007
N	.0021	.0030	.0027	.0002
O	.0019	.0100	.0130	.0036
Si	.0002	.0003	.0005	-
Metals	.0002	.0015	.0017	.0010
Total	0.9774	1.0160	1.0041	0.9729
Principal Ratio	4.40	2.215	11.96	12.57

Stoichiometric Composition

Aℓ		.55513	.17217	.17217
B	.7826	.44487	.82783	.82783
C	.2174			

The analysis gives little or no information about the distribution of impurities in the compound. Because of an ambiguity here the calculation of heat of formation would be ambiguous even if no uncertainty existed in the elemental analysis. In treating the distribution of impurities, four methods have been applied:

(1), (2) The compound is considered to be stoichiometric and the non metal impurities are combined all with one element. Excess B or Aℓ remaining is considered to be present as the free element.

(3) The compound is considered to be stoichiometric and the non-metal impurities are distributed between B and Aℓ in proportion to the stoichiometric ratio of B to Aℓ. Excess B or Aℓ is considered to be present as the free element.

(4) The compound is considered to be non-stoichiometric and the non-metal impurities are distributed between B and Aℓ in proportion to the number of moles of B and Aℓ.

Table XV gives heats of formation calculated for each of the samples studied on each basis. The combustion data (item 10) given in Table XII was used in calculating the heats of formation of $A\ell B_{2.215}$ by method (4), and of α-$A\ell B_{12}$ and γ-$A\ell B_{12}$ by method (3). For auxiliary data we used the heats of formation of CF_4 and BF_3 given in Tables VI and X, respectively, and the heat of formation of $A\ell F_3$(c), -360.37 kcal mol^{-1}, from Domalski and Armstrong [5]. In calculating the heats of formation of B_4C and the other values for the aluminum borides, the intermediate calculations are not shown in Table XII.

Table XII illustrates a calculation of the heat of combustion of B_4C, which would lead to ΔH°_{f298} = -19.5 kcal mol^{-1}. This calculation illustrates the effect of an uncertainty in the relative amounts of the elements present. In making this calculation, because of the variability in the analysis for B and C, we made the assumption that all material in the sample not present as Si, metals, B_2O_3 or BN is B_4C in which the elements are present in their proper stoichiometric proportions, and that there was no excess B or C present.

TABLE XV. EFFECT OF TREATMENT OF COMPOSITION ON THE VALUES CALCULATED FOR HEATS OF FORMATION OF ALUMINUM BORIDES AND BORON CARBIDE

Formula Assumed	ΔH_f, kcal/mol		(kcal/g atom)	
Method	(1) (Aℓ)	(2) (B)	(3)	(4)
$A\ell B_2$	-15.9	-15.8	-16.1 (-5.37)	
$A\ell B_{2.215}$				-16.2 (-5.04)
α-$A\ell B_{12}$	-65.0	-61.9	-61.5 (-4.73)	
α-$A\ell B_{11.96}$				-61.3 (-4.73)
γ-$A\ell B_{12}$	-39.4	-39.0	-39.1 (-3.01)	
γ-$A\ell B_{12.57}$				-37.9 (-2.79)
B_4C		-26.5 (-5.30)		
$B_{4.4}C$				-27.2 (-5.04)

NOTE: For the above calculations the observed compositions were normalized to a total of 1.0000 by assuming the error in each element to be proportional to the amount of it present.

The heats of formation calculated on the bases (1), (2), (3), (4), have ranges of 0.4 kcal mol^{-1} for AlB_2, 3.1 kcal mol^{-1} for α-AlB_{12}, 2.5 kcal mol^{-1} for γ-AlB_{12} and 0.7 kcal mol^{-1} for B_4C. Some of the values have been converted to kcal $(gram\ atom)^{-1}$ as shown in parantheses. These differences, while large in some cases, are not intolerable in all cases. However, if one, as we have done for B_4C, now admits the possibility that an error of analysis could also be present, immediately errors of 20 to 50 kcal mol^{-1} or even more may be introduced. In the case of B_4C as compared to $B_{4.4}C$ the large calculated difference is due to the assumption that the apparent non-stoichiometry is actually an error of analysis in a compound which is truly B_4C. If, in addition, an attempt was made to account for the 2.26 percent unaccounted for in the analysis, an uncertainty up to 25 kcal mol^{-1} could occur. Similarly, the large difference of 22 kcal mol^{-1} shown in Table XV between the heats of formation of α-AlB_{12} and γ-AlB_{12} may be partly or wholly due to error of analysis. Such a large difference seems hardly reasonable for two crystal phases of the same substance.

It is apparent on the basis of the above discussion that analysis of the samples can be a major factor in obtaining reliable thermochemical data on refractory compounds. One should not presume that an adequate analysis can be obtained in a routine way.

8. CALORIMETRIC METHODS APPLICABLE TO REFRACTORY COMPOUNDS

We resumé briefly here some possible experimental methods applicable to the calorimetry of refractory compounds, with special reference to the difficulties of stoichiometry and analysis posed in the preceding section.

8.1 Direct Combination of the Elements The great advantage of this method is that the total heat measured is the heat of formation of the compound. Impurities and non-stoichiometry affect the heat of formation only in proportion to their uncertainty, whereas in processes described in section 2 below, the errors of uncertainties, impurities, and non-stoichiometry are magnified. This method may be very successful in a bomb calorimeter if one of the elements is a gas, and if the resulting compound can be assayed for amount of reaction, either by weighing or by chemical analysis of the products. Direct combination of oxygen with many metals has been very successful. Direct combination of nitrogen with boron has achieved good success also.

However, in the direct combination of two solid elements, a metal with carbon, boron, phosphorus, etc., it is difficult to obtain good results. The principal difficulty is not in initiating the reaction but in determining the amount of reaction and the identity of the phases present in the product. If one recognizes the difficulty that one has in obtaining good quality single phase compounds in a preparative furnace process, in which great care can be taken in temperature control, zone refining, selective extraction and so on, it seems probable that when the elements combine rapidly in an uncontrolled process the quality of the product will suffer.

A slight modification of direct combination is a displacement reaction involving two solid materials. While Gross [4] has had good success in the reaction of Al with PbF_2 in such a displacement reaction, the questions raised in the previous paragraph become of equally great importance here, when very refractory materials are considered.

8.2 Combustion of the Compound and of the Separate Elements in a Reactive Atmosphere This is the procedure used in the combustion of refractory borides in fluorine. It can be successful because of the high precision of the bomb calorimetric process. Even when small differences between large heats of combustion are taken, the residual error in the heat of formation of the compound may be less than 1 kcal mol^{-1}. However, much depends upon the knowledge of the composition of the sample and the completeness of reaction. Because of the taking of differences between large heats of combustion an uncertainty in composition or in completeness of combustion affects the heat of formation in a disproportionate way.

8.3 Solution of the Compound and of the Separate Elements in a Suitable Solvent in a Calorimeter The principal problem in applying this technique to refractory compounds is to find a suitable solvent. Provided this is done, the heat of solution is generally a much smaller number than the heat of combustion. While differences must be taken as in section 8.2, the differences are between much smaller numbers. The effect of lack of knowledge about the composition is correspondingly less. The potentialities of boric oxide or some similar solvent at a high temperature should be examined.

9. REFERENCES

[1] J. D. Cox, H. A. Gundry, and A. J. Head, Trans. Faraday Soc. 61, 1594-1600 (1965).

[2] G. K. Johnson, H. M. Feder, and W. N. Hubbard, J. Phys. Chem. 70, 1-6 (1966).

[3] (a) G. H. Andersen, General Atomic, San Diego, California, private communication
(b) Kaman Nuclear, Technical Note (TN-105), 10 June 1965.

[4] P. Gross, C. Hayman, and D. L. Levi, Trans. Faraday Soc. 50, 477-80 (1954).

[5] E. S. Domalski and G. T. Armstrong, J. Research NBS 69A, 137-147 (1965).

[6] E. S. Domalski and G.T. Armstrong, Technical Report AFAPL-TR-65-110, "Heats of Formation of Metallic Borides by Fluorine Bomb Calorimetry", prepared under USAF Delivery Order Nr. 33(615)64-1003, for the Air Force Aero Propulsion Laboratory, Res. and Devel. Div., Air Force Systems Command, Wright-Patterson Air Force Base, Ohio.

[7] G.T. Armstrong and E. S. Domalski, Interagency Chemical Rocket Propulsion Group, Working Group on Thermochemistry, Proceedings of the 4th Meeting, Vol. I, March 1966, Cape Kennedy, Fla.

Chapter 15

HEATS OF FORMATION OF SOME FLUORINE CONTAINING OXIDIZERS

George T. Armstrong
Heat Division, Institute for Basic Standards

ABSTRACT

The status of our knowledge of the heats of formation of selected fluorides of oxygen, nitrogen, chlorine and carbon is reviewed. A brief description is given of a flame-calorimetry study of oxygen difluoride at the National Bureau of Standards.

INTRODUCTION

This report is a review of the status of the knowledge of the heats of formation of a number of oxidizers commonly considered for use in propulsion. The work was supported in part by the Bureau of Naval Weapons, and in part by the Air Force Office of Scientific Research.

1. OXYGEN DIFLUORIDE

The importance of the heat of formation of oxygen difluoride is based on several factors. The compound provides a mixed oxygen-fluorine oxidizer which is readily liquified, and which is less reactive than fluorine (higher activation energy). It provides a reference value for the O-F bond energy, useful for estimating energy potentialities of more complex propellants containing O-F linkages. A relevant bond energy can be derived most nearly unambiguously from F_2O.

Complications make a difficult problem of the determination of the heat of formation. Although the heat of formation is small, no study has been reported which is based on a reaction liberating only a small amount of heat. No direct combination of the elements has been carried out. The reaction energies of F_2O and of the separate elements F_2 and O_2 with hydrogen are large, leading to a loss of accuracy in taking the difference. The corrosive character of HF, found among the products, leads to difficulties of checking the stoichiometry of the reaction and also results in extra energy from corrosion. Reactions with reducing solutions may lead to multiple products for which the problems of stoichiometry and of determining the amount of each reaction become difficult. The reaction of a polyvalent element would be expected to lead to complex products, such as a mixture of the oxide, the fluoride and the oxyfluoride.

In Table I are three reactions studied some years ago by Ruff and Menzel [1]. When treated together, $\Delta H_f[F_2O(g)] = -\Delta H(a) + \Delta H(b) + \Delta H(c) = +4.7$ kcal mol^{-1}. Our recalculation from equation (a) alone leads to $\Delta H_f[F_2O(g)] = -1.1$ kcal mol^{-1}.

TABLE I. $F_2O(g)$ HEAT OF FORMATION

Measurements of Ruff and Menzel [1].

(a) $OF_2(g) + 2H_2(g) + 2NaOH$ (excess aq. 20%) = 2NaF (in aq. NaOH) + $3H_2O(\ell)$
$\Delta H = -254.9$ kcal mol^{-1} $\quad\sigma = 0.6$ kcal mol^{-1}

(b) $1/2\ O_2(g) + H_2(g) = H_2O(\ell)$
$\Delta H = -68.5$ kcal mol^{-1} $\quad\sigma = 0.1$ kcal mol^{-1}

(c) $F_2 + H_2 + 2NaOH$ (excess aq. 20%) = 2NaF (in aq. NaOH) + $2H_2O(\ell)$
$\Delta H = -181.7$ kcal mol^{-1} $\quad\sigma = 1.15$ kcal mol^{-1}

In Table II are shown three reactions studied by Wartenberg and Klinkott [2]. When Evans, et al. [3] recalculated $\Delta H_f^o[F_2O(g)]$ using auxiliary data current at the time, they found +7.1, +6.0, and +9.7 kcal mol^{-1}, respectively, from equations (a), (b) and (c). More recently Evans [4] recalculated the same values, using auxiliary data prepared for NBS Technical Note 270-1 [5] et seq. and found +6.9, +1.4, and +8.8 kcal mol^{-1}, respectively.

TABLE II. $F_2O(g)$ HEAT OF FORMATION

Measurements of Wartenberg and Klinkott [2].

(a) $F_2O(g) + 2KOH$ (in excess KOH aq. 40%) = $[2KF + H_2O]$(in aq. KOH) + $O_2(g)$
$\Delta H^o_{291} = -125.75$ kcal mol^{-1} $\quad\sigma = 0.75$ kcal mol^{-1}

(b) $F_2O(g)+[6KI+2HF]$(in excess aq. sol'n) = $[4KF+2KI_3+H_2O]$(in aq. KI HF sol'n)
$\Delta H^o_{291} = -176.55$ kcal mol^{-1} $\quad\sigma = 0.82$ kcal mol^{-1}

(c) $F_2O(g) + 4HBr$ (in excess HBr aq. 45%) = $[2HF + 4Br_2]$ (in aq. HBr)
$\Delta H^o_{291} = -134.36$ kcal mol^{-1} $\quad\sigma = 0.51$ kcal mol^{-1}

The experiments of Ruff and Menzel, and of Wartenberg and Klinkott were done many years ago, at a time when techniques for handling and analyzing fluorine compounds were relatively little developed. Characterization of the reactions and description of the experiments were limited. They have been reworked until probably all the useful information that can be drawn from them has been obtained, still without reconciliation.

In a more recent study, Bisbee and Hamilton [6,7], measured the reaction of F_2O with H_2 in a bomb calorimeter. (Table III). The reported value, $\Delta H_{f298}[F_2O(g)] = -4.4$ kcal mol^{-1}, is undoubtedly the best value available today for this substance. Nevertheless, certain objections can be raised to the work, which may not be trivial. The measurements were made in a stationary bomb, using a fairly massive internal container for $F_2O(g)$ which was ruptured to initiate reaction with H_2. The reaction products consisted of H_2O and HF in a condensed phase, formed in the presence of excess $H_2O(\ell)$. The formation of a homogeneous HF (aq) phase was presumed. However, experience in reactions in which condensation occurs in a stationary bomb indicates that much of the condensation would occur on the walls and would form droplets of a solution quite different from the bulk solution. Mixing these two solutions would evolve heat in addition to that which was measured. The massive F_2O ampoule could also retain significant quantities of heat for an appreciable time and the complete equilibration of the heat distribution was not described. Both of these processes would appear to act in the same direction, causing the measured amount of heat to be less than could have been evolved if equilibrium had been achieved. If any error of these types exists in these experiments, a less negative heat of formation would be indicated for F_2O than was reported.

TABLE III. $F_2O(g)$ HEAT OF FORMATION

Measurements of W. R. Bisbee and J. V. Hamilton [6,7].

(a) $F_2O(g) + H_2 = H_2O(\ell) + 2HF(aq.\infty)$

$\Delta H^o_{298} = -222.93$ kcal mol^{-1} ± 0.76 kcal mol^{-1}

$\Delta H^o_{f298}[F_2O(g)] = -4.4$ kcal mol^{-1} (reported)

Without going into detail with respect to the other oxygen fluorides, we list a summary in Table IV of the best values available for the heats of formation of the known compounds of oxygen with fluorine.

TABLE IV. OXYGEN FLUORIDES, HEATS OF FORMATION

			ΔH_f kcal mol^{-1}	
FO			41	[5,8]
FO_2			(>38)	[9]
F_2O			-4.4	[6,7]
F_2O_2	+4.73	→	+4.3	[5,10]
F_2O_3	+6.24	→	+3.8	[5,10]
F_2O_4			-	-

On the basis of the information given above, it appears that there is a substantial basis for doubt that the heat of formation of $F_2O(g)$ has been finally settled. However, pending the results of other work now under way (see section 6) little benefit would be expected to accrue from starting additional work.

2. CHLORINE FLUORIDES

In Table V are listed six reactions which have been used for calculating the heats of formation of chlorine mono- and trifluoride. These reactions have been reviewed by Evans, et al. [3], and by Stull, et al. [7], and it appears that all information that can be gleaned from them has been obtained. In view of the relative lack of attention to detail in most of the early work, no further resolution of the discrepancies that remain can be expected without additional work. About 1.5 kcal ambiguity exists in the dissociation energy of $C\ell F$ as measured spectroscopically because of lack of information about the assignment of states to the product atoms. The heat of formation of $C\ell F$ can be -11.9 or -13.5 kcal mol^{-1} depending on the choice. The less negative value is favored by direct calorimetric measurements of the combination of F_2 and $C\ell_2$; however, these are suspect because of the possible concurrent formation of $C\ell F_3$. The more negative value is more consistent with a variety of calculations relating $C\ell F$ to $C\ell F_3$ by means of the other reactions listed. For $C\ell F_3$ values range from -37.5 to -40.5 kcal mol^{-1} based on combinations of references [12], [14], and [16]. However, a discordant value for the heat of reaction (a) by Wartenberg and Riteris prevents full agreement, and would lead to a value of about -26.5 kcal mol^{-1}. Additional evidence is sketchy and includes reports of measurements made at Harshaw Chemical Company and Rocketdyne, Inc., both undocumented by reported literature, which tend to support the less negative value for $C\ell F_3(g)$.

TABLE V. $C\ell F$ AND $C\ell F_3$ HEATS OF FORMATION

Reaction		kcal mol^{-1}		Ref.
(a) $C\ell F_3(g) + 3NaC\ell(c) = 3NaF(c) + 2C\ell_2(g)$	$\Delta H^\circ_{18^\circ}$ =	-86.6	±0.3	[11]
	$\Delta H^\circ_{18^\circ}$ =	-76.5		[12]
(b) $C\ell F(g) + NaC\ell(c) = NaF(c) + C\ell_2(g)$	$\Delta H^\circ_{18^\circ}$ =	-24.5	±0.1	[12]
(c) $C\ell F_3(g) = C\ell F(g) + F_2(g)$	ΔH° =	24.5		[11,13]
	ΔH° =	24.6		[14,3]
(d) $C\ell F = C\ell + F$	ΔH°_0 =	58.96 or 60.35		[12,5,6,16]
(e) $\frac{1}{2}C\ell_2(g) + \frac{1}{2}F_2(g) = C\ell F(g)$	ΔH =	-11.6	±0.4	[13]
		-11.7		[15]
(f) $\frac{1}{2}F_2(g) + NaC\ell(c) = \frac{1}{2}C\ell_2(g) + NaF(c)$	ΔH =	-39.5		[12]
		-39.3		[17]

3. TETRAFLUOROHYDRAZINE

A single study [18] has been reported of the heat of formation of $N_2F_4(g)$, leading to a heat of formation of -2.0 ± 2.5 kcal mol^{-1}. The study was made very soon after the discovery of N_2F_4, and the quantity and the purity of the available sample were not adequate for a high precision study. The corrections for impurities were large, though based upon a detailed analysis of the sample. A study of a pure sample would be warranted.

4. CARBONYL FLUORIDE

While not an oxidizer, carbonyl fluoride seems more relevant at this point than later in the program. One calorimetric determination [19] has been reported of the heat of formation of $COF_2(g)$. Two studies [20,21] are available of equilibrium in the reaction involving CO_2, CF_4 and COF_2 which can be used for calculating the heat of formation. The equations and calculated values are summarized in Table VIII. The calculations based on observed equilibria lead to values more negative by 3 to 5 kcal mol^{-1} than the calorimetric determination. The equilibria indicate that a large fraction of product gases may consist of COF_2 under conditions when an organic compound is burned in an oxidizer containing both oxygen and fluorine. It is therefore of importance comparable to CF_4 and CO_2 in such combustions. A more careful calorimetric study than that reported by Wartenberg [19] seems to be justified.

TABLE VIII. COF_2 HEAT OF FORMATION

$COF_2(g) + H_2O(\ell)$	=	$2HF(aq) + CO_2(g)$	$\Delta H = -26.73$	[11]
$\Delta H^\circ_{f298}[COF_2(g)]$	=	-151.7* kcal mol^{-1}		
$CO_2(g) + CF_4(g)$	=	$2COF_2(g)$	$\Delta F^\circ_{298} \approx 0$	[20]
$\Delta H^\circ_{f298}[COF_2(g)]$	=	-156.9* kcal mol^{-1}		
$CO_2(g) + CF_4(g)$	=	$2COF_2(g)$	$\Delta H^\circ_{298} = -7.5 \pm 4.9$	[21,22]
$\Delta H^\circ_{f298}[COF_2(g)]$	=	-154.7* kcal mol^{-1}	(Third-Law analysis of equilibrium)	

* Calculated from recent thermodynamic data. See heat of formation of CF_4 reported by Armstrong in another section.

6. NEW WORK ON OXYGEN DIFLUORIDE (with R. C. King)

A study at NBS on the heat of formation of F_2O using a flame calorimeter has reached the stage at which some preliminary information can be given. In Table X are listed reactions which will be carried out in determining the heat of formation. The combustion in the calorimeter leads to a condensed and gaseous phase mixture of H_2O and HF, equation (1), which are mixed, still in the calorimeter, with excess H_2O, equation (2), forming a homogeneous single phase system. The overall reaction occurring in the calorimeter is equation (3). A reaction vessel designed for carrying out this reaction is shown schematically in Figure 1. The burner detail and gas dispersion system are given in Figure 2.

TABLE X. REACTIONS LEADING TO THE HEAT OF FORMATION OF OF_2

$$0.06\ OF_2(g) + 0.12\ H_2(g) = [0.12\ HF \times 0.06\ H_2O](g+\ell) \qquad (1)$$

$$[0.12\ HF \times 0.06\ H_2O](g+\ell) + 5.55\ H_2O(\ell) = [0.12\ HF \times 5.61\ H_2O](\ell) \qquad (2)$$

$$0.06\ OF_2(g) + 0.12\ H_2(g) + 5.55\ H_2O(\ell) = [0.12\ HF \times 5.61\ H_2O](\ell) \qquad (3)$$

The study has reached the stage in which the stoichiometry of the reaction is under reasonably good control. Table XI shows the tests which have been made of recovery of HF in the resulting aqueous solution. The collection shows a gradual improvement until a sudden drop-off occurs in the last two experiments. The factor causing this change is still under investigation. Table XII shows the reproducibility of the resistance change per unit mass for these same preliminary experiments. Aside from the first experiment, which probably suffered from a conditioning process, the reproducibility has been within 0.01 per cent until a slight drop-off occurs in the two final experiments. This last observation may be related to the low HF collection observed for these two experiments.

The same general process is suitable for the study of $C\ell F_3$ and for other gaseous fluorine compounds.

TABLE XI. EARLY TESTS OF THE STOICHIOMETRY OF THE REACTION OF OF_2 WITH H_2

Experiment No.	Mass of OF_2 g	HF(obs)/HF(calc) ratio
1	3.5496	0.99288
2	2.9080	.99710
3	3.4370	.99633
4	3.5261	.99836
5	3.0869	1.00093
6	3.4556	0.99714
7	3.4512	.99469

TABLE XII. REPRODUCIBILITY OF CALORIMETRY OF OF_2-H_2 REACTION

	m_s	ΔRc	$\Delta Rc/m_s$
	g	ohm	ohm g^{-1}
1	3.5496	0.291760	0.0821951
2	2.9080	.235144	.0808611
3	3.4370	.277914	.0808595
4	3.0869	.249608	.0808604
5	3.5261	.285151	.0808687
6*	3.4556	.279298	.0808247
7*	3.4512	.278765	.0807733

* 1.8709 g neoprene added to burner.

7. REFERENCES

[1] Ruff, O. and Menzel, W., Z. anorg. u. allgem. Chem. 190, 257-66 (1930).

[2] Wartenberg, H. V. and Klinkott, G. Z., Z. anorg. u. allgem. Chem. 193, 409-19 (1930).

[3] Evans, W. H., Munson, T. R., and Wagman, D. D., J. Research Natl. Bur. Standards 55, 147 (1955).

[4] Evans, W. H., Private Communication, March 1966.

[5] Wagman, D. D., Evans, W. H., Halow, I., Parker, V. B., Bailey, S.M., and Schumm, R. H., Natl. Bur. Standards Tech. Note 270-1,-2 (U.S. Government Printing Office, Washington, D.C. (1965, 1966).

[6] Bisbee, W. R. and Hamilton, J. V., Am. Chem. Soc., Proc. 149th Meeting, April 4-9, 1965, Detroit, Michigan, Abstracts, p. 13-J.

[7] JANAF Thermochemical Tables, Dow Chemical Co., Midland, Michigan, Sept. 30, 1964.

[8] Dibeler, V. H., Reese, R. M., and Franklin, J. L., J. Phys. Chem. 27, 1296-7 (1957).

[9] Brewer, L. and Rosenblatt, G. M., Chem. Rev. 61, 257-63 (1961).

[10] Kirshenbaum, A. D., Grosse, A. V., and Aston, J. G., J. Am. Chem. Soc. 81, 6398-6402 (1959).

[11] Wartenberg, J. V. and Riteris, G., Z. anorg. Chem. 258, 356-60. (1949).

[12] Schmitz, H. and Schumacher, H. J., Z. Naturforsch 2a, 362 (Col. 2) 1947.

[13] Wicke, E., Machr. Akad. Wiss. Gottingen, Math. phys. chem. Abt. 1946. 89-90.

[14] Schafer, K. and Wicke, E., Z. Elektrochem. 52, 205 (1958).

[15] Wicke, E. and Friz, H., Z. Elektrochem. 57, 9-16 (1953).

[16] Wahrhaftig, A. L., J. Chem. Phys. 10, 248 (1942).

[17] Wartenberg, H. V. and Fitzner, O., Z. anorg. u. allgem. Chem. 151, 313 (1926).

[18] Armstrong, G. T., Marantz, S., and Coyle, C. F., Natl. Bur. Standards Report 6584, October 1959.

[19] Wartenberg, H. v., Z. anorg. Chem 258, 356 (1949).

[20] Armstrong, G. T., Coyle, C. F., and Krieger, L. A., WADC TR58-541, October 1958.

[21] Ruff, O. and Li, S., Z. anorg. Chem. 242, 272 (1939).

[22] JANAF Thermochemical Tables, Dow Chemical Co., Midland, Michigan, March 31, 1965.

Chapter 16

A REVIEW OF THE HEAT OF FORMATION OF TETRAFLUOROMETHANE

George T. Armstrong

Introduction

The first attempts to measure the heat of formation of CF_4, by von Wartenberg and Schuette (1933) [1] and by von Wartenberg (1949) [2], involved different processes, and showed such a wide disparity that interest in the problem was aroused. The method used by von Wartenberg and Schuette, the combination of the elements, was the most direct, but the value, -162 ± 2 kcal mol^{-1} which they obtained was criticized by Ruff and Bretschneider [3] because of the simultaneous formation of unknown amounts of higher fluorocarbon homologs. Ruff and Bretschneider suggested a revision to -183.5 kcal mol^{-1}, a change which was far too little as evidenced by later measurements.

The measurement by von Wartenberg [2] was on the reaction of CF_4 with potassium, for which he found $\Delta H_r = -307 \pm 3$ kcal mol^{-1}, and from which he calculated $\Delta H_f[CF_4(g)] = -231$ kcal mol^{-1}. This was so different from the preceding value that over a period of years numerous investigations [4,5,6,7,8,9,10,11,12,14,15,16,17] were carried out and in addition efforts were made to adduce information from other sources. The reactions carried out in the above work are summarized in Table 1, and they will be discussed below.

For the purposes of this discussion, the reactions involving CF_4 in Table 1 may be divided into two groups, those for which a calculation of $\Delta H_f[CF_4(g)]$ involves the heat of formation of gaseous or aqueous HF, and those for which the calculation is independent of HF. Because of current uncertainty about the heat of formation of HF, we first examine those reactions that do not involve HF, and then examine the consistency of the remainder with respect to the heat of formation of HF.

<u>The combustion of graphite in fluorine</u>. In addition to the work of von Wartenberg and Schuette [1], previously mentioned, this reaction (equation 1, Table 1) has been reported from only one other study, by Domalski and Armstrong [5,6]. The reaction as carried out by von Wartenberg and Schuette suffered from the failure to obtain a good analysis of the product gases, which probably contained substantial amounts of higher fluorocarbons. In addition, the residual ash (containing some CaF_2) also contained unspecified amounts of unburned material which von Wartenberg and Schuette presumed to be carbon. The large discrepancy of this series of experiments, together with the incomplete characterization of the products cause us to believe that the work of von Wartenberg and Schuette should no longer be considered except for its historical interest.

The work of Domalski and Armstrong [5,6] on graphite led to a value of -222.87 ± 0.38 kcal mol^{-1} for the heat of formation of $CF_4(g)$. The combustion was performed in a high pressure of fluorine and was promoted by Teflon powder admixed with the graphite. The reaction was carried out on a well characterized sample, combustion was nearly complete, and the reaction products were carefully analyzed. We believe that all relevant factors were considered in this work, and consider that it offers the best value available today for $\Delta H_f[CF_4(g)]$. This value will be used as a basis for discussion of the other work in Table 1.

Reactions of polytetrafluoroethylene (Teflon).

Scott, Good and Waddington [10] reported burning C_2F_4(solid polymer) in oxygen in a series of conditions which were extrapolated at one limit to the condition of no HF(aq) in the products (Equation 4a). Domalski and Armstrong [5,6] reported the heat of combustion of polytetrafluoroethylene in fluorine (Equation 6a), as -247.85 kcal mol^{-1}, and have previously [13] reported a slightly less reliable value, -247.43 kcal mol^{-1}. The more recent work is supported by additional unpublished work of Dr. K. L. Churney in this laboratory, in which the heat of combustion was found to be -247.89 kcal mol^{-1}.

Equation (6c) is obtained by combining Equations (4a) and (6a), and involves only the heat of formation of $CO_2(g)$. For reaction (6a) we find ΔH° = (preferably) -129.05, or -128.63 kcal mol^{-1}. These values, combined with the heat of formation of $CO_2(g)$, which we take from Wagman, et al. [24] to be -94.051 kcal mol^{-1}, give $\Delta H_f[CF_4(g)]$ = (preferably) -223.10, or -222.68 kcal mol^{-1}. The two values differ by not more than 0.23 kcal mol^{-1} from the value found by combustion of graphite in florine, and bracket it. As far as we can discern, the latter method of calculation gives values of $\Delta H_f[CF_4(g)]$ which are independent of the heat of formation found in the graphite combustion. However, because reaction (1) and reaction (6a) were carried out using similar techniques, it is possible that a systematic error common to them both could cause them both to be in error in the same direction. In addition, because C_2F_4 (solid polymer) was used as a combustion aid in the combustion of graphite, the value used for the heat of combustion of C_2F_4 affects the value found for the combustion of graphite. It is not apparent to us, however, what, if any, dependence between the values can be attributed to these experimental prodedures.

The values reported in the preceeding paragraphs for $\Delta H_f[CF_4(g)]$ differ from the value -221.77 kcal mol^{-1} calculated by Domalski and Armstrong [13] by another treatment of the same reactions, in that the earlier treatment [13] introduced the heat of formation of HF(aq) which we are here trying to avoid. A certain amount of inconsistency had thereby been introduced into the previous calculations.

Heat of formation of polytetrafluorethylene. The heat of formation of $CF_4(g)$ as derived from the work of ref. [5,6], when combined with the heat of reaction (6a) leads to $\Delta H_f[C_2F_4$ (solid polymer)] = (preferably) -197.89, or 198.29 kcal mol^{-1}. When it is combined with the heat of reaction (4a) it leads to $\Delta H_f[C_2F_4$ (solid polymer)] = -198.13 kcal mol^{-1}.

Relationships between the heats of formation of $CF_4(g)$, NaF(c), and KF(c). Reactions involving CF_4 and NaF or KF were carried out by von Wartenberg [2,4], Kirkbride and Davidson [16], and Vorob'ev and Skuratov [17], and are listed as reactions (8) and (9). The heat of formation of $CF_4(g)$ can thus be calculated if the heats of formation of NaF(c) or KF(c) are known.

While the heat of formation of NaF has been most commonly determined by reference to reactions involving hydrofluoric acid, as was done by Vorob'ev and Skuratov [17], or as is illustrated in the JANAF Thermochemical Tables [25], there are available heat measurements on two reactions not involving HF which lead to the heat of formation of sodium fluoride. These are listed as reactions (10a) and (10b) of Table 1.

The measurements of von Wartenberg and Fitzner [18] and of Schmitz and Schumaker [19] on reaction (10a) are in good agreement with each other and require only the heat of formation of NaCl (c) to permit calculation of the heat of formation of NaF(c). Using ΔH_f[NaCl(c)] = -98.232 kcal mol^{-1} [26], we obtain for ΔH_f[NaF(c)], -137.5 kcal mol^{-1} from the work of von Wartenberg and Fitzner, and -137.7 kcal mol^{-1} from the work of Schmitz and Schumaker. Applying these results to equation (9), for which the reaction heat was measured by Vorob'ev and Skuratov [17], we calculate $\Delta H_f[CF_4(g)]$ = -224.5 and -225.3 kcal mol^{-1}, respectively. The average of these is more negative by about 2 kcal mol^{-1} than the value reported by Domalski and Armstrong[5,6].

We see some possible uncertainties in the processes involved in this calculation. Some ClF may have formed in the reaction of NaCl with fluorine. If so observed heat is excessively exothermic for reaction (9). The calculated heats of formation of NaF(c) and $CF_4(g)$ would be less negative if an adjustment were required for formation of ClF.

The carbonaceous reaction product of sodium with CF_4 in the work of Vorob'ev and Skuratov [17] was identified by x-ray analysis as β-graphite, and no correction was applied for its heat of formation. Such an identification can be made even when only a fraction of the material is actually crystalline. In a similar study by von Wartenberg [2,4] the carbon was tested by combustion and x-ray and in that work, also, no correction was applied for the heat of formation of the product.

However, in other similar studies by Kirkbride and Davidson [16] a correction of 2.5 kcal mol^{-1} was made for the heat of formation of the carbon formed. In a study by Neugebauer and Margrave [9] in which finely divided carbon (soot) was formed in other reactions (reactions (3a) and (3b)), they measured the heat of combustion of the soot and determined its heat of formation to be 1.5 or 1.9 kcal mol^{-1}. In the early combustion study by von Wartenberg [1], as previously noted, his starting material was active charcoal (Norite). For this he applied a heat of formation of 2.4 kcal mol^{-1}, based on a measurement of its heat of combustion.

Evidence that the carbon obtained by Vorob'ev and Skuratov[17] was actually an active form, is found in their statement that they observed an exothermic post-reaction process, which they attributed to absorption of CF_4 by the carbon. They did not include this heat in their measurement or make any correction based on it. In a later similar experiment involving Na(c) and C_2F_4(g), Kolesov, Zenkov, and Skuratov [27] found amorphous carbon among the products. They measured its heat of conbustion from which they concluded that it had a heat of formation of 3.95 kcal mol^{-1}.

Thus, while no firm information is available as to the heat of formation of the carbon formed in the experiments of Vorob'ev and Skuratov, the preponderance of findings of other experimenters suggests that its heat of formation could have been from 1.5 to 4 kcal mol^{-1}. If the reaction heat they reported is adjusted for this positive heat of formation, the standard heat of reaction to form graphite is more negative, and the heat of formation calculated for CF_4(g) is more positive. Values of $\Delta H_f[CF_4(g)]$ ranging from -220.5 to -223.8 kcal mol^{-1} can be calculated. These values bracket the value of Domalski and Armstrong [5,6].

Not much additional information can be derived from reaction (10b) because of the uncertainty of the heat of formation of ClF(g). ΔH_f[ClF(g)] (see the JANAF tables [25] for a discussion) was found (a) by direct reaction of the elements to be -11.6 or -11.7 kcal mol^{-1} (Wicke [22];Wicke and Friz [23]) (b) by comparison of the heats of reaction of ClF and F_2 with NaCl(c) (Schmitz and Schumaker [19]) to be -15.0 kcal mol^{-1}, and (c) by dissociation energy measurements (Schmitz and Schumaker [20], Wahrhaftig [21], see also Stricker [28]) to be -12.14 or -13.51 kcal mol^{-1} depending on the state of the products. These values can be combined with the known heat of formation of NaCl(c) (-98.232 kcal mol^{-1} [26]) and the heat of reaction (10b) to give the heat of formation of NaF(c). Values obtained in this way for ΔH_f[NaF(c)] range from -137.7 kcal mol^{-1}, consistent with the previous discussion, to -134.3 kcal mol^{-1}, Application of these values to reaction (9) leads to values for $\Delta H_f[CF_4(g)]$ ranging from -225.3 kcal mol^{-1} to -212.8 kcal mol^{-1}. Thus, again, the most negative value tenable for the heat of formation of CF_4 on the basis of the work of Vorob'ev and Skuratov [17] without reference to HF is -225.3 kcal mol^{-1}, and as before such values are subject to revision in the positive direction if the carbon resulting from reaction (9) had a positive heat of formation.

We have not found a reaction scheme by which the heat of formation of KF(c) can be obtained without reference to HF. On this account, reaction (8) cannot be given the same treatment as reaction (9). However, if we presume that the heats of formation of NaF(c) and KF(c) bear the proper relationship to one another in NBS Circular 500 [26], ($\Delta H_f[NaF(c)] - \Delta H_f[KF(c)] = -136.0 + 134.46 = 1.54$ kcal mol^{-1}) the most negative value attributable to $\Delta H_f[KF(c)]$ would be -136.16 kcal mol^{-1} on the basis of the previous discussion of NaF(c). If we apply this information to reaction (8) we find $\Delta H_f[CF_4(g)] \geq -224.6$ kcal mol^{-1}. Here we must bear in mind, however, that Kirkbride and Davidson [16] applied an arbitrary correction for the heat of formation of carbon, of 2.5 kcal mol^{-1}, which may be too large by 1.0 kcal mol^{-1} or two small by 1.5 kcal mol^{-1} on the basis of reported measurements of the heat of formation of amorphous carbon found in other laboratories.

It is evident that failures of Kirkbride and Davidson [16] and of Vorob'ev and Skuratov [17] to measure the heat of combustion of the carbon which was formed in their experiments has reduced the ultimate usefulness of their measurements on CF_4, because there seems now to be no way to relate their measurements clearly to a well defined standard state of carbon.

Summary of the work on $\Delta H_f[CF_4]$ without reference to $\Delta H_f[HF]$.

In summary, the values for the heat of formation of CF_4 as calculated from the reaction of graphite with fluorine, and from the reactions of Teflon with fluorine and oxygen are in good agreement, and indicate $\Delta H_f[CF_4(g)] = -222.87 \pm 0.38$. The values which can be derived from other reactions not involving HF are consistent with them, but allow a range of values which bracket them in every instance.

Relationship of $\Delta H_f[CF_4(g)]$ to $\Delta H_f[HF(aq)]$.

Reactions (2), (3a,b,c,d,e), (4a,b,c), (5a,b,c) involve both $CF_4(g)$ and HF (aq) or HF(g) directly. In addition reactions (8) and (9) involve hydrofluoric acid indirectly if one derives the heats of formation of the alkali fluorides from cycles involving HF(aq). In this section we infer as much information as we can about the heat of formation of HF by application of the proposed heat of formation of CF_4. The work of Jessup, McCoskey, and Nelson [7] on the gas phase combustion of CH_4 in fluorine, is the only study listed here which involves HF(g). Its limited accuracy is indicated by the large uncertainty (2% or 9 kcal mol^{-1}) attributed to it by the authors. Applying $\Delta H_f[CF_4(g)] = -222.87$ and $\Delta H_f[CH_4(g)] = -17.889$ kcal mol^{-1}, we find $\Delta H_f[HF(g)] = -63.6$ kcal mol^{-1}, about one kcal mol^{-1} less negative than any currently acceptable value. At this time we can find no justification for its validity.

Reactions (3a) and (3c), the decomposition of tetrafluoroethylene gas into tetrafluoromethane and carbon, and the reduction of tetrafluoroethylene gas to hydrogen fluoride and carbon, were carried out by Duus [8] in a bomb calorimeter. Several experimental difficulties encountered by Duus were remedied in a study of similar reactions (3a and 3b) by Neugebauer and Margrave [9]. Neugebauer and Margrave measured the heat of formation of the carbon produced in each experiment, while Duus did not. A significant heat of formation was found. In the reduction of tetrafluoroethylene by hydrogen, Neugebauer and Margrave caused the hydrogen fluoride product to be dissolved in water, and thus overcame the problem, encountered by Duus, of large and uncertain corrections for the amount of HF present as gas. Because of these differences we consider only the experiments of Neugebauer and Margrave. Reactions (3a) and (3b) can be combined to eliminate C_2F_4 which was common to both. For the resulting reaction, (3d), the work of Neugebauer and Margrave [9] gives $\Delta H_r = 85.4 \pm 1.5$ kcal mol^{-1}. Applying $\Delta H_f[CF_4(g)] = -222.87 \pm 0.38$ kcal mol^{-1}, to this reaction leads to $\Delta H_f[HF \cdot 1815 H_2O] = -77.07 \pm 0.4$ kcal mol^{-1}.

The work of Good, Scott, and Waddington [10,11] on the combustion of polytetrafluoroethylene was extrapolated to the condition of no $CF_4(g)$ on the one extreme and the condition of no HF(aq) on the other extreme, and led them to reactions (4a) and (4b). Elimination of polytetrafluoroethylene from these reactions by subtraction led to reaction (4c) for which their measurements give $\Delta H_r = 41.5 \pm 1.0$ kcal mol^{-1}. Applying the values $\Delta H_f[H_2O(l)] = -68.317$, $\Delta H_f[CO_2(g)] = -94.05$, and $\Delta H_f[CF_4(g)] = -222.87 \pm 0.38$ kcal mol^{-1} we calculate $\Delta H_f[HF \cdot 10 H_2O] = -76.74 \pm 0.35$ kcal mol^{-1}.

Cox, Gundry, and Head [12] measured the heat of combustion of docosafluorobicyclohexyl in oxygen, under a similar range of conditions to that used by Good, Scott and Waddington on polytetrafluoroethylene. Their limits of extrapolation led them to reactions (5a) and (5b), from which reaction (5c) is obtained by difference. For reaction (5c) they obtained $\Delta H_r = 41.38 \pm 0.32$ kcal mol^{-1}. Applying the same auxiliary data as above we calculate $\Delta H_f[HF \cdot 20H_2O] = -76.71 \pm 0.2$ kcal mol^{-1}.

The values found above for the heats of formation of aqueous HF of three concentrations are shown in Table 2 in the column headed A. For comparison in columns B and C are values for the same concentrations of HF, calculated from two recent tabulations. The work of Cox and Harrop [29] (Column B) is based on a new determination of the heat of solution of HF combined with the value $\Delta H_f[HF(g)] = -64.92$ kcal mol^{-1}. The survey by Wagman et al. [24] is based on older work, but uses $\Delta H_f[HF(g)] = -64.8$ kcal mol^{-1}.

The first point to be noted is that columns A, B, and C are each internally self consistent and show differences from one another that are constant at least within the uncertainties of the three measurements upon which Column A is based. The second point to be noted is that a difference of Column A from the work of Cox and Harrop requires 0.4 to 0.7 kcal less negative heat of formation for the HF solutions than they arrived at. The difference from Column C requires heat of formation of HF (aq) more negative by 0.4 to 0.7 kcal mol^{-1} than Wagman, et al. [24] proposed.

We propose several possibilities for the sources of the discrepancy and will examine them briefly, but not exhaustively.

(1) The heat of formation reported by Domalski and Armstrong [5,6] may be in error. To place the calculated results on HF in concordance with that of Cox and Harrop [29] would require that the heat of formation of $CF_4(g)$ be more negative by 1.6 to 2.8 kcal mol^{-1}, $\Delta H_f = -224.5$ to -225.7 kcal mol^{-1}. These values are similar to those suggested by Cox, Gundry, and Head [12] as a result of applying the work of Cox and Harrop [29] to the same experiments. An error this large in the work of Domalski and Armstrong is hard to visualize in view of the internal consistency of their work. To put the calculated results on HF into concordance with those of Wagman, et al. [24] requires similarly large changes, bringing ΔH_f for CF_4 to -220.1 to -221.3 kcal mol^{-1}. The large error is no easier to justify in this case.

Turning to the tabulations of heats of formation of HF(aq), Columns B and C, we find, first of all, that the tabulation of Wagman, et al. [24] is based upon such an elaborate appraisal of many processes, that we are not prepared to indicate which key data would affect the tabulation in the direction of conformity with Column A. A reappraisal of the whole array of data would be necessary. The calorimetric work of Cox and Harrop [29] seems to have no possible source of an error as large as we are looking for. We must then turn to the non-calorimetric and auxiliary information used by Cox and Harrop, if we wish to account for the discrepancy.

(2) A poor value for the heat of formation of HF(g) may have been used by Cox and Harrop [29]. To bring their data into agreement with Column A would require that ΔH_f for HF(g) be taken as -64.3 to -64.6 kcal mol^{-1}. Such values are quite conceivable, as several experimental determinations of this quantity fall in the range given.

(3) An error may be present in the heat of vaporization of HF(g) from $LiHF_2$(c) as found by Cox and Harrop [29]. Their determination consisted of a measurement of the vapor pressure of HF(g) over $LiHF_2$(c), from which they calculated $\Delta G^\circ_{298} = -RT\ln P = 3.553 \pm 0.044$ kcal mol^{-1} for reaction (a).

$$LiHF_2(c) = LiF(c) + HF(g) \qquad \text{(a)}$$

They calculated ΔH_{298} for reaction (a) from the formula $\Delta H_{298} = \Delta G_{298} + T\Delta S_{298}$. They took values of $(S_{298} - S^\circ_o)$ from low temperature calorimetric studies of LiF(c) and $LiHF_2$(c) and a statistical thermodynamic calculation for HF(g) with which no significant fault has been found. They added the value $\Delta H^\circ_{298} = 13.410 \pm 0.048$ kcal mol^{-1}, which they thus found for reaction (a), to several calorimetrically determined heats of solution and dilution in order to obtain for reaction (b), $\Delta H^\circ_{298} = 13.172 \pm 0.068$ kcal mol^{-1}.

$$HF(aq, 6017\ H_2O) = HF(g) \qquad \text{(b)}$$

Combining this with $\Delta H_f{}^\circ{}_{298}[HF(g)] = -64.92$ kcal mol^{-1}, they obtained $\Delta H_f{}^\circ{}_{298}[HF \cdot 6017 H_2O] = -78.09$ kcal mol^{-1}, from which their other solution data were derived.

Two features of this experiment and calculation may be pointed out as sources of possible difficulty.

<u>Possible non-standard state of LiF in reaction (a).</u> Because HF vaporizing from $LiHF_2$ will come from within the lattice a porous structure is formed when this process occurs. If the resulting solid has a high free energy relative to the bulk crystal, the free energy change of vaporization will be greater than for the process leaving LiF in the standard state. The vapor pressure in this case would be

lower than the equilibrium vapor pressure. Some evidence for a behavior of this type is found in the preparation of active NaF by removal of HF from $NaHF_2$, which is known to produce a solid that absorbs HF more readily than bulk NaF.

The necessary reduction of the vapor pressure, however is improb - ably large, approximately a factor of two in pressure being necessary to account for the observed energy error. It appears very unlikely that such a far departure from a well defined equilibrium could occur.

Possible zero point entropy of $LiHF_2(c)$. If crystalline $LiHF_2$ has an entropy equal to Rln2 at the absolute zero, a contribution of -1.377 cal deg^{-1} mol^{-1} would be added to ΔS^o_{298} for reaction (a), or a contribution of about -0.4 kcal mol^{-1} to ΔH^o_{298}. This would remove the major part of the discrepancy between Columns A and B of Table 2.

We may presume that as a simple substance in a cubic lattice LiF will have $S^o_o = 0$, and that for ideal-gas HF, $S^o_o = 0$. However, in $LiHF_2(c)$ we find a much more complicated structure. In particular the possibility of two equivalent positions for the hydrogen atom in the HF_2^- ion should be considered. Two such equivalent positions would exist if there were a double minimum in the potential between the two fluorine atoms. This is a question which is susceptible to unambiguous determination but requires very careful experimentation.

The question of a double minimum in the bifluoride ion, analogous to the double minimum in the potential between oxygen atoms in a hydrogen bonded substance has been repeatedly examined by Westrum and his co-workers [32-37] and by others [38-61]. Little, if any, positive evidence has been found: yet the continuing work indicates lingering doubts about the precise conditions under which the unsymmetrically located proton will occur. In particular, little evidence referring specifically to $LiHF_2$ has been presented except the crystal structure [56], which gives the F-F bond distance, and a heat capacity and vapor pressure study by Westrum and Burney [35]. Unfortunately, the calorimetric and vapor pressure measurements by Westrum and Burney, which could give decisive information on this point, are not complete. The heat capacity measurements do not extend into the region of the vapor pressure measurements.

A more detailed review of the background and present status of the problem of the double minimum, and its application as a possible source of error in the thermodynamic analysis by Cox and Harrop is inappropriate here. Such a review is given in the appendix.

Appendix.

Evidence concerning a possible residual entropy in $LiHF_2(c)$.

1. Thermochemical evidence. Perhaps the strongest piece of directly relevant evidence that a residual entropy exists is, as shown in the main text, the discrepancy between the heat of formation of HF(aq) calculated by Cox and Harrop [29] and that found by applying the heat of formation of $CF_4(g)$ given by Domalski and Armstrong [5,6] to several thermochemical processes involving $CF_4(g)$ and HF(aq). This is not decisive, because the discrepancy can be attributed to another source, an error in the heat of formation selected by Cox and Harrop [29] for $\Delta H_f[HF(g)]$. A thermochemical study of $LiHF_2$ by Westrum and Burney [35] gives an incomplete cycle. Data presently exist for the vapor pressure of HF(g) in reaction (a)

$$LiHF_2(c) = LiF(c) + HF(g) \qquad (a)$$

and for the heat capacity of LiF(c). But the low temperature heat capacity measurements of $LiHF_2(c)$ [35] stop short of the range in which pressure measurements were made. Only an isolated vapor pressure point in the range of the heat capacity measurements exists, and this was ued by Cox and Harrop [29] in their calculation. The constancy of ΔH°_0 or ΔH°_{298} for reaction (a) in a third law analysis of the vapor pressure data would provide a sensitive enough test to indicate absence of a residual entropy of magnitude Rln2.

2. Structural evidence. The crystal structure of $LiHF_2(c)$ was determined by Frevel and Rinn [56]. They found the F-F distance to be 2.27A°, in good agreement with, but slightly greater than, the value of 2.26A° in $KHF_2(c)$ (Helmholtz and Rogers [62]).

A short hydrogen bond length is taken to be a sensitive criterion of a symmetrical position of the proton. In crystalline HF, R_{F-F} is 2.49A°, as found by Atoji and Lipscomb [61], and in that structure the proton is assymmetric. In the $H_2F_3^-$ ion as found in $NaH_2F_3(c)$ and $KH_2F_3(c)$ Blinc, Trontelj, and Volavšek [59] find by NMR analysis, that the protons are not placed equally distant from the F atoms, but are displaced about 0.10A° toward the outer F atoms. In these salts R_{F-F} was found to be 2.33A° by Forrester, Senter, Zalhim , and Templeton [63]. In the HF^-_2 ion, as measured in $NaHF_2(c)$ and $NaDF_2(c)$, and in $KHF_2(c)$, the evidence presented by Peterson and Levy [48] indicates that the proton must be within 0.1 A° of the center, and Ibers [57] states (with an unspecified uncertainty) that the proton is symmetrically located. The neutron diffraction data alone is inadequate to distinguish an unsymmetric location of the proton displaced as much as 0.16A°, but combination of the neutron diffraction data with spectroscopic data reduces this lower limit to a smaller value.

Ibers [57] found $R_{F-F} = 2.277 \pm 0.006 A^{o}$ in $KHF_2(c)$. In $NaHF_2(c)$, Megaw and Ibers [58] found $R_{F-F} = 2.269$, and in $NH_4HF_2(c)$ McDonald [64] found $R_{F-F} = 2.269$ to $2.275 A^{o}$. Godycki, Rundle, Voter, and Banks [52], in speculating about a possible symmetrical O-H-O hydrogen bond in dimethylglyoxime, discuss the distance between oxygen atoms or between fluorine atoms as a valid criterion of the existence of a double or a single minimum in the potential. Referring to the work of Donahue [65], and Pauling [53], they mention the prediction of an R_{F-F} of $2.24 A^{o}$ for a symmetrical (single minimum) configuration. The observed bond lengths are only slightly greater than this.

The structural evidence removes all but limited possibilities for an unsymmetrical location of the hydrogen atom in any of the bifluorides thus far examined. This work has been discussed by Pauling [41].

All the above studies were made at temperature far above the absolute zero. It is improbable that any assymmetry would appear, on the average, until the crystal is cooled to a temperature near or below the kT corresponding to the height of any barrier between two minima. This may require cooling the crystal to very low temperatures.

3. Spectroscopic evidence. No attempt will be made here to make a critical review of the spectroscopic evidence concerning a potential hill centrally located between the fluorine atoms in the HF_2^- ion. No data specific to $LiHF_2(c)$ has been reported. However, Westrum and Pitzer [33] reviewed and commented on the infrared spectrum of KHF_2. A principle problem in this case is the assignment of certain observed frequencies. There are certain unresolved ambiguities or difficulties; but the general picture of a single minimum seems to be more easily justified.

Newman and Badger [54] point out that thespectrum of $KHF_2(c)$ is unique in the wealth of combination and overtone bands. In such a simple structure, they suggest that a detailed interpretation may ultimately be anticipated, but that a more satisfactory theory is necessary then now exists. Various other features of the spectrum were discussed by Buswell, Maycock and Rodebush [38], Glockler and Evans [39], Polder [43], Couture and Mathieu [45], Mathieu and Couture -- Mathieu [46], Halverson [47], Ketelaar [40], and Ketelaar and Vedder [55].

Analogy to the thermochemistry of other bifluorides. Westrum and Pitzer [33] measured the heat capacities from low temperatures to above 500°K, of KF(c) and KHF_2(c) and also measured the dissociation pressure of HF(g) over KHF_2(c) in the range from 450 to 500°K. They state that on the basis of free energy functions calculated from their data a zero point entropy of KHF_2(c) of $R\ln 2$ would lead to a calculated vapor pressure at variance with their observations. However, in the JANAF thermochemical tables [25] is noted a variation of ΔH°_0 with temperatures when ΔH°_0 is calculated from their vapor pressure data. We have calculated ΔH°_0 from their vapor pressure data and free energy functions, and find no trend with temperature if we presume S°_0 [$LiHF_2$(c)] to be zero. If we presume S°_0 [LiHF2(c)] to be Rln2, calculated values of ΔH°_0 show a pronounced trend. Assuming $\Delta S^\circ_0 = 0$, we calculate $\Delta H^\circ_0 = 20.52$ kcal mol^{-1}. Applying thermal functions from Westrum and Pitzer, we calculate $\Delta H^\circ_{305} = 21.31$ hcalmol^{-1}. If we were to assume $\Delta S^\circ_0 = -R\ln 2$, we would abtain $\Delta H^\circ_0 = 19.85$ hcalmol^{-1}. This seems to rule out any but the most speculative possibilities that KHF_2(c) has a residual entropy at 0°K.

Another interesting side of this question, however, is suggested by the results of some heat of solution measurements made by Westrum and Pitzer [33]. These measurements seem to have been largely overlooked, yet they bear a close relationship to the measurements of Cox and Harrop [29] on $LiHF_2$ and LiF. Westrum and Pitzer reported the enthalpy changes of reactions (1) and (2), below, but did not carry out sufficient measurements to close a thermodynamic cycle. They found $\Delta H(1) = -4.378$ and $\Delta H(2) = 10.946$ kcal mol^{-1} at 32°C.

$$KF(c) + [0.6647KOH + 922.6H_2O](\ell) = [KF + 0.6647\ KOH + 922.6H_2O]\ (\ell) \qquad (1)$$
(KOH in 1388 H_2O)

$$KHF_2(c,\alpha) + [2.323\ KOH + 1842H_2O] = [2KF + 1.323KOH\ 1843H_2O](\ell) \qquad (2)$$
(KOH in $793H_2O$)

$$KF(c) = KF(aq,\infty) \qquad (1a)$$

$$KHF_2(c,\alpha) + KOH\ (aq,\infty) = KF(aq,\infty) + H_2O \qquad (2a)$$

$$HF\ (aq,\infty) + KOH\ (aq,\infty) = KF(aq,\infty) + H_2O(\ell) \qquad (3)$$

$$KHF_2(c,\alpha) = KF(c) + HF(g) \qquad (4)$$

$$HF\ (aq,\infty) = HF(g) \qquad (5)$$

$$HF(aq,6017\ H2O) = HF(aq,\infty) \qquad (6)$$

$$HF(aq,\ 6017\ H_2O) = HF(g) \qquad (7)$$

By applying dilution data from NBS Circular 500 [26], to equation (1) we calculate, for the dilution of the final solution to one in which KF and KOH are present separate in infinite dilution, ΔH = -0.199 kcal mol^{-1}. In this calculation we assume KOH and KF are separately present in solutions of the same ionic strength as the final solution of equation (1). We also calculate, for the dilution of the given initial amount of KOH(aq) to KOH(aq,∞), ΔH = -0.063 kcal mol^{-1}. Adding these terms, each with the proper sign, to ΔH (1), we find ΔH (1a) = -4.514 kcal mol^{-1}.

Similarly, by applying dilution data from NBS Circular 500 [26] to equation (2), we calculate, for the dilution of the final solution to one in which KOH and KF are separately present in infinite dilution, ΔH = -0.394 kcal mol^{-1}, using the same ionic strength criterion as before. We calculate, for the dilution of the given initial amount of KOH(aq) to KOH(aq,∞), ΔH = -0.272 kcal mol^{-1}. The amounts of heat involved in this hypothetical dilution of reaction (2) are roughly twice the magnitude of those involved in reaction (1) because approximately twice as much substance is involved. Adding these dilution terms, each with the proper sign, to $\Delta H(2)$ we find $\Delta H(2a)$ = -11.068 kcal mol^{-1}.

The heat of neutralization of KOH(aq) and HF(aq) in infinite dilution (Reaction 3), is the heat of formation of water from its ions. For this we take $\Delta H(3)$ = -13.336 kcal mol^{-1} from Vanderzee and Swenson [67]. Finally, for $\Delta H(4)$ we take +21.31 kcal mol^{-1} from our recalculation of the work of Westrum and Pitzer [33]. Reactions (1a,2a,3 and 4) when added with proper regard for sign give Reaction (5), the heat of vaporization of HF(g) from HF(aq,∞), for which we calculate $\Delta H(5)$ = 14.528 kcal mol^{-1}.

For the dilution of HF(aq, 6017H_2O) to HF(aq,∞) we find, from Wagman, et al. [24], $\Delta H(b)$ = -2.30 kcal mol^{-1}. Thus we find for reaction (7), $\Delta H(7)$ = 12.228 kcal mol^{-1} by extension of the work of Westrum and Pitzer [33]. This may be compared with the value +13.172 kcal mol^{-1} reported by Cox and Harrop [29], and with 12.4 kcal mol^{-1} from Wagman, et al. [24].

The difference that is noted above of the work of Cox and Harrop [29] from that of Westrum and Pitzer [33] combined with other auxiliary data, is in the direction but somewhat larger than would be expected if $LiHF_2$(c) had a zero point entropy and KHF_2(c) had none. One must take this as only a suggestion, in view of the approximations applied by us to the measurements of Westrum and Pitzer. One should, for instance, note that the dilution of HF(aq, 6017H_2O) to HF(aq,∞) requires 2.30 kcal mol^{-1}, which is largely based on a theoretical extrapolation. Such an extrapolation (which is necessary in order to apply the work of Vanderzee and Swenson [67]) may be viewed with some skepticism in the light of the cautious approach used by Vanderzee and Swenson.

Equilibrium studies involving the vapor pressure of HF(g) over $NaHF_2$(c) were made by Fischer [66] , and by Froning, et al. [51]. The difference in the heats of vaporization reported in these two studies, indicates that a careful review of both pieces of work would be necessary to decide between them. Because we are not prepared to do this at present, no further inferences can be drawn, using their data.

The general conclusion of the inferences from other work is that little if any positive evidence for a residual zero point entropy of $LiHF_2$(c) can be found. The evidence with regard to KHF_2(c) seems to be firmly in favor $S^\circ_o[KHF_2(c)] = 0$. Despite the negative indications of the structural information, the possibility remains open that $LiHF_2$(c) has a real zero point entropy, not equal to zero, on the basis of a disagreement in the value of the heat of vaporization of HF(g) from HF(aq) as measured in two different laboratories using cycles involving $LiHF_2$(c) and KHF_2(c) respectively. In addition, there remains the discrepancy between the heats of formation HF(aq) found by Cox and Harrop [29] and those calculated from several reactions involving CF_4(g), using the heat of formation of CF_4(g) determined by Domalski and Armstrong [5,6] .

Notes to Table 1

1. a) The original authors made an adjustment of 2.4 kcal mol^{-1} for the estimated heat of formation of the Norite (activated wood charcoal) they burned. They obtained -165.0 ±1.5 kcal mol^{-1} for the combustion of Norite in fluorine. When adjusted by +2.4 kcal mol^{-1} this gives -162.6 kcal mol^{-1} which they apparently rounded to -162 kcal mol^{-1}, increasing the uncertainty to 2 kcal mol^{-1}.

   b) This is an adjustment by Ruff and Bretschneider [3] of the work of von Wartenberg and Schuette [1], taking into account the formation of several percent of higher fluorocarbons in the combustion of Norite. The recalculation changes the original data far too little. A recalculation using a more current value for the fluorination of a C-C bond (142.7 kcal mol^{-1}, instead of 107 kcal mol^{-1} as was used by Ruff and Bretschneider) leads to ΔH_r = -190.5 kcal mol^{-1}. Hence it appears that the formation of other products would have to be greater than was suggested by Ruff and Bretschneider. The uncertainty in amount of products seems to preclude further consideration of the work of von Wartenberg and Schuette.

2. As a part of its uncertainty the work of Jessup, McCoskey and Nelson [7] contains an uncertain correction of 1.5 to 2.0 kcal mol^{-1} (of CF_4) for nonideality of HF. This now appears to have been an excessive correction. In the extreme case, if this correction is reduced to zero, the heat of reaction becomes -461.2 kcal mol^{-1}. The large uncertainty assigned by the authors is apparently a 95 percent confidence limit.

3. a) The carbon formed in the reaction by Duus [8] was weakly crystalline. Duus made no adjustment to the heat for the physical state of the graphite. An adjustment of the magnitude made by Neugebauer and Margrave [9] would bring Duus' value to -63.3 kcal mol^{-1}. Neugebauer and Margrave [9] measured the heat of reaction, with the formation amorphous carbon, to be -63.5 kcal mol^{-1}, and measured the heat of formation of the amorphous carbon to be 1.9 kcal mol^{-1}. We have combined their measurements to give the heat of decomposition to form graphite, -65.4 kcal mol^{-1}.

   b,c) Neugebauer and Margrave [9] measured the heat of hydrogenation of C_2F_4(g), with the formation of HF(aq) and amorphous carbon, to be -147.8 kcal mol^{-1}, and measured the heat of formation of the amorphous carbon to be 3.0 kcal mol^{-1}. We have combined their measurements to give the heat of hydrogenation to form HF(aq) and graphite, ΔH = -150.8 kcal mol^{-1}. Their reaction is definitely superior to reaction 3(c) as carried out by Duus, who was forced to make large corrections for the presence of HF(g), and did not attempt any correction for the physical state of the carbon formed. Neither reaction 3(b) nor 3(c) can be used by themselves to calculate the heat of formation of CF_4, but are included because they can be combined with other work done in the same laboratory to obtain a relationship leading to the desired value.

d) This reaction is obtained by subtracting 3(b) from 3(a). The heat value cited was obtained using the heat of reaction 3(a) determined by Neugebauer and Margrave [9].

e) The heat of this reaction was determined by combining the energy of reaction 3(c) with that for 3(a) determined by Duus [8] and reported in the same paper.

4. a,b) The energies of these reactions were obtained by Good, et al. [11] by extrapolating respectively to x = 1 and x = 0 from measurements covering the range x = 0.0285 to x = 0.8162 of the reaction C_2F_4(solid polymer) + O_2(g) + 42(1-x)H_2O(l) = (2-x)CO_2(g) + xCF_4 + 4(1-x)[HF + 10H_2O](l). The experiments are carefully described.

c) The heat of this reaction was obtained by combining the heats of reactions 4(a) and 4(b) determined in the same laboratory.

5. c) The heat of this reaction was obtained by Cox Gundry, and Head [12] by appropriately combining reactions 5(a) and 5(b).

6. a) An earlier (in parentheses) and a more recent and more amply substantiated value are listed.

c) The heat of this reaction is obtained by combining the heats of reaction 6(a) and 4(a). This reaction does not in any way involve the heat of formation of HF, but in order for it to be valid, the C_2F_4(solid polymer) used in the two different experiments must be similar.

7. Baibuz and Medvedev [15] recalculated the work of Baibuz [14] and reported $\Delta H_f[CF_4(g)] = -220.6$. The work of Baibuz is not available to us in sufficient detail to allow us to write the equation for the reaction or to know the dependence of the reported heat of formation of CF_4 on other auxiliary data.

8. Von Wartenberg [2,4] reported $\Delta H = -307$ kcal mol^{-1}, and although he indicated the carbon was graphite, the evidence for other sources is that probably only a slight amount of graphite was present. On the basis of information supplied by Neugebauer and Margrave (1.5 to 1.9 kcal mol^{-1}) [9], von Wartenberg and Schuette (2.4 kcal mol^{-1})

[1], and Kirkbride and Davidson (2.5 kcal mol^{-1}) [16] if we assume the heat of formation of the carbon residue to be +2 ±1 kcal mol^{-1} and apply a correction, the heat of reaction to that in which graphite is formed would be -307, which is still far less negative than the result of Kirkbride and Davidson.

Kirkbride and Davidson [16] reported $\Delta H_f[CF_4(g)] = -218 \pm 2$ kcal mol^{-1}, together with auxiliary data for KF(c) and amorphous carbon. We have back calculated to obtain $\Delta H_r = -320 \pm 2$ kcal mol^{-1}.

9. Vorob'ev and Skuratov [17] reported $\Delta H_r = -325.5 \pm 2.2$ kcal mol^{-1} and that their reaction led to formation of β-graphite. If we presume, on the basis of the work of Kirkbride and Davidson [16], that only a small amount of crystalline material was present and apply a correction of 2 kcal mol^{-1} for the heat of formation of amorphous carbon, the heat of reaction 9 would be -327.5 kcal mol^{-1}. See 8 above.

10. This series of reactions does not involve $CF_4(g)$, but is a route by which the heat of formation of NaF(c) can be obtained as auxiliary data for reaction 9.

The two different values given for the heat of reaction 10(c) are not due to experimental differences, but to an ambiguity in the nature of the reaction products. The spectroscopically observed reaction leads to an excited and a normal atom, but it is unclear which of the atoms is excited. The two different values, each accurately known, depend on the assignment.

Table 1 Thermochemical Studies Involving Tetrafluoromethane

	Reaction	ΔH°_{298}	Process for $\Delta H_f[CF_4(g)]$	Reference
1.	$C(c,graphite) + 2F_2(g) = CF_4(g)$	-162 ± 2^a	ΔH_r	Wartenberg and Schuette [1]
		$(-183.5 \pm 2)^b$		Ruff and Bretschneider[4]
		-222.87 ± 0.38		Domalski and Armstrong[5,6,]
2.	$CH_4(g) + 4F_2(g) = CF_4(g) + 4HF(g)$	-459.3 ± 9	$\Delta H_r + \Delta H_f[CH_4(g)] - 4\Delta H_f[HF(g)]$	Jessup, McCoskey and Nelson[7]
3.(a)	$C_2F_4(g) = CF_4(g) + C(c,graphite)^a$	-61.43 ± 1.4	$\Delta H_r + \Delta H_f[C_2F_4(g)]$	Duus[8]
		-65.4 ± 0.42		Neugebauer and Margrave[9]
(b)	$C_2F_4(g) + 2H_2(g) + 4[181.5H_2O](\ell) = 4[HF+181.5H_2O](\ell) + 2\ C(c,graphite)$	-150.8 ± 1.1		Neugebauer and Margrave[9]
(c)	$C_2F_4(g) + 2H_2(g) = 4HF(\ell) + 2\ C(c,graphite)$	-132.72 ± 0.7		Duus[8]
(d)	$4[HF+181.5H_2O](\ell) + C(c,graphite) = CF_4(g) + 2H_2(g) + 4[181.5H_2O](\ell)$	$+85.4 \pm 1.5$	$\Delta H_r + 4\Delta H_f$[HF in $181.5H_2O$]	
(e)	$4HF(\ell) + C(c,graphite) = CF_4(g) + 2H_2(g)$	$+67.32$	$\Delta H_r + 4\Delta H_f[HF(\ell)]$	
4.(a)	C_2F_4(solid polymer) $+ O_2(g) = CO_2(g) + CF_4(g)$	-118.8 ± 0.5	$\Delta H_r + \Delta H_f[C_2F_4$(solid polymer)$] - \Delta H_f[CO_2(g)]$	Scott, Good and Waddington[10]
(b)	C_2F_4(solid polymer) $+ O_2(g) + 42H_2O(\ell) = 2CO_2(g) + 4[HF+10H_2O](\ell)$	-160.3 ± 0.9		Scott, Good and Waddington[11]
				Scott, Good and Waddington[10]
(c)	$CO_2(g) + 4[HF+10H_2O](\ell) = CF_4(g) + 42H_2O(\ell)$	$+41.5 \pm 1.0$	$\Delta H_r + \Delta H_f[CO_2(g)] + 4\Delta H_f$[HF in $10H_2O(\ell)$]	
5.(a)	$C_{12}F_{22}(\ell) + 6.5O_2(g) + 401.8\ H_2O(\ell) = 0.6CF_4(g) + 11.4\ CO_2(g) + 19.6[HF+20H_2O](\ell)$	4067.9/4.184		Cox, Gundry and Head[12]
(b)	$C_{12}F_{22}(\ell) + 6.5O_2(g) + 131.2\ H_2O(\ell) = 3.9CF_4(g) + 8.1\ CO_2(g) + 6.4[HF+20H_2O](\ell)$	3496.5/4.184		Cox, Gundry and Head[12]
(c)	$CO_2(g) + 4[HF + 20H_2O](\ell) = CF_4(g) + 82\ H_2O(\ell)$	$+41.38 \pm 0.32$	$\Delta H_r + \Delta H_f[CO_2(g)] + 4\Delta H_f$[HF in $20H_2O(\ell)$]	

Table 1 (continued)

	Reaction	ΔH^o_{298} Kcal mol^{-1}	Process for $\Delta H_f[CF_4(g)]$	Reference
6.(a)	C_2F_4(solid polymer) + $F_2(g)$ = 2 $CF_4(g)$	-247.85(-247.43	$1/2[\Delta H_r + \Delta H_f[C_2F_4$(solid polymer)$]]$	Domalski and Armstrong[5,6,13]
(b)=4(a)	C_2F_4(solid polymer) + $O_2(g)$ = $CO_2(g)$ + $CF_4(g)$	-118.8		
(c)	$CO_2(g) + F_2(g) = O_2(g) + CF_4(g)$	-129.05(128.63)	$\Delta H_r + \Delta H_f[CO_2(g)]$	
7.	H_2, O_2, CO, CF_4	-220.1±1.4		Baibuz[14]
		-220.6		Baibuz and Medvedev[15]
8.	$CF_4(g) + 4K(c) = 4KF(c)$ + C(graphite)	-307±4	$4\Delta H_f[KF(c)] - \Delta H_r$	Wartenberg[2,3]
		-320±2		Kirkbride and Davidson[16]
9.	$CF_4(g) + 4Na(c) = 4NaF(c)$ + C(graphite)	-325.5±2.2	$4\Delta H_f[NaF(c)] - \Delta H_r$	Vorob'ev and Skuratov[17]
10.(a)	Na Cl(c) + 1/2 $F_2(g)$ = NaF(c) + $Cl_2(g)$	-39.3±0.1		Wartenberg and Litzner[18]
		-39.5±0.5		Schmitz and Schumacher[19]
(b)	NaCl + ClF(g) = NaF(c) + $Cl_2(g)$	-24.5±0.5		Schmitz and Schumacher[19]
(c)	ClF(g) = Cl(g) + F(g)	+60.355		Schmitz and Schumacher[20]
		+58.96		Wahrhaftig[21]
(d)	$1/2Cl_2(g) + 1/2\ F_2(g)$ = ClF(g)	-11.6		Wicke[22]
		-11.7		Wicke and Friz [23]

Table 2

Comparison of $\Delta H_f[HF \cdot nH_2O]$ From Several Sources

n	A	B	e_B	C	e_C
181.5	-77.07 ±0.4	-77.46	+.39	-76.35	-.72
20	-76.71 ±0.2	-77.396	+.69	-76.28	-.43
10	-76.74 ±0.35	-77.367	+.63	-76.235	-.50

A Calculations shown in the text.

B Values interpolated from the work of Cox and Harrop [29].

C Values interpolated from the review by Wagman, et al. [24].

Note: Recent work on the heat of reaction of NF_3 with hydrogen combined with heats of formation of NF_3 determined by dissociation measurements, [30] and also from the reaction of NF_3 with sulfur and the heat of formation of SF_6 [31] leads to a heat of formation of HF (aq,123H_2O) in good agreement with Column A.

[1] Wartenberg, H. v., and Schutte, R., Z. Anorg. Allgem. Chem. 211, 222-6 (1933).

[2] Wartenberg, H. von, Z. Anorg. Chem. 258, 356-60 (1949).

[3] Ruff, O., and Bretschneider, O., Z. Anorg. Allgem. Chem. 210, 173-83 (1933).

[4] Wartenberg, H., Nachr. Akad. Wiss. Goettingen, Math. Physik. Kl. 1946, 57.

[5] Domalski, E. S., and Armstrong, G. T., U. S. Air Force, Tech. Rept. AFAPL-TR-65-110 (1965).

[6] Domalski, E. S. and Armstrong, G. T., J. Research Natl. Bur. Standards, Submitted for Publication.

[7] Jessup, R. S., McCoskey, R. E., and Nelson, R. A., J. Am. Chem. Soc. 77, 244-5 (1955).

[8] Duus, H. C., Ind. Eng. Chem. 47, 1445-9 (1955).

[9] Neugebauer, C. A., and Margrave, J. L., J. Phys. Chem. 60, 1318-21 (1956).

[10] Good, W. D., Scott, D. W., and Waddington, G., J. Phys. Chem. 60, 1080-9 (1956).

[11] Scott, D. W., Good, W. D., and Waddington, G., J. Am. Chem. Soc. 77, 245-6 (1955).

[12] Cox, J. D., Gundry, H. A., and Head, A. J., Trans. Faraday Soc. 60, 653-65 (1964).

[13] Domalski, E. S., and Armstrong, G. T., J. Res. Natl. Bur. Standards 69A, 137-47 (1965).

[14] Baibuz, V. F., Doklady Akad. Nauk S.S.S.R. 140, 1358-60 (1961).

[15] Baibuz, V. F., and Medvedev, V. A., Tr. Gos. Inst. Prikl. Khim., No 49, 84 (1942).

[16] Kirkbride, F. W., and Davidson, F. G., Nature 174, 79-80 (1954).

[17] Vorob'ev, A. F., and Skuratov, S. M., Zh. Fiz. Khim., 32, 2580-5 (1958).

[18] Wartenberg, H. v., and Fitzner, O., Z. Anorg. Allgem. Chem. 151, 313-25 (1926).

[19] Schmitz, H., and Schumacher, H. J., Z. Naturforsch. 2A, 362 (1947).

[20] Schmitz, H., and Schumacher, H. J., Z. Naturforsch. 2A, 359-62 (1947).

[21] Wahrhaftig, A. L., J. Chem. Phys. 10, 248 (1942).

[22] Wicke, E., Nachr. Akad. Wiss. Gottingen 7, 89-90 (1946).

[23] Wicke, E., and Friz, H., Z. Elektrochem. 57, 9-16 (1953).

[24] Wagman, D. D., Evans, W. H., Halow, I., Parker, V. B., Bailey, S. M., and Schumm, R. H., Natl. Bur. Standards Tech. Note 270-2. 1-62 (1966).

[25] JANAF Thermochemical Tables, The Dow Chemical Company, Midland, Michigan, Dec. 31, 1960.

[26] Rossini, F. D., Wagman, D. D., Evans, W. H., Levine, S., and Jaffa, I., Selected Values of Chemical Thermodynamic Properties, NBS Circular 500 (U.S. Government Printing Office. Washington, 25, D. C. 1952).

[27] Kolesov, V. P., Zenkov, I. D., and Skuratov, S. M., Zh. Fiz. Khim. 37, 720 (1963); See also Russ. J. Phys. 37, 378-9 (1963).

[28] Stricker, W., Deutsch Luft and Raumfahrn Report 66-06,(1966).

[29] Cox, J. D., and Harrop, D., Trans. Faraday Soc. 61, 1328-37 (1965).

[30] Sinke, G. C.,Reported at the 21st calorimetry conference, Boulder, Colorado, June, 1966.

[31] Walker, L. C., Reported at the 21st calorimetry conference, Boulder, Colorado, June, 1966.

[32] Pitzer, K. S., and Westrum, E. F., J. Chem. Phys., 15, 526 (1947).

[33] Westrum, E. F., Jr., and Pitzer, K. S., J. Am. Chem. Soc. 71, 1940-48 (1949).

[34] Davis, M. L., and Westrum, E. F., Jr., J. Phys. Chem. 65, 338 (1961).

[35] Westrum, E. F., Jr., and Burney, G. A., J. Phys. Chem. 65, 344-8 (1961).

[36] Higgins, T. L., and Westrum, E. F., Jr., J. Phys. Chem. 65, 830-6 (1961).

[37] Benjamins, E., Burney, G. A., and Westrum, E. F. Jr., See Higgins, T. L., and Westrum, E. F. Jr., J. Phys. Chem., 65, 830 - 6 (1961).

[38] Buswell, A. M., Maycock, R. L., and Rodebush, W. H., J. Chem. Phys., 8, 362 (1940).

[39] Glockler, G., and Evans, G. E., J. Chem. Phys., 10, 607 (1942).

[40] Ketalaar, J. A. A., Rec. Trav. Chim., 60, 523 (1941).

[41] Pauling, L., "The Nature of the Chemical Bond," (Cornell University Press, Ithaca, New York, 1939) p 296 ff. See also (3rd Ed. 1960) pp 460 - 464.

[42] Davis, M., J. Chem Phys., 15, 739 (1947).

[43] Polder, D., Nature, 160, 870 (1947).

[44] Bernal, J. D., and Megaw, H. D., Proc. Roy. Soc. (London), A151, 384 (1935).

[45] Couture, L., and Mathieu, J. P., Compt. rend. 228, 555 (1949).

[46] Mathieu, J P., and Couture-Mathieu, L., Compt. rend., 230, 1054 (1950).

[47] Halverson, F., Rev. Modern Phys., 19, 87 (1947).

[48] Peterson, S. W., and Levy, H. A., J. Chem. Phys., 20, 704 (1952).

[49] Waddington, T. C., J. Chem. Soc., 1708 (1958).

[50] Anderson, C. C., and Hassel, O., Z. Physik. Chem., 123, 151 (1926).

[51] Froning, J. F., Richard, M. K., Stricklin, T. W., and Turnbull, S. G., Ind. Eng. Chem. , 39, 275 (1947).

[52] Godycki, L. E., Rundle, R. E., Voter, C., and Banks, C. V., J. Chem Phys., 19, 1205-6 (1951).

[53] Pauling, L., J. Am. Chem. Soc., 69, 542 (1947).

[54] Newman, R., and Badger, R. M., J. Chem. Phys., 19, 1207-8 (1951).

[55] Katelaar, J. A. A., and Vedder, W., J. Chem. Phys., 19, 654 (1951).

[56] Frevel, L. K. and Rinn, H. W. Acta. Cryst. 15, 286 (1962).

[57] Ibers, J. A., J. Chem. Phys., 40, No.2 402-4 (1964).

[58] Megaw, B. L., and Iber, J. A., J. Chem. Phys., 39, 2677 (1963).

[59] Blinc, R., Trontelj, Z., and Volausek, B., J. Chem. Phys. 44, No. 3 1028-33 (1966).

[60] Waugh, J. S., Humphrey, F. B., and Yost, D. M., J. Phys. Chem., 57, 486 (1953).

[61] Atoji, M., and Lipscomb, W. N., Acta. Cryst., 7, 173 (1954).

[62] Helmholz, L., and Rogers, M. T., J. Am. Chem. Soc., 61, 2590 (1949).

[63] Forrester, J. D., Senter, M. E., Zalhim, A., and Templeton, D. H., Acta. Cryst., 16, 58 (1963).

[64] McDonald, T. R. R., Acta. Cryst. 13, 113 (1960).

[65] Donahue, J., Am Chem. Soc. Meeying, April 9, 1951.

[66] Fischer, J., J. Am. Chem. Soc. 79, 6363-4 (1957).

[67] Vanderzee, C. E., and Swanson, J. A., J. Phys. Chem. 67, 2608-12 (1963).

Chapter 17

EQUATION OF STATE OF SOLID HYDROGEN

by

R. C. Thompson

and

C. W. Beckett

INTRODUCTION

The equation of state of solid hydrogen is of great theoretical interest because hydrogen is the simplest of all atoms and because of the simplicity of the interactions between hydrogen molecules as well as hydrogen atoms. Theoretical calculations of the equation of state and properties of solid hydrogen can be used to evaluate theoretical methods before they are tried on more complicated systems. The normal solid form of hydrogen is the molecular crystal, which we will call solid molecular hydrogen. The calculations of this phase of solid hydrogen can be compared with experimental measurements.

The first suggestion of a metallic modification of solid hydrogen at high pressures seems to have been made by Wigner and Huntington[1]. This phase of solid hydrogen is of great theoretical interest since, if it exists, solid atomic hydrogen would be the simplest of metals. Since the pressures at which metallic hydrogen would be formed are predicted to be of the order of one million atmospheres, it has been impossible to prove or disprove this hypothesis. The possibility of metallic hydrogen is of great interest to geophysicists and astrophysicists. The hypothesis that the core of the earth consists of iron and nickel was made to explain the discontinuity in the velocity of seismic waves which occurs at a depth of around 2900 km. In 1941, Kuhn and Rittman[2] proposed that the core of the earth contains considerable amounts, perhaps up to some 30 percent of solid hydrogen, and that the transition from the core to the outer silicate shell, which has lost its hydrogen by degassing, is quite gradual. They proposed the discontinuity was due to a change in viscosity of the solid hydrogen. Kronig, DeBoer and Korringa[3] calculated the pressure at which there would be a transition from solid molecular to metallic hydrogen, found it compatible with the pressure of about 1.5×10^6 atm prevailing at a depth of 2900 km, and proposed the transition as the cause of the discontinuity. Although Kronig et al made their calculation to support the hypothesis of Kuhn and Rittman, their work is now considered to form an argument against this hypothesis. On the other hand, it seems much more plausible, that the giant planets might contain metallic hydrogen. A number of papers [4-17] have used the suggested equation of state in the speculations on the compositions of the planets.

Of great interest in connection with the proposed transition from solid molecular hydrogen to metallic hydrogen is that a phase transition of this kind seems to have been observed experimentally by Alder and Christian[18] in shock-wave experiments on crystalline iodine. They used their results to estimate the pressure at which the phase transition would occur in hydrogen and obtained a value of about 20 megabars.

This paper is a review of the theory and calculations of the equation of state of solid hydrogen.

The calculation of the ground state energy of metallic hydrogen is divided into three parts. One is the energy of the electron gas system, the second is the energy of the lattice, and the third is the interaction terms. The energy of the electron gas consists of:

1. the Fermi energy (average kinetic energy);

2. the average Coulomb interaction energy between the electrons;

3. the energy of the exchange correlations of the Pauli principle which acts to keep electrons of parallel spin apart; and

4. the correlation energy.

1, 2, and 3 are calculated using the Hartree-Fock approximation. The correlation energy is defined as the difference between the energy calculated in the Hartree-Fock approximation and that calculated using any better approximation. The total energy equals the ground state energy plus the zero point energy.

The Correlation Energy

The ground state energy of a free electron gas has been calculated accurately in both the high and low density limit. The results of such calculations may be conveniently expressed in terms of the extent to which they represent an improvement over the Hartree-Fock calculation of the system energy. Thus we may write

$$E_0 = (2.21/r_s^2 - 0.916/r_s + E_{corr}) \cdot \qquad (1)$$

where r_s is the radius of the Fermi sphere, $E_0 = (22.1/r_s^2 - 0.916/r_s)$ is the ground state energy calculated in the Hartree-Fock approximation, and e_{corr} is the correlation energy. This name was introduced by Wigner[1, 25] who called attention to its importance in solid state problems.

As Wigner[19] first remarked, at sufficiently low densities the electrons may be expected to form a stable lattice in a sea of uniform positive charge. The potential energy keeps the electrons apart, and the kinetic energy for larger r_s (r_s>>10) is sufficient to prevent the electrons becoming localized at fixed sites. The correlation energy may then be expanded as a power series in $(1/r_s)^{1/2}$

$$E_{corr} = (U/r_s + V/r_s^{3/2} + W/r_s^2 + \cdots) \cdot \qquad (2)$$

The coefficients U and V were estimated by Wigner.

Macke[22] gave a treatment of the correlation energy which is based on the use of perturbation theory in determining the effect of the Coulomb interactions on the energy of the system. By including certain terms of higher order than the second, he was able to get convergence.

Gell-Mann and Brueckner [23] determined the correlation energy for high density or small r_s. Their method was based on summing the most highly divergent terms of the perturbation series under the integral sign to give a convergent result. The summation was performed by a technique similar to Feynman's methods in field theory. They get

$$E_{corr} \doteq 0.0622 \ln(r_s) - 0.98 + D r_s \ln(r_s) + E r_s + \cdots \qquad (3)$$

Where D and E were not evaluated. They also made a calculation using the methoc reported by Macke[22] to get

$$E_{corr} = 0.0622 \ln(r_s) - 0.128 . \quad (4)$$

Results which are equivalent to those of Gell-Mann and Brueckner in the high-density limit were subsequently obtained by a number of investigators[24-29].

DuBois[30] extended the work of Gell-Mann and Brueckner using third order perturbation theory to calculate an additional term. His expression for the correlation energy is

$$E_{corr} = 0.0622 \ln(r_s) - 0.096 + 0.0049\, r_s \ln(r_s) + 0(r_s) . \quad (5)$$

The region of actual metallic densities ($1.0<r_s<10$) is essentially an intermediate density region. There exists no simple rigorous series expression for the correlation energy in this region. It is usually found by interpolation between the high and low density limits.

Wigner[1] states that the correlation energy for $r_s>1$ can be represented rather closely by

$$E_{corr} = -0.584/(r_s + 5.1) . \quad (6)$$

Pines[31] states that this value of Wigner's approximation formulae was based on the incorrect low density limit of $-0.58/r_s$ as Wigner[20] points out in a footnote. Pines shows the correct low density limit to be $-0.88/r_s$. On combining this with Wigner's high-density calculation, he obtains as an approximate expression for the correlation energy

$$E_{corr}= -0.88/(r_s + 7.8) . \quad (7)$$

Using the collective description of electron interactions developed by Bohm and Pines[32-34], Pines determined a correlation energy of

$$E_{corr} = 0.0313 \ln(r_s) - 0.114 -0.005 r_s . \quad (8)$$

Later Nozieres and Pines[35] used this method to develop an interpolation procedure that gives for metallic densities the equation

$$E_{corr}= 0.031 \ln(r_s) - 0.115 . \quad (9)$$

Carr, Coldwell-Horsfall and Fein[36] calculated the first anharmonic contribution to the ground state energy of an electron gas. They found for low densities or large r_s the approximation

$$E_{corr} = E_{exp} - 1.792/r_s + 2.65/r_s^{3/2} - 0.73/r_s^2 . \quad (10)$$

where

$$E_{exp} = (21 r_s^{-1} - 4.8 r_s^{-3/4} - 1.16 r_s^{-5/4}) \,\mathrm{Exp}(- 2.06 r_s^{1/2})$$
$$-(2.06 r_s^{-5/4} - 0.66 r_s^{-7/4}) \,\mathrm{Exp}(-0.55 r_s^{1/2}) .$$

By interpolation between this result and that of Gell-Mann and Brueckner, assuming the expression of DuBois was correct, they determined the interpolation equation for metallic densities

$$E_{corr} = 0{\cdot}0622\ln(r_s) - 0{\cdot}096 + r_s[0{\cdot}0049\ln(r_s) - 0{\cdot}02]\cdot \qquad (11)$$

Recently Carr and Maradudin[37] calculated an additional term in the ground state energy of a high density electron gas using perturbation theory· They confirmed the results of Gell-Mann and Brueckner but obtained a coefficient of 0·018 for the $r_s\ln r_s$ term to be compared with 0·0049 given by DuBois· They say the reason for the discrepancy is a number of errors found in the calculation by DuBois· The additional term is r_s (E′ – ·036)· This makes the expression for the correlation energy at high densities

$$E_{corr} = (0{\cdot}0622\ln(r_s) - 0{\cdot}096) + r_s[0{\cdot}018\ln(r_s) + E' - 0{\cdot}036]\cdot \qquad (12)$$

E′ is given as the sum of a twelve-dimensional integral which is not evaluated· However, E′ must be positive if the r_s term of the correlation energy is to be quite small compared with the first term· To get a smooth curve between this high density expression and the low density expression of equation 10, they set E′ ≈0 and assume the high-density expression is then correct for $r_s<1$· The results of their interpolation are compared with other calculations in table I· The results of Wigner , Pines modification of Wigner, Nozieres and Pines, Macke, Gell-Man and Brueckner, and Carr et al were calculated from the equations above· The results of Hubbard, Carr et al tabulated and Carr and Maradudin are from table I of Carr and Maradudin· There is a discrepancy between the values calculated from the Carr et al equation and those tabulated by them·

The various expressions for the correlation energy are plotted in Figure 1· Note that the low density approximation of Carr et al falls almost on the Wigner interpolation curve· The interpolation curves of Wigner, Wigner as modified by Pines, Nozieres and Pines, and that of Carret al are quite similar in the region $2<r_s<20$· Accepting the Gell-Mann and Brueckner expression as correct for high densities, it would appear that Carr et al's interpolation equation is best in the region $1<r_s<10$·

Energy Calculations

Wigner and Huntington[1] were the first to calculate the energy of metallic hydrogen· Using the Wigner-Seitz method, they performed a numerical calculation for a body-centered cubic lattice· No equation for the energy was given, but their results were shown graphically· Using for the zero point energy

$$E_z = 0{\cdot}0244(\partial^2E/\partial r^2)^{1/2}. \qquad (13)$$

they found a minimum in the energy curve at 0·05 Ry (heat of vaporization about 16 kcal) for $r_s=1{\cdot}63$· They predicted a pressure of more than 250,000 atms would be required to form metallic hydrogen·

Eleven years later, Kronig, DeBoer and Korringa[3] (referred to subsequently as KBK) calculated the energies of solid metallic and molecular hydrogen to determine the pressure required for the transition· They used the Wigner-Seitz method for the metallic phase and gave a complete set of equations· They used the method proposed by Bardeen[21] to calculate the Fermi energy and Bardeen's equation for the exchange and correlation energy for the electrons, which was the same as that used by Wigner and Huntington· There is a problem with their expression for α in the Fermi-energy term

$$F = 2{\cdot}21\alpha/r^2\cdot \qquad (14)$$

KBK's equation for α is given as

$$\alpha = [1 - f(u)/2]^2[1 + (1 + f(u))/10r_s]/[1 + 13f(u)/28] \quad (15)$$

where

$$f(u) = u - 13u^3/28 + \cdots, \quad u = 7r_s/(70 - 13r_s). \quad (16)$$

These equations combine to give $\alpha = 0.827$ at $r_s = 1.8$ while they state in the paper that $\alpha = 0.966$ at $r_s = 1.8$.

March[38] recalculated the Fermi energy correction term α, and E_0 which represents the ''inferior limit'' of the lowest energy band which an electron in the atomic hydrogen lattice can occupy. His solution was constructed by means of a Taylor series expansion around the point $r/r_s = 1$. KBK had used a mutually orthogonal set of polynomials in r/r_s. March gave as KBK's value of α

$$\alpha = 1 - (61r^2/7000) + 0(r^3). \quad (17)$$

March gave as his value

$$\alpha = 1 - 13r^2/2100 + r^3/420 + 0(r^4) \quad (18)$$

Which gives $\alpha = 0.966$ at $r_s = 1.8$ This value of α can be put into KBK's energy equation to get

$$E_{at} = \frac{2.21}{r^2} - \frac{2.716}{r_s} - \frac{f(u)}{r_s} + 1.1563 - 0.0526r_s - \frac{0.58}{(r_s + 5.1)}. \quad (19)$$

Where f(u) is defined in equation (16), E is in Rydbergs and r_s is in Bohr radii; after conversion to kcal/mole and cc/mole, it is

$$E_{at} = \frac{359.6}{V^{2/3}} - \frac{613.5 + 225.9f(u)}{V^{1/3}} + 362.6 - 22.9V^{1/3} - \frac{131.0}{(V^{1/3} - 3.67)} \quad (20)$$

Where V is in cubic centimeters per mole, E is in kilocalories, and

$$f(u) = u - 13u^3/28, \quad u = 9.72V^{1/3}/(70 - 18.0\,V^{1/3}).$$

They disregarded zero point energy because of its smallness. KBK calculated the transition pressure to be 7×10^5 atm; the densities at this pressure were found to be $0.4 g/cm^3$ for the molecular phase and $0.8 g/cm^3$ for the metallic phase.

In 1954, a Russian, A. A. Abrikosov[39] calculated the equation of state of metallic hydrogen. Instead of using the Wigner-Seitz method, he selected a single parameter family of electronic wave functions which represent plane waves modulated by functions which have the required symmetry

$$\psi(k,r) = e^{ikr}\sum_n e^{-|r-r_n|}$$

and performed a quantum mechanical calculation for the simple, body-centered, and face-centered cubic lattice. The effect of the correlation of the positions of the electrons is not included. It is claimed that the correction is small and decreases rapidly with decreasing volume. His expression for the zero point energy is

$$E_z = 0.0768\ V^{2/3}(\partial^2E/\partial V^2)^{1/2}. \quad (21)$$

In the region of the minimum of the energy curve, this gives a value about 2/3 of that given by the Wigner and Huntington expression which is equivalent to

$$E_z = 0.118[V^{4/3}(\partial^2E/\partial V^2)\ 2/3\ V^{1/3}(\partial E/\partial V)]^{1/2}.$$

After adding I + D/2 - Eo/2 where Eo is the zero point energy of a molecule, his equation in atomic units is

$$E_{at} = 3.02/V^{2/3} - 2.26/V^{1/3} + 0.55\ . \quad (22)$$

This gives a minimum in the energy at V = 19.1 (r_s = 1.66) but no binding energy. After converting to kcal/mole and cc/mole, the equation becomes

$$E_{at} = 378.2/V^{2/3} - 632.2/V^{1/3} + 345.\ . \quad (23)$$

Abrikosov calculated the transition pressure to be 2.4×10^6 atm; the densities for this pressure were found to be $0.62 g/cm^3$ for the molecular phase and $1.12 g/cm^3$ for the metallic phase.

In 1958, W. C. DeMarcus[14] reviewed the the theoretical calculations and experimental data on the physical properties of solid hydrogen. He performed his own calculations and then applied his results to a discussion to the composition of the planets Jupiter and Saturn. His calculations for metallic hydrogen were based on the paper of Wigner and Huntington. He used Pines modification of Wigners equation for the correlation energy (equation 7). For the zero point energy, he used

$$E_z = 0.0244[\partial^2E/\partial r_s^2 - 2(\partial E/\partial r_s)/r_s]^{1/2}. \quad (24)$$

The corrections for the fact that the wave functions are not plane were taken directly from the graphs of Wigner and Huntington. He gave his results in the form of a table and stated that the calculation gives a cohesive energy of 13.3 kcal/mole at a density of $0.525\ g/cm^3$ and that the equation of state for pressures greater than 300,000 atms was very close to the one obtained by Kronig, DeBoer and Korringa if the zero point energy was added to their results.

In 1961, Bellemans and DeLeener[40] used the quantum statistical formalism of Block and deDominicis to determine the ground-state energy of a simple cubic lattice. They found a minimum in the energy curve at r = 1.59 and E(r) = + 0.01. This meant they found no binding energy.

In a later paper, Bellemans and DeLeener[41] state that they were making a consistent expansion of the ground state energy in terms of λ up to terms λ^2 (i.e., up to the same order as the Gell-Mann and Brueckner expression). This way of proceeding is very different from the Wigner-Seitz method and may eventually be a weaker type of approach on account of the slow convergence of a series in λ. However, it permits the case of multicomponent lattices (i.e., lattices with more than one type of positive charge located on the sites) to be treated in practically the same way as one component lattices. Hence, their method gives some hope for applications to metallic solutions. They compared their results with those of Wigner and Huntington to show their method gives approximately the correct solutions.

Carr[42] calculated the ground state energy of metallic hydrogen using a Rayleigh- Schrodinger perturbation expansion divided into three parts. One part was the electron gas system, the second was the lattice, and the third represented the interaction terms. For a body centered cubic lattice in atomic units, he got

$$E_{at} = 2.21r_s^{-2} - 2.708r_s^{-1} - 0.0905 - 0.018r_s - 0.005r_s^2 + E_{corr} \quad (25)$$

If the correlation energy found by Carr et al (equation 11) is used, then

$$E_{at} = \frac{2.21}{r_s^2} - \frac{2.708}{r_s} - 0.1865 + 0.0622\ln(r_s) - 0.38r_s - 0.005r_s^2 + 0.0049r_s\ln(r_s). \quad (26)$$

This equation does not include the terms for ionization energy, dissociation energy, or zero point energy. After conversion to kcal and cc/mole,

$$E_{at} = \frac{359.6}{V^{2/3}} - \frac{611.7}{V^{1/3}} - 52.09 + 19.5\ln(V^{1/3}) - 15.8V^{1/3} - 3.02V^{2/3} + 2.13V^{1/3}\ln(V^{1/3}). \quad (27)$$

Finally, a recent calculation has been carried out to test the so-called alternate molecular orbital method. Calais[43] applied Lowden's alternate molecular orbital method to the calculation of the potential energy curve of a body centered cubic lattice of hydrogen atoms. The results of the numerical calculation were given in graphical form for $1.59<r_s<7$. He found a minimum of 0.096 Rydbergs at $r_s = 1.89$. He did not make any estimate of the zero point energy because of the relative uncertainty of the calculations at small intermolecular distances.

Figure 2 compares the energy calculations for metallic hydrogen when the zero point energy is not included. The curves for Bellemans and DeLeener, Calais, and Wigner and Huntington are obtained from the graphs in their papers. The values for Kronig, DeBoer and Korringa, and those of Carr are calculated using equations 19 and 27, respectively. The dashed portions of the curves are arbitrary extensions of the data in the papers. If the correlation energy of Carr et al is used in the equations of KBK, the minimum energy becomes about the same as that of Calais but the value of r_s remains unchanged. Figure 3 compares the energy calculations for metallic hydrogen when the zero point energy is included. The values for the Abrikosov curve are calculated from equation 22. The values for Wigner and Huntington are taken from their graph and those for KBK and Carr are calculated as for Figure 2 with the addition of the zero point energy equation of Wigner and Huntington (equation 13). The Abrikosov curve is much too high, with a minimum of 0.09 Rydbergs.

A summary of the metallic hydrogen calculations is shown in Table II. In some cases estimates were made when the values or necessary information to calculate them were not given in the paper. These estimates are indicated by parenthesis. a is the coefficient in the equivalent Morse potential function.

The normal solid form of hydrogen is the molecular crystal. Solid molecular hydrogen belongs to the wider group of so-called molecular solids. In molecular crystals, the molecule preserves its individuality, i.e., its properties are very little different from those of an isolated molecule as present in a gas. In other words, molecular crystals consist of rather compact cells held together by the weak Van der Waals attractive forces.

The total energy of the crystal lattice at absolute zero (U_0) is the sum of the potential energy of the lattice (V_0) and the zero-point energy (U_z) associated with the zero-point vibrations of the molecules in the lattice.

$$U_0 = V_0 + U_z$$

The separation between nearest neighbors in a crystal at absolute zero differs from the separation (r_m) at which the intermolecular potential is a minimum. This is due to the opposing effects of the zero-point energy and the attraction of a molecule to molecules beyond its nearest neighbors. The effect of the zero-point energy is to expand the lattice. The attraction of non-nearest neighbors tends to contract the lattice. In molecular hydrogen the effect of the zero-point energy is much greater than the attraction of non-nearest neighbors.

The usual theory of molecular crystals assumes the forces between molecules are central forces, additive and the potential energy of the crystal can be written as

$$V_0 = \frac{N}{2} \sum_i n_i \phi(r_i) \qquad (28)$$

where N is the number of molecules in the lattice, r_i is the distance from a particular molecule to the i^{th} kind of lattice point, n_i is the number of molecules which occupy such lattice points, and $\phi(r_i)$ is the intermolecular potential function. The values of r_i and n_i for five types of crystal lattices and the relations between d_0 (the distance between nearest neighbors) and V_0 (the specific volume of the crystal) have been calculated by Kihara and Koba [44], Prins and Petersen[45] and are found in Hirschfelder, Curtiss and Bird[46].

For the Lennard-Jones intermolecular potential function [$\phi(r) = Ar^{-m} - Br^{-n}$], the potential energy of the crystal at absolute zero can be expressed in the form

$$V_o = (N/2)[AC_m d^{-m} - BC_n d^{-n}] \ . \qquad (29)$$

The constants C_i have been calculated by Lennard-Jones and Ingham[47] and Kihara and Koba[44] and are available in Hirschfelder, Curtiss and Bird[46].

To the potential energy must be added the zero-point energy (due to quantum effects) which is usually determined from the Debye expression

$$U_z = (9/8)Nk\Theta_D \qquad (30)$$

where Θ_D is the Debye characteristic temperature.

EXPERIMENTAL DATA

A fair amount of experimental data is available that can be used to check the theoretical calculations and to guide in the selection of parameters in the theoretical calculation of the properties of solid molecular hydrogen. Unfortunately, the experimental data is mostly in the low pressure region. The review of hydrogen and its isotopes by Woolley, Scott and Brickwedde [48] has an extensive bibliography covering all the data published up to 1947. The Cryogenic Data Center of NBS Boulder has published a comprehensive bibliography[49] of cryogenic fluids and their mixtures including hydrogen and its isotopes. This paper will not be as comprehensive, but will refer only to those papers that have come to the authors' attention and are considered useful for the calculation of the equation of state of solid hydrogen.

CRYSTAL STRUCTURE OF SOLID MOLECULAR HYDROGEN

The earliest investigation of the crystal structure of any of the solid isotopic hydrogens was that of Keesom, DeSmedt and Mooy[50] in 1930. The observed X-ray Debye-Scherrer patterns of more or less randomly oriented cyrstals of solid parahydrogen at liquid helium temperatures were indexed on the basis of a close-packed hexagonal structure; $a = 3.75A^\circ$, $c/a = 1.633$.

The initial results of Kogan and collaborators[51-55] were interpreted on the basis of a body- centered tetragonal structure for both hydrogen and deuterium. Independent Russian nuclear magnetic resonance measurements [56,57] were said to confirm this. However, the more recent X-ray studies of Kogan et al [58] confirm the hexagonal close- packed structure of Keesom et al with $a = 3.78A^\circ$ and $c/a = 1.63$ for hydrogen and $a = 3.54A^\circ$ and $c/a = 1.67$ for deuterium. They explain their earlier results as due to the texture of the samples, i.e., due to not having randomly oriented crystalline samples.

The infrared absorption spectrum of solid parahydrogen has been measured at temperatures above $10^\circ K$ by Gush et al[59]. The $S_1(0)$ line arises from the quadrupolar induction effect. The intensity is proportional to the square of the sum of the dipole moments induced by the quadrupole field of the absorbing molecule in all neighboring molecules. Van Kranendonk and Gush[60,61] have shown that for parahydrogen this sum vanishes if the central molecule is at the center of inversion symmetry. In a body centered tetragonal structure, the parahydrogen molecule would be at a center of inversion while in a close-packed hexagonal structure it would not. The fact that the $S_1(0)$ line is observed in parahydrogen is given as proof by Van Kranendonk and Gush that the parahydrogen crystal does not possess inversion symmetry and, therefore, cannot have a body centered tetragonal structure.

Curzon and Pawlowicz[62-64] found their electron diffraction patterns of a thin film of solid deuterium at $7^\circ K$ were consistent with a face-centered cubic lattice with four molecules per unit cell and a lattice parameter $a = 5.07 \pm 0.02A^\circ$. They state their pattern could not possibly have been produced by a close-packed hexagonal structure.

Mucker et al[65] studied the neutron diffraction patterns of randomly oriented crystalline samples of ortho-deuterium (97.8% ortho) and normal deuterium (66 2/3% ortho) at $13^\circ K$. They found it impossible to index the observed reflections as a single phase on the basis of either a cubic or tetragonal lattice. The assignment of indices is made on the basis of a hexagonal close-packed structure containing two molecules per cell with $a = 3.63A^\circ$ and $c/a = 1.61$.

Curzon and Mascal [66] studied the electron diffraction patterns of thin films of solid hydrogen at $5^\circ K$ and solid deuterium at 5 and $7^\circ K$. They did not specify the ortho-para concentrations. The pattern for deuterium was indexed according to a face-centered cubic lattice with a parameter $a_0 = 5.07 \pm 0.05A^\circ$ at about $5^\circ K$. The pattern for hydrogen was indexed as a mixture of a face-centered cubic lattice with a parameter $a_0 = 5.29 \pm 0.05A^\circ$ and a hexagonal close-packed lattice with parameters $a = 3.73 \pm 0.05\ A^\circ$, $c/a = 1.63$. The face-centered cubic lattice was predominant.

O. Bostanjoglo [67] used electron diffraction to study the crystalline structure of normal-hydrogen, para-hydrogen, and normal-deuterium layers at temperatures of 2.8 to 4.5°K. Five of the seven Debye-Sherrer rings found in the diffraction pattern were ascribed to a face-centered cubic lattice with a_0 =5.08 ± 0.02 A° for hydrogen and 5.08 ± 0.03 A° for deuterium. The remaining two diffraction rings could be due to (1) diffraction from cross-gratings and double diffraction by twinned crystals or (2) from a hexagonal lattice. He said the first explanation was more probable.

The specific heat measurements of Mendelssohn et al [68] Hill and Ricketson [69], and Ahlers and Orttung [70] have established that solid hydrogen with a high ortho-hydrogen content (> 60%) exhibits a λ anomaly below 2°K. Nuclear-magnetic-resonance measurements [71, 72] indicate that solid hydrogen undergoes a cooperative transition in this same region.

In their study of the infrared absorption spectrum of solid normal hydrogen in the neighborhood of 1.5°K, Clouter and Gush [73] found evidence of a transition. A reversible change in the spectrum was found to occur at the same temperature as the λ anomaly in the specific heat. The spectrum change can be accounted for if it is assumed that at temperatures above the transition, the crystal does not have a center of inversion symmetry and that when the crystal is cooled, there is a change in crystal structure to one possessing inversion symmetry. The mechanism by which the ortho-hydrogen molecules could cause this transition is by the splitting of the J = 1 state which is triply degenerate M = 0, ±1). This degeneracy can be removed by an electric field which could be exerted by the surrounding molecules. Bell and Fairbairn [74-76] and Danielian [77] have calculated this transition theoretically. They have found for pure ortho-hydrogen in a hexagonal close-packed lattice, a second order transition to an ordered state. The transition found by Danielian occured at 3°K. This is in agreement with Smith and Housley's experimental temperature of 2.6°K for 80% ortho-hydrogen and their extrapolated value of 3°K for 100% ortho-hydrogen.

Mills and Schuch [78] studied this transition by investigating the x-ray diffraction of normal hydrogen and 50% ortho-hydrogen at liquid helium temperatures. Normal hydrogen was found to have a hexagonal close-packed structure from 4°K to about 1.3°K and to transform below this temperature to face-centered cubic structure. For the 50% ortho-hydrogen, the structure was found to remain hexagonal to 1.25°K, the low temperature limit of the cryostat. The face-centered cubic lattice in the temperature region 1.25 to 1.3°K had a lattice parameter a_0 = 5.312 ± 0.010 A° and a calculated average volume of 22.57 cc/mole. The hexagonal closest-packing lattice parameters above 1.3°K were a = 3.76. ± 0.007 A°, c = 6.105 ± 0.011 A°, c/a = 1.623, and the calculated average volume was 22.52 cc/mole.

P V T Data of Solid Molecular Hydrogen

The molar volumes of solid hydrogen and deuterium at 4.2°K in the pressure range 0 to 100 kg/cm were measured by Megaw [79] with a picnometer in which the solid H_2 or D_2 was surrounded with liquid helium. The volume of the picnometer had been previously measured as a function of pressure at 4.2°K. Miss Megaw calculated the compressibilities from the results of these measurenents. Stewart [80-82] measured the relative volume changes of solid hydrogen and deuterium for pressures to 20,000 kg/cm by using the piston displacement method developed by Bridgman. The molar volumes were calculated from the results by assuming that Megaw's volume for zero pressure was correct. Stewart fit the data to the Birch-Murnaghan equation

$$P = (3/2\beta)[y^7 - y^5]\ [2 - \xi(y^2 - 1)] \quad (31)$$

where y = (Vo/V) . The values of ξ and $3/2\,\beta$ obtained from the fit were -1.9±0.1 and 3060 kg/cm , respectively.

Table III shows the molar volumes of solid hydrogen. The values for Megaw were obtained by reading the density from the graph and dividing by the molecular weight (2.0159 g/mole from ref [83]). Stewart's values are taken directly from his papers. The values given in Woolley et al (WSB) and the values calculated from the Murnaghan equation as fit by Stewart (SFM) are shown for comparison. The Murnaghan equation fits the experimental data of Stewart to well within his experimental accuracy, ±5 percent in the volume change.

The latent heat of fusion of normal hydrogen was measured by Simon and Lange[90] as 28.0±0.15 cal/g·mole at the triple point. The latent heat of fusion of parahydrogen as measured by Clusius and Hillier[91], Johnston et al[94], Ahlers [99], and Dwyer et al[84], is 28.04±0.19 cal/g·mole at the triple point. Stewart and Roder [85] have calculated the heat of fusion of parahydrogen from the Clapeyron equation using the volume change on fusion of normal hydrogen of Bartholome[86] and the volume of the freezing liquid given by Goodwin and Roder[114] with the assumption that the volume change on fusion is the same for normal and parahydrogen. Dwyer et al measured the heat of fusion at pressures up to 340 atm. and found the data could be represented by the equation

$$\Delta H = 0.04415P + 28.04 \quad (32)$$

where ΔH is in cal/g·mole and the pressure P is in atm. The heat of fusion calculated from this equation are given in Table IV.

Simon[87] calculated the heat of sublimation of solid hydrogen at absolute zero from the data of Simon and Lange[90] to be 183.4 cal/g·mole. The heats of sublimation of parahydrogen calculated by Mullins et al [88,89] are shown in Table V. If these results are extrapolated to 0°K, the result is 182.4 cal/g·mole.

SPECIFIC HEAT DATA OF SOLID MOLECULAR HYDROGEN

The specific heat at saturation pressure (C_s) of solid hydrogen was measured by Simon and Lange[90] from 10°K to the melting point before the discovery of parahydrogen. Clusius and Hillier[91] performed the same measurements for parahydrogen and obtained the same values within experimental error, for the specific heats of parahydrogen as had been obtained by Simon and Lange for supposedly normal hydrogen. Mendelssohn, Ruhemann, and Simon[92] measured the specific heats of several mixtures of ortho- and parahydrogen between 2.5° and 11.5°K. At temperatures below 11°K, the specific heats of the mixtures containing orthohydrogen are larger than for pure parahydrogen. The results on pure parahydrogen were in agreement with the earlier measurements of Clusius and Hillier, the data from 2.5° to 14°K fitting rather closely a Debye function with Θ = 91°K. However, the Debye theta is related theoretically to the specific heat at constant volume (C_V) not the specific heat at constant pressure (C_P) or at saturation pressure. The specific heats of solid hydrogen and deuterium at constant volume was measured by Bartholome and Eucken[93]. The Debye Θ that fit the C_V data of solid hydrogen best was 105° and for solid deuterium was 97°K.

Johnston et al [94] measured specific heat at constant pressure (C_P) of solid (99.8% pure) parahydrogen from 12.71°K to the melting point. Their results are in good agreement with those of Clusius and Hillier.

Hill and Ricketson[95] measured the temperature time curve for several mixtures of ortho- and parahydrogen as the sample warmed up due to heat liberated by the conversion of ortho- to parahydrogen. Assuming the rate at which heat was liberated in the hydrogen remains unchanged through and below the anomaly, the heating curves were translated into specific heat versus temperature curves. The heat capacity was found to have a sharp maximum of the type at about 1.5°K for orthohydrogen concentrations greater than 62%. The specific heat values were not very accurate, but the main interest was in the specific heat anomaly. Ahlers and Orttung [96] studied the λ anomaly in the heat capacity of solid hydrogen as a function of orthohydrogen concentration and molar volume. The anomaly was found to have structure with three distinguishable maxima. The maximum at the lowest temperature was invariably the largest of the three and was taken as the main peak. The temperature of the main peak was fit to the equation

$$T = (-226 + 6.93q)\,(V^{-5/3} - 120\times10^{3}V^{-5}) \tag{33}$$

where q is the orthohydrogen concentration in percent.

Hill and Lounasmaa [97] measured the specific heats of solid parahydrogen and orthodeuterium in the temperature range 2 to 18°K. The specific heats of parahydrogen at constant pressure were fit by the equation

$$C_p = 1.21\times10^{-3}T^3 + 8.5\times10^{-6}T^5 \tag{34}$$

Where C_p is in joule per mole per degree. Gruneisen's law was assumed to hold and the variation of compressibility with temperature was neglected to permit the calculation of the specific heat at constant volume from the equation

$$C_p - C_v = ATC_v^2 \tag{35}$$

The constant $A = 1.60 \times 10^{-3}$. was determined from the Bartholome and Eucken values for C_v. The calculation was admittedly approximate and had the particular defect that the C_v values were made to agree with those of Bartholome and Eucken so the latter were in no sense confirmed.

Ahlers[98,99] measured the heat capacity of solid parahydrogen at zero pressure and at three constant volumes. The C_p data agree with that of Hill and Lounasmaa above 4°K. Below 4°K, however, the Hill and Lounasmaa data was greater than this by more than can be explained by the scatter in the data. The heat capacity at constant volume was measured at 22.56, 19.83, and 18.73 cc/mole. The Debye thetas at 0°K were 128°, 169°, and 189°K, respectively. The temperature dependence of the Debye thetas was found to be similar to those for other simple solids. It is difficult to compare the data of Bartholome and Eucken with this because the molar volume used by Bartholome is unknown. Ahlers found the Gruneisen relation does not hold and, therefore, Hill and Lounasmaa's values for C_v are likely to be in error by a considerable amount.

Table VI contains the smoothed heat capacity at saturation pressure (C_s) of Ahlers and Hill and Lounasmaa. The measurements of Johnston et al, taken between 12 and 14°K, agree with Ahlers data within experimental error. The constant volume heat capacity (C_v) and Debye thetas are shown in Table VII. The molar volume at which the Bartholome and Eucken data were taken was unspecified. Ahlers gives an upper limit of 22.1 cc/mole for Bartholome's volume since the measurements extend to at least 17.9°K. Nonetheless, their heat capacity is 7% larger than Ahlers.

The relation between pressure and temperature along the melting line is usually expressed as some form of the Simon melting equation [100,101]. This equation was determined semi-empirically and found to fit the experimental melting curves of most substances. Domb[102] and DeBoer[103], by extending the Lennard-Jones and Devonshire theory of melting, and Salter[104], using the Gruneisen equation of state and the Lindemann melting formula, have derived the Simon melting equation giving it a theoretical basis.

The early measurements of Onnes[105], Keesom et al [106-108], and Simon et al [109] were correlated by Woolley et al[48] in their compilation of the properties of hydrogen. Woolley et al represented the melting curve by the Simon equation

$$\log_{10}(237.1 + P) = 1.85904 \log_{10}(T) + 0.24731 \qquad (36)$$

where the pressure is in kg/cm and the temperature is in °K on the NBS 1939 low temperature scale. Since then, Chester and Dugdale[110] have published a table of the separation of the melting curves of hydrogen and deuterium along with a small graph of the melting curves. Mills and Grilly measured the melting curves of hydrogen and deuterium first to 1920 kg/cm [111] and then to 3700 kg/cm [112]. They did not report the data but least squares fit their results to a Simon melting equation of the form

$$P = a + bT^c \qquad (37)$$

where P is in kg/cm , and T is in °K. The constants were determined as a = -279.63, b = 2.749629, and c = 1.744070 with a rms derivation of 5.98.

In 1962, Goodwin[113] measured the melting pressure of parahydrogen at three temperatures. Because the Simon equation used by Mills and Grilly in the region of the triple point is not satisfactory for hydrogen when least- squared to a wide range of data, Goodwin developed a new equation

$$(P - P_t)/(T - T_t) = A \exp(-\alpha T) + BT + C \qquad (38)$$

the subscript t refers to the triple point. The value B = 2/3 atm/deg was estimated from the behavior of normal hydrogen at the higher temperatures as given by Mills and Grilly and by Woolley, Scott, and Brickwedde. Values of the constants A = 30.3312 atm/deg and α = 5.693 were then determined from his measurements. Table VIII contains the melting pressures of normal hydrogen calculated from the equation of Woolley et al[48], the equations of Mills and Grilly [111,112], and the equation of Goodwin [113]. The values for parahydrogen were calculated from the equation of Goodwin. Temperatures are on the NBS 1955 temperature scale.

In 1963, Goodwin and Roder[114] applied Goodwin's equation without the constant C to parahydrogen. Using these pressures, they extrapolated the PVT data for fluid parahydrogen of Goodwin, Diller, Roder, and Weber[115] to determine the densities of the liquid in equilibrium with the solid.

In 1965, Dwyer, Cook, Berwaldt, and Nevins[116] measured the molar volume of solid parahydrogen along the melting line from the triple point to about 24°K. They computed additional values of the molar volume in this range from their heat of fusion data [117] and Goodwin et al's[115] PVT data for liquid parahydrogen. Dwyer et al[118] also measured the molar volume of the solid at temperatures somewhat lower than the melting temperature. These results indicate that at pressures above 150 atm there is a narrow temperature region near the melting line in which the molar volume of the solid parahydrogen increases as the temperature is decreased at constant pressure.

ZERO POINT ENERGY CALCULATIONS

Hobbs[119] calculated the zero-point energy, total energy, and volume of solid hydrogen and deuterium in face- centered cubic, simple cubic, and diamond lattices. An expression developed by London[120] was used for the zero- point energy. The results were closest to experimental values of hydrogen for a Lennard-Jones 9-6 potential in a face-centered cubic lattice.

DeBoer and Blaisse[121] derived a reduced equation of state for the solid state of the condensed permanent gases Ne, Ar, Kr, Xe, N_2, D_2, H_2, and He in a face-centered cubic lattice using a Lennard-Jones 12-6 potential. The zero-point energy was determined from the Debye expression

$$U_z = (9/8)\,Nk\Theta \tag{39}$$

using a formula proposed by Herzfeld and Mayer[122]. Their expression for the zero point energy (U_z) involves the elastic constants in a rather complicated fashion, so that numerical calculations are somewhat involved.

Salter[123,124] derived a reduced equation of state using a modified Debye expression

$$U_z = (9/8)\,Nk\Theta_\infty \tag{40}$$

to calculate the zero-point energy. Θ_∞ is the limiting value of Θ for high temperature. Central forces were assumed to allow the expression of the results in terms of DeBoer's reduced units. The method of Montroll[125-127] and Thirring was used to get a better estimate of the frequency spectrum. The zero-point energy is given as

$$U_z = \frac{3Nh}{16\pi}\left[5/m\sum\nabla^2\phi(r)\right]^{1/2} \tag{41}$$

For the Lennard-Jones 12-6 potential, the zero-point energy is very close to that of DeBoer and Blaisse.

I. J. Zucker[128] used a theoretical treatment based on the Einstein model of a crystal modified to account for large vibrations of the crystal atoms to calculate the harmonic and first two anharmonic terms in the zero-point energy. His harmonic term, which is quite similar to that of Salter's, is

$$U_z = \frac{3Nh}{16\pi}\left[\frac{16}{3m}\sum\nabla^2\phi(r)\right]^{1/2} \tag{42}$$

The first anharmonic term calculated from perturbation theory, the inclusion of which has been shown by Henkel [129], Johns[130], and Zucker[131] to improve the treatment of the heavier inert gas crystals, is given as

$$U_{zah} = \frac{3Nh^2\sum[(\partial^4\phi/\partial r^4) + (4/r)(\partial^3\phi/\partial r^3)]}{128\pi^2 m\sum[(\partial^2\phi/\partial r^2) + (2/r)(\partial\phi/\partial r)]} \tag{43}$$

However, for hydrogen this term is not small enough to be considered a perturbation when the volume is greater than 1/2 the zero pressure volume. Furthermore, an additional term is required. The zero-point energy was set up in the form of a Schrodinger equation which was solved by a numerical method due to Coulson and McWeeny. The calculations were made using a Lennard-Jones 12-6 potential. His results are given graphically and as he states, the procedure is excellent for the heavier inert gas solids but not too good for the hydrogen or helium isotopes.

J. M. H. Levelt and R. P. Hurst[132,133] recast the cell model for the liquid state, as proposed by Lennard-Jones and Devonshire, in terms of quantum statistical mechanics and applied it first to liquid hydrogen and deuterium at a density near that of the crystals at 0°K. They then adapted this method to crystals and evaluated the zero-point properties of the noble gases, hydrogen, and deuterium. The zero-point energy was obtained from an accurate solution of the Schrodinger equation using a Lennard-Jones 12-6 potential. The procedure requires lengthy numerical calculations that are very time-consuming even using a computer. The results for hydrogen are given in the pressure range of 0-300 atm with the calculated volumes being within four percent of the experimental values.

D. Henderson and R. Reed[134,135] also used the quantum cell model to find the thermodynamic properties of liquid hydrogen but calculated the energy levels by means of the WKB method rather than the numerical method used by Levelt and Hurst. Their results are compared with those of Levelt and Hurst and there is good agreement.

Hillier and Walkley[136-140] have written a series of papers on quantum cell model. They also find the WKB approximation gives results close to those of the exact calculation. They report calculations on the hard sphere potential, cubical cell model [140], and Lennard-Jones 12-6 potential.

EQUATION OF STATE CALCULATIONS

Kronig, DeBoer, and Korringa[3] calculated the equation of state of a face-centered cubic crystal of molecular hydrogen at absolute zero using the Lennard-Jones 12-6 potential. They assumed the forces were additive and used the lattice potential constants of Lennard-Jones and Ingham in an equation of the form of equation 29. They neglected the zero-point energy.

DeMarcus[14] in his paper on the constitution of planets Jupiter and Saturn objects to the pressure density relation of KBK for molecular hydrogen because it crosses the Fermi gas curve. The possibility that the equation of state of any cold matter can cross its Fermi gas curve can be questioned on general theoretical grounds. He compared the calculation of DeBoer and Blaisse with Stewart's experimental results and states the peculiar behavior of DeBoer theoretical densities at low pressures is convincingly explained as due to the neglect of anharmonic terms in calculating the zero- point energy. The subsequent gradual rise in the ratio of experimental to theoretical densities confirms that the Lennard-Jones potential is too hard. DeMarcus obtained his equation of state for the molecular form by an empirical extrapolation of the experimental data of Stewart. Stewart estimates the error in his measurements as five percent in the relative volume change from zero pressure so that the densities at the higher pressures are most uncertain. DeMarcus made two extrapolations; one assumes Stewart's data are correct as they stand and an alternative equation of state which is based on the assumption that Stewart's densities are too high by two percent at 20,000 kg/cm, are progressively more accurate at lower pressures, and completely accurate below 10,000 kg/cm The alterenate equation of state was calculated as a possible resolution of a dilemma that arose when model planets of Saturn were calculated. He presents his results in tables and graphs.

Abrikosov[39] had three objections to the calculations of Kronig et al on solid molecular hydrogen: (1) for the small spacings of interest for the phase transition, one cannot assume that the molecules interact as entities; (2) the experimental data used to determine the law of interaction between two molecules are valid only for normal pressures and cannot be used for high pressures; (3) the lattice has been assumed to be face – centered cubic without sufficient evidence. Abrikosov calculated the equation of state at T = 0 of the nonrotating modification of a hexagonal close – packed crystal of molecular hydrogen. The first order perturbation theory was based on the assumption that the energy of the molecular lattice is the sum of the interaction energies of individual atoms. The zero – point energy was included but the energy of the Van der Waals attraction of the molecules was neglected. Abrikosov estimates these forces would be important only at densities below 0.226 gm/cm . The calculations are numerical and an exact formula is not given. An interpolation formula that fits the results in the range V = 10 to 55 is given in atomic units as

$$P = 7.91\exp(-2.62V^{1/3}) \tag{44}$$

This expression can be integrated to give

$$E_{mol} = (1.145V^{2/3} + 0.87V^{1/3} + 0.334)\ [7.91\exp(-2.62V^{1/3})] \tag{45}$$

After converting to atmospheres, kilocalories, and cubic centimeters, these equations become

$$P = 2.278\times10^{8}\exp(-5.86V^{1/3}) \quad (46)$$

and

$$E_{mol} = (143.5V^{2/3} + 243.9V^{1/3} + 209.5)[\ 7.91\exp(-5.86V^{1/3})] \tag{47}$$

Trubitsyn[141] has shown that the Van der Waals energy in order of magnitude may be comparable with the first order approximation of the energy for pressure up to one million atm and objects [142] to the neglect of the Van der Waals forces by Abrikosov. This means the energy and pressures calculated in (39) are overestimated for all pressures.

Trubitsyn[142] calculated the energy and pressure of a crystal of molecular hydrogen as functions of volume and temperature in the pressure region from zero up to 10^6 atm. The intermolecular potential was assumed to be the sum of the interatomic potentials of all atoms in the two molecules. The interaction energy of two atoms of hydrogen was represented as the sum of the Heitler-London and the Van der Waals interaction energies. The intermolecular potential is found to be for R > 3.5

$$(R) = a\exp(-bR) - cR^{-6}(1 + dR^{-2}) \tag{48}$$

where a = 5.6, b = 1.81, c = 10.9, and d = 10.6. All quantities are expressed in atomic units where one atomic unit of energy is 27.2 ev, one unit of distance is 0.529×10^{-8} cm, and a unit of pressure is 3.0×10^{8} atm. The lattice constants of Hirschfelder, Curtiss, and Bird were rounded off to where the calculation applied to both the face-centered cubic and the hexagonal close – packing lattices. The Debye theory was used to obtain for the zero-point energy.

$$U_z = 0.026\nu^{4/3}v^{1/6}(v\partial^2 V_o/\partial v^2)^{1/2} \tag{49}$$

where ν was set equal to one since $3N\nu$ is the number of vibrational degrees of freedom and the crystal modification considered is one in which the molecules are rotating. This formula is good only for $v < 90$. In the region $100 < v < 170$, the zero-point energy was taken as that calculated by Levelt and Hurst [132] approximated by

$$U_z = 290v^{-3} \tag{50}$$

Trubitsyn fit Stewart's compressibility data with an exp-6 expression for the energy to obtain

$$U_o(v) = 11.5\exp(-2.19v^{1/3}) - 5.6/v^2 \tag{51}$$

in atomic units. Since this curve closely approximates the one calculated theoretically, Trubitsyn adds the thermal contribution calculated from the Debye theory to this to get his final equation.

To compare the results of these calculations, the internal energy of both solid molecular hydrogen and metallic hydrogen are shown in Figure 4. Two curves are given for metallic hydrogen. The values for Carr were calculated from equation 27 with the addition of the zero-point energy equation of Wigner and Huntington (equation 13). The curve labeled atomic hydrogen was calculated from the equations of Kronig, DeBoer, and Korringa using March's correction to the Fermi term (α), the correlation energy equation of Carr et al., and Wigner and Huntington's equation for the zero-point energy. This equation in cc/mole and kcal/mole is

$$\begin{aligned} E_{at} = {} & 359.6V^{-2/3} - 613.5V^{-1/3} - 225.9f(u)V^{-1/3} + 312.1 \\ & - 19.5\ln(V^{1/3}) - 18.3V^{1/3} + 2.13V^{1/3}\ln(V^{1/3}) - 1.8V^{2/3} \\ & + 0.0244[1119.6V^{-4/3} - 636.7V^{-1} - 10.1V^{-2/3} + 1.1V^{-1/3} - 1.87] \end{aligned} \tag{52}$$

where $f(u) = u - 13u^3/28$

and $u = 9.72V^{1/3}/(70 - 18.0V^{1/3})$.

The properties of solid atomic hydrogen calculated from this equation are given in Table IX.

There are several curves for molecular hydrogen. The curve labeled DeBoer was taken from DeBoer and Blaisse[121] whose equations are given below.

$$E_{mol} = N\epsilon\,(6.066V^{*-4} - 14.454V^{*-2} + (9/8)(3/4)^{1/3}\Lambda^{*}[V^{*}F(c^{*}_{ik})]^{1/6}) \qquad (53)$$

where

$$F(c^{*}_{ik}) = \frac{305534}{V^{*15}} - \frac{425900}{V^{*13}} + \frac{192503}{V^{*11}} - \frac{28373.1}{V^{*9}}$$

The values

$$N\sigma^{3} = 15.12 \text{ cc/mole}, \quad N\epsilon = 73.52 \text{ cal/mole}$$

$$E/k = 37°K \text{ and } P/\sigma^{3} = 200.8 \text{ atm}$$

were taken from a paper by DeBoer[142].

The equations of Salter[124]

$$E_{mol} = N\,[6.066V^{*-4} - 14.454V^{*-2} + 2.291\Lambda^{*}V^{*-7/2}(4.283 - 2.00V^{*2})^{1/2}] \qquad (54)$$

using the same variables and values as for DeBoer and Blaisse give a curve which differs from that of DeBoer only by the width of a line. The values for Trubitsyn were calculated from equation 54 which converted to cc/mole and kcal is

$$E_{mol} = 627.3[11.5\exp(-0.979V^{1/3}) - 703.2V^{-2} \qquad (55)$$

The values for Stewart were calculated by integrating the Murnaghan equation (equation 31) using ξ = −1.9 and 3060 kg/cm for 3/2 β. The values for Abrikosov were calculated from equation 50.

Because Abrikosov neglected the Van der Waals forces his values are much too high at volumes greater than 3 cc/mole and are probably too high throughout. The Lennard - Jones 12-6 potential is too hard at high densities making the DeBoer values too high at volumes smaller than 4 cc/mole. The Trubitsyn curve does not extend any further because the maximum of the exp-6 curve has been reached. However, if it were extended as a pure exponential curve, it would probably not intersect the atomic hydrogen curve. It is to be expected that the true curve should be somewhere near Stewart's curve.

To make it easier to determine the pressure at which the transition from molecular to metallic hydrogen occurs, the pressure versus the Gibb's free energy at 0°K were plotted in Figure 5. From this, it can be seen that the pressure would be between a low of 600,000 atmospheres, using DeBoer's parameters for the Lennard-Jones 12-6 potential, and a high of 2.4×10^{6} atmospheres, calculated using Abrikosov's equations.

DISCUSSION

From the experimental measurements of the crystal lattice structure it would seem that parahydrogen has a hexagonal close-packed lattice, and normal hydrogen has a mixture of a hexagonal close-packed (hcp) and face-centered cubic lattice (fcc). From the calculations of the lattice potential constants [155,156], it has been shown theoretically that for a Lennard-Jones m-n potential the energy of a hcp lattice is less than one percent smaller than a fcp lattice. This means the hcp lattice is favored. However, this should hold for the inert gas solids which have been found experimentally to be face-centered cubic. For a modified Buckingham equation [44]

$$\phi(r) = \frac{\varepsilon}{(\alpha - 6)} [6 \exp(\alpha - \alpha r/r_m) - \alpha(r_m/r)^6] \quad (56)$$

there exists a critical value of α, $\alpha = 8.675$. If α is greater than 8.675 the hcp lattice has the lower energy while for α less than this value the fcc lattice is favored. However, since the difference in energy is small compared with the difference due to the choice of potential functions, the choice of hcp or fcc is relatively unimportant.

A major problem in calculating the energy of a molecular crystal is determining the intermolecular potential to be used. The forces between two hydrogen atoms [143-145] are known with an accuracy which is probably greater than that for any other system. The forces between two hydrogen molecules is much less accurately known. It appears that no satisfactory inverse pair potential can be found which allows ε and σ to be uniquely evaluated over any large range of temperatures [146,147].

To determine how the choice of different intermolecular potentials would affect the calculations, the authors have chosen several of the potentials proposed for gaseous hydrogen using equation 29 to calculate the potential energy and Salter's equation (41) to calculate the zero-energy. The results are shown in figure 6.

The Buckingham Corner curve is given by the equation

$$\phi(r) = A \exp[-a(y-1)] - (By^{-6} + Cy^{-8}) \exp[-4(y-1)^3] \quad \text{for } y \leq 1 \quad (57)$$

where $y = r/r_m$ and the values of the constants A, B, and C were taken from the paper by Buckingham et al[148]. Since the main contribution is due to the 12 nearest neighbors, a value of 12 was used for C_i in all equations for the exponential functions. The curve labeled Fisher was calculated from a Morse Function

$$\phi(r) = \varepsilon\{\exp[-2A(y-1)] - 2 \exp[-A(y-1)]\} \quad (58)$$

where $y = r/r_m$, $r_m = [1 + \ln(2)/C]$, $A = Cr_m/\sigma$

The values of $\varepsilon/k = 39.75°K$, $\sigma = 3.011 \times 10^{-8}$cm, and $C = 5.003$ determined by Fisher[149] are based on high temperature viscosity measurements.

Bahethi and Saxena[150] evaluated the Morse potential parameters using second virial, viscosity, and diffusion data. They found that different choices of parameters were essential to represent the equilibrium and nonequilibrium properties. Their values evaluated from second virial coefficients give a curve very close to that of Fisher's. The values evaluated from the viscosity data give a curve which lies between the DeBoer and Blaisse curve and the Buckingham Corner curve.

Mason and Rice[151] calculated the parameters of the modified Buckingham potential

$$\phi(r) = \frac{\varepsilon}{1 - 6/\alpha} \left\{ \frac{6}{\alpha} \exp[\alpha(1 - r/r_0)] - (r_0/r)^6 \right\} \quad (59)$$

from experimental values of second virial coefficients and viscosity coefficients. They get $r_0 = 3.337\text{A}^\circ$, $\varepsilon/k = 37.3^\circ k$, and $\alpha = 14$. The curve calculated for solid molecular hydrogen using this potential and their coefficients falls close to the Buckingham Corner curve.

Gordon and Cashion[152] in their comparison of infrared spectroscopic data to potential functions used as parameters in the modified Buckingham equation

$$\varepsilon/k = 33^\circ K, \quad r_0 = 3.45 \times 10^{-8} \text{cm}, \quad \text{and} \quad \alpha = 11.5$$

which they fit to the results of the quantum mechanical calculation of Evett and Margenau[154] on the $H_2 - H_2$ interaction. Using this potential results in a curve which follows the Stewart curve to v = 1.5 and the atomic hydrogen curve for v less than 1 cc/mole. In the calculations for all potentials other than the 12-6, Salter's equation for Debye theta was used to determine the zero- point energy.

Figure 7 shows the results of these calculations on a Gibb's free energy versus pressure plot. It is to be expected that the correct solid molecular hydrogen curve would lie somewhere between the Fisher curve and the Gordon and Cashion curve. Because the slope of the metallic and molecular hydrogen curves are so similar a relatively small change in either of them will cause a large change in the predicted transition pressure.

The intermolecular potential for hydrogen molecules calculated by Vanderslice and Mason [157] for small intermolecular distances lies between the Morse potential fit to experimental data by Fisher and the modified Buckingham potential fit to the theoretical calculations of Evett and Margenau by Gordon and Cashion. At intermolecular distances corresponding to those at which the transition from solid molecular to metallic hydrogen takes place the Fisher potential and the Vanderslice and Mason potential are almost identical. This indicates that the Fisher Morse potential is probably better than the Lennard-Jones 12 - 6 potential for hydrogen. The zero point energy equations of DeBoer and Blaisse or Salter contain only the harmonic approximation so they are not accurate enough to use at low pressures where the zero point energy and potential energy are of opposite sign and both are larger than the total energy. In addition the expressions become imaginary for molar volumes near the zero pressure volume. However, at high pressures where the zero point energy is a fraction of the total energy the neglect of the anharmonic terms should cause only a small differance. The Murnaghan equation correlates the experimental pressure-volume data very well. This equation can be integrated using an integration constant that will give an energy at zero pressure equal to the sublimation energy. This gives results that fall between those of Fisher and those of Gordon and Cashion. However, this method takes no account of the possible transition from a rotating to a nonrotating form as proposed by London[158]. The best calculations of the zero point properties of solid hydrogen were performed by Levelt and Hurst, but this method requires very time consuming machine calculations.

The calculations of Kronig, DeBoer and Koringa give the largest binding energy of the cell type calculations for metallic hydrogen. This suggests the choice of the KBK equations using Marche's expression for the Fermi correction term α and Carr et al's expression for the correlation energy as the best expression for the energy for metallic hydrogen. The curves labeled atomic hydrogen were calculated from these equations. The recent calculations of Calais using the molecular orbital method give a minimum in the energy curve without the zero point energy which agrees very well with that calculated from the KBK equations. It would appear from figures 5 and 7 that the transition pressure is between 8×10^5 and 3×10^6 atm. Assuming the curves labeled Fisher and atomic hydrogen are the best approximations, the best value for the transition pressure is 1×10^6 atm. The properties of solid hydrogen at 0°K calculated according to these approximations are given in Tables IX and X. The properties of metallic hydrogen contained in Table IX were calculated from equation 52 which contains I plus D/2 where D/2 is taken as 54.71 kcal. The properties of solid molecular hydrogen contained in Table X were calculated from equation 28 considering only nearest neighbors to give $V_o = 6N\phi(r)$. The Morse function of Fisher (equation 58) was used for the intermolecular potential $\phi(r)$, and the Salter expression (equation 41) was used for the zero point energy. This table goes no lower than 10^4 atm because the Salter approximation is no good at low pressures.

A treatment of solid molecular hydrogen that will permit the correlation of the thermodynamic properties over a fairly wide range of temperatures and pressures is desirable. For this purpose one may use the Morse potential function combined with the Gruneisen approximation for the equation of state of a simple solid. Although this is probably the best currently available method for obtaining thermodynamic properties over a wide range of temperatures and pressures, it is not very satisfactory because the specific heat at constant volume does not appear to be in agreement with estimates of the Gruneisen approximation at zero pressure.

REFERENCES

[1] E. Wigner and H. B. Huntington, ''On the Possibility of a Metallic Modification of Hydrogen,'' J. Chem. Phys. 3, 764 (1935).

[2] W. Kuhn and A. Rittman, ''About the Condition of the Earths Inner Core and its Formation from a Homogeneous Initial State'' (in German) Geol. Rundschau 32, 215 (1941).

[3] R. Kronig, J. De Boer and J. Korringa, ''On the Internal Constitution of the Earth,'' Physica XII, 245 (1946).

[4] R. Wildt, ''On the State of Matter in the Interior of the Planets,'' Astrophys. J. 87, 508 (1938).

[5] D. S. Kothari, ''The Theory of Pressure Ionization and its Applications,'' Proc. Roy. Soc. (London) A165, 486 (1938).

[6] C. L. Critchfield, ''Theoretical Properties of Dense Hydrogen,'' Astrophys. J. 96, 1 (1942).

[7] H. Brown, ''On the Composition and Structures of the Planets,'' Astrophys. J. 111, 641 (1950).

[8] W. H. Ramsey, ''The Planets and the White Dwarfs,'' Monthly Notices Roy. Astron. Soc. 110, 444 (1950).

[9] W. H. Ramsey, ''On the Constitution of the Major Planets,'' Monthly Notices Roy. Astron. Soc. 111, 427 (1951).

[10] V. G. Fesenkov and A. G. Masevich, ''The Structure and Chemical Composition of the Large Planets,'' Soviet Astron. AJ 28, 317 (1951).

[11] R. Wildt, ''The Constitution of the Planets,'' Mon. Not. Roy. Astron. Soc. 107, 84 (1954).

[12] L. Knopoff and R. J. Uffen, ''The Densities of Compounds at High Pressures and the State of the Earth's Interior,'' J. Geophys. Res. 59, 471 (1954).

[13] R. Wildt, ''Inside the Planets,'' Publ. Astron. Soc. Pacific 70, 237 (1958).

[14] W. C. DeMarcus, ''The Constitution of Jupiter and Saturn,'' Astron. J. 63, 2 (1958).

[15] W. C. DeMarcus, ''Planetary Interiors,'' Handbuch der Physik 52, 419 (1959).

[16] W. E. De Marcus, ''Theoretical Pressure-Density Relations with Applications to the Constitution of the Planets,'' Thesis Yale Univ. (1951).

[17] R. Wildt, ''Planetary Interiors,'' Chap. 5 of The Solar System III Planets and Satellites, edited by C. P. Kuiper and B. M. Middlehurst, Univ. Chicago Press (1961).

[18] B. J. Alder and R. H. Christian, ''Destruction of Diatomic Bonds by Pressure,'' Phys. Rev. Letters 4, 450 (1960).

[19] E. P. Wigner, ''On the Interaction of Electrons in Metals,'' Phys. Rev. 46, 1002 (1934).

[20] E. Wigner, ''Effect of the Electron Interaction on the Energy Levels of Electrons in Metals,'' Trans. Faraday Soc. 34, 678 (1938).

[21] J. Bardeen, ''An Improved Calculation of the Energies of Metallic Li and Na '' J. Chem. Phys. 6, 367 (1938).

[22] W. Macke, ''On the Collective Effect in a Fermi Gas'' (in German) Z. Naturforsch 5a, 192 (1950).

[23] M. Gell-Mann and K. A. Brueckner, ''Correlation Energy of an Electron Gas at High Density,'' Phys. Rev. 106, 364 (1957).

[24] K. Sawada, K. A. Brueckner, N. Fukuda and R. Brout, ''Correlation Energy of an Electron Gas at High Density; Plasma Oscillations,'' Phys. Rev. 108, 507 (1957).

[25] R. Brout, ''Correlation Energy of High-Density Gas: Plasma Coordinates,'' Phys. Rev. 108, 515 (1957).

[26] J. Hubbard, ''The Description of Collective Motions in Terms of Many-Body Perturbation Theory,'' Proc. Roy. Soc. (London) A240, 539 (1957).

[27] J. Hubbard, ''The Description of Collective Motions in Terms of Many-Body Perturbation Theory II The Correlation Energy of a Free-Electron Gas,'' Proc. Roy. Soc. (London) A243, 336 (1958).

[29] P. Nozieres and D. Pines, ''Ground-State Energy and Stopping Power of an Electron Gas,'' Phys. Rev. 109, 1009 (1958).

[30] D. F. DuBois, ''Electron Interactions Part I. Field Theory of a Degenerate Electron Gas,'' Ann. Phys. 7, 174 (1959).

[31] D. Pines, ''Electron Interaction in Metals,'' Solid State Physics 1, 367 (1955).

[32] D. Bohm and D. Pines, ''A Collective Description of Electron Interactions II Collective vs. Individual Particle Aspects of the Interactions,'' Phys. Rev. 85, 332 (1952).

[33] D. Bohm and D. Pines, ''A Collective Description of Electron Interactions III Coulomb Interactions in a Degenerate Electron Gas,'' Phys. Rev. 92, 609 (1953).

[34] D. Pines, ''A Collective Description of Electron Interactions IV Electron Interaction in Metals,'' Phys. Rev. 92, 626 (1953).

[35] P. Nozieres and D. Pines, ''Correlation Energy of Free Electron Gas,'' Phys. Rev. 111, 442 (1958).

[36] W. J. Carr, Jr., R. A. Coldwell-Horsfall and A. E. Fein, ''Anharmonic Contribution to Energy of a Dilute Electron Gas Interpolation for the Correlation Energy,'' Phys. Rev. 124, 747 (1961).

[37] W. J. Carr, Jr. and A. A. Maradudin, ''Ground-State Energy of a High-Density Electron Gas,'' Phys. Rev. 133, A371 (1964).

[38] N. H. March, ''On Metallic Hydrogen,'' Physica XXII, 311 (1956).

[39] A. A. Abrikosov, ''The Equation of State of Hydrogen at High Pressures,'' U.S.S.R. Astronomical Journal 31, 112 (1954) available in English as Rand translation T-81 (1958), AD605743 translated by M. Kivelson.

[40] A. Bellemans and M. DeLeener, ''Ground-State Energy of an Electron Gas in a Lattice of Positive Point Charges,'' Phys. Rev. Letters 6, 603 (1961).

[41] A. Bellemans and M. DeLeener, ''Electron Gas in a Lattice of Positive Charges,'' Adv. Chem. Phys. 6, 85 (1964).

[42] W. J. Carr, Jr., ''Ground State of Metallic Hydrogen I,'' Phys. Rev. 128, 120 (1962).

[43] J. L. Calais, ''Different Bands for Different Spins III. Solid Atomic Hydrogen,'' Arkiv Fysik 29, 255 (1965).

[44] T. Kihara and S. Koba, ''Crystal Structures and Intermolecular Forces of Rare Gases,'' J. Phys. Soc. Japan 7, 384 (1952).

[45] J. Prins and H. Petersen, ''Theoretical Diffraction Patterns Coorresponding to some simple types of Molecular Arrangements'' Physica 3, 147 (1936).

[46] J. O. Hirschfelder, C. F. Curtiss and R. B. Bird, ''Molecular Theory of Gases and Liquids,'' John Wiley and Sons (1954).

[47] J. E. Lennard-Jones and A. E. Ingham, ''On the Calculation of Certain Crystal Potential Constants and on the Cubic Crystal of Least Potential Energy,'' Proc. Roy. Soc. (London) A107, 636 (1925).

[48] H. W. Woolley, R. B. Scott, F. G. Brickwedde, ''Compilation of Thermal Properties of Hydrogen in its Various Isotopic and Ortho- Para Modifications,'' J. Research NBS 41, 379 (1948). (Res. Paper R. P. 1932)

[49] NBS Cryogenic Data Center Report 8808 (1965).

[50] W. H. Keesom, J. DeSmedt and H. H. Mooy, ''On the Crystal Structure of Para- Hydrogen at Liquid Helium Temperatures,'' Comms. Kamerlingh Onnes Lab. Univ. Leiden No. 209-d, 35, (1930).

[51] V. S. Kogan, B. G. Lazarev and R. F. Bulatova, ''The Crystalline Structure of Hydrogen and Deuterium,'' Soviet Phys. JETP 4, 593 (1957).

[52] V. S. Kogan, B. G. Lazarev and R. F. Bulatova, ''Diffraction of X-rays by Polycrystalline Samples of Hydrogen Isotopes,'' Soviet Phys. JETP 10, 485 (1960).

[53] V. S. Kogan, B. G. Lazerov, R. P. Ozerov and G. S. Zhdanov, ''Neutron Diffraction Study of the Crystalline Structure of Solid Hydrogen and Deuterium,'' Soviet Phys. JETP 13, 718 (1961).

[54] R. P. Ozerov, V. S. Kogan, G. S. Zhdanov and O. H. Kuto, ''The Crystalline Structure of Solid Isotopes of Hydrogen,'' Soviet Phys. Cryst. 6, 507 (1962).

[55] R. P. Ozerov, V. S. Kogan, G. S. Zhdanov and B. G. Lazarov, ''Neutron Diffraction Study of the Crystal Structure of Solid Hydrogen and Deuterium,'' J. Phys. Soc. Japan 17, (Suppl. B-II) 385 (1962).

[56] A. A. Galkin and I. V. Matyash, ''On the Structure of Solid Hydrogen,'' Soviet Phys. JETP 10, 1292 (1960).

[57] S. S. Duklin, ''Specific Heat Anomaly and Nuclear Resonance in Crystalline Hydrogen in Connection with New Data on its Structure,'' Soviet Phys. JETP 10, 1054 (1960).

[58] V. S. Kogan, A. S. Bulatov and L. F. Yakimenko, ''Texture in Layers of Hydrogen Isotopes Condensed on a Cooled Substrate,'' Soviet Phys. JETP 19, 107 (1964).

[59] H. F. Gush, W. F. J. Hare, E. J. Allen and H. L. Welsh, ''The Infrared Fundamental Band of Liquid and Solid Hydrogen,'' Can. J. Phys. 38, 176 (1960).

[60] J. Van Kranendonk and H. P. Gush, ''The Crystal Structure of Solid Hydrogen,'' Phys. Letters 1, 22 (1962).

[61] H. P. Gush and J. Van Kranendonk, ''Calculation of the Structure of the $S_1(0)$ and $S_1(0)$ $+S_1(0)$ Lines in the Infrared Spectrum of Solid Hydrogen,'' Can. J. Phys. 40, 1463 (1962).

[62] A. E. Curzon and A. T. Pawlowicz, ''Electron Diffraction Patterns from Solid Deuterium,'' Proc. Phys. Soc. (London) 83, 499 (1964).

[63] A. E. Curzon and A. T. Pawlowicz, ''Electron Diffraction Patterns from Solid Deuterium -- A Correction,'' Proc. Phys. Soc. (London) 83, 888 (1964).

[64] M. Blackman and A. E. Curzon, ''On the Crystal Structure of Solid Deuterium,'' Proc. Phys. Soc. (London) 87, 588 (1966).

[65] K. F. Mucker, S. Talhouk, P. M. Harris, D. White, and R. A. Erickson, ''On the Crystal Structure of Solid Deuterium,'' Phys. Rev. Letters 15, 586 (1965).

[66] A. E. Curzon and A. J. Mascall, ''The Crystal Structures of Solid Hydrogen and Solid Deuterium in Thin Films,'' Brit. J. Appl. Phys. 16, 1301 (1965).

[67] O. Bostanjoglo, ''Electron Diffraction of Crystalline Hydrogen''(in German), Z. Physik 187, 444 (1965).

[68] K. Mendelssohn, M. Ruhemann and F. Simon, ''The Specific Heat of Hydrogen at Helium Temperatures,'' Z. Physik. Chem. (Leipzig) B15, 121 (1931).

[69] R. W. Hill and B. W. A. Ricketson, ''A λ Anomaly in the Specific Heat of Solid Hydrogen,'' Phil. Mag. 45, 277 (1954).

[70] G. Ahlers and W. H. Orttung, '' λ Anomaly in the Heat Capacity of Solid Hydrogen at Small Molar Volumes,'' Phys. Rev. 133, A1642 (1964).

[71] F. Reif and E. M. Purcell, ''Nuclear Magnetic Resonance in Solid Hydrogen,'' Phys. Rev. 91, 631 (1953).

[72] G. W. Smith and R. M. Housley, ''Nuclear Magnetic Resonance of Solid Hydrogen (67-86% Ortho) and Solid Deuterium (33% and 55% Para),'' Phys. Rev. 117, 732 (1960).

[73] M. Clouter and H. P. Gush, ''Change in Crystal Structure of Solid Normal Hydrogen Near 1.5°K,'' Phys. Rev. Letters 15, 200 (1965).

[74] G. M. Bell and W. M. Fairbairn, ''Regular Model for Solid Hydrogen I,'' Mol. Phys. 4, 481 (1961).

[75] G. M. Bell and W. M. Fairbairn, ''Regular Model for Solid Hydrogen II,'' Mol. Phys. 5, 605 (1962).

[76] G. M. Bell and W. M. Fairbairn, ''Regular Model for Solid Hydrogen III,'' Mol. Phys. 7, 497 (1964).

[77] A. Danielian, ''Ordering in Solid Hydrogen,'' Phys. Rev. 138, A282 (1965).

[78] R. L. Mills and A. F. Schuch, ''Crystal Structure of Normal Hydrogen at Low Temperatures,'' Phys. Rev. Letters 15, 722 (1965).

[79] H. D. Megaw, ''The Density and Compressibility of Solid Hydrogen and Deuterium at 4.2°K,'' Phil. Mag. 28, 129 (1939).

[80] J. W. Stewart and C. A. Swenson, ''Compression to 10,000 Atms of Solid Hydrogen and Deuterium at 4.2°K,'' Phys. Rev. 94, 1069 (1954).

[81] J. W. Stewart, ''Compressibilities of Some Solidified Gases at Low Temperatures,'' Phys. Rev. 97, 578 (1955).

[82] J. W. Stewart, ''Compression of Solidified Gases to 20,000 kg/cm at Low Temperatures,'' J. Phys. Chem. Solids 1, 146 (1956).

J. W. Stewart, ''Compression of Solid Helium and other Condensed Gases at Low Temperatur,'' Bull. Am. Phys. Soc. [2] 1, 218 (1956).

[83] D. D. Wagman, W. H. Evans, I. Halow, V. B. Parker, S. M. Bailey, and R. H. Schumm, NBS Tech. Note 270-1 (1965).

[84] R. F. Dwyer, G. A. Cook, B. M. Shields, and D. H. Stellrecht, ''Heat of Fusion of Solid Parahydrogen,'' J. Chem. Phys. 42, 3809 (1965).

[85] R. B. Stewart and H. M. Roder, ''Properties of Normal and Para-Hydrogen,'' Chapter 11 of Technology and Uses of Liquid Hydrogen edited by R. B. Scott, The Macmillan Company, New York (1964).

[86] E. Bartholome, ''On Thermal and Calometric Equations of State of Condensed Hydrogen Isotopes'' (in German), Z. Physik. Chem. (B) 33, 387 (1936).

[87] F. Simon, ''The Chemical Constants of Hydrogen'' (in German), Z. Physik 15, 307 (1923).

[88] J. C. Mullins, W. T. Ziegler, and B. S. Kirk, ''The Thermodynamic Properties of Parahydrogen from 1° to 22°K,'' Tech. Rept. No. 1, Eng. Expt. Sta., Geo. Inst. Tech. (1961).

[89] J. C. Mullins, W. T. Ziegler, and B. S. Kirk, ''The Thermodynamic Properties of Parahydrogen,'' Adv. Cryogenics Eng. 8, 116 (1962).

[90] F. Simon and F. Lange, ''The Thermal Data of Condensed Hydrogen'' (in German), Z. Physik 15, 312 (1923).

[91] K. Clusius and K. Hiller, ''The Specific Heat of Parahydrogen in Solid, Liquid, and Gas States'' (in German), Z. Physik. Chem. (B) 4, 158 (1929).

[92] K. Mendelssohn, M. Ruhemann, and F. Simon, ''The Specific Heat of Hydrogen at Helium Temperatures'' (in German), Z. Physik. Chem. (B) 15, 121 (1931).

[93] E. Bartholome and A. Eucken, ''The Direct Calorimetric Estimation of Specific Heat at Constant Volume for the Isotopes of Hydrogen in Solid and Liquid State'' (in German), Z. Elecktrochem. 42, 547 (1936).

[94] H. L. Johnston, J. T. Clarke, E. B. Rifkin, and E. C. Kerr, ''Condensed Gas Calorimetry. I. Heat Capacities, Latent Heats, and Entropies of Pure Para- Hydrogen from 12.7 to 20.3°K. Description of the Condensed Gas Calorimeter in Use in the Cryogenics Laboratory of the Ohio State University,'' J. Am. Chem. Soc. 72, 3933 (1950).

[95] R. W. Hill and B. W. A. Ricketson, ''A λ-Anomaly in the Specific Heat of Solid Hydrogen,'' Phil. Mag. (7) 45, 277 (1954).

[96] G. Ahlers and W. H. Orttung, ''λ Anomaly in the Heat Capacity of Solid Hydrogen at Small Molar Volumes,'' Phys. Rev. 133, A1642 (1964).

[97] R. W. Hill and O. V. Lounasmaa, ''The Lattice Specific Heats of Solid Hydrogen and Deuterium,'' Phil. Mag. (8) 4, 785 (1959).

[98] G. Ahlers, ''Some Properties of Solid Hydrogen at Small Molar Volumes,'' AEC Report UCRL-10757 (1963).

[99] G. Ahlers, ''Lattice Heat Capacity of Solid Hydrogen,'' J. Chem. Phys. 41, 86 (1964).

[100] F. Simon and G. Glatzel, ''Observations on the Melting Curve''(in German), Z. Anorgan. Chem. 178, 309 (1929).

[101] F. Simon, ''On the Range of Stability of the Fluid State,'' Trans. Faraday Soc. 33, 65 (1937).

[102] C. Domb, ''The Melting Curve at High Pressures,'' Phil. Mag. (7) 42, 1316 (1951).

[103] J. DeBoer, ''Theories of the Liquid State,'' Proc. Roy. Soc. (London) 215A, 4 (1952).

[104] L. Salter, ''The Simon Melting Equation,'' Phil. Mag. (7) 45, 369 (1954).

J. S. Dugdale and F. E. Simon, ''Thermodynamic Properties and Melting of Solid Helium,'' Proc. Roy. Soc. (London) 218A, 219 (1953).

[105] K. Kamerlingh Onnes and W. Van Gulick, ''The Melting Curve of Hydrogen to 55 kg/cm,'' Commun. Phys. Lab. Univ. Leiden No. 184 (1926).

[106] W. Van Gulik and W. H. Keesom, ''The Melting Curve of Hydrogen to 245 kg/cm,'' Commun. Phys. Lab. Univ. Leiden No. 192b (1928).

[107] W. H. Keesom and J. H. C. Lisman, ''The Melting Curve of Hydrogen to 450 kg/cm,'' Commun. Phys. Lab. Univ. Leiden No. 213e (1931).

[108] W. H. Keesom and J. H. C. Lisman, ''The Fusion Curve of Hydrogen up to 610.5 kg/cm ''(in French), Comm. Phys. Lab. Univ. Leiden No. 22/a (1932).

[109] F. Simon, M. Ruhemann, and W. A. M. Edwards, ''The Melting curve of Hydrogen, Neon, Nitrogen and Argon ''(in German), Z. Physik. Chem. B6, 331 (1930).

[110] P. F. Chester and J. S. Dugdale, ''Melting Curves of Deuterium and Hydrogen,'' Phys. Rev. 95, 278 (1954).

[111] R. L. Mills and E. R. Grilly, ''Melting Curves of He^3, He^4, H_2, D_2, Ne, N_2 and O_2 up to 3500 kg/cm,'' Phys. Rev. 99, 480 (1955).

[112] R. L. Mills and E. R. Grilly, ''Melting Curves of H_2, D_2, and T_2 up to 3500 kg/cm,'' Phys. Rev. 101, 1246 (1956).

[113] R. D. Goodwin, ''Melting Pressure Equation for the Hydrogens,'' Cryogenics 2, 352 (1962).

[114] R. D. Goodwin and H. M. Roder, ''Pressure - Density - Temperature Relations of Freezing Liquid Parahydrogen to 350 Atmospheres,'' Cryogenics 3, 12 (1963).

[115] R. D. Goodwin, D. E. Diller, H. M. Roder, and L. A. Weber, ''Pressure-Density-Temperature Relations of Fluid Para Hydrogen from 15 to 100°K at Pressures to 350 Atmospheres,'' J. Res. N.B.S. 67A, 173 (1963).

[116] R. F. Dwyer, G. A. Cook, O. E. Berwaldt, and H. E. Nevins, ''Molar Volume of Solid Parahydrogen Along the Melting Line,'' J. Chem. Phys. 43, 801 (1965).

[117] G. A. Cook, R. F. Dwyer, O. E. Berwaldt, and H. E. Nevins, ''Pressure-Volume-Temperature Relations in Solid Parahydrogen,'' J. Chem. Phys. 43, 1313 (1965).

[118] R. F. Dwyer, G. A. Cook, B. M. Shields, and D. H. Stellrecht, ''Heat of Fusion of Solid Parahydrogen,'' J. Chem. Phys. 42, 3809 (1965).

[119] M. E. Hobbs, ''The Solid State of H_2, HD, and D_2,'' J. Chem. Phys. 7, 318 (1939).

[120] F. London, ''On Condensed Helium at Absolute Zero,'' Proc. Toy. Soc. (London) A153, 576 (1936).

[121] J. DeBoer and B. S. Blaisse, ''Quantum Theory of Condensed Permanent Gases II The Solid State and the Melting Line,'' Physica XIV, 149 (1948).

[122] K. F. Herzfeld and M. Goeppert-Mayer, ''On the Theory of Fusion,'' Phys. Rev. 46, 995 (1934).

[123] C. Domb and L. Salter, ''The Zero Point Energy and Values of Crystals,'' Phil. Mag. (7) 43, 1083 (1952).

[124] L. Salter, ''The Ideal Crystal at Absolute Zero,'' Phil. Mag. (7) 45, 360 (1954).

[125] E. W. Montroll, ''Frequency Spectrum of Crystalline Solids,'' J. Chem. Phys. 10, 218 (1942).

[126] E. W. Montroll, ''Frequency Spectrum of Crystalline Solids II General Theory and Applications to Simple Cubic Lattices,'' J. Chem. Phys. 11, 481 (1943).

[127] E. W. Montroll, ''Frequency Spectrum of Crystalline Solids III Body-Centered Lattices,'' J. Chem. Phys. 12, 98 (1944).

[128] I. J. Zucker, ''The Reduced Equation of State of the Inert Gas Solids at the Absolute Zero,'' Proc. Phys. Soc. (London) 77, 889 (1961).

[129] I. J. Zucker, ''Anharmonic Effects in the Theory of Solid Argon,'' Phil. Mag. (8) 3, 987 (1958).

[130] H. H. Henkel, ''Equation of State and the Thermal Dependence of the Elastic Coefficients of Crystalline Argon,'' J. Chem. Phys. 23, 681 (1955).

[131] T. F. Johns, ''Calculations of the Solid State Data of Neon and the Vapour Pressure Ratio of its Isotopes,'' Phil. Mag. (8) 3, 229 (1958).

[132] J. M. H. Levelt and R. P. Hurst, ''Quantum Mechanical Cell Model of the Liquid State. I,'' J. Chem. Phys. 32, 96 (1960).

[133] R. P. Hurst and J. M. H. Levelt, ''Quantum Mechanical Cell Model of the Liquid State II Application to the Zero Point Properties of Close Packed Crystals,'' J. Chem. Phys. 34, 54 (1961).

[134] D. Henderson and R. D. Reed, ''Cell Model for Quantum Fluids. I,'' J. Chem. Phys. 40, 975 (1964).

[135] R. D. Reed, D. Henderson, and R. Chen, ''Isotopic Effects in Liquid Hydrogen,'' J. Chem. Phys. 43, 1836 (1965).

[136] I. H. Hillier and J. Walkley, ''Quantum Cell Model Equation of State,'' J. Chem. Phys. 41, 2168 (1964).

[137] I. H. Hillier and J. Walkley, ''Quantum Cell Model I. The Uniform Potential Function,'' J. Chem. Phys. 41, 3205 (1964).

[138] I. H. Hillier and J. Walkley, ''Quantum Cell Model. II. A Corresponding States Approach to an Equation of State at High Densities,'' J. Chem. Phys. 42, 3414 (1965).

[139] I. H. Hillier, M. S. Islam, and J. Walkley, ''Single- Particle Theory for Systems at High Densities. I Characteristic Reduction Parameters for the Mie-Lennard- Jones Pai Interaction Potential from Zero Point Crystal Data,'' J. Chem. Phys. 43, 3705 (1965).

[140] I. H. Hillier and J. Walkley, ''A Quantum Hard- Sphere Equation of State,'' Trans. Faraday Soc. 59, 1093 (1963).

[141] V. P. Trubitsyn, ''Van der Waals Forces at High Pressures,'' Soviet Phys. Solid State 7, 2779 (1966).

[142] V. P. Trubitsyn, ''Equation of State of Solid Hydrogen,'' Soviet Phys. Solid State 7, 2708 (1966). 0

[142] J. DeBoer, ''Theories of the Liquid State,'' Proc. Roy. Soc. (London) A215, 4 (1952).

[143] W. Kolos and L. Wolniewicz, ''Accurate Adiabatic Treatment of the Ground State of the Hydrogen Molecule,'' J. Chem. Phys. 41, 3663 (1964).

[144] W. Kolos. and L. Wolniewicz, ''Accurate Computation of Vibronic Energies and of Some Expectation Values of H_2, D_2, and T_2,'' J. Chem. Phys. 41, 3674 (1964).

[145] W. Kolos and L. Wolniewicz, ''Potential-Energy Curves for the $X\,{}^1\Sigma_g^+$, and $C\,{}^1\Pi_u$ States of the Hydrogen Molecule,'' J. Chem. Phys. 43, 2429 (1964).

[146] A. E. Sherwood and J. M. Prausnitz, ''Intermolecular Potential Functions and the Second and Third Virial Coefficients,'' J. Chem. Phys. 41, 429 (1964).

[147] J. H. Dymond, M. Rigby, and E. B. Smith, ''Intermolecular Potential Energy Functions for Simple Molecules,'' Nature 204, 678 (1964).

[148] R. A. Buckingham, A. E. Davies, and A. R. Davies, ''The Deduction of Intermolecular Forces from the Transport Properties of Hydrogen and Helium,'' Proc. Conf. Therm. and Trans. Props., Fluids (London) 111, (1957).

[149] B. B. Fisher, ''Calculation of the Thermal Properties of Hydrogen,'' AEC Report LA-3364 to be published.

[150] O. P. Bahethi and S. C. Saxena, ''Morse Potential Parameters for Hydrogen,'' Indian J. Pure Appl. Phys. 2, 267 (1964).

[151] E. A. Mason and W. E. Rice, ''The Intermolecular Potentials for Some Simple Non- Polar Molecules,'' J. Chem. Phys. 22, 843 (1954).

[152] E. A. Mason and W. E. Rice, ''Intermolecular Potentials of Helium and Hydrogen,'' J. Chem. Phys. 22, 522 (1954).

[153] K. G. Gordon and J. K. Cashion, ''Intermolecular Potentials and the Infrared Spectrum of the Molecular Complex (H_2),'' J. Chem. Phys. 44, 1190 (1966).

[154] A. A. Evett and H. Margenau, ''The Forces Between Hydrogen Molecules,'' Phys. Rev. 90, 1021 (1953).

[155] J.A.Prins, J.M.Dumore and L.T.Tjoan, ''Factors affecting the Choice Between Cubical and Hexagonal Close Packing'', Physica 18, 307 (1952).

[156] T. K. H. Barron and C. Domb, ''On the Cubic and Hexagonal Close-Packed Lattice'', Proc. Roy. Soc. (London) A227, 447 (1955).

[157] J. T. Vanderslice and E. A. Mason, ''Quantum Mechanical Calculations of Short- Range Intermolecular Forces'', Rev. Mod. Phys. 32, 417 (1960).

[158] F. London, ''Alignment of Hydrogen Molecules by High Pressure,'' Phys. Rev. 102, 168 (1956).

TABLE I· CORRELATION ENERGY OF AN ELECTRON GAS·

Negative Values Given in Rydberg Units as Function of the Fermi Sphere Radius (r_s) in Bohr Radii)

1 Rydberg = 1,312·04 kilojoules = 313·585 kilocalories = 13·598 electron volts

1 Bohr Radius = 5·29167 x 10^{-8}cm, $V_s = \frac{4\pi}{3} r_s^3$ = 11·2058 (V in cc/mol electrons)

r_s Bohr	V_s $Bohr^3$	log r_s	Wigner	Wigner Pines	Nozieres Pines	Macke	Gell-Mann Brueckner	Carr et al	Hubbard	Carr table	Carr Maradudin
0·00	0·0000	∞	0·1145	0·1128							
0·10	0·0042	-1·0000	0·1123	0·1114	0·1864	0·2712	0·2392	0·2413			
0·20	0·0335	-0·6990	0·1102	0·1100	0·1649	0·2281	0·0961	0·2017			
0·50	0·5236	-0·3010	0·1042	0·1060	0·1365	0·1711	0·1391	0·1508			
1·00	4·1888	0·0000	0·0957	0·1009	0·1150	0·1280	0·0960	0·1160			
1·10	5·5753	0·0414	0·0942	0·0989	0·1120	0·1221	0·0901	0·1116			
1·20	7·2382	0·0792	0·0927	0·0978	0·1093	0·1167	0·0847	0·1076			
1·25	8·1812	0·0969	0·0920	0·0972	0·1081	0·1141	0·0821	0·1058			
1·30	9·2028	0·1139	0·0912	0·0967	0·1069	0·1117	0·0797	0·1040			
1·40	11·494	0·1461	0·0898	0·0957	0·1040	0·1071	0·0751	0·1008			
1·50	14·137	0·1761	0·0885	0·0946	0·1024	0·1028	0·0708	0·0978			
1·60	17·157	0·2041	0·0872	0·0936	0·1004	0·0988	0·0668	0·0951			
1·65	18·817	0·2175	0·0865	0·0931	0·0995	0·0969	0·0649	0·0938			
1·70	20·580	0·2304	0·0859	0·0926	0·0986	0·0950	0·0630	0·0926			
1·80	24·429	0·2553	0·0846	0·0917	0·0968	0·0914	0·0594	0·0903			
1·90	28·731	0·2788	0·0834	0·0907	0·0951	0·0881	0·0561	0·0881			
2·00	33·510	0·3010	0·0823	0·0898	0·0935	0·0849	0·0529	0·0861	0·099	0·085	0·096
3·00	113·10	0·4771	0·0721	0·0815	0·0809	0·0597	0·0277	0·0715	0·086	0·068	0·076
4·00	268·08	0·6020	0·0642	0·0746	0·0720	0·0418	0·0098	0·0626	0·074	0·058	0·064
5·00	523·60	0·6990	0·0578	0·0688	0·0651	0·0279	-0·0041	0·0565	0·067	0·051	0·054
6·00	904·78	0·7782	0·0526	0·0623	0·0595	0·0166	-0·0154	0·0519		0·046	0·048
10·00	4188·8	1·0000	0·0388	0·0494	0·0436	-0·0152	-0·0472	0·0400			
20·00	33510·	1·3010	0·0233	0·0317	0·0221	-0·0583	-0·0903	0·0161			
100·00		2·0000	0·0056	0·0082	-0·0278	-0·1584	-0·1904	-0·4470			
∞	∞	∞	0	0	- ∞	- ∞	- ∞	- ∞			

TABLE II· SUMMARY OF CALCULATED PROPERTIES OF METALLIC HYDROGEN·

Energy is in Rydberg units and distance in Bohr radii·

1 Rydberg = 1312·04 kilojoules = 313·585 kilocalories = 13·598 electron volts

1 Bohr radius = $5{\cdot}29167 \times 10^{-8}$ cm, $V_s = \frac{4\pi}{3} r_s^3$ = 11·2058 (V in cc/mole electron)

Author	Wigner Huntington	Kronig et al	Abrikosov	Bellemanns DeLeener	Carr	Calais
Date	1935	1946	1954	1961	1962	1965
-E	0·50	0·0775	-(0·0900)	-0·01	0·056	0·096
+Ez	0·0173	0·0192	0·0320		0·0213	
-(E+Ez)	0·0327	-0·0583	-0·0897	0·0347		
Without Zero Point Energy						
Re	1·64	1·68	(1·62)	1·59	1·66	1·89
Ro	1·36	1·284			1·31	
Ro/Re	0·829	0·764			0·752	
a	4·05	2·94			3·24	
Ve	18·48	20·0	(17·81)	16·84	19·16	25·69
Vo	10·54	8·86			9·31	
Including Zero Point Energy						
Re	1·67	(1·65)	1·66		(1·69)	
Ro	1·40	(1·24)			(1·35)	
Ro/Re	0·838	(0·752)			(0·799)	
a	4·28	(2·79)			(3·45)	
Ve	19·51	(18·8)	19·1		(20·2)	
Vo	11·49	(7·99)			(10·3)	
Ve	2·692	(2·66)			(2·73)	
Vo	2·256	(2·00)			(2·18)	

E is the energy at the minimum of the potential energy curve·
Ez is the zero point energy at the minimum of the energy curve·
Re is the radius at the minimum of the energy curve·
Ve is the volume in bohr units at the minimum of the energy curve·
Ro is the radius at which the energy is equal to zero·
Vo is the volume at which the energy is zero·
a is the coefficient in the equivalent Morse function·
In some cases estimates were made when not given in the paper·
These estimates are indicated by parenthesis·

TABLE III. MOLAR VOLUMES OF SOLID HYDROGEN.

T °K	P kg/cm	Megaw V cc/mole	Stewart V cc/mole	SFM V cc/mole	WSB V cc/mole	Compressibility Megaw in 10^{-5} cm^2/kg	Compressibility Stewart in 10^{-5} cm^2/kg
0	0	22.57					
4.2	0	22.65		22.65		68+15	49
	10			22.54	22.49		
	20	22.37		22.44			
	25			22.38	22.30		
	30	22.25		22.33			
	40	22.15		22.23			
	50	22.01		22.14	22.03		
	60	21.91		22.05			
	70	21.86		21.96			
	75			21.91	21.80		
	80	21.77		21.87			
	90	21.64		21.78			
	100	21.60		21.70	21.60	32	
	143		21.4	21.37			
	200		21.0	20.98			31
	300			20.40			
	400		20.0	19.90			23
	600		19.2	19.10			19
	1,000		18.0	17.94			14
	2,000		16.1	16.17			
	2,043		16.1	16.11			8.1
	3,000		15.1	15.07			6.1
	4,000		14.3	14.28			4.8
	6,000		13.2	13.18			3.5
	8,000		12.4	12.40			2.7
	10,000		11.8	11.81			2.3
	12,000		11.3	11.34			1.9
	16,000		10.6	10.61			1.4
	18,000		10.3	10.34			
	20,000		10.1	10.08			1.2

TABLE IV· FUSION CURVE·

T °K	Pressure Atmos	Heat of Fusion Cal/g Mole
14	5·88698	28·2999
15	36·8797	29·6682
16	70·1908	31·1389
17	105·676	32·7056
18	143·217	34·363
19	182·717	36·107
20	224·096	37·9338
21	267·286	39·8407
22	312·23	41·825
23	358·88	43·8846
24	407·196	46·0177
25	457·14	48·2227
26	508·684	50·4984
27	561·801	52·8435
28	616·466	55·257
29	672·662	57·738
30	730·368	60·2858

TABLE V· HEAT OF SUBLIMATION

T °K	Heat of Sublimation Cal/g mole
13·813	244·90
13	242·30
12	238·71
11	234·77
10	230·55
9	226·12
8	221·53
7	216·82
6	212·02
5	207·15
4	202·24
3	197·30
2	192·34
1	187·37

TABLE VI· HEAT CAPACITY OF SOLID MOLECULAR HYDROGEN AT SATURATION PRESSURE·

Heat capacity in millijoules per mole per degree

T °K	Hill and Lounasmmaa	Ahlers
1	1·22	1·03
2	9·95	8·57
3	34·7	30·7
4	86·1	78·7
5	178·	168·
6	327·	319·
7	557·	551·
8	898·	882·
9	1384·	1333·
10	2060·	1917·
11		2651·
12		3548·
13		4618·
14		5910·

TABLE VII· SMOOTHED VALUES OF HEAT CAPACITY AT CONSTANT VOLUME AND THE DEBYE THETAS FOR HYDROGEN·

T °K	Bartholome and Eucken		Hill and Lounasmma		Ahlers 22·56 cc/mole		Ahlers 19·83 cc/mole		Ahlers 18·73 cc/mole	
	C_v	Θ_D	C_v	Θ_D	C_v	Θ_D	C_v	Θ_D	C_v	Θ_D
0					0·0	128·1	0·00	169·0	0·00	189·4
1					0·93	127·8	0·40	168·8	0·29	189·2
2			9·95	116·0	7·58	127·0	3·26	168·3	2·31	188·8
3			34·7	114·8	26·4	125·7	11·18	167·4	7·88	188·1
4			85·6	113·2	65·3	123·9	27·1	166·2	18·94	187·3
5			176·	111·3	134·6	121·8	54·2	164·9	37·5	186·4
6			317·	109·8	247·	119·3	96·8	163·1	66·3	185·0
7			527··	108·1	418·	116·9	159·1	161·2	107·7	183·6
8			813·	106·9	662·	114·5	247·	159·1	164·9	182·1
9			1170·	106·0	990·	112·5	367·	156·9	242·	180·0
10			1570·	104·5	1413·	110·7	523·	154·9	343·	178·3
11	2220·	103·9			1919·	109·4	723·	15298	471·	176·4
12	2740·	104·9			2499·	108·5	968·	151·2	632·	174·4
13	3330·	105·4			3124·	107·8	1259·	149·8	830·	172·4
14	4000·	105·5			3866·	107·0	1597·	148·6	1067·	170·7
15	4740·	105·2			4678·	105·8	1979·	147·6	1340·	169·2
16	5540·	104·7					2405·	146·7	1655·	167·7
17	6390·	103·9					2869·	146·0	2009·	166·4
18							3359·	145·5	2409·	165·1
19							3882·	144·9	2860	163·4
20							4432·	144·4	3360·	161·6

C_v in Millijoules per mole per degree K

Θ_D in °K·

TABLE VIII· MELTING PRESSURE OF MOLECULAR HYDROGEN·

Pressure in atmospheres

T[°K]	Woolley[48]	Mills[111]	Mills[112]	Goodwin[113] Normal Hydrogen	Goodwin[113] Parahydrogen
14	1·93822	-3·37034	-5·17337	1·63611	5·88698
15	33·5836	30·0929	28·7707	32·4529	36·8797
16	67·0938	65·3072	64·4419	65·5962	70·1908
17	102·452	102·246	101·812	100·921	105·676
18	139·642	140·885	140·854	138·307	143·217
19	178·649	181·202	181·545	177·658	182·717
20	219·461	223·175	223·861	218·892	224·096
21	262·062	266·785	267·782	261·941	267·286
22	306·443	312·012	313·288	306·748	312·23
23	352·59	358·84	360·359	353·264	358·88
24	400·492	407·25	408·977	401·448	407·196
25	450·14	457·229	459·128	451·264	457·14
26	501·523	508·76	510·793	502·681	508·684
27	554·632	561·83	563·959	555·673	561·801
28	609·457	616·424	618·61	610·216	616·466
29	665·989	672·531	674·734	666·29	672·662
30	724·222	730·137	732·316	723·877	730·368
32	845·751	849·799	851·807	843·528	850·255
34	973·985	975·323	976·988	969·064	976·021
36	1108·87	1106·62	1107·77	1100·4	1107·58
38	1250·34	1243·63	1244·08	1237·46	1244·87
40	1398·35	1386·26	1385·83	1380·21	1387·83
42	1552·87	1534·45	1532·95	1528·58	1536·42
44	1713·83	1688·13	1685·39	1682·54	1690·6
46	1881·21	1847·26	1843·06	1842·06	1850·34
48	2054·95	2011·77	2005·93	2007·12	2015·6
50	2235·02	2181·6	2173·92	2177·69	2186·38
55	2712·67	2629·16	2616·	2628·09	2637·31
60	3229·14	3108·97	3089·04	3112·59	3122·32
65	3783·96	3620·38	3592·37	3631·01	3641·25
70	4376·69	4162·8	4125·36	4183·23	4193·98
75	5006·95	4735·68	4687·47	4769·17	4780·42
80	5674·37	5338·55	5278·17	5388·75	5400·49
85	6378·61	5970·94	5897·01	6041·92	6054·16
90	7119·36	6632·43	6543·54	6728·63	6741·37
95	7896·32	7322·65	7217·37	7448·86	7462·1
100	8709·22	8041·22	7918·11	8202·59	8216·31

TABLE IX. PROPERTIES OF METALLIC HYDROGEN AT 0 °K.

Pressure 10^6 Atm	Volume cc/mole	Energy kcal	Gibb's free Energy kcal
0·0	1·85	31·64	31·64
0·1	1·71	31·84	36·01
0·2	1·60	32·24	40·07
0·3	1·52	32·77	43·90
0·4	1·45	33·38	47·53
0·5	1·39	34·04	51·01
0·6	1·34	34·74	54·35
0·7	1·29	35·47	57·57
0·8	1·25	36·21	60·69
0·9	1·22	36·97	63·71
1·0	1·19	37·73	66·65
1·1	1·16	38·48	69·42
1·2	1·13	39·28	72·31
1·3	1·10	40·06	75·04
1·4	1·08	40·84	77·70
1·5	1·06	41·62	80·31
1·6	1·04	42·40	82·87
1·7	1·02	43·17	85·39
1·8	1·00	43·95	87·85
1·9	0·98	44·73	90·28
2·0	0·97	45·50	92·66
2·2	0·94	47·02	97·30
2·4	0·91	48·55	101·82
2·6	0·88	50·05	106·20
2·8	0·86	51·54	110·47
3·0	0·84	53·01	114·63
3·2	0·82	54·47	118·70
3·4	0·80	55·91	122·67
3·6	0·79	57·35	126·56
3·8	0·77	58·77	130·37
4·0	0·76	60·17	134·11
4·5	0·72	63·61	143·15
5·0	0·70	66·97	151·81
5·5	0·67	70·26	160·14
6·0	0·65	73·47	168·18
6·5	0·63	76·62	175·95
7·0	0·61	79·70	183·48
7·5	0·59	82·72	190·79
8·0	0·57	85·68	197·90
8·5	0·56	88·60	204·83
9·0	0·55	91·46	211·58
9·5	0·53	94·28	218·19
10·0	0·52	97·04	224·64

TABLE X. PROPERTIES OF SOLID MOLECULAR HYDROGEN AT 0°K.

Pressure 10^5 Atm	Volume cc/mole	Energy kcal/mole	Gibbs Free Energy kcal/mole
.1	14.18	.26	3.69
.2	11.69	.93	6.59
.3	10.43	1.60	9.18
.4	9.61	2.26	11.57
.5	9.01	2.91	13.83
.6	8.55	3.54	15.97
.8	7.86	4.78	20.01
.9	7.59	5.39	21.93
1.0	7.35	5.99	23.80
2.0	5.95	11.59	40.42
3.0	5.23	16.73	54.76
4.0	4.77	21.56	67.75
5.0	4.43	26.15	79.81
6.0	4.16	30.58	91.18
7.0	3.94	35.00	102.33
8.0	3.76	39.23	112.88
9.0	3.61	43.22	122.69
10.0	3.49	46.98	131.81
12.0	3.27	54.39	149.61
14.0	3.10	61.63	166.71
16.0	2.95	68.63	183.03
18.0	2.84	74.84	197.33
20.0	2.72	82.02	213.71

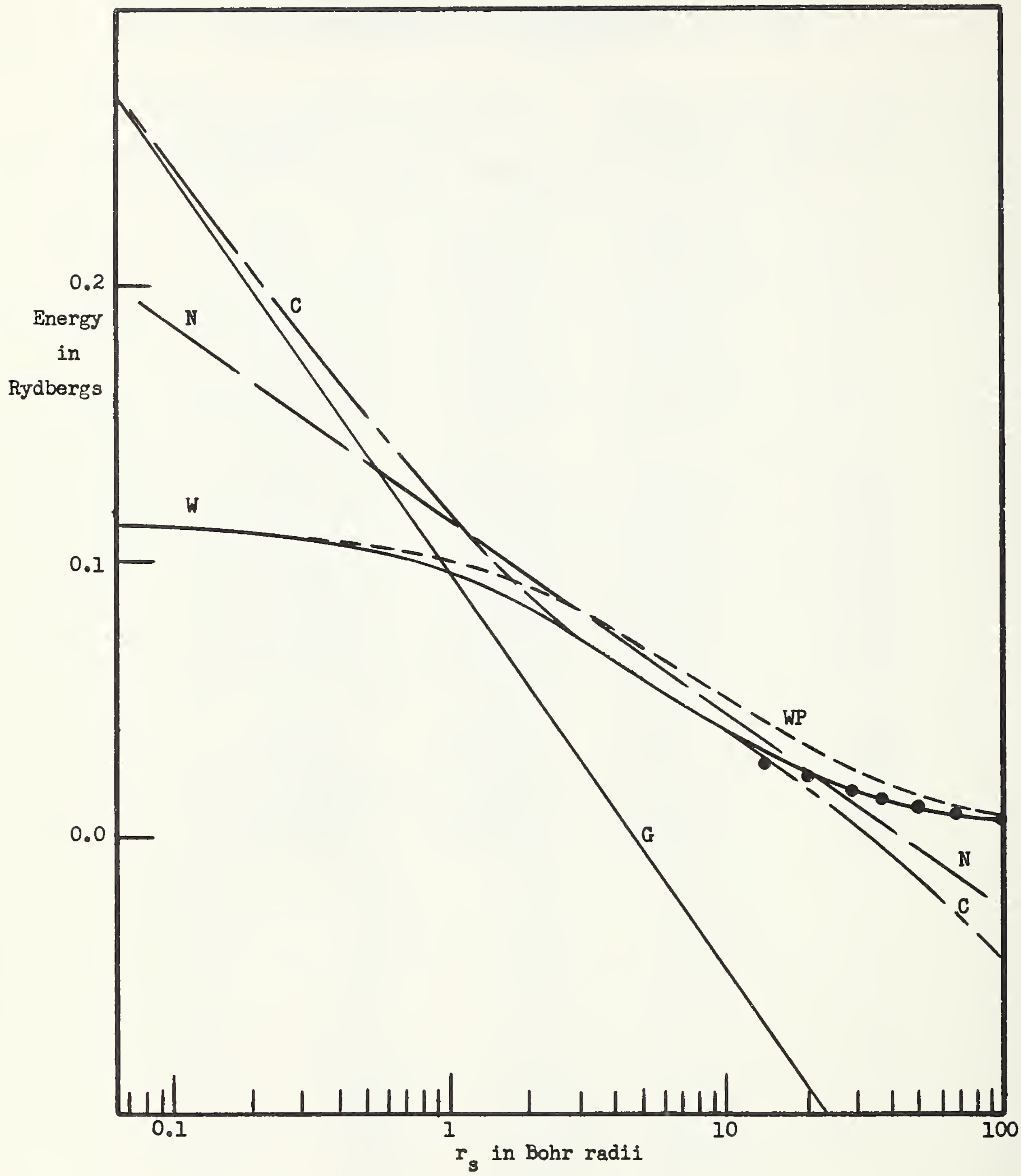

Figure 1. Correlation Energy

● Carr et.al low density
C Carr et al interpolation
G Gell-Mann and Breuckner
N Nozieres and Pines
W Wigner
WP Pines modification of Wigner

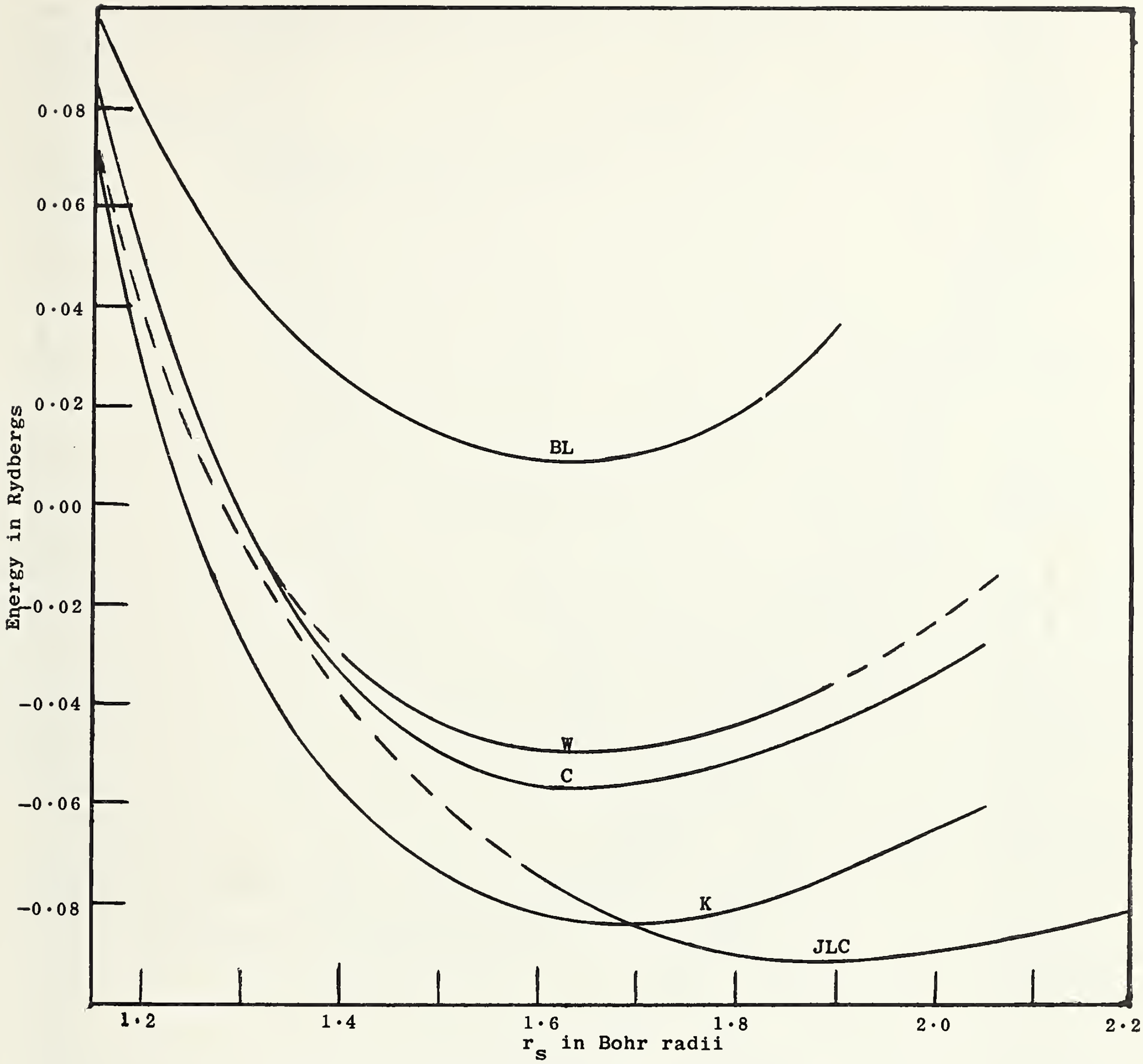

Figure 2· Ground State Energy of Metallic Hydrogen

BL Bellemans and DeLeener
C W·J·Carr, Jr·
JLC J·L·Calais
K Kronig, DeBoer and Korringa
W Wigner and Huntington

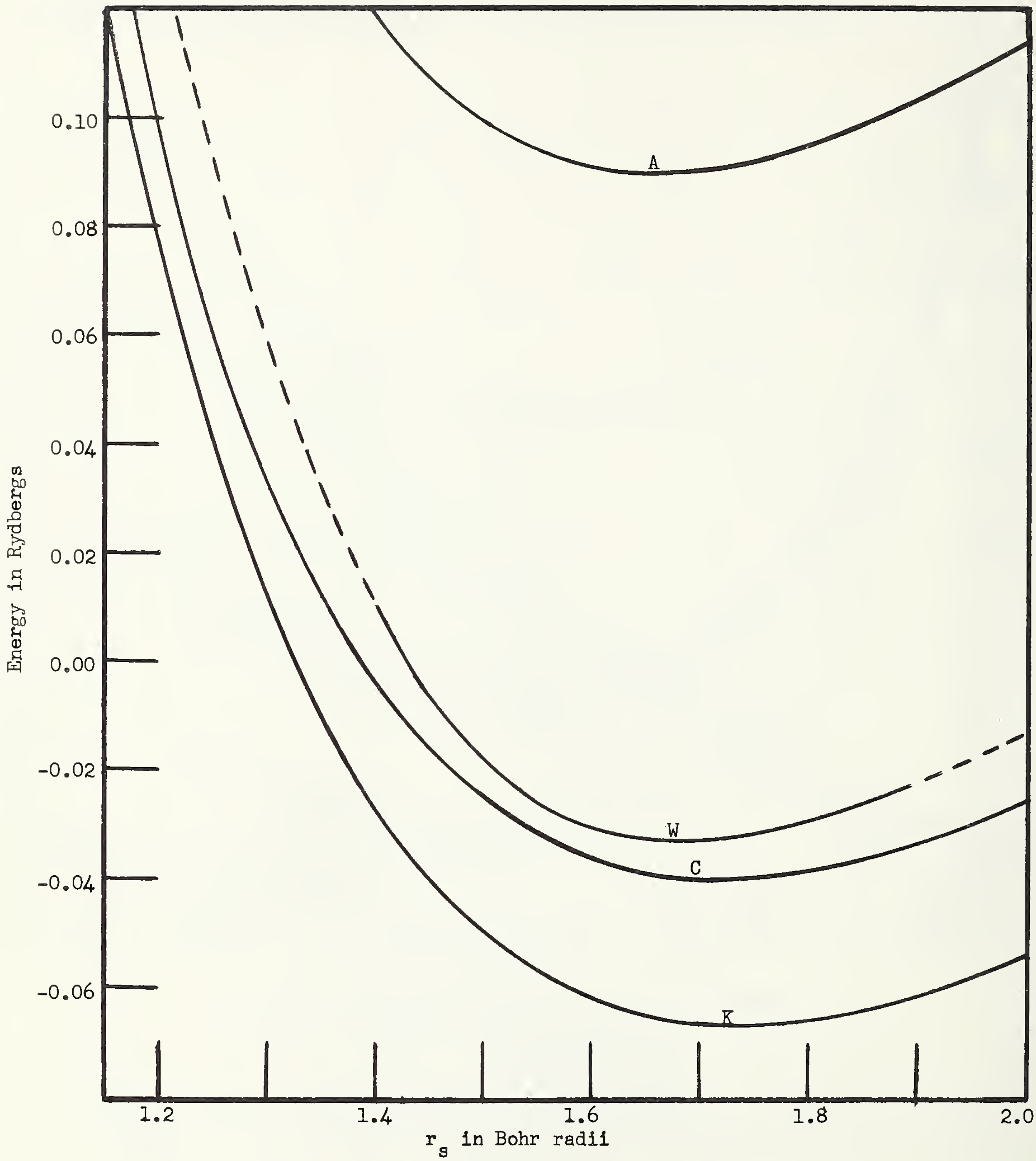

Figure 3. Internal Energy of Metallic Hydrogen.

A A. A. Abrikosov
C W. J. Carr, Jr.
K Kronig, DeBoer, and Korringa
W Wigner and Huntington

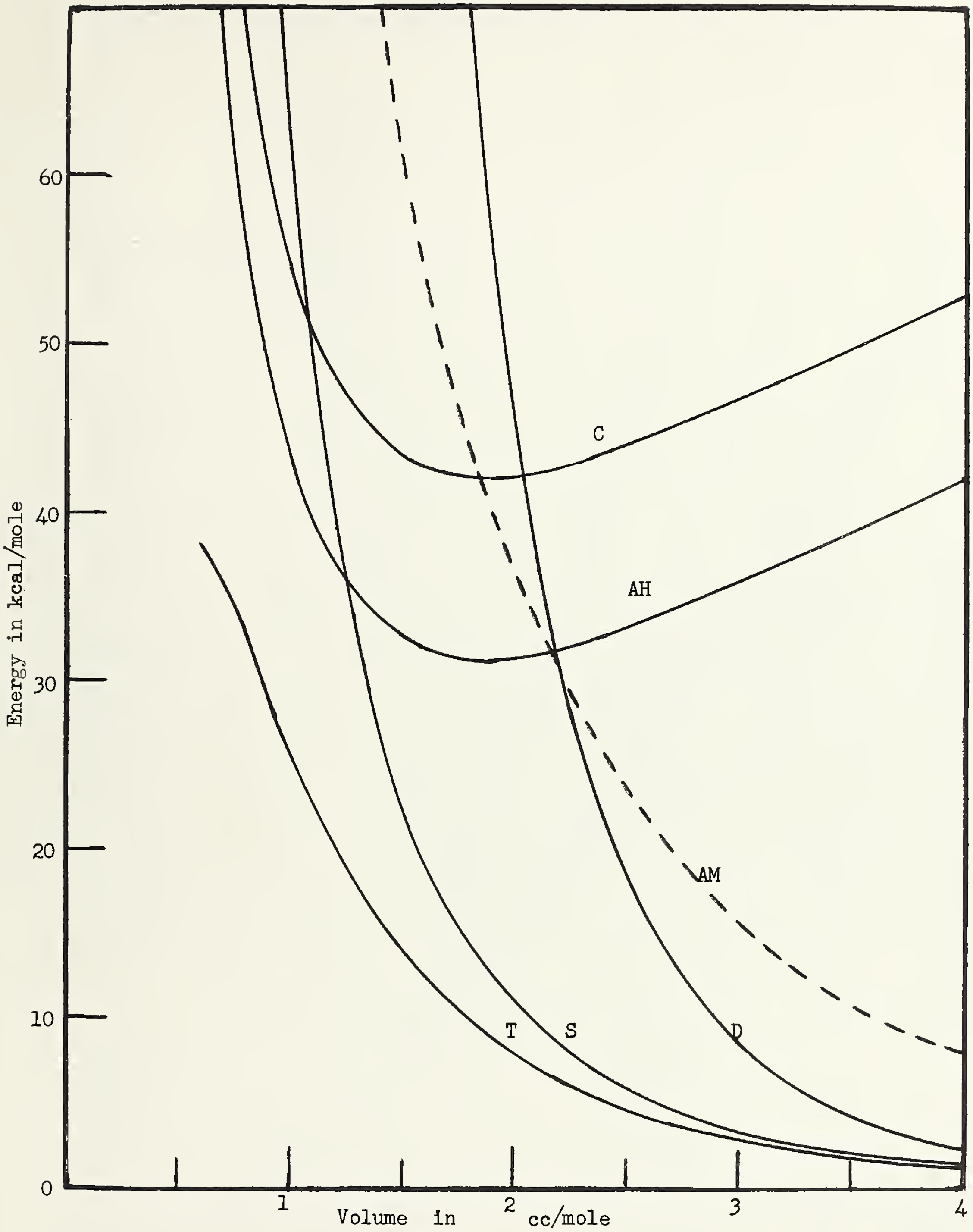

Figure 4. Internal Energy of Solid Hydrogen.

AH Atomic Hydrogen
C W. J. Carr, Jr.
AM Abrikosov
D DeBoer and Blaisse
S Stewart
T Trubitsyn

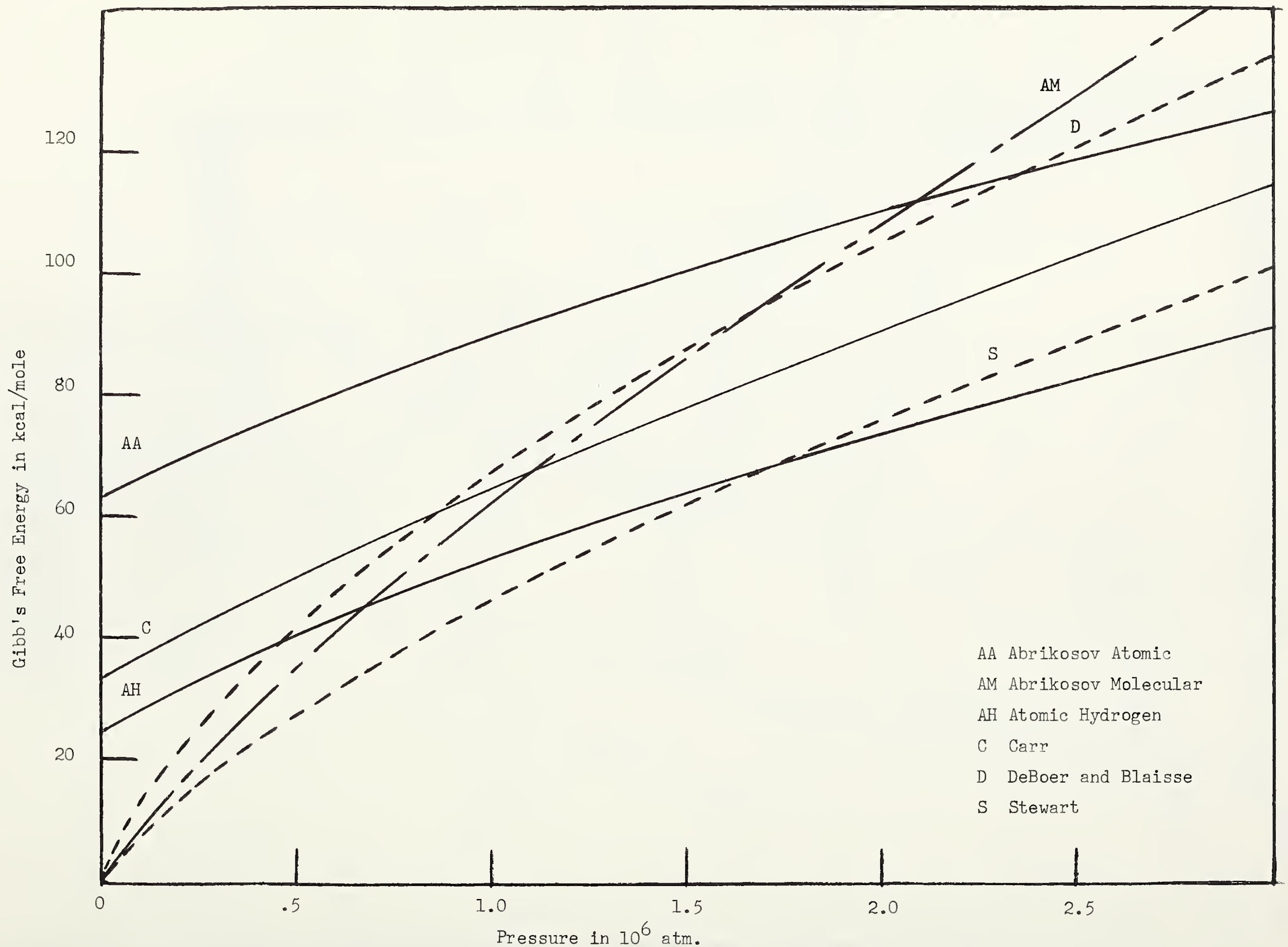

Figure 5. Gibb's Free Energy of Solid Hydrogen

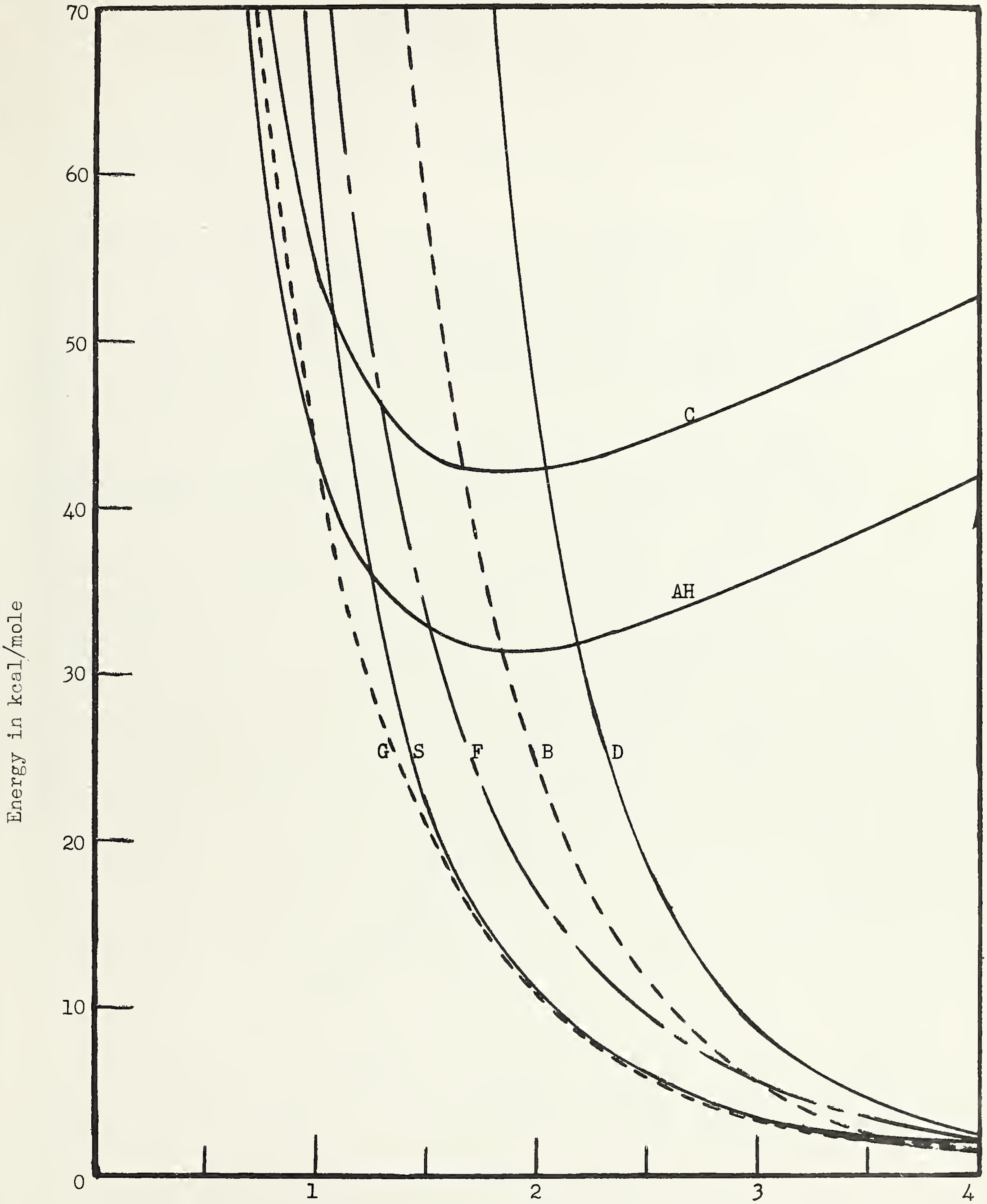

AH Atomic Hydrogen
C W. J. Carr, Jr.
B Buckingham Corner
F Fisher
G Gordon Cashion
S Stewart
D DeBoer

Figure 6. Internal Energy of Solid Hydrogen

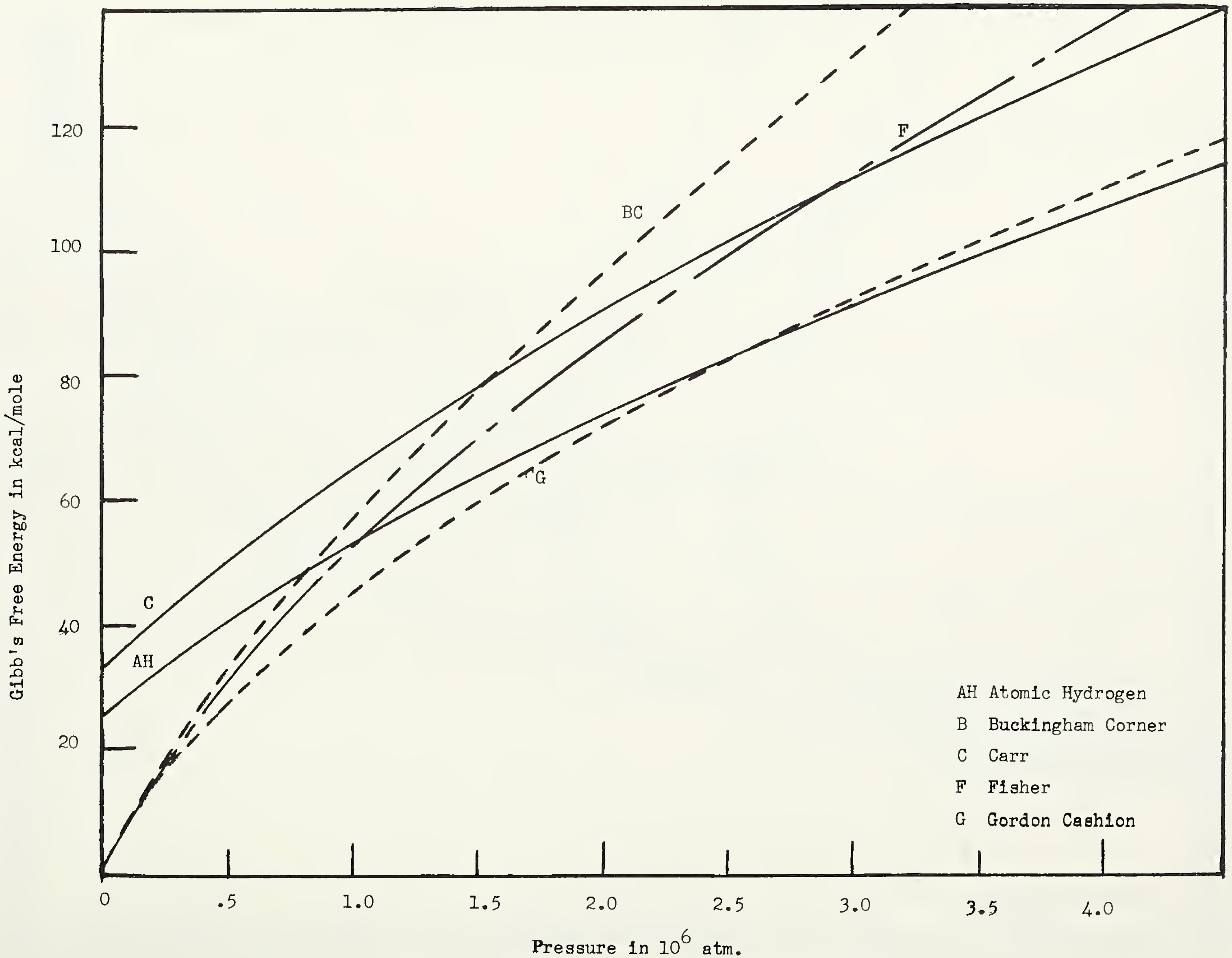

Figure 7. Gibb's Free Energy of Solid Hydrogen

APPENDIX A

SELECTED THERMOCHEMICAL VALUES

W. H. Evans, V. B. Parker, S. Bailey, and R. H. Schumm

In preceding reports (NBS Reports 8504 and 8628) selections of values from data prepared by the Chemical Thermodynamic Properties Group for the revision of NBS Circular 500 have been presented in condensed form. More complete tables will be published initially in the NBS Technical Note 270 Series; however in order to make these data available to research groups prior to completion we present in the accompanying table the results of some additional compounds of interest to this program.

These new data will form a self-consistent set of thermodynamic tables; extreme caution should be used if they are combined with data from other sources.

Substance	State	ΔHf°₀	ΔHf°	ΔGf°	S°	C_p°
		0°K	298.15°K			
		kcal/mol			cal/deg mol	
Cd	c,α	0	0	0	12.37	6.21
	g	26.78	26.77	18.51	40.066	4.968
in Hg, 2 phase			-5.078	-2.328	3.145	
Cd^{+}	g	234.18	235.65			
Cd^{++}	g	624.09	627.04			
std. state	aq		-18.14	-18.542	-17.5	
CdO	c		-61.7	-54.6	13.1	10.38
$Cd(OH)_2$	c		-134.0	-113.2	23.	
CdF_2	c		-167.4	-154.8	18.5	
std. state	aq		-172.14	-151.82	-24.1	
$CdCl_2$	c	-93.677	-93.57	-82.21	27.55	17.85
in 200 H_2O	aq		-96.863			
500 H_2O	aq		-97.069			
1000 H_2O	aq		-97.192			
10000 H_2O	aq		-97.608			
100000 H_2O	aq		-97.932			
$CdCl_2 \cdot H_2O$	c		-164.54	-140.31	40.1	
$Cd(ClO_4)_2$						
in 10 H_2O	aq		-78.3			
100 H_2O	aq		-79.9			
$Cd(ClO_4)_2 \cdot 6H_2O$	c		-490.6			
$CdBr_2$	c		-75.57	-70.82	32.8	18.32
in 100 H_2O	aq		-76.259			
500 H_2O	aq		-76.344			
1000 H_2O	aq		-76.376			
10000 H_2O	aq		-76.309			
$CdBr_2 \cdot 4\ H_2O$	aq		-356.73	-298.287	75.6	

Substance	State	ΔHf_0°	ΔHf°	ΔGf°	S°	C_p°
		0°K	298.15°K			
		kcal/mol			cal/deg mol	
CdI_2	c	-48.52	-48.6	-48.13	38.5	19.11
in 400 H_2O	aq		-47.325			
1000 H_2O	aq		-46.875			
10000 H_2O	aq		-45.705			
$Cd(IO_3)_2$	c			-90.13		
CdS	c		-38.7	-37.4	15.5	
$CdSO_4$	c	-220.719	-223.06	-196.66	29.407	23.80
in 20 H_2O	aq		-232.87			
100 H_2O	aq		-233.72			
1000 H_2O	aq		-234.344			
10000 H_2O	aq		-234.806			
100000 H_2O	aq		-235.250			
$CdSO_4 \cdot H_2O$	c	-292.786	-296.26	-255.46	36.814	32.16
$CdSO_4 \cdot 8/3\ H_2O$	c	-406.960	-413.33	-350.224	54.883	50.97
$CdSeO_3$	c		-137.5	-119.0	34.0	
$CdSeO_4$	c		-151.3	-127.1	39.3	
CdTe	c		-22.1	-22.0	24.	
$Cd(N_3)_2$	c		108.			
	aq		113.4			
Cd_3N_2	c		38.7			
$Cd(NO_3)_2$	c		-109.06			
in 5 H_2O	aq		-114.19			
10 H_2O	aq		-115.80			
50 H_2O	aq		-116.725			
400 H_2O	aq		-116.84			
1000 H_2O	aq		-116.864			
10000 H_2O	aq		-116.896			
$Cd(NO_3)_2 \cdot 2H_2O$	c		-252.30			

Substance	State	ΔHf_0°	ΔHf°	ΔGf°	S°	C_p°
		0°K	298.15°K			
		kcal/mol			cal/deg mol	
$Cd(NO_3)_2 \cdot 4H_2O$	c		-394.11			
Cd_3P_2	c		-27.4			
$Cd_3(PO_4)_2$	c			-587.1		
$CdAs_2$	c		-4.2			
Cd_3As_2	c		-10.0			
CdSb	c		-3.44	-3.11	22.2	
Cd_3Sb_2			-13.9			
$CdCO_3$	c		-179.4	-160.0	22.1	
CdC_2O_4	c		-218.1			
std. state, m = 1	aq		-215.3	-179.6	-6.6	
$Cd(CH_3)_2$	liq		15.2	33.2	48.25	
	g		24.27	35.09	72.4	
$CdSiO_3$	c		-284.20	-264.29	23.3	21.17
$Cd(BO_2)_2$	c			-354.87		

Substance	State	ΔHf_0°	ΔHf°	ΔGf°	S°	Cp°
		0°K	298.15°K			
		kcal/mol			cal/deg mol	
Zn	c	0	0	0	9.95	6.07
	g	31.114	31.245	22.748	38.450	4.968
Zn^+	g	247.74	249.352			
Zn^{++}	g	662.00	665.09			
std. state, m = 1	aq		-36.78	-35.14	-26.8	11.
ZnO	c		-83.24	-76.08	10.43	9.62
ZnO_2^{--}						
std. state, m = 1	aq			-91.85		
$HZnO_2^-$						
std. state, m = 1	aq			-109.26		
$Zn(OH)_2$	c,β		-153.42	-132.31	19.4	
	c,ε		-153.74	-132.68	19.5	17.3
ZnF_2	c	-182.07	-182.7	-107.5	17.61	15.69
ionized,std.state	aq		-195.78	-168.42	-33.4	-40.
$ZnCl_2$	c	-99.255	-99.20	-88.296	26.64	17.05
ionized,std.state	aq		-116.68	-97.88	0.2	-54.
in 10 H_2O			-109.17			
20 H_2O			-110.66			
50 H_2O			-112.70			
100 H_2O			-114.24			
500 H_2O			-115.72			
1000 H_2O			-116.02			
$Zn(ClO_4)_2$						
in 20 H_2O	aq		-97.78			
50 H_2O			-98.10			
100 H_2O			-98.20			
500 H_2O			-98.60			
1000 H_2O			-98.6			

Substance	State	ΔHf°_0	ΔHf°	ΔGf°	S°	Cp°
		0°K	298.15°K			
		kcal/mol			cal/deg mol	
$Zn(ClO_4)_2 \cdot 6H_2O$	c		-509.89	-371.8	130.4	
$ZnBr_2$	c		-78.55	-74.60	33.1	
in 400 H_2O	aq		-93.78			
$ZnBr_2 \cdot 2H_2O$	c		-224.0	-191.1	47.5	
ZnI_2	c		-49.72	-49.94	38.5	
in 3000 H_2O	aq		-61.4			
$Zn(IO_3)_2$	c			-103.68		
std.state, m = 1	aq		-142.6	-96.3	29.8	
ZnS wurtzite	c		-46.04			
spholerite	c		-49.23	-50.12	13.8	11.0
$ZnSO_4$	c		-234.9	-209.0	28.6	
in 20 H_2O	aq		-252.258			
50 H_2O			-252.799			
100 H_2O			-252.897			
500 H_2O			-253.108			
1000 H_2O			-253.225			
5000 H_2O			-253.503			
10000 H_2O			-253.628			
$ZnSO_4 \cdot H_2O$	c		-311.78	-270.58	33.1	
$ZnSO_4 \cdot 6H_2O$	c		-663.83	-555.64	86.9	
$ZnSO_4 \cdot 7H_2O$	c		-735.60	-612.59	92.9	
ZnSe	c		-31.2			
$ZnSeO_4$	c		-158.8			
ZnTe	c		-28.1			
Zn_3N_2	c		-5.4			26.

Substance	State	ΔHf_0°	ΔHf°	ΔGf°	S°	C_p°
		0°K	298.15°K			
		kcal/mol			cal/deg mol	
$Zn(NO_3)_2$	c		-115.6			
in 5 H_2O	aq		-129.8			
10 H_2O			-133.99			
50 H_2O			-135.56			
100 H_2O			-135.67			
500 H_2O			-135.51			
$Zn(NO_3)_2 \cdot 6H_2O$			-551.30	-423.79	109.2	77.2
$Zn(NH_2)_2$	c		-38.2			
Zn_3P_2	c		-113.			
$Zn(PO_3)_2$	c		-479.9			
$Zn_3(PO_4)_2$	c		-691.3			
$ZnAs_2$	c		-7.6			
Zn_3As_2	c		-0.8			
ZnSb	c		-3.5			
$ZnCO_3$	c		-194.26	-174.85	19.7	19.05
$ZnC_2O_4 \cdot 2H_2O$	c		-374.0	-321.7	45.3	
$Zn(CH_3)_2$	liq		5.6			
	g		12.67			
$Zn(C_2H_5)_2$	liq		2.5			
	g		12.1			
$Zn(CN)_2$	c		22.9			
Zn_2SiO_4	c		-391.19	-364.15	31.4	29.48
$ZnAl_2O_4$	c		-502.2			

Substance	State	ΔHf_0°	ΔHf°	ΔGf°	S°	Cp°
		0°K	298.15°K			
		kcal/mol			cal/deg mol	
Cu	c	0	0	0	7.97	5.86
	g	80.58	80.86	71.39	39.74	4.968
Cu^+	g	258.752	260.513			
std. state, m = 1	aq		17.13	11.95	9.7	
Cu^{++}	g	726.69	729.93			
std. state, m = 1	aq		15.48	15.66	-23.8	
Cu_2	g	115.7	115.73	103.28	57.71	8.75
CuO	c		-37.6	-31.0	10.19	10.11
Cu_2O	c		-40.3	-34.9	22.26	15.21
CuH	c		5.1			
	g		70.			
$Cu(OH)_2$	c		-107.5			
CuF_2	c		-129.7			
$CuF_2 \cdot 2H_2O$	c		-275.4	-234.6	42.	
CuCl	c		-32.8	-28.65	20.7	
$CuCl_2$	c	-52.79	-52.6	-42.0	25.83	13.82
in 10 H_2O	aq		-58.70			
50 H_2O	aq		-62.40			
100 H_2O	aq		-63.23			
500 H_2O	aq		-64.42			
1000 H_2O	aq		-64.70			
$CuCl_2 \cdot 2H_2O$	c		-196.3	-156.8	40.	
$Cu(ClO_3)_2$						
in 1000 H_2O	aq		-32.			
$Cu(ClO_4)_2$						
std. state, m = 1	aq		-46.34	11.54	63.2	
$Cu(ClO_4)_2 \cdot 6H_2O$	c		-460.9			

Substance	State	ΔHf_0°	ΔHf°	ΔGf°	S°	Cp°
		0°K	298.15°K			
		kcal/mol			cal/deg mol	
CuBr	c		-25.0	-24.0	22.97	13.08
$CuBr_2$	c		-33.9			
in 400 H_2O	aq		-42.5			
$CuBr_2 \cdot 4H_2O$	c		-317.0			
CuI	c		-16.3	-16.6	23.1	12.92
$Cu(IO_3)_2 \cdot H_2O$	c		-165.4	-112.0	59.1	
CuS	c		-12.7	-12.6	15.9	11.43
Cu_2S	c,α		-19.0	-20.6	28.9	18.24
$CuSO_4$	c		-184.36	-158.2	26.	23.9
std. state, m = 1	aq		-201.84	-162.31	-19.0	
in 50 H_2O	aq		-200.284			
100 H_2O	aq		-200.374			
400 H_2O	aq		-200.58			
1000 H_2O	aq		-200.76			
10000 H_2O	aq		-201.254			
$CuSO_4 \cdot 5\ H_2O$	c		-544.85	-449.344	71.8	67.
Cu_2SO_4	c		-179.6			
CuSe	c		-9.45			
$CuSe_2$	c		-10.3			
Cu_2Se	c		-14.2			
$CuSeO_4$	c		-114.36			
Cu_2Te	c		5.			
CuN_3	c		66.7	82.4	24.	
$Cu(N_3)_2$	c		143.0			
Cu_3N	c		17.8			

Substance	State	ΔHf_0°	ΔHf	ΔGf	S°	Cp°
		0°K	298.15°K			
		kcal/mol			cal/deg mol	
$Cu(NO_3)_2$	c		-72.4			
in 10 H_2O	aq		-82.76			
100 H_2O	aq		-83.75			
800 H_2O	aq		-84.4			
$Cu(NO_3)_2 \cdot 6H_2O$	c		-504.5			
$Cu(NH_3)_4(NO_3)_2$	c		-198.0			
in 250 H_2O	aq		-181.56			
CuP_2	c		-29.			
Cu_3P	c		-36.2			
$Cu_2P_2O_7$	c			-448.0		
std. state, m = 1	aq		-511.8	-427.4	-76.	
$Cu_3(PO_4)_2$	c			-490.3		
Cu_3As	c		-2.8			
$Cu_3(AsO_4)_2$	c			-310.9		
Cu_2Sb	c		-2.8			
Cu_3Sb	c		-2.			
CuC_2O_4	c			-158.2		
std. state, m = 1	aq		-181.7	-145.5	-12.9	
$Cu(CHO_2)_2$	c		-186.7			
$Cu(CH_3COO)_2$	c		-213.5			
CuCN	c		23.0	26.6	20.5	
Cu(ONC) cuprous fulminate	c		26.3			
CuCNS	c			16.7		
CuAl	c		-9.8			
Cu_3Al_2	c		-26.2			
$CuAl_2O_4$	c		-445.3			

APPENDIX B

THERMODYNAMIC FUNCTIONS OF SOME SELECTED SUBSTANCES IN THE SOLID AND LIQUID STATES

George T. Furukawa and Martin L. Reilly

(See Chapter 13 for discussion concerning the substances for which thermodynamic functions are tabulated.)

TABLE B-152

THERMODYNAMIC FUNCTIONS FOR BERYLLIUM SULFATE (BE S O_4)
SOLID PHASE

GRAM MOLECULAR WT.= 105.0738 GRAMS   1 CAL=4.1840 JOULES

T DEG K = 273.15 + T DEG C

T	$-(G^0_T-H^C_0)/T$	$(H^0_T-H^C_0)/T$	$(S_T-S^C_0)$	$(H^0_T-H^C_0)$	C^0_P	$-(G^0_T-H^C_0)$
DEG K	CAL / DEG MOLE	CAL / DEG MOLE	CAL / DEG MOLE	CAL / MOLE	CAL / DEG MOLE	CAL / MOLE
0.00	0.000	0.000	0.000	0.000	0.000	0.000
5.00	0.001	0.002	0.003	0.010	0.008	0.003
10.00	0.005	0.015	0.020	0.145	0.055	0.051
15.00	0.016	0.045	0.061	0.668	0.166	0.240
20.00	0.035	0.096	0.132	1.927	0.352	0.706
25.00	0.065	0.173	0.238	4.323	0.618	1.614
30.00	0.105	0.275	0.380	8.246	0.966	3.142
35.00	0.156	0.403	0.559	14.089	1.374	5.473
40.00	0.220	0.549	0.769	21.968	1.777	8.781
45.00	0.293	0.709	1.002	31.887	2.194	13.199
50.00	0.377	0.879	1.256	43.956	2.636	18.835
55.00	0.469	1.059	1.528	58.267	3.089	25.788
60.00	0.569	1.247	1.817	74.848	3.543	34.144
65.00	0.677	1.441	2.118	93.697	3.995	43.975
70.00	0.791	1.640	2.431	114.80	4.443	55.342
75.00	0.911	1.842	2.752	138.13	4.888	68.296
80.00	1.036	2.046	3.082	163.67	5.329	82.878
85.00	1.166	2.252	3.418	191.41	5.763	99.126
90.00	1.301	2.459	3.760	221.29	6.188	117.07
95.00	1.439	2.666	4.105	253.27	6.604	136.73
100.00	1.581	2.873	4.454	287.31	7.013	158.13
105.00	1.726	3.080	4.806	323.39	7.416	181.28
110.00	1.874	3.286	5.161	361.47	7.817	206.19
115.00	2.025	3.492	5.517	401.55	8.215	232.89
120.00	2.178	3.697	5.875	443.62	8.611	261.36
125.00	2.333	3.901	6.234	487.66	9.004	291.64
130.00	2.490	4.105	6.595	533.66	9.394	323.71
135.00	2.649	4.308	6.957	581.59	9.780	357.59
140.00	2.809	4.510	7.319	631.45	10.161	393.28
145.00	2.971	4.712	7.683	683.20	10.539	430.79
150.00	3.134	4.912	8.046	736.83	10.913	470.11
155.00	3.298	5.112	8.410	792.32	11.284	511.25
160.00	3.464	5.310	8.774	849.66	11.653	554.21
165.00	3.630	5.508	9.138	908.84	12.020	598.99
170.00	3.798	5.705	9.503	969.85	12.385	645.59
175.00	3.966	5.901	9.867	1032.7	12.748	694.02
180.00	4.135	6.096	10.231	1097.3	13.108	744.26
185.00	4.304	6.291	10.595	1163.8	13.465	796.33
190.00	4.475	6.484	10.959	1232.0	13.819	850.21
195.00	4.646	6.677	11.322	1301.9	14.168	905.91
200.00	4.817	6.868	11.685	1373.6	14.512	963.43
205.00	4.989	7.059	12.048	1447.1	14.852	1022.8
210.00	5.161	7.248	12.410	1522.2	15.186	1083.9
215.00	5.334	7.437	12.771	1598.9	15.515	1146.9
220.00	5.507	7.624	13.131	1677.3	15.840	1211.6
225.00	5.681	7.810	13.491	1757.3	16.161	1278.2
230.00	5.854	7.995	13.850	1838.9	16.479	1346.5
235.00	6.028	8.179	14.207	1922.1	16.793	1416.7
240.00	6.203	8.362	14.564	2006.8	17.105	1488.6
245.00	6.377	8.543	14.920	2093.1	17.414	1562.3
250.00	6.551	8.724	15.275	2181.0	17.720	1637.8
255.00	6.726	8.903	15.629	2270.3	18.024	1715.1
260.00	6.900	9.082	15.982	2361.2	18.325	1794.1
265.00	7.075	9.259	16.334	2453.6	18.623	1874.9
270.00	7.250	9.435	16.685	2547.4	18.917	1957.4
273.15	7.360	9.545	16.905	2607.3	19.100	2010.3
275.00	7.424	9.610	17.034	2642.7	19.207	2041.7
280.00	7.599	9.784	17.383	2739.5	19.492	2127.8
285.00	7.774	9.957	17.731	2837.6	19.771	2215.6
290.00	7.949	10.128	18.077	2937.2	20.045	2305.1
295.00	8.123	10.299	18.422	3038.1	20.313	2396.3
298.15	8.233	10.405	18.638	3102.3	20.478	2454.7
300.00	8.298	10.468	18.765	3140.3	20.574	2489.3

H^C_0 AND S^C_0 APPLY TO THE REFERENCE STATE OF THE SOLID AT ZERO DEG K

TABLE B-152 (CONT.)

THERMODYNAMIC FUNCTIONS FOR BERYLLIUM SULFATE ($BE\ S\ O_4$)
SOLID PHASE

GRAM MOLECULAR WT.= 105.0738 GRAMS 1 CAL=4.1840 JOULES

T DEG K = 273.15 + T DEG C

T	$-(G_T^0-H_0^C)/T$	$(H_T^0-H_0^C)/T$	$(S_T-S_0^C)$	$(H_T^0-H_0^C)$	C_P^0	$-(G_T^0-H_0^C)$
DEG K	CAL/DEG MOLE	CAL/DEG MOLE	CAL/DEG MOLE	CAL/MOLE	CAL/DEG MOLE	CAL/MOLE
300.00	8.298	10.468	18.765	3140.3	20.574	2489.3
310.00	8.646	10.802	19.448	3348.6	21.078	2680.4
320.00	8.994	11.131	20.125	3561.8	21.556	2878.2
330.00	9.342	11.453	20.795	3779.6	22.009	3082.8
340.00	9.689	11.770	21.459	4001.9	22.438	3294.1
350.00	10.034	12.081	22.115	4228.3	22.845	3512.0
360.00	10.379	12.385	22.764	4458.7	23.233	3736.4
370.00	10.722	12.684	23.406	4692.9	23.603	3967.2
373.15	10.830	12.776	23.606	4767.4	23.716	4041.3
380.00	11.064	12.976	24.040	4930.7	23.958	4204.5
390.00	11.405	13.262	24.667	5172.0	24.300	4448.0
400.00	11.744	13.542	25.286	5416.7	24.632	4697.8
425.00	12.586	14.218	26.804	6042.5	25.430	5349.0
450.00	13.417	14.862	28.279	6688.0	26.207	6037.6
475.00	14.237	15.480	29.717	7352.9	26.981	6762.7
500.00	15.046	16.074	31.121	8037.1	27.758	7523.2
550.00	16.632	17.207	33.839	9463.9	29.311	9147.6
600.00	18.176	18.280	36.455	10968.	30.843	10905.
650.00	19.680	19.304	38.984	12548.	32.348	12792.
700.00	21.146	20.289	41.435	14202.	33.832	14802.
750.00	22.579	21.241	43.820	15931.	35.304	16934.
800.00	23.979	22.166	46.145	17733.	36.769	19183.
850.00	25.350	23.068	48.418	19608.	38.228	21548.
900.00	26.694	23.950	50.644	21555.	39.674	24025.

H_0^C AND S_0^C APPLY TO THE REFERENCE STATE OF THE SOLID AT ZERO DEG K

TABLE B-153

THERMODYNAMIC FUNCTIONS FOR STRONTIUM FLUORIDE (SR F_2)
SOLID PHASE

GRAM MOLECULAR WT.= 125.6168 GRAMS   1 CAL=4.1840 JOULES

T DEG K = 273.15 + T DEG C

T	$-(G_T^0-H_0^C)/T$	$(H_T^0-H_0^C)/T$	$(S_T-S_0^C)$	$(H_T^0-H_0^C)$	C_P^0	$-(G_T^0-H_0^C)$
DEG K	CAL/DEG MOLE	CAL/DEG MOLE	CAL/DEG MOLE	CAL/MOLE	CAL/DEG MOLE	CAL/MOLE
0.00	0.000	0.000	0.000	0.000	0.000	0.000
5.00	0.001	0.002	0.002	0.008	0.006	0.003
10.00	0.004	0.012	0.016	0.123	0.048	0.041
15.00	0.013	0.037	0.051	0.559	0.133	0.201
20.00	0.029	0.077	0.106	1.547	0.277	0.583
25.00	0.053	0.140	0.193	3.499	0.520	1.316
30.00	0.086	0.230	0.316	6.908	0.859	2.571
35.00	0.130	0.349	0.479	12.228	1.280	4.543
40.00	0.186	0.495	0.681	19.794	1.754	7.427
45.00	0.253	0.663	0.917	29.841	2.272	11.406
50.00	0.333	0.852	1.185	42.595	2.837	16.646
55.00	0.424	1.059	1.483	58.266	3.436	23.304
60.00	0.525	1.283	1.809	76.991	4.056	31.522
65.00	0.637	1.521	2.158	98.837	4.683	41.429
70.00	0.759	1.769	2.528	123.82	5.309	53.136
75.00	0.890	2.026	2.915	151.92	5.931	66.738
80.00	1.029	2.289	3.318	183.11	6.543	82.315
85.00	1.176	2.557	3.732	217.32	7.137	99.937
90.00	1.330	2.827	4.157	254.44	7.705	119.66
95.00	1.490	3.098	4.588	294.33	8.244	141.51
100.00	1.655	3.368	5.024	336.84	8.755	165.54
105.00	1.826	3.637	5.463	381.84	9.241	191.76
110.00	2.002	3.902	5.903	429.21	9.704	220.17
115.00	2.181	4.164	6.345	478.84	10.144	250.79
120.00	2.363	4.422	6.785	530.61	10.561	283.62
125.00	2.549	4.675	7.224	584.41	10.955	318.64
130.00	2.737	4.924	7.661	640.12	11.327	355.86
135.00	2.928	5.168	8.095	697.64	11.677	395.25
140.00	3.120	5.406	8.526	756.85	12.005	436.81
145.00	3.314	5.639	8.953	817.66	12.314	480.51
150.00	3.509	5.866	9.375	879.97	12.605	526.33
155.00	3.705	6.088	9.793	943.68	12.878	574.25
160.00	3.902	6.305	10.206	1008.7	13.135	624.25
165.00	4.099	6.515	10.614	1075.0	13.378	676.30
170.00	4.296	6.720	11.017	1142.5	13.606	730.38
175.00	4.494	6.920	11.414	1211.1	13.822	786.46
180.00	4.692	7.115	11.807	1280.7	14.025	844.52
185.00	4.889	7.304	12.194	1351.3	14.217	904.52
190.00	5.087	7.489	12.575	1422.8	14.398	966.44
195.00	5.283	7.668	12.951	1495.2	14.568	1030.3
200.00	5.480	7.842	13.322	1568.5	14.728	1095.9
205.00	5.675	8.012	13.688	1642.5	14.878	1163.5
210.00	5.871	8.177	14.048	1717.3	15.021	1232.8
215.00	6.065	8.338	14.403	1792.7	15.155	1303.9
220.00	6.258	8.495	14.753	1868.8	15.283	1376.8
225.00	6.451	8.647	15.098	1945.5	15.405	1451.5
230.00	6.643	8.795	15.438	2022.8	15.521	1527.8
235.00	6.833	8.939	15.773	2100.7	15.632	1605.8
240.00	7.023	9.080	16.103	2179.1	15.740	1685.5
245.00	7.212	9.217	16.428	2258.1	15.843	1766.9
250.00	7.399	9.350	16.749	2337.6	15.942	1849.8
255.00	7.586	9.480	17.066	2417.5	16.039	1934.3
260.00	7.771	9.608	17.378	2498.0	16.131	2020.5
265.00	7.955	9.731	17.687	2578.8	16.221	2108.1
270.00	8.138	9.852	17.991	2660.2	16.307	2197.3
273.15	8.253	9.927	18.180	2711.6	16.359	2254.3
275.00	8.320	9.971	18.291	2741.9	16.389	2288.0
280.00	8.501	10.086	18.587	2824.0	16.469	2380.2
285.00	8.680	10.199	18.879	2906.6	16.545	2473.9
290.00	8.859	10.309	19.167	2989.5	16.619	2569.0
295.00	9.036	10.416	19.452	3072.8	16.689	2665.5
298.15	9.147	10.483	19.629	3125.4	16.732	2727.1
300.00	9.212	10.521	19.733	3156.4	16.757	2763.5

H_0^C AND S_0^C APPLY TO THE REFERENCE STATE OF THE SOLID AT ZERO DEG K

TABLE B-154

THERMODYNAMIC FUNCTIONS FOR STRONTIUM CHLORIDE ($SR\ CL_2$)
SOLID PHASE

GRAM MOLECULAR WT.= 158.526 1 CAL=4.1840 JOULES

T DEG K = 273.15 + T DEG C

T DEG K	$-(G^0_T-H^C_0)/T$ CAL/DEG MOLE	$(H^0_T-H^C_0)/T$ CAL/DEG MOLE	$(S_T-S^C_0)$ CAL/DEG MOLE	$(H^0_T-H^C_0)$ CAL/MOLE	C^0_P CAL/DEG MOLE	$-(G^0_T-H^C_0)$ CAL/MOLE
0.00	0.000	0.000	0.000	0.000	0.000	0.000
5.00	0.001	0.003	0.004	0.016	0.013	0.005
10.00	0.009	0.026	0.035	0.260	0.107	0.085
15.00	0.030	0.096	0.126	1.437	0.407	0.452
20.00	0.075	0.236	0.312	4.727	0.941	1.504
25.00	0.149	0.444	0.593	11.106	1.636	3.728
30.00	0.253	0.712	0.965	21.365	2.494	7.587
35.00	0.386	1.035	1.421	36.224	3.456	13.520
40.00	0.548	1.398	1.946	55.933	4.428	21.914
45.00	0.735	1.789	2.524	80.511	5.404	33.070
50.00	0.944	2.199	3.143	109.95	6.367	47.224
55.00	1.174	2.620	3.794	144.10	7.287	64.556
60.00	1.420	3.045	4.465	182.73	8.153	85.197
65.00	1.680	3.470	5.150	225.53	8.957	109.23
70.00	1.953	3.889	5.842	272.20	9.699	136.71
75.00	2.235	4.299	6.534	322.42	10.384	167.65
80.00	2.526	4.699	7.225	375.95	11.016	202.05
85.00	2.822	5.088	7.910	432.49	11.590	239.89
90.00	3.124	5.464	8.588	491.75	12.105	281.14
95.00	3.429	5.826	9.255	553.45	12.565	325.75
100.00	3.737	6.173	9.910	617.32	12.980	373.67
105.00	4.046	6.506	10.552	683.18	13.359	424.83
110.00	4.356	6.826	11.182	750.86	13.707	479.17
115.00	4.666	7.132	11.799	820.21	14.030	536.63
120.00	4.976	7.426	12.402	891.12	14.328	597.13
125.00	5.285	7.708	12.993	963.45	14.602	660.63
130.00	5.593	7.978	13.570	1037.1	14.854	727.04
135.00	5.899	8.237	14.135	1112.0	15.086	796.31
140.00	6.203	8.485	14.688	1187.9	15.298	868.37
145.00	6.505	8.724	15.228	1264.9	15.493	943.17
150.00	6.804	8.952	15.756	1342.8	15.672	1020.6
155.00	7.101	9.172	16.273	1421.6	15.837	1100.7
160.00	7.396	9.382	16.778	1501.2	15.991	1183.3
165.00	7.688	9.585	17.273	1581.5	16.133	1268.5
170.00	7.977	9.779	17.756	1662.5	16.266	1356.1
175.00	8.263	9.967	18.230	1744.1	16.390	1446.0
180.00	8.546	10.147	18.693	1826.4	16.506	1538.3
185.00	8.827	10.320	19.147	1909.2	16.615	1632.9
190.00	9.104	10.487	19.591	1992.5	16.716	1729.8
195.00	9.379	10.648	20.027	2076.3	16.811	1828.8
200.00	9.650	10.803	20.453	2160.6	16.899	1930.0
205.00	9.919	10.953	20.872	2245.3	16.983	2033.3
210.00	10.184	11.097	21.282	2330.4	17.061	2138.7
215.00	10.447	11.237	21.684	2415.9	17.135	2246.2
220.00	10.707	11.372	22.079	2501.8	17.206	2355.6
225.00	10.964	11.502	22.466	2588.0	17.273	2466.9
230.00	11.218	11.628	22.847	2674.5	17.338	2580.2
235.00	11.470	11.750	23.220	2761.4	17.400	2695.4
240.00	11.718	11.869	23.587	2848.5	17.460	2812.4
245.00	11.964	11.983	23.948	2936.0	17.518	2931.2
250.00	12.207	12.095	24.302	3023.7	17.575	3051.9
255.00	12.448	12.203	24.651	3111.7	17.630	3174.3
260.00	12.686	12.308	24.994	3200.0	17.684	3298.4
265.00	12.921	12.410	25.331	3288.5	17.738	3424.2
270.00	13.154	12.509	25.663	3377.4	17.790	3551.7
273.15	13.300	12.570	25.870	3433.4	17.822	3632.8
275.00	13.385	12.605	25.990	3466.4	17.841	3680.8
280.00	13.613	12.699	26.312	3555.8	17.892	3811.6
285.00	13.838	12.791	26.629	3645.4	17.942	3943.9
290.00	14.062	12.880	26.941	3735.2	17.991	4077.8
295.00	14.282	12.967	27.249	3825.3	18.039	4213.3
298.15	14.420	13.021	27.441	3882.1	18.069	4299.5
300.00	14.501	13.052	27.553	3915.6	18.086	4350.3

H^C_0 AND S^C_0 APPLY TO THE REFERENCE STATE OF THE SOLID AT ZERO DEG K

TABLE B-155

THERMODYNAMIC FUNCTIONS FOR TITANIUM TETRAFLUORIDE (TI F_4)
SOLID PHASE

GRAM MOLECULAR WT.= 123.8936 GRAMS   1 CAL=4.1840 JOULES

T DEG K = 273.15 + T DEG C

T DEG K	$-(G^0_T-H^C_0)/T$ CAL/DEG MOLE	$(H^0_T-H^C_0)/T$ CAL/DEG MOLE	$(S_T-S^C_0)$ CAL/DEG MOLE	$(H^0_T-H^C_0)$ CAL/MOLE	C^0_P CAL/DEG MOLE	$-(G^0_T-H^C_0)$ CAL/MOLE
0.00	0.000	0.000	0.000	0.000	0.000	0.000
5.00	0.003	0.008	0.011	0.040	0.034	0.013
10.00	0.024	0.077	0.101	0.772	0.318	0.239
15.00	0.084	0.242	0.326	3.635	0.841	1.256
20.00	0.183	0.464	0.647	9.288	1.435	3.657
25.00	0.314	0.725	1.038	18.117	2.106	7.846
30.00	0.471	1.014	1.485	30.420	2.820	14.134
35.00	0.651	1.326	1.976	46.396	3.577	22.771
40.00	0.849	1.655	2.504	66.202	4.345	33.958
45.00	1.064	1.997	3.060	89.854	5.117	47.858
50.00	1.292	2.348	3.640	117.39	5.897	64.599
55.00	1.532	2.706	4.238	148.83	6.677	84.287
60.00	1.783	3.069	4.853	184.14	7.447	107.01
65.00	2.044	3.435	5.479	223.27	8.203	132.83
70.00	2.312	3.802	6.114	266.16	8.949	161.81
75.00	2.586	4.170	6.756	312.74	9.683	193.98
80.00	2.867	4.537	7.404	362.96	10.401	229.38
85.00	3.153	4.903	8.056	416.71	11.096	268.03
90.00	3.444	5.265	8.709	473.87	11.763	309.94
95.00	3.738	5.624	9.362	534.30	12.405	355.12
100.00	4.036	5.979	10.014	597.88	13.024	403.56
105.00	4.336	6.329	10.665	664.52	13.628	455.26
110.00	4.638	6.674	11.312	734.14	14.217	510.21
115.00	4.942	7.014	11.957	806.66	14.791	568.38
120.00	5.248	7.350	12.598	882.02	15.347	629.77
125.00	5.555	7.681	13.236	960.10	15.884	694.36
130.00	5.862	8.006	13.869	1040.8	16.400	762.12
135.00	6.171	8.326	14.497	1124.1	16.895	833.03
140.00	6.479	8.641	15.120	1209.7	17.373	907.08
145.00	6.788	8.950	15.738	1297.8	17.833	984.23
150.00	7.096	9.254	16.350	1388.1	18.279	1064.4
155.00	7.405	9.552	16.956	1480.5	18.712	1147.7
160.00	7.713	9.845	17.557	1575.2	19.133	1234.0
165.00	8.020	10.132	18.152	1671.8	19.541	1323.3
170.00	8.327	10.415	18.742	1770.5	19.936	1415.5
175.00	8.632	10.693	19.325	1871.2	20.320	1510.7
180.00	8.938	10.965	19.903	1973.7	20.693	1608.8
185.00	9.242	11.233	20.475	2078.1	21.055	1709.7
190.00	9.545	11.496	21.041	2184.3	21.406	1813.5
195.00	9.847	11.755	21.601	2292.1	21.747	1920.1
200.00	10.147	12.009	22.156	2401.7	22.079	2029.5
205.00	10.447	12.258	22.705	2512.9	22.401	2141.7
210.00	10.745	12.503	23.249	2625.7	22.714	2256.5
215.00	11.042	12.744	23.787	2740.0	23.019	2374.1
220.00	11.338	12.981	24.319	2855.9	23.315	2494.4
225.00	11.633	13.214	24.847	2973.2	23.605	2617.3
230.00	11.925	13.443	25.369	3091.9	23.887	2742.9
235.00	12.217	13.668	25.885	3212.0	24.164	2871.0
240.00	12.507	13.890	26.397	3333.5	24.436	3001.7
245.00	12.796	14.108	26.903	3456.4	24.702	3135.0
250.00	13.083	14.322	27.405	3580.6	24.965	3270.7
255.00	13.369	14.533	27.902	3706.0	25.224	3409.0
260.00	13.653	14.742	28.394	3832.8	25.479	3549.7
265.00	13.936	14.946	28.882	3960.8	25.731	3692.9
270.00	14.217	15.149	29.365	4090.1	25.980	3838.6
273.15	14.393	15.274	29.668	4172.2	26.135	3931.5
275.00	14.497	15.348	29.844	4220.6	26.225	3986.6
280.00	14.775	15.544	30.319	4352.3	26.467	4137.0
285.00	15.052	15.738	30.790	4485.3	26.706	4289.8
290.00	15.327	15.929	31.256	4619.4	26.941	4444.9
295.00	15.601	16.118	31.719	4754.7	27.173	4602.3
298.15	15.773	16.235	32.008	4840.5	27.318	4702.7
300.00	15.874	16.304	32.177	4891.1	27.402	4762.1

H^C_0 AND S^C_0 APPLY TO THE REFERENCE STATE OF THE SOLID AT ZERO DEG K

TABLE B-156

THERMODYNAMIC FUNCTIONS FOR ZIRCONIUM TETRAFLUORIDE ($ZR F_4$)
SOLID AND LIQUID PHASES

GRAM MOLECULAR WT.= 167.2136 GRAMS 1 CAL=4.1840 JOULES

T DEG K = 273.15 + T DEG C

T	$-(G^0_T-H^C_0)/T$	$(H^0_T-H^C_0)/T$	$(S_T-S^C_0)$	$(H^0_T-H^C_0)$	C^0_P	$-(G^0_T-H^C_0)$
DEG K	CAL/DEG MOLE	CAL/DEG MOLE	CAL/DEG MOLE	CAL/MOLE	CAL/DEG MOLE	CAL/MOLE
			SOLID PHASE			
0.00	0.000	0.000	0.000	0.000	0.000	0.000
5.00	0.000	0.000	0.001	0.002	0.002	0.001
10.00	0.001	0.005	0.006	0.047	0.022	0.014
15.00	0.006	0.022	0.027	0.323	0.104	0.088
20.00	0.017	0.062	0.079	1.248	0.282	0.339
25.00	0.038	0.132	0.170	3.311	0.559	0.946
30.00	0.070	0.233	0.303	6.990	0.926	2.113
35.00	0.116	0.363	0.479	12.711	1.375	4.051
40.00	0.174	0.521	0.695	20.843	1.887	6.970
45.00	0.246	0.704	0.950	31.662	2.449	11.067
50.00	0.330	0.908	1.239	45.414	3.059	16.524
55.00	0.427	1.133	1.560	62.311	3.706	23.509
60.00	0.536	1.375	1.912	82.517	4.381	32.177
65.00	0.656	1.633	2.290	106.15	5.075	42.669
70.00	0.787	1.904	2.691	133.29	5.783	55.112
75.00	0.928	2.187	3.115	164.00	6.501	69.620
80.00	1.079	2.479	3.558	198.32	7.227	86.293
85.00	1.238	2.780	4.018	236.27	7.953	105.22
90.00	1.405	3.087	4.492	277.83	8.670	126.49
95.00	1.581	3.399	4.980	322.94	9.374	150.17
100.00	1.763	3.715	5.479	371.54	10.063	176.31
105.00	1.952	4.034	5.986	423.55	10.738	204.97
110.00	2.147	4.354	6.501	478.90	11.399	236.18
115.00	2.348	4.674	7.022	537.52	12.046	269.99
120.00	2.553	4.994	7.548	599.33	12.677	306.41
125.00	2.764	5.314	8.078	664.26	13.292	345.47
130.00	2.978	5.632	8.611	732.22	13.889	387.19
135.00	3.197	5.949	9.146	803.12	14.467	431.59
140.00	3.419	6.263	9.682	876.86	15.025	478.66
145.00	3.644	6.575	10.219	953.33	15.562	528.41
150.00	3.872	6.883	10.755	1032.4	16.079	580.84
155.00	4.103	7.188	11.291	1114.1	16.575	635.96
160.00	4.336	7.489	11.824	1198.2	17.051	693.75
165.00	4.571	7.785	12.356	1284.6	17.507	754.20
170.00	4.808	8.078	12.885	1373.2	17.944	817.31
175.00	5.046	8.366	13.412	1464.0	18.362	883.05
180.00	5.286	8.649	13.935	1556.8	18.763	951.42
185.00	5.526	8.927	14.454	1651.6	19.147	1022.4
190.00	5.768	9.201	14.969	1748.2	19.516	1095.9
195.00	6.011	9.470	15.481	1846.7	19.869	1172.1
200.00	6.254	9.735	15.988	1946.9	20.209	1250.7
205.00	6.497	9.994	16.491	2048.8	20.535	1332.0
210.00	6.741	10.249	16.990	2152.2	20.848	1415.7
215.00	6.985	10.499	17.484	2257.2	21.149	1501.8
220.00	7.229	10.744	17.974	2363.7	21.438	1590.5
225.00	7.474	10.985	18.458	2471.6	21.716	1681.6
230.00	7.718	11.221	18.939	2580.8	21.983	1775.1
235.00	7.961	11.453	19.414	2691.4	22.241	1870.9
240.00	8.205	11.680	19.885	2803.2	22.488	1969.2
245.00	8.448	11.903	20.351	2916.3	22.726	2069.8
250.00	8.691	12.122	20.813	3030.5	22.955	2172.7
255.00	8.933	12.336	21.269	3145.8	23.175	2277.9
260.00	9.175	12.547	21.722	3262.2	23.387	2385.4
265.00	9.416	12.753	22.169	3379.7	23.592	2495.1
270.00	9.656	12.956	22.612	3498.1	23.789	2607.1
273.15	9.807	13.082	22.888	3573.2	23.910	2678.7
275.00	9.895	13.155	23.050	3617.5	23.980	2721.2
280.00	10.134	13.350	23.484	3737.9	24.164	2837.6
285.00	10.372	13.541	23.913	3859.2	24.343	2956.1
290.00	10.609	13.729	24.338	3981.3	24.515	3076.7
295.00	10.846	13.913	24.758	4104.3	24.683	3199.4
298.15	10.994	14.027	25.021	4182.2	24.786	3277.8
300.00	11.081	14.094	25.175	4228.1	24.846	3324.3

H^C_0 AND S^C_0 APPLY TO THE REFERENCE STATE OF THE SOLID AT ZERO DEG K

TABLE B-156 (CONT.)

THERMODYNAMIC FUNCTIONS FOR ZIRCONIUM TETRAFLUORIDE ($ZR\ F_4$)
SOLID AND LIQUID PHASES

GRAM MOLECULAR WT.= 167.2136 GRAMS 1 CAL=4.1840 JOULES

T DEG K = 273.15 + T DEG C

T	$-(G^0_T-H^C_0)/T$	$(H^0_T-H^C_0)/T$	$(S_T-S^C_0)$	$(H^0_T-H^C_0)$	C^0_P	$-(G^0_T-H^C_0)$
DEG K	CAL / DEG MOLE	CAL / DEG MOLE	CAL / DEG MOLE	CAL / MOLE	CAL / DEG MOLE	CAL / MOLE
			SOLID PHASE			
300.00	11.081	14.094	25.175	4228.1	24.846	3324.3
310.00	11.549	14.446	25.995	4478.2	25.158	3580.1
320.00	12.013	14.785	26.798	4731.2	25.452	3844.1
330.00	12.473	15.113	27.585	4987.2	25.729	4116.0
340.00	12.929	15.429	28.357	5245.8	25.990	4395.8
350.00	13.380	15.734	29.114	5506.9	26.234	4683.1
360.00	13.828	16.029	29.857	5770.4	26.463	4978.0
370.00	14.271	16.314	30.585	6036.1	26.678	5280.2
373.15	14.410	16.402	30.811	6120.3	26.743	5376.9
380.00	14.710	16.589	31.299	6303.9	26.880	5589.6
390.00	15.144	16.856	32.000	6573.7	27.069	5906.1
400.00	15.574	17.113	32.687	6845.3	27.247	6229.6
425.00	16.630	17.721	34.351	7531.6	27.651	7067.7
450.00	17.659	18.283	35.942	8227.4	28.007	7946.5
475.00	18.662	18.803	37.465	8931.7	28.325	8864.3
500.00	19.639	19.287	38.925	9643.4	28.613	9819.3
550.00	21.519	20.158	41.677	11087.	29.119	11835.
600.00	23.306	20.924	44.230	12554.	29.556	13984.
650.00	25.008	21.603	46.611	14042.	29.945	16255.
700.00	26.632	22.212	48.843	15548.	30.299	18642.
750.00	28.183	22.762	50.945	17071.	30.627	21138.
800.00	29.669	23.263	52.932	18611.	30.936	23735.
850.00	31.093	23.723	54.816	20165.	31.229	26429.
900.00	32.461	24.148	56.609	21733.	31.510	29215.
950.00	33.777	24.543	58.320	23316.	31.782	32089.
1000.00	35.046	24.911	59.957	24911.	32.046	35046.
1050.00	36.270	25.257	61.527	26520.	32.304	38083.
1100.00	37.452	25.583	63.036	28142.	32.558	41197.
1150.00	38.596	25.892	64.488	29776.	32.809	44386.
1200.00	39.705	26.185	65.890	31422.	33.055	47645.
1205.00	39.813	26.213	66.027	31587.	33.079	47975.
			LIQUID PHASE			
1205.00	39.813	38.952	78.766	46937.	29.000	47975.

H^C_0 AND S^C_0 APPLY TO THE REFERENCE STATE OF THE SOLID AT ZERO DEG K

TABLE B-157

THERMODYNAMIC FUNCTIONS FOR ZIRCONIUM DIBORIDE ($ZR\ B_2$)

SOLID PHASE

GRAM MOLECULAR WT.= 112.842 GRAMS 1 CAL=4.1840 JOULES

T DEG K = 273.15 + T DEG C

T	$-(G_T^0-H_0^C)/T$	$(H_T^0-H_0^C)/T$	$(S_T-S_0^C)$	$(H_T^0-H_0^C)$	C_P^0	$-(G_T^0-H_0^C)$
DEG K	CAL/DEG MOLE	CAL/DEG MOLE	CAL/DEG MOLE	CAL/MOLE	CAL/DEG MOLE	CAL/MOLE
0.00	0.000	0.000	0.000	0.000	0.000	0.000
5.00	0.000	0.000	0.000	0.002	0.001	0.001
10.00	0.001	0.001	0.002	0.014	0.004	0.006
15.00	0.002	0.003	0.005	0.046	0.009	0.023
20.00	0.003	0.006	0.009	0.118	0.021	0.055
25.00	0.005	0.011	0.015	0.267	0.041	0.113
30.00	0.007	0.018	0.025	0.551	0.076	0.213
35.00	0.011	0.030	0.041	1.067	0.135	0.377
40.00	0.016	0.049	0.065	1.955	0.225	0.639
45.00	0.023	0.075	0.098	3.369	0.346	1.042
50.00	0.033	0.109	0.142	5.475	0.502	1.637
55.00	0.045	0.153	0.199	8.439	0.689	2.484
60.00	0.061	0.207	0.267	12.400	0.899	3.644
65.00	0.080	0.269	0.348	17.454	1.125	5.178
70.00	0.102	0.338	0.440	23.667	1.362	7.145
75.00	0.128	0.415	0.542	31.088	1.608	9.597
80.00	0.157	0.497	0.654	39.753	1.859	12.585
85.00	0.190	0.585	0.775	49.684	2.113	16.154
90.00	0.226	0.676	0.903	60.883	2.366	20.343
95.00	0.265	0.772	1.037	73.344	2.617	25.190
100.00	0.307	0.871	1.178	87.056	2.868	30.725
105.00	0.352	0.972	1.324	102.02	3.118	36.977
110.00	0.400	1.075	1.475	118.24	3.370	43.971
115.00	0.450	1.180	1.630	135.72	3.624	51.731
120.00	0.502	1.287	1.790	154.48	3.879	60.279
125.00	0.557	1.396	1.953	174.51	4.135	69.634
130.00	0.614	1.506	2.120	195.83	4.391	79.817
135.00	0.673	1.618	2.291	218.42	4.647	90.843
140.00	0.734	1.731	2.465	242.30	4.903	102.73
145.00	0.797	1.845	2.641	267.46	5.159	115.49
150.00	0.861	1.959	2.820	293.89	5.413	129.15
155.00	0.927	2.075	3.002	321.59	5.666	143.70
160.00	0.995	2.191	3.186	350.55	5.917	159.17
165.00	1.064	2.308	3.372	380.76	6.167	175.56
170.00	1.135	2.425	3.559	412.21	6.414	192.89
175.00	1.207	2.542	3.749	444.89	6.659	211.16
180.00	1.280	2.660	3.940	478.79	6.901	230.38
185.00	1.354	2.778	4.132	513.89	7.140	250.56
190.00	1.430	2.896	4.326	550.19	7.376	271.70
195.00	1.507	3.014	4.520	587.65	7.609	293.82
200.00	1.585	3.131	4.716	626.28	7.839	316.91
205.00	1.663	3.249	4.912	666.04	8.065	340.98
210.00	1.743	3.366	5.109	706.92	8.287	366.03
215.00	1.824	3.483	5.307	748.90	8.505	392.07
220.00	1.905	3.600	5.505	791.97	8.720	419.10
225.00	1.987	3.716	5.703	836.09	8.929	447.12
230.00	2.070	3.832	5.902	881.25	9.135	476.13
235.00	2.154	3.947	6.100	927.44	9.337	506.14
240.00	2.238	4.061	6.299	974.62	9.534	537.13
245.00	2.323	4.175	6.498	1022.8	9.728	569.13
250.00	2.408	4.288	6.696	1071.9	9.917	602.11
255.00	2.494	4.400	6.894	1121.9	10.102	636.09
260.00	2.581	4.511	7.092	1172.9	10.284	671.05
265.00	2.668	4.622	7.290	1224.8	10.461	707.01
270.00	2.755	4.732	7.487	1277.5	10.635	743.95
273.15	2.811	4.800	7.611	1311.2	10.742	767.73
275.00	2.843	4.840	7.684	1331.1	10.804	781.87
280.00	2.931	4.948	7.880	1385.5	10.970	820.78
285.00	3.020	5.055	8.075	1440.8	11.132	860.67
290.00	3.109	5.162	8.270	1496.9	11.290	901.54
295.00	3.198	5.267	8.465	1553.7	11.444	943.37
298.15	3.254	5.333	8.587	1589.9	11.539	970.23
300.00	3.287	5.371	8.658	1611.3	11.594	986.18
310.00	3.467	5.576	9.043	1728.7	11.882	1074.7
320.00	3.647	5.778	9.425	1848.9	12.154	1167.0
330.00	3.828	5.975	9.803	1971.7	12.410	1263.2
340.00	4.009	6.168	10.177	2097.0	12.650	1363.1
350.00	4.191	6.356	10.547	2224.7	12.874	1466.7

H_0^C AND S_0^C APPLY TO THE REFERENCE STATE OF THE SOLID AT ZERO DEG K

TABLE B-158

THERMODYNAMIC FUNCTIONS FOR STRONTIUM 1:1-SILICATE (SR O .SI O_2)

SOLID PHASE

GRAM MOLECULAR WT.= 163.7042 GRAMS 1 CAL=4.1840 JOULES

T DEG K = 273.15 + T DEG C

T DEG K	$-(G^0_T-H^C_0)/T$ CAL/DEG MOLE	$(H^0_T-H^C_0)/T$ CAL/DEG MOLE	$(S_T-S^C_0)$ CAL/DEG MOLE	$(H^0_T-H^C_0)$ CAL/MOLE	C^0_P CAL/DEG MOLE	$-(G^0_T-H^C_0)$ CAL/MOLE
0.00	0.000	0.000	0.000	0.000	0.000	0.000
5.00	0.001	0.002	0.003	0.010	0.008	0.003
10.00	0.005	0.016	0.022	0.164	0.066	0.055
15.00	0.018	0.055	0.074	0.830	0.220	0.277
20.00	0.044	0.129	0.173	2.587	0.505	0.872
25.00	0.084	0.243	0.327	6.087	0.913	2.099
30.00	0.141	0.395	0.536	11.848	1.400	4.237
35.00	0.215	0.576	0.791	20.159	1.931	7.538
40.00	0.305	0.780	1.086	31.208	2.493	12.216
45.00	0.410	1.003	1.413	45.128	3.080	18.449
50.00	0.528	1.241	1.769	62.060	3.699	26.392
55.00	0.658	1.494	2.152	82.181	4.354	36.184
60.00	0.799	1.761	2.560	105.63	5.026	47.955
65.00	0.951	2.037	2.988	132.41	5.683	61.817
70.00	1.112	2.320	3.433	162.42	6.314	77.863
75.00	1.282	2.607	3.889	195.51	6.922	96.162
80.00	1.460	2.895	4.355	231.59	7.506	116.77
85.00	1.644	3.183	4.826	270.53	8.066	139.72
90.00	1.834	3.469	5.303	312.22	8.604	165.04
95.00	2.029	3.753	5.782	356.55	9.124	192.75
100.00	2.229	4.034	6.263	403.43	9.626	222.86
105.00	2.432	4.312	6.744	452.78	10.114	255.38
110.00	2.639	4.587	7.226	504.54	10.587	290.31
115.00	2.849	4.858	7.707	558.63	11.045	327.64
120.00	3.061	5.125	8.186	614.97	11.489	367.37
125.00	3.276	5.388	8.664	673.50	11.920	409.50
130.00	3.492	5.647	9.140	734.14	12.336	454.01
135.00	3.710	5.902	9.613	796.84	12.739	500.89
140.00	3.930	6.154	10.083	861.51	13.129	550.13
145.00	4.150	6.401	10.550	928.10	13.505	601.72
150.00	4.371	6.644	11.014	996.54	13.868	655.63
155.00	4.593	6.882	11.475	1066.8	14.219	711.86
160.00	4.815	7.117	11.932	1138.7	14.559	770.37
165.00	5.037	7.347	12.385	1212.3	14.887	831.17
170.00	5.260	7.574	12.834	1287.6	15.204	894.22
175.00	5.483	7.796	13.279	1364.4	15.511	959.50
180.00	5.706	8.015	13.720	1442.7	15.809	1027.0
185.00	5.928	8.229	14.157	1522.4	16.099	1096.7
190.00	6.150	8.440	14.591	1603.6	16.382	1168.6
195.00	6.372	8.647	15.020	1686.2	16.659	1242.6
200.00	6.594	8.851	15.445	1770.2	16.929	1318.8
205.00	6.815	9.051	15.866	1855.5	17.195	1397.0
210.00	7.035	9.248	16.284	1942.2	17.455	1477.4
215.00	7.255	9.442	16.697	2030.1	17.709	1559.9
220.00	7.474	9.633	17.107	2119.2	17.958	1644.4
225.00	7.693	9.821	17.514	2209.6	18.202	1730.9
230.00	7.911	10.005	17.916	2301.2	18.439	1819.5
235.00	8.128	10.187	18.315	2394.0	18.671	1910.1
240.00	8.344	10.366	18.711	2487.9	18.897	2002.7
245.00	8.560	10.543	19.103	2583.0	19.117	2097.2
250.00	8.775	10.716	19.491	2679.1	19.332	2193.7
255.00	8.989	10.887	19.876	2776.3	19.541	2292.1
260.00	9.202	11.056	20.257	2874.5	19.745	2392.4
265.00	9.414	11.222	20.635	2973.7	19.944	2494.7
270.00	9.625	11.385	21.010	3073.9	20.139	2598.8
273.15	9.758	11.487	21.244	3137.6	20.260	2665.3
275.00	9.836	11.546	21.381	3175.1	20.330	2704.8
280.00	10.045	11.704	21.749	3277.2	20.516	2812.6
285.00	10.254	11.861	22.114	3380.3	20.699	2922.3
290.00	10.461	12.015	22.476	3484.2	20.877	3033.7
295.00	10.668	12.166	22.834	3589.0	21.052	3147.0
298.15	10.798	12.261	23.058	3655.5	21.161	3219.3
300.00	10.874	12.316	23.189	3694.7	21.224	3262.1

H^C_0 AND S^C_0 APPLY TO THE REFERENCE STATE OF THE SOLID AT ZERO DEG K

TABLE B-159

THERMODYNAMIC FUNCTIONS FOR STRONTIUM 2:1-SILICATE (2SR O .SI O_2)
SOLID PHASE

GRAM MOLECULAR WT.= 267.3236 GRAMS 1 CAL=4.1840 JOULES

T DEG K = 273.15 + T DEG C

T	$-(G^O_T-H^C_O)/T$	$(H^O_T-H^C_O)/T$	$(S_T-S^C_O)$	$(H^O_T-H^C_O)$	C^O_P	$-(G^O_T-H^C_O)$
DEG K	CAL / DEG MOLE	CAL / DEG MOLE	CAL / DEG MOLE	CAL / MOLE	CAL / DEG MOLE	CAL / MOLE
0.00	0.000	0.000	0.000	0.000	0.000	0.000
5.00	0.001	0.003	0.003	0.013	0.010	0.004
10.00	0.007	0.020	0.027	0.203	0.081	0.068
15.00	0.023	0.068	0.091	1.024	0.272	0.342
20.00	0.054	0.161	0.215	3.215	0.637	1.077
25.00	0.105	0.310	0.415	7.750	1.214	2.615
30.00	0.179	0.524	0.703	15.725	2.009	5.371
35.00	0.280	0.804	1.084	28.142	2.983	9.802
40.00	0.409	1.144	1.553	45.747	4.074	16.359
45.00	0.566	1.533	2.099	68.977	5.223	25.457
50.00	0.749	1.960	2.709	97.996	6.383	37.452
55.00	0.957	2.414	3.371	132.77	7.524	52.633
60.00	1.187	2.886	4.074	173.19	8.635	71.230
65.00	1.437	3.370	4.807	219.05	9.703	93.421
70.00	1.705	3.859	5.564	270.14	10.726	119.34
75.00	1.988	4.350	6.338	326.24	11.707	149.09
80.00	2.284	4.839	7.123	387.14	12.644	182.74
85.00	2.592	5.325	7.917	452.60	13.532	220.34
90.00	2.910	5.804	8.714	522.38	14.369	261.91
95.00	3.237	6.276	9.513	596.22	15.160	307.48
100.00	3.570	6.739	10.310	673.92	15.917	357.04
105.00	3.910	7.194	11.104	755.34	16.647	410.57
110.00	4.255	7.640	11.895	840.36	17.355	468.07
115.00	4.604	8.077	12.681	928.85	18.039	529.52
120.00	4.957	8.506	13.463	1020.7	18.696	594.88
125.00	5.313	8.926	14.239	1115.8	19.324	664.14
130.00	5.671	9.338	15.009	1213.9	19.923	737.26
135.00	6.031	9.740	15.772	1315.0	20.494	814.22
140.00	6.393	10.134	16.527	1418.8	21.040	894.96
145.00	6.755	10.519	17.274	1525.3	21.564	979.47
150.00	7.118	10.896	18.014	1634.4	22.069	1067.7
155.00	7.481	11.264	18.746	1746.0	22.557	1159.6
160.00	7.845	11.625	19.469	1859.9	23.029	1255.1
165.00	8.208	11.977	20.185	1976.2	23.486	1354.3
170.00	8.570	12.322	20.893	2094.8	23.929	1457.0
175.00	8.933	12.660	21.593	2215.5	24.359	1563.2
180.00	9.294	12.991	22.285	2338.4	24.776	1672.9
185.00	9.654	13.315	22.969	2463.3	25.181	1786.0
190.00	10.014	13.632	23.646	2590.1	25.575	1902.6
195.00	10.372	13.943	24.315	2719.0	25.957	2022.5
200.00	10.729	14.249	24.977	2849.7	26.330	2145.7
205.00	11.084	14.548	25.632	2982.3	26.693	2272.2
210.00	11.438	14.841	26.279	3116.6	27.047	2402.0
215.00	11.791	15.129	26.920	3252.7	27.392	2535.0
220.00	12.142	15.411	27.553	3390.5	27.727	2671.2
225.00	12.491	15.689	28.180	3530.0	28.054	2810.5
230.00	12.839	15.961	28.800	3671.1	28.373	2953.0
235.00	13.185	16.228	29.414	3813.7	28.683	3098.5
240.00	13.530	16.491	30.021	3957.9	28.985	3247.1
245.00	13.872	16.749	30.621	4103.5	29.279	3398.7
250.00	14.213	17.003	31.216	4250.6	29.566	3553.3
255.00	14.552	17.252	31.804	4399.2	29.847	3710.9
260.00	14.890	17.497	32.386	4549.1	30.123	3871.3
265.00	15.225	17.737	32.963	4700.4	30.394	4034.7
270.00	15.559	17.974	33.533	4853.0	30.661	4201.0
273.15	15.768	18.121	33.890	4949.9	30.827	4307.2
275.00	15.891	18.207	34.098	5007.0	30.924	4370.0
280.00	16.221	18.437	34.658	5162.3	31.185	4541.9
285.00	16.550	18.663	35.212	5318.9	31.444	4716.6
290.00	16.876	18.885	35.761	5476.7	31.700	4894.0
295.00	17.201	19.105	36.305	5635.9	31.955	5074.2
298.15	17.404	19.241	36.646	5736.8	32.114	5189.1
300.00	17.524	19.321	36.845	5796.3	32.207	5257.1

H^C_O AND S^C_O APPLY TO THE REFERENCE STATE OF THE SOLID AT ZERO DEG K

TABLE B-160
THERMODYNAMIC FUNCTIONS FOR BARIUM 1:1-SILICATE (BA O .SI O_2)
SOLID PHASE

GRAM MOLECULAR WT.= 213.4242 GRAMS   1 CAL=4.1840 JOULES

T DEG K = 273.15 + T DEG C

T	$-(G^O_T-H^C_0)/T$	$(H^O_T-H^C_0)/T$	$(S_T-S^C_0)$	$(H^O_T-H^C_0)$	C^O_P	$-(G^O_T-H^C_0)$
DEG K	CAL/DEG MOLE	CAL/DEG MOLE	CAL/DEG MOLE	CAL/MOLE	CAL/DEG MOLE	CAL/MOLE
0.00	0.000	0.000	0.000	0.000	0.000	0.000
5.00	0.001	0.004	0.006	0.021	0.017	0.007
10.00	0.011	0.034	0.045	0.338	0.135	0.113
15.00	0.038	0.113	0.150	1.690	0.442	0.568
20.00	0.088	0.256	0.345	5.125	0.965	1.766
25.00	0.167	0.464	0.631	11.608	1.650	4.168
30.00	0.274	0.726	0.999	21.769	2.422	8.214
35.00	0.408	1.026	1.433	35.894	3.233	14.271
40.00	0.566	1.352	1.918	54.096	4.045	22.632
45.00	0.745	1.695	2.440	76.284	4.822	33.515
50.00	0.941	2.045	2.986	102.23	5.548	47.072
55.00	1.153	2.394	3.547	131.69	6.227	63.400
60.00	1.376	2.741	4.117	164.44	6.869	82.557
65.00	1.609	3.082	4.691	200.31	7.471	104.57
70.00	1.849	3.416	5.265	239.09	8.036	129.46
75.00	2.096	3.742	5.838	280.61	8.568	157.22
80.00	2.348	4.059	6.407	324.73	9.074	187.83
85.00	2.603	4.368	6.972	371.31	9.555	221.28
90.00	2.862	4.669	7.531	420.25	10.018	257.54
95.00	3.122	4.963	8.085	471.46	10.465	296.58
100.00	3.384	5.249	8.633	524.88	10.900	338.38
105.00	3.647	5.528	9.175	580.45	11.324	382.90
110.00	3.910	5.801	9.711	638.10	11.735	430.12
115.00	4.174	6.068	10.242	697.78	12.134	480.00
120.00	4.438	6.329	10.766	759.42	12.522	532.52
125.00	4.701	6.584	11.285	822.98	12.899	587.65
130.00	4.964	6.834	11.798	888.39	13.266	645.36
135.00	5.227	7.079	12.306	955.62	13.623	705.63
140.00	5.489	7.319	12.807	1024.6	13.970	768.41
145.00	5.750	7.554	13.303	1095.3	14.307	833.69
150.00	6.010	7.784	13.794	1167.7	14.635	901.43
155.00	6.269	8.011	14.279	1241.6	14.953	971.62
160.00	6.526	8.232	14.759	1317.2	15.261	1044.2
165.00	6.783	8.450	15.233	1394.2	15.560	1119.2
170.00	7.038	8.663	15.702	1472.8	15.850	1196.5
175.00	7.293	8.873	16.165	1552.7	16.132	1276.2
180.00	7.545	9.078	16.624	1634.1	16.407	1358.2
185.00	7.797	9.280	17.077	1716.8	16.675	1442.4
190.00	8.047	9.478	17.525	1800.8	16.936	1528.9
195.00	8.296	9.672	17.968	1886.1	17.192	1617.7
200.00	8.543	9.864	18.407	1972.7	17.443	1708.6
205.00	8.789	10.051	18.840	2060.5	17.689	1801.7
210.00	9.033	10.236	19.270	2149.6	17.930	1897.0
215.00	9.276	10.418	19.694	2239.8	18.167	1994.4
220.00	9.518	10.597	20.115	2331.3	18.398	2093.9
225.00	9.758	10.773	20.531	2423.8	18.625	2195.6
230.00	9.997	10.946	20.942	2517.5	18.847	2299.2
235.00	10.234	11.116	21.350	2612.3	19.064	2405.0
240.00	10.470	11.284	21.754	2708.1	19.276	2512.7
245.00	10.704	11.449	22.153	2805.0	19.484	2622.5
250.00	10.937	11.612	22.549	2903.0	19.688	2734.3
255.00	11.169	11.772	22.941	3001.9	19.888	2848.0
260.00	11.399	11.930	23.329	3101.8	20.085	2963.7
265.00	11.627	12.086	23.713	3202.8	20.279	3081.3
270.00	11.855	12.239	24.094	3304.6	20.471	3200.8
273.15	11.997	12.335	24.332	3369.3	20.591	3277.1
275.00	12.081	12.391	24.472	3407.5	20.661	3322.2
280.00	12.305	12.540	24.846	3511.2	20.849	3445.5
285.00	12.529	12.688	25.216	3616.0	21.036	3570.7
290.00	12.751	12.833	25.584	3721.6	21.221	3697.7
295.00	12.971	12.977	25.948	3828.2	21.406	3826.5
298.15	13.109	13.066	26.176	3895.8	21.521	3908.6
300.00	13.190	13.119	26.309	3935.7	21.589	3957.1

H^C_0 AND S^C_0 APPLY TO THE REFERENCE STATE OF THE SOLID AT ZERO DEG K

TABLE B-161

THERMODYNAMIC FUNCTIONS FOR BARIUM 1:2-SILICATE ($BA\ O\ .2SI\ O_2$)
SOLID PHASE

GRAM MOLECULAR WT.= 273.509 GRAMS 1 CAL=4.1840 JOULES

T DEG K = 273.15 + T DEG C

T DEG K	$-(G^0_T-H^C_0)/T$ CAL/DEG MOLE	$(H^0_T-H^C_0)/T$ CAL/DEG MOLE	$(S_T-S^C_0)$ CAL/DEG MOLE	$(H^0_T-H^C_0)$ CAL/MOLE	C^0_P CAL/DEG MOLE	$-(G^0_T-H^C_0)$ CAL/MOLE
0.00	0.000	0.000	0.000	0.000	0.000	0.000
5.00	0.003	0.008	0.011	0.042	0.034	0.014
10.00	0.022	0.067	0.089	0.671	0.266	0.224
15.00	0.074	0.217	0.291	3.248	0.817	1.117
20.00	0.168	0.461	0.629	9.220	1.593	3.365
25.00	0.304	0.771	1.075	19.279	2.435	7.588
30.00	0.474	1.120	1.594	33.599	3.292	14.235
35.00	0.675	1.494	2.168	52.274	4.188	23.621
40.00	0.900	1.888	2.788	75.539	5.122	35.996
45.00	1.146	2.300	3.446	103.50	6.062	51.568
50.00	1.410	2.722	4.132	136.12	6.980	70.503
55.00	1.690	3.150	4.840	173.25	7.868	92.926
60.00	1.982	3.579	5.561	214.75	8.726	118.92
65.00	2.285	4.007	6.292	260.45	9.549	148.55
70.00	2.598	4.431	7.029	310.17	10.335	181.86
75.00	2.918	4.850	7.768	363.75	11.091	218.85
80.00	3.244	5.263	8.507	421.04	11.822	259.53
85.00	3.575	5.670	9.245	481.93	12.534	303.92
90.00	3.911	6.071	9.981	546.35	13.229	351.98
95.00	4.250	6.465	10.715	614.21	13.911	403.73
100.00	4.591	6.854	11.446	685.44	14.581	459.13
105.00	4.935	7.238	12.173	759.99	15.239	518.18
110.00	5.280	7.616	12.897	837.81	15.885	580.85
115.00	5.627	7.990	13.617	918.82	16.520	647.14
120.00	5.975	8.358	14.333	1003.0	17.142	717.02
125.00	6.324	8.722	15.046	1090.2	17.751	790.47
130.00	6.673	9.081	15.753	1180.5	18.345	867.47
135.00	7.022	9.434	16.457	1273.6	18.921	947.99
140.00	7.372	9.783	17.155	1369.7	19.481	1032.0
145.00	7.721	10.127	17.848	1468.4	20.025	1119.5
150.00	8.070	10.466	18.536	1569.9	20.554	1210.5
155.00	8.419	10.800	19.218	1673.9	21.068	1304.9
160.00	8.767	11.128	19.895	1780.5	21.570	1402.7
165.00	9.114	11.452	20.566	1889.6	22.061	1503.8
170.00	9.461	11.771	21.232	2001.1	22.540	1608.3
175.00	9.806	12.086	21.892	2115.0	23.010	1716.1
180.00	10.151	12.396	22.547	2231.2	23.469	1827.2
185.00	10.495	12.701	23.196	2349.7	23.918	1941.6
190.00	10.838	13.002	23.840	2470.4	24.359	2059.2
195.00	11.179	13.299	24.478	2593.3	24.790	2180.0
200.00	11.520	13.591	25.111	2718.3	25.212	2304.0
205.00	11.859	13.880	25.739	2845.4	25.626	2431.1
210.00	12.197	14.164	26.361	2974.5	26.031	2561.3
215.00	12.533	14.445	26.978	3105.7	26.429	2694.7
220.00	12.869	14.722	27.590	3238.8	26.819	2831.1
225.00	13.203	14.995	28.197	3373.8	27.201	2970.6
230.00	13.535	15.264	28.799	3510.8	27.575	3113.1
235.00	13.866	15.530	29.396	3649.6	27.943	3258.6
240.00	14.196	15.792	29.988	3790.2	28.303	3407.0
245.00	14.524	16.051	30.576	3932.6	28.657	3558.4
250.00	14.851	16.307	31.158	4076.8	29.004	3712.8
255.00	15.177	16.559	31.736	4222.6	29.345	3870.0
260.00	15.501	16.808	32.309	4370.2	29.680	4030.1
265.00	15.823	17.054	32.877	4519.4	30.010	4193.1
270.00	16.144	17.297	33.441	4670.3	30.333	4358.9
273.15	16.346	17.449	33.794	4766.2	30.535	4464.8
275.00	16.464	17.537	34.001	4822.7	30.652	4527.5
280.00	16.782	17.774	34.556	4976.8	30.965	4698.9
285.00	17.098	18.008	35.107	5132.4	31.273	4873.1
290.00	17.414	18.240	35.653	5289.5	31.577	5050.0
295.00	17.727	18.468	36.196	5448.1	31.875	5229.6
298.15	17.924	18.611	36.535	5548.8	32.061	5344.1
300.00	18.040	18.694	36.734	5608.3	32.169	5411.9

H^C_0 AND S^C_0 APPLY TO THE REFERENCE STATE OF THE SOLID AT ZERO DEG K

TABLE B-162

THERMODYNAMIC FUNCTIONS FOR BARIUM 2:3-SILICATE (2BA O .3SI O_2)
SOLID PHASE

GRAM MOLECULAR WT.= 486.9332 GRAMS　　　1 CAL=4.1840 JOULES

T DEG K = 273.15 + T DEG C

T	$-(G^O_T-H^C_0)/T$	$(H^O_T-H^C_0)/T$	$(S_T-S^C_0)$	$(H^O_T-H^C_0)$	C^O_P	$-(G^O_T-H^C_0)$
DEG K	CAL/DEG MOLE	CAL/DEG MOLE	CAL/DEG MOLE	CAL/MOLE	CAL/DEG MOLE	CAL/MOLE
0.00	0.000	0.000	0.000	0.000	0.000	0.000
10.00	0.033	0.099	0.132	0.991	0.389	0.333
15.00	0.109	0.312	0.421	4.680	1.153	1.638
20.00	0.243	0.653	0.896	13.060	2.245	4.857
25.00	0.435	1.103	1.539	27.587	3.612	10.876
30.00	0.683	1.653	2.336	49.584	5.215	20.501
35.00	0.985	2.285	3.270	79.974	6.956	34.464
40.00	1.335	2.979	4.314	119.17	8.719	53.383
45.00	1.728	3.712	5.440	167.05	10.418	77.739
50.00	2.157	4.464	6.621	223.19	12.024	107.87
55.00	2.618	5.221	7.840	287.16	13.551	144.01
60.00	3.105	5.976	9.081	358.58	15.005	186.31
65.00	3.613	6.725	10.338	437.12	16.404	234.85
70.00	4.139	7.465	11.604	522.57	17.773	289.70
75.00	4.679	8.197	12.876	614.81	19.117	350.90
70.00	4.139	7.465	11.604	522.57	17.773	289.70
75.00	4.679	8.197	12.876	614.81	19.117	350.90
80.00	5.231	8.921	14.152	713.67	20.415	418.47
85.00	5.793	9.634	15.427	818.86	21.651	492.42
90.00	6.364	10.334	16.698	930.09	22.834	572.73
95.00	6.941	11.022	17.963	1047.1	23.981	659.39
100.00	7.524	11.699	19.222	1169.9	25.106	752.35
105.00	8.110	12.363	20.474	1298.2	26.213	851.60
110.00	8.701	13.018	21.718	1431.9	27.299	957.08
115.00	9.294	13.662	22.955	1571.1	28.360	1068.8
120.00	9.889	14.296	24.184	1715.5	29.393	1186.6
125.00	10.485	14.920	25.405	1865.0	30.396	1310.6
130.00	11.082	15.534	26.616	2019.4	31.370	1440.7
135.00	11.680	16.138	27.818	2178.6	32.315	1576.7
140.00	12.277	16.732	29.009	2342.5	33.234	1718.8
145.00	12.875	17.317	30.191	2510.9	34.127	1866.8
150.00	13.471	17.892	31.363	2683.7	34.996	2020.7
155.00	14.067	18.457	32.524	2860.9	35.844	2180.4
160.00	14.662	19.013	33.676	3042.1	36.670	2345.9
165.00	15.256	19.561	34.816	3227.5	37.475	2517.2
170.00	15.848	20.099	35.947	3416.9	38.261	2694.1
175.00	16.438	20.629	37.067	3610.1	39.028	2876.6
180.00	17.026	21.151	38.177	3807.1	39.776	3064.7
175.00	16.438	20.629	37.067	3610.1	39.028	2876.6
180.00	17.026	21.151	38.177	3807.1	39.776	3064.7
185.00	17.613	21.664	39.277	4007.8	40.506	3258.4
190.00	18.197	22.169	40.366	4212.1	41.219	3457.5
195.00	18.780	22.667	41.446	4420.0	41.916	3662.0
200.00	19.360	23.156	42.516	4631.3	42.597	3871.9
205.00	19.937	23.639	43.576	4845.9	43.264	4087.2
210.00	20.513	24.114	44.627	5063.9	43.918	4307.7
215.00	21.086	24.582	45.667	5285.1	44.560	4533.4
220.00	21.656	25.043	46.699	5509.5	45.189	4764.3
225.00	22.224	25.498	47.722	5737.0	45.807	5000.4
230.00	22.789	25.946	48.735	5967.5	46.414	5241.5
235.00	23.352	26.388	49.740	6201.1	47.010	5487.7
240.00	23.912	26.823	50.736	6437.6	47.595	5738.9
245.00	24.470	27.253	51.723	6677.0	48.170	5995.1
250.00	25.025	27.677	52.702	6919.3	48.734	6256.1
255.00	25.577	28.096	53.672	7164.4	49.288	6522.1
260.00	26.126	28.508	54.635	7412.2	49.831	6792.8
265.00	26.673	28.916	55.589	7662.6	50.363	7068.4
270.00	27.217	29.318	56.535	7915.8	50.885	7348.7
273.15	27.559	29.568	57.127	8076.6	51.208	7527.7
275.00	27.759	29.714	57.474	8171.5	51.396	7633.7
280.00	28.298	30.106	58.404	8429.7	51.897	7923.4
285.00	28.834	30.493	59.327	8690.4	52.388	8217.8
290.00	29.368	30.874	60.242	8953.6	52.868	8516.7
295.00	29.899	31.251	61.150	9219.1	53.338	8820.2
298.15	30.232	31.486	61.718	9387.6	53.629	9013.7
300.00	30.427	31.623	62.050	9486.9	53.798	9128.2

H^C_0 AND S^C_0 APPLY TO THE REFERENCE STATE OF THE SOLID AT ZERO DEG K

TABLE B-163

THERMODYNAMIC FUNCTIONS FOR BARIUM 2:1-SILICATE (2BA O .SI O_2)
SOLID PHASE

GRAM MOLECULAR WT.= 366.7636 GRAMS   1 CAL=4.1840 JOULES

T DEG K = 273.15 + T DEG C

T	$-(G_T^O-H_0^C)/T$	$(H_T^O-H_0^C)/T$	$(S_T-S_0^C)$	$(H_T^O-H_0^C)$	C_P^O	$-(G_T^O-H_0^C)$
DEG K	CAL/DEG MOLE	CAL/DEG MOLE	CAL/DEG MOLE	CAL/MOLE	CAL/DEG MOLE	CAL/MOLE
0.00	0.000	0.000	0.000	0.000	0.000	0.000
5.00	0.003	0.010	0.013	0.048	0.038	0.016
10.00	0.025	0.076	0.101	0.760	0.300	0.254
15.00	0.084	0.244	0.328	3.659	0.918	1.263
20.00	0.190	0.521	0.711	10.418	1.821	3.798
25.00	0.344	0.887	1.231	22.164	2.903	8.600
30.00	0.543	1.322	1.865	39.661	4.108	16.296
35.00	0.783	1.811	2.594	63.378	5.387	27.408
40.00	1.059	2.339	3.398	93.544	6.674	42.360
45.00	1.366	2.890	4.256	130.03	7.912	61.474
50.00	1.700	3.452	5.151	172.58	9.102	84.979
55.00	2.055	4.019	6.074	221.02	10.270	113.03
60.00	2.429	4.587	7.016	275.22	11.398	145.75
65.00	2.819	5.152	7.971	334.88	12.451	183.21
70.00	3.221	5.708	8.929	399.59	13.423	225.46
75.00	3.633	6.253	9.887	469.00	14.330	272.50
80.00	4.054	6.785	10.839	542.79	15.178	324.32
85.00	4.481	7.302	11.783	620.68	15.969	380.88
90.00	4.913	7.804	12.717	702.40	16.709	442.14
95.00	5.348	8.292	13.639	787.70	17.406	508.03
100.00	5.785	8.764	14.549	876.40	18.069	578.51
105.00	6.224	9.222	15.446	968.34	18.704	653.50
110.00	6.663	9.667	16.330	1063.4	19.314	732.95
115.00	7.102	10.100	17.202	1161.4	19.900	816.78
120.00	7.541	10.520	18.061	1262.4	20.463	904.95
125.00	7.979	10.928	18.907	1366.0	21.002	997.37
130.00	8.415	11.326	19.741	1472.3	21.518	1094.0
135.00	8.850	11.712	20.563	1581.2	22.013	1194.8
140.00	9.283	12.089	21.372	1692.4	22.486	1299.6
145.00	9.714	12.455	22.169	1806.0	22.941	1408.5
150.00	10.142	12.812	22.954	1921.8	23.380	1521.3
155.00	10.568	13.160	23.727	2039.8	23.803	1638.0
160.00	10.991	13.499	24.490	2159.8	24.213	1758.5
165.00	11.411	13.830	25.241	2281.9	24.611	1882.9
170.00	11.829	14.152	25.981	2405.9	24.996	2010.9
175.00	12.244	14.468	26.711	2531.8	25.371	2142.7
180.00	12.656	14.776	27.431	2659.6	25.735	2278.0
185.00	13.065	15.077	28.141	2789.2	26.089	2416.9
190.00	13.471	15.371	28.842	2920.5	26.432	2559.4
195.00	13.874	15.659	29.532	3053.5	26.767	2705.3
200.00	14.274	15.941	30.214	3188.1	27.092	2854.7
205.00	14.671	16.217	30.887	3324.4	27.409	3007.5
210.00	15.065	16.487	31.551	3462.2	27.718	3163.6
215.00	15.456	16.751	32.207	3601.6	28.019	3323.0
220.00	15.844	17.011	32.855	3742.4	28.313	3485.6
225.00	16.229	17.265	33.494	3884.7	28.600	3651.5
230.00	16.611	17.515	34.126	4028.4	28.880	3820.6
235.00	16.990	17.759	34.750	4173.5	29.153	3992.8
240.00	17.367	18.000	35.366	4319.9	29.422	4168.0
245.00	17.740	18.235	35.976	4467.7	29.685	4346.4
250.00	18.111	18.467	36.578	4616.7	29.943	4527.8
255.00	18.479	18.694	37.174	4767.1	30.197	4712.2
260.00	18.844	18.918	37.762	4918.7	30.447	4899.5
265.00	19.207	19.138	38.345	5071.6	30.694	5089.8
270.00	19.566	19.354	38.921	5225.6	30.939	5283.0
273.15	19.792	19.489	39.280	5323.3	31.091	5406.1
275.00	19.924	19.567	39.491	5380.9	31.180	5479.0
280.00	20.278	19.777	40.055	5537.4	31.420	5677.8
285.00	20.630	19.983	40.613	5695.1	31.657	5879.5
290.00	20.979	20.186	41.165	5854.0	31.892	6084.0
295.00	21.326	20.387	41.713	6014.0	32.126	6291.2
298.15	21.543	20.511	42.055	6115.5	32.272	6423.1
300.00	21.670	20.584	42.254	6175.3	32.357	6501.1

H_0^C AND S_0^C APPLY TO THE REFERENCE STATE OF THE SOLID AT ZERO DEG K

TABLE B-164

THERMODYNAMIC FUNCTIONS FOR CALCIUM 1:1-ZIRCONATE (CA O .ZR O_2)
SOLID PHASE

GRAM MOLECULAR WT.= 179.2982 GRAMS 1 CAL=4.1840 JOULES

T DEG K = 273.15 + T DEG C

T DEG K	$-(G^O_T-H^C_0)/T$ CAL/DEG MOLE	$(H^O_T-H^C_0)/T$ CAL/DEG MOLE	$(S_T-S^C_0)$ CAL/DEG MOLE	$(H^O_T-H^C_0)$ CAL/MOLE	C^O_P CAL/DEG MOLE	$-(G^O_T-H^C_0)$ CAL/MOLE
0.00	0.000	0.000	0.000	0.000	0.000	0.000
5.00	0.000	0.001	0.002	0.006	0.005	0.002
10.00	0.003	0.009	0.012	0.092	0.037	0.031
15.00	0.010	0.031	0.041	0.465	0.124	0.155
20.00	0.024	0.073	0.098	1.464	0.291	0.489
25.00	0.048	0.141	0.189	3.529	0.551	1.190
30.00	0.081	0.237	0.319	7.119	0.898	2.442
35.00	0.127	0.361	0.488	12.637	1.321	4.443
40.00	0.185	0.511	0.696	20.438	1.809	7.386
45.00	0.255	0.685	0.940	30.825	2.354	11.459
50.00	0.337	0.881	1.218	44.053	2.945	16.839
55.00	0.431	1.097	1.528	60.342	3.577	23.691
60.00	0.536	1.331	1.867	79.876	4.241	32.167
65.00	0.652	1.581	2.234	102.79	4.925	42.409
70.00	0.779	1.845	2.624	129.14	5.615	54.545
75.00	0.916	2.119	3.035	158.93	6.302	68.684
80.00	1.062	2.402	3.463	192.15	6.981	84.923
85.00	1.216	2.691	3.907	228.73	7.653	103.34
90.00	1.378	2.985	4.363	268.66	8.317	124.01
95.00	1.547	3.283	4.830	311.89	8.971	146.99
100.00	1.723	3.584	5.307	358.35	9.613	172.33
105.00	1.905	3.886	5.791	407.99	10.240	200.07
110.00	2.093	4.188	6.282	460.73	10.850	230.25
115.00	2.286	4.491	6.777	516.47	11.445	262.90
120.00	2.484	4.793	7.277	575.15	12.026	298.03
125.00	2.685	5.094	7.779	636.71	12.596	335.67
130.00	2.891	5.393	8.284	701.10	13.155	375.82
135.00	3.100	5.691	8.791	768.24	13.701	418.51
140.00	3.312	5.986	9.299	838.09	14.233	463.73
145.00	3.528	6.280	9.807	910.54	14.746	511.50
150.00	3.745	6.570	10.315	985.51	15.238	561.81
155.00	3.965	6.857	10.823	1062.9	15.710	614.65
160.00	4.188	7.141	11.329	1142.6	16.162	670.03
165.00	4.412	7.421	11.833	1224.5	16.594	727.94
170.00	4.637	7.697	12.334	1308.5	17.008	788.35
175.00	4.864	7.969	12.833	1394.5	17.407	851.27
180.00	5.093	8.236	13.329	1482.5	17.792	916.68
185.00	5.322	8.500	13.822	1572.4	18.164	984.56
190.00	5.552	8.759	14.311	1664.1	18.523	1054.9
195.00	5.783	9.014	14.796	1757.6	18.870	1127.7
200.00	6.014	9.264	15.278	1852.8	19.206	1202.8
205.00	6.246	9.511	15.757	1949.7	19.530	1280.4
210.00	6.478	9.753	16.231	2048.1	19.842	1360.4
215.00	6.710	9.991	16.701	2148.1	20.143	1442.7
220.00	6.943	10.225	17.168	2249.5	20.433	1527.4
225.00	7.175	10.455	17.630	2352.4	20.712	1614.4
230.00	7.407	10.681	18.088	2456.6	20.981	1703.7
235.00	7.640	10.903	18.542	2562.2	21.240	1795.3
240.00	7.871	11.121	18.992	2669.0	21.490	1889.1
245.00	8.103	11.335	19.438	2777.1	21.731	1985.2
250.00	8.334	11.545	19.879	2886.3	21.965	2083.5
255.00	8.565	11.752	20.316	2996.7	22.190	2184.0
260.00	8.795	11.955	20.749	3108.2	22.409	2286.7
265.00	9.024	12.154	21.178	3220.8	22.620	2391.5
270.00	9.253	12.350	21.603	3334.4	22.825	2498.4
273.15	9.397	12.471	21.869	3406.5	22.951	2566.9
275.00	9.482	12.542	22.024	3449.0	23.023	2607.5
280.00	9.710	12.731	22.440	3564.6	23.216	2718.7
285.00	9.936	12.916	22.853	3681.2	23.403	2831.9
290.00	10.163	13.099	23.261	3798.6	23.584	2947.2
295.00	10.388	13.278	23.666	3917.0	23.759	3064.5
298.15	10.530	13.389	23.919	3992.0	23.867	3139.5
300.00	10.613	13.454	24.067	4036.2	23.930	3183.8

H^C_0 AND S^C_0 APPLY TO THE REFERENCE STATE OF THE SOLID AT ZERO DEG K

TABLE B-165

THERMODYNAMIC FUNCTIONS FOR STRONTIUM 1:1-ZIRCONATE ($SR\ O\ .ZR\ O_2$)
SOLID PHASE

GRAM MOLECULAR WT.= 226.8382 GRAMS 1 CAL=4.1840 JOULES

T DEG K = 273.15 + T DEG C

T	$-(G_T^O-H_0^C)/T$	$(H_T^O-H_0^C)/T$	$(S_T-S_0^C)$	$(H_T^O-H_0^C)$	C_P^O	$-(G_T^O-H_0^C)$
DEG K	CAL / DEG MOLE	CAL / DEG MOLE	CAL / DEG MOLE	CAL / MOLE	CAL / DEG MOLE	CAL / MOLE
0.00	0.000	0.000	0.000	0.000	0.000	0.000
5.00	0.001	0.003	0.003	0.013	0.010	0.004
10.00	0.007	0.021	0.028	0.210	0.084	0.070
15.00	0.024	0.071	0.094	1.058	0.280	0.353
20.00	0.055	0.164	0.219	3.270	0.631	1.109
25.00	0.106	0.304	0.410	7.590	1.115	2.654
30.00	0.177	0.485	0.662	14.555	1.679	5.310
35.00	0.267	0.699	0.967	24.473	2.297	9.362
40.00	0.376	0.940	1.316	37.600	2.960	15.052
45.00	0.502	1.203	1.705	54.127	3.654	22.589
50.00	0.643	1.484	2.127	74.179	4.371	32.155
55.00	0.798	1.780	2.578	97.879	5.114	43.905
60.00	0.966	2.089	3.056	125.35	5.877	57.978
65.00	1.146	2.410	3.556	156.65	6.640	74.498
70.00	1.337	2.739	4.076	191.72	7.385	93.571
75.00	1.537	3.073	4.610	230.46	8.110	115.28
80.00	1.746	3.410	5.156	272.79	8.817	139.69
85.00	1.963	3.748	5.711	318.61	9.508	166.85
90.00	2.187	4.087	6.274	367.84	10.182	196.81
95.00	2.417	4.425	6.842	420.39	10.836	229.60
100.00	2.652	4.762	7.414	476.16	11.468	265.24
105.00	2.893	5.096	7.988	535.03	12.078	303.75
110.00	3.138	5.426	8.564	596.90	12.666	345.13
115.00	3.386	5.754	9.140	661.66	13.237	389.38
120.00	3.638	6.077	9.715	729.24	13.792	436.52
125.00	3.892	6.396	10.289	799.56	14.333	486.53
130.00	4.149	6.712	10.861	872.55	14.860	539.40
135.00	4.408	7.023	11.432	948.13	15.369	595.14
140.00	4.669	7.330	11.999	1026.2	15.860	653.72
145.00	4.932	7.632	12.564	1106.7	16.331	715.13
150.00	5.196	7.930	13.126	1189.5	16.782	779.35
155.00	5.460	8.223	13.683	1274.5	17.213	846.38
160.00	5.726	8.510	14.236	1361.6	17.626	916.18
165.00	5.992	8.792	14.785	1450.7	18.022	988.73
170.00	6.259	9.069	15.328	1541.8	18.403	1064.0
175.00	6.526	9.341	15.867	1634.7	18.770	1142.0
180.00	6.793	9.608	16.401	1729.5	19.125	1222.7
185.00	7.059	9.870	16.930	1826.0	19.468	1306.0
190.00	7.326	10.127	17.453	1924.1	19.800	1392.0
195.00	7.592	10.379	17.972	2023.9	20.121	1480.5
200.00	7.858	10.627	18.485	2125.3	20.431	1571.7
205.00	8.124	10.869	18.993	2228.2	20.729	1665.4
210.00	8.389	11.108	19.496	2332.6	21.017	1761.6
215.00	8.653	11.341	19.994	2438.4	21.293	1860.3
220.00	8.916	11.570	20.486	2545.5	21.558	1961.5
225.00	9.179	11.795	20.974	2653.9	21.813	2065.2
230.00	9.440	12.016	21.456	2763.6	22.058	2171.3
235.00	9.701	12.232	21.933	2874.5	22.294	2279.7
240.00	9.961	12.444	22.405	2986.5	22.521	2390.6
245.00	10.219	12.652	22.871	3099.7	22.741	2503.8
250.00	10.477	12.856	23.333	3213.9	22.953	2619.3
255.00	10.734	13.056	23.789	3329.2	23.159	2737.1
260.00	10.989	13.252	24.241	3445.5	23.359	2857.2
265.00	11.243	13.445	24.688	3562.8	23.553	2979.5
270.00	11.496	13.633	25.130	3681.0	23.742	3104.0
273.15	11.655	13.751	25.406	3756.0	23.858	3183.6
275.00	11.748	13.819	25.567	3800.2	23.925	3230.8
280.00	11.999	14.001	26.000	3920.3	24.104	3359.7
285.00	12.248	14.180	26.428	4041.2	24.278	3490.8
290.00	12.496	14.355	26.852	4163.1	24.448	3624.0
295.00	12.743	14.528	27.271	4285.7	24.614	3759.3
298.15	12.898	14.635	27.533	4363.4	24.717	3845.6
300.00	12.989	14.697	27.686	4409.2	24.776	3896.7

H_0^C AND S_0^C APPLY TO THE REFERENCE STATE OF THE SOLID AT ZERO DEG K

TABLE B-166

THERMODYNAMIC FUNCTIONS FOR BARIUM 1:1-ZIRCONATE (BA O .ZR O_2)

SOLID PHASE

GRAM MOLECULAR WT.= 276.5582 GRAMS 1 CAL=4.1840 JOULES

T DEG K = 273.15 + T DEG C

T	$-(G^O_T-H^C_0)/T$	$(H^O_T-H^C_0)/T$	$(S_T-S^C_0)$	$(H^O_T-H^C_0)$	C^O_P	$-(G^O_T-H^C_0)$
DEG K	CAL/DEG MOLE	CAL/DEG MOLE	CAL/DEG MOLE	CAL/MOLE	CAL/DEG MOLE	CAL/MOLE
0.00	0.000	0.000	0.000	0.000	0.000	0.000
5.00	0.002	0.005	0.006	0.024	0.019	0.008
10.00	0.013	0.039	0.052	0.389	0.155	0.130
15.00	0.044	0.129	0.173	1.938	0.504	0.654
20.00	0.101	0.289	0.390	5.787	1.064	2.021
25.00	0.188	0.511	0.699	12.770	1.741	4.711
30.00	0.304	0.775	1.080	23.253	2.454	9.132
35.00	0.446	1.068	1.513	37.364	3.198	15.594
40.00	0.608	1.382	1.991	55.290	3.978	24.336
45.00	0.790	1.715	2.506	77.187	4.784	35.563
50.00	0.989	2.063	3.052	103.14	5.596	49.444
55.00	1.202	2.421	3.623	133.13	6.399	66.121
60.00	1.428	2.785	4.213	167.10	7.185	85.704
65.00	1.666	3.153	4.819	204.96	7.956	108.28
70.00	1.913	3.523	5.436	246.61	8.703	133.91
75.00	2.169	3.892	6.061	291.94	9.422	162.65
80.00	2.432	4.260	6.691	340.78	10.113	194.53
85.00	2.701	4.624	7.325	393.02	10.779	229.57
90.00	2.975	4.984	7.959	448.53	11.421	267.78
95.00	3.254	5.339	8.593	507.19	12.040	309.16
100.00	3.537	5.689	9.226	568.89	12.634	353.71
105.00	3.823	6.033	9.856	633.49	13.203	401.42
110.00	4.112	6.372	10.483	700.88	13.748	452.27
115.00	4.402	6.704	11.106	770.94	14.272	506.24
120.00	4.694	7.030	11.724	843.57	14.776	563.32
125.00	4.988	7.349	12.337	918.68	15.265	623.48
130.00	5.282	7.663	12.945	996.19	15.738	686.68
135.00	5.577	7.971	13.548	1076.0	16.195	752.92
140.00	5.873	8.272	14.145	1158.1	16.635	822.15
145.00	6.168	8.568	14.736	1242.3	17.056	894.36
150.00	6.463	8.858	15.321	1328.6	17.458	969.50
155.00	6.758	9.141	15.900	1416.9	17.841	1047.6
160.00	7.053	9.419	16.472	1507.0	18.206	1128.5
165.00	7.347	9.690	17.038	1598.9	18.556	1212.3
170.00	7.640	9.956	17.597	1692.6	18.891	1298.9
175.00	7.933	10.216	18.149	1787.8	19.213	1388.2
180.00	8.224	10.470	18.694	1884.7	19.524	1480.3
185.00	8.514	10.719	19.233	1983.0	19.824	1575.2
190.00	8.803	10.963	19.766	2082.9	20.114	1672.7
195.00	9.091	11.201	20.292	2184.2	20.394	1772.8
200.00	9.378	11.434	20.812	2286.8	20.665	1875.6
205.00	9.663	11.662	21.325	2390.8	20.926	1980.9
210.00	9.947	11.886	21.833	2496.1	21.177	2088.8
215.00	10.229	12.105	22.334	2602.6	21.420	2199.2
220.00	10.510	12.319	22.829	2710.2	21.653	2312.1
225.00	10.789	12.529	23.318	2819.1	21.877	2427.5
230.00	11.067	12.735	23.801	2929.0	22.091	2545.3
235.00	11.343	12.936	24.279	3040.0	22.297	2665.5
240.00	11.617	13.133	24.750	3151.9	22.494	2788.1
245.00	11.890	13.326	25.216	3264.9	22.683	2913.0
250.00	12.161	13.515	25.676	3378.8	22.865	3040.2
255.00	12.430	13.700	26.131	3493.5	23.039	3169.7
260.00	12.698	13.881	26.580	3609.1	23.206	3301.5
265.00	12.964	14.059	27.023	3725.6	23.368	3435.5
270.00	13.229	14.233	27.461	3842.8	23.523	3571.7
273.15	13.394	14.340	27.735	3917.1	23.619	3658.7
275.00	13.491	14.403	27.894	3960.8	23.674	3710.1
280.00	13.752	14.570	28.322	4079.5	23.820	3850.7
285.00	14.012	14.733	28.745	4199.0	23.961	3993.4
290.00	14.269	14.894	29.163	4319.2	24.099	4138.1
295.00	14.525	15.051	29.576	4440.0	24.233	4285.0
298.15	14.686	15.148	29.834	4516.4	24.315	4378.5
300.00	14.780	15.205	29.985	4561.5	24.363	4433.9

H^C_0 AND S^C_0 APPLY TO THE REFERENCE STATE OF THE SOLID AT ZERO DEG K

TABLE B-167

THERMODYNAMIC FUNCTIONS FOR SODIUM 1:1-TUNGSTATE ($NA_2O \cdot WO_3$)
SOLID PHASE

GRAM MOLECULAR WT.= 293.8272 GRAMS   1 CAL=4.1840 JOULES

T DEG K = 273.15 + T DEG C

T	$-(G_T^0-H_0^C)/T$	$(H_T^0-H_0^C)/T$	$(S_T-S_0^C)$	$(H_T^0-H_0^C)$	C_P^0	$-(G_T^0-H_0^C)$
DEG K	CAL / DEG MOLE	CAL / DEG MOLE	CAL / DEG MOLE	CAL / MOLE	CAL / DEG MOLE	CAL / MOLE
0.00	0.000	0.000	0.000	0.000	0.000	0.000
5.00	0.001	0.003	0.004	0.015	0.012	0.005
10.00	0.008	0.025	0.033	0.245	0.098	0.082
15.00	0.028	0.082	0.110	1.235	0.327	0.413
20.00	0.065	0.192	0.256	3.831	0.745	1.296
25.00	0.125	0.361	0.486	9.028	1.367	3.115
30.00	0.210	0.594	0.804	17.822	2.178	6.302
35.00	0.323	0.888	1.211	31.070	3.143	11.303
40.00	0.464	1.236	1.699	49.426	4.212	18.546
45.00	0.631	1.629	2.260	73.286	5.337	28.417
50.00	0.825	2.056	2.881	102.80	6.467	41.247
55.00	1.042	2.507	3.549	137.90	7.568	57.305
60.00	1.280	2.974	4.254	178.46	8.653	76.800
65.00	1.537	3.453	4.990	224.44	9.741	99.899
70.00	1.811	3.941	5.752	275.87	10.830	126.74
75.00	2.099	4.436	6.535	332.71	11.900	157.45
80.00	2.402	4.935	7.337	394.81	12.935	192.13
85.00	2.716	5.435	8.151	462.00	13.934	230.84
90.00	3.041	5.934	8.975	534.09	14.897	273.65
95.00	3.375	6.431	9.805	610.91	15.824	320.60
100.00	3.717	6.923	10.640	692.26	16.711	371.71
105.00	4.067	7.409	11.476	777.95	17.559	427.00
110.00	4.422	7.889	12.311	867.78	18.367	486.47
115.00	4.784	8.361	13.145	961.56	19.139	550.11
120.00	5.149	8.826	13.975	1059.1	19.877	617.91
125.00	5.519	9.282	14.801	1160.3	20.585	689.85
130.00	5.892	9.730	15.622	1264.9	21.264	765.91
135.00	6.267	10.169	16.437	1372.9	21.913	846.06
140.00	6.645	10.600	17.245	1484.0	22.532	930.27
145.00	7.024	11.022	18.046	1598.1	23.120	1018.5
150.00	7.405	11.434	18.839	1715.1	23.677	1110.7
155.00	7.786	11.838	19.624	1834.9	24.204	1206.9
160.00	8.168	12.232	20.401	1957.1	24.704	1306.9
165.00	8.551	12.617	21.168	2081.9	25.180	1410.9
170.00	8.933	12.994	21.927	2208.9	25.633	1518.6
175.00	9.315	13.361	22.676	2338.2	26.067	1630.1
180.00	9.696	13.720	23.416	2469.6	26.485	1745.4
185.00	10.077	14.070	24.147	2603.0	26.888	1864.3
190.00	10.457	14.413	24.870	2738.4	27.277	1986.8
195.00	10.836	14.747	25.583	2875.7	27.653	2112.9
200.00	11.213	15.075	26.288	3014.9	28.018	2242.6
205.00	11.589	15.395	26.984	3155.9	28.370	2375.8
210.00	11.964	15.708	27.672	3298.6	28.712	2512.4
215.00	12.337	16.014	28.351	3443.0	29.042	2652.5
220.00	12.709	16.314	29.022	3589.0	29.361	2795.9
225.00	13.079	16.607	29.686	3736.6	29.669	2942.7
230.00	13.447	16.894	30.341	3885.7	29.968	3092.8
235.00	13.813	17.175	30.989	4036.2	30.257	3246.1
240.00	14.178	17.451	31.629	4188.2	30.537	3402.7
245.00	14.540	17.721	32.261	4341.6	30.810	3562.4
250.00	14.901	17.985	32.886	4496.3	31.075	3725.3
255.00	15.260	18.244	33.504	4652.3	31.335	3891.2
260.00	15.617	18.449	34.115	4809.7	31.589	4060.3
265.00	15.971	18.748	34.719	4968.2	31.839	4232.4
270.00	16.324	18.993	35.317	5128.0	32.084	4407.5
273.15	16.545	19.145	35.690	5229.3	32.237	4519.3
275.00	16.675	19.233	35.908	5289.1	32.326	4585.5
280.00	17.023	19.469	36.492	5451.3	32.565	4766.5
285.00	17.370	19.701	37.071	5614.7	32.800	4950.5
290.00	17.715	19.929	37.643	5779.3	33.033	5137.2
295.00	18.057	20.153	38.210	5945.0	33.264	5326.9
298.15	18.272	202922	38.564	6050.0	33.408	5447.8
300.00	18.398	20.373	38.771	6111.9	33.492	5519.3

H_0^C AND S_0^C APPLY TO THE REFERENCE STATE OF THE SOLID AT ZERO DEG K

TABLE B-168

THERMODYNAMIC FUNCTIONS FOR SODIUM 1:2-TUNGSTATE (NA_2O .2W O_3)
SOLID PHASE

GRAM MOLECULAR WT.= 525.6754 GRAMS 1 CAL=4.1840 JOULES

T DEG K = 273.15 + T DEG C

T	$-(G^0_T-H^C_0)/T$	$(H^0_T-H^C_0)/T$	$(S_T-S^C_0)$	$(H^0_T-H^C_0)$	C^0_P	$-(G^0_T-H^C_0)$
DEG K	CAL/DEG MOLE	CAL/DEG MOLE	CAL/DEG MOLE	CAL/MOLE	CAL/DEG MOLE	CAL/MOLE
0.00	0.000	0.000	0.000	0.000	0.000	0.000
5.00	0.003	0.008	0.010	0.039	0.031	0.013
10.00	0.021	0.062	0.083	0.623	0.247	0.208
15.00	0.069	0.202	0.272	3.035	0.772	1.039
20.00	0.158	0.441	0.599	8.816	1.582	3.157
25.00	0.290	0.771	1.061	19.271	2.644	7.250
30.00	0.466	1.191	1.657	35.723	3.983	13.989
35.00	0.687	1.701	2.389	59.552	5.588	24.047
40.00	0.952	2.298	3.250	91.906	7.374	38.091
45.00	1.261	2.965	4.226	133.43	9.244	56.737
50.00	1.610	3.687	5.297	184.34	11.110	80.510
55.00	1.997	4.444	6.441	244.41	12.905	109.83
60.00	2.417	5.221	7.637	313.24	14.612	145.00
65.00	2.866	6.006	8.872	390.41	16.248	186.26
70.00	3.340	6.795	10.134	475.62	17.826	233.77
75.00	3.835	7.581	11.416	568.59	19.352	287.64
80.00	4.349	8.363	12.713	669.05	20.825	347.96
85.00	4.880	9.138	14.018	776.74	22.241	414.78
90.00	5.424	9.904	15.328	891.37	23.600	488.14
95.00	5.980	10.659	16.639	1012.6	24.905	568.06
100.00	6.545	11.403	17.949	1140.3	26.159	654.53
105.00	7.119	12.135	19.254	1274.2	27.365	747.54
110.00	7.701	12.854	20.554	1413.9	28.524	847.06
115.00	8.288	13.559	21.847	1559.3	29.637	953.07
120.00	8.879	14.252	23.131	1710.2	30.705	1065.5
125.00	9.475	14.930	24.405	1866.3	31.729	1184.4
130.00	10.073	15.595	25.669	2027.4	32.708	1309.6
135.00	10.674	16.247	26.921	2193.3	33.643	1441.0
140.00	11.277	16.884	28.161	2363.8	34.537	1578.7
145.00	11.880	17.508	29.388	2538.6	35.389	1722.6
150.00	12.484	18.117	30.601	2717.6	36.203	1872.6
155.00	13.088	18.713	31.801	2900.6	36.982	2028.6
160.00	13.691	19.296	32.987	3087.4	37.727	2190.6
165.00	14.294	19.865	34.159	3277.8	38.443	2358.5
170.00	14.895	20.422	35.317	3471.7	39.132	2532.2
175.00	15.495	20.966	36.461	3669.1	39.795	2711.6
180.00	16.093	21.498	37.591	3869.7	40.434	2896.7
185.00	16.689	22.018	38.707	4073.4	41.053	3087.5
190.00	17.283	22.527	39.810	4280.1	41.652	3283.8
195.00	17.875	23.025	40.900	4489.9	42.233	3485.6
200.00	18.464	23.512	41.976	4702.4	42.797	3692.8
205.00	19.050	23.989	43.040	4917.8	43.345	3905.3
210.00	19.634	24.457	44.091	5135.9	43.878	4123.1
215.00	20.215	24.914	45.129	5356.6	44.397	4346.2
220.00	20.793	25.363	46.156	5579.8	44.902	4574.4
225.00	21.368	25.802	47.170	5805.6	45.393	4807.7
230.00	21.940	26.234	48.173	6033.7	45.870	5046.1
235.00	22.508	26.656	49.165	6264.2	46.334	5289.4
240.00	23.074	27.071	50.145	6497.0	46.786	5537.7
245.00	23.636	27.478	51.114	6732.1	47.225	5790.9
250.00	24.195	27.877	52.073	6969.3	47.653	6048.8
255.00	24.751	28.269	53.020	7208.6	48.071	6311.6
260.00	25.304	28.654	53.958	7450.0	48.479	6579.0
265.00	25.853	29.032	54.885	7693.4	48.878	6851.1
270.00	26.399	29.403	55.802	7938.7	49.270	7127.9
273.15	26.742	29.633	56.375	8094.3	49.513	7304.5
275.00	26.942	29.767	56.710	8186.1	49.654	7409.1
280.00	27.482	30.126	57.608	8435.3	50.032	7694.9
285.00	28.018	30.478	58.497	8686.4	50.404	7985.2
290.00	28.551	30.825	59.377	8939.3	50.771	8279.9
295.00	29.081	31.166	60.248	9194.1	51.132	8579.0
298.15	29.413	31.378	60.792	9355.5	51.357	8769.6
300.00	29.608	31.502	61.110	9450.6	51.488	8882.4

H^C_0 AND S^C_0 APPLY TO THE REFERENCE STATE OF THE SOLID AT ZERO DEG K

TABLE B-169

THERMODYNAMIC FUNCTIONS FOR MAGNESIUM 1:1-TUNGSTATE (MG O .W O_3)
SOLID PHASE

GRAM MOLECULAR WT.= 272.1596 GRAMS 1 CAL=4.1840 JOULES

T DEG K = 273.15 + T DEG C

T	$-(G^O_T-H^C_0)/T$	$(H^O_T-H^C_0)/T$	$(S_T-S^C_0)$	$(H^O_T-H^C_0)$	C^O_P	$-(G^O_T-H^C_0)$
DEG K	CAL / DEG MOLE	CAL / DEG MOLE	CAL / DEG MOLE	CAL / MOLE	CAL / DEG MOLE	CAL / MOLE
0.00	0.000	0.000	0.000	0.000	0.000	0.000
5.00	0.000	0.001	0.002	0.006	0.005	0.002
10.00	0.003	0.009	0.012	0.092	0.037	0.031
15.00	0.010	0.031	0.041	0.465	0.124	0.155
20.00	0.024	0.073	0.098	1.465	0.291	0.489
25.00	0.048	0.141	0.189	3.532	0.552	1.190
30.00	0.081	0.238	0.319	7.135	0.902	2.444
35.00	0.127	0.362	0.489	12.679	1.327	4.449
40.00	0.185	0.512	0.697	20.498	1.809	7.401
45.00	0.255	0.685	0.940	30.840	2.333	11.482
50.00	0.337	0.877	1.215	43.869	2.880	16.858
55.00	0.430	1.085	1.515	59.656	3.436	23.672
60.00	0.534	1.304	1.838	78.248	4.004	32.046
65.00	0.648	1.534	2.182	99.741	4.597	42.088
70.00	0.770	1.775	2.545	124.26	5.215	53.898
75.00	0.901	2.026	2.926	151.92	5.850	67.570
80.00	1.040	2.285	3.325	182.78	6.497	83.191
85.00	1.186	2.552	3.738	216.90	7.153	100.84
90.00	1.340	2.826	4.166	254.31	7.814	120.60
95.00	1.500	3.106	4.606	295.04	8.475	142.52
100.00	1.667	3.391	5.057	339.06	9.132	166.67
105.00	1.839	3.679	5.519	386.34	9.781	193.11
110.00	2.017	3.971	5.988	436.85	10.422	221.87
115.00	2.200	4.266	6.466	490.55	11.055	253.01
120.00	2.388	4.562	6.949	547.39	11.680	286.54
125.00	2.580	4.859	7.439	607.34	12.298	322.51
130.00	2.776	5.157	7.933	670.35	12.906	360.94
135.00	2.977	5.455	8.431	736.37	13.501	401.85
140.00	3.180	5.752	8.933	805.34	14.083	445.25
145.00	3.387	6.050	9.437	877.18	14.650	491.18
150.00	3.598	6.345	9.943	951.81	15.200	539.63
155.00	3.810	6.640	10.450	1029.1	15.733	590.61
160.00	4.026	6.932	10.958	1109.1	16.250	644.13
165.00	4.244	7.222	11.466	1191.6	16.752	700.19
170.00	4.463	7.509	11.973	1276.6	17.239	758.78
175.00	4.685	7.794	12.479	1364.0	17.712	819.91
180.00	4.909	8.076	12.985	1453.7	18.173	883.58
185.00	5.134	8.355	13.489	1545.7	18.620	949.76
190.00	5.360	8.631	13.991	1639.9	19.056	1018.5
195.00	5.588	8.904	14.492	1736.2	19.481	1089.7
200.00	5.817	9.173	14.990	1834.7	19.894	1163.4
205.00	6.047	9.440	15.487	1935.2	20.296	1239.6
210.00	6.277	9.703	15.980	2037.6	20.686	1318.2
215.00	6.509	9.963	16.472	2142.0	21.066	1399.4
220.00	6.741	10.219	16.960	2248.3	21.434	1482.9
225.00	6.973	10.473	17.446	2356.3	21.790	1569.0
230.00	7.206	10.722	17.928	2466.1	22.136	1657.4
235.00	7.439	10.969	18.408	2577.7	22.472	1748.2
240.00	7.673	11.212	18.885	2690.8	22.798	1841.5
245.00	7.906	11.452	19.358	2805.6	23.114	1937.1
250.00	8.140	11.688	19.828	2922.0	23.422	2035.1
255.00	8.374	11.921	20.295	3039.8	23.722	2135.4
260.00	8.608	12.151	20.758	3159.2	24.014	2238.0
265.00	8.841	12.377	21.219	3280.0	24.300	2342.9
270.00	9.075	12.601	21.675	3402.2	24.580	2450.2
273.15	9.222	12.740	21.961	3479.9	24.753	2518.9
275.00	9.308	12.821	22.129	3525.8	24.854	2559.7
280.00	9.541	13.038	22.579	3650.7	25.124	2671.5
285.00	9.774	13.253	23.026	3777.0	25.389	2785.5
290.00	10.006	13.464	23.470	3904.6	25.649	2901.7
295.00	10.238	13.673	23.911	4033.5	25.906	3020.2
298.15	10.384	13.803	24.187	4115.3	26.065	3095.9
300.00	10.469	13.879	24.348	4163.6	26.158	3140.8

H^C_0 AND S^C_0 APPLY TO THE REFERENCE STATE OF THE SOLID AT ZERO DEG K

TABLE B-170

THERMODYNAMIC FUNCTIONS FOR CALCIUM 1:1-TUNGSTATE ($CA\ O\ .W\ O_3$)
SOLID PHASE

GRAM MOLECULAR WT.= 287.9276 GRAMS 1 CAL=4.1840 JOULES

T DEG K = 273.15 + T DEG C

T	$-(G^O_T-H^C_0)/T$	$(H^O_T-H^C_0)/T$	$(S_T-S^C_0)$	$(H^O_T-H^C_0)$	C^O_P	$-(G^O_T-H^C_0)$
DEG K	CAL / DEG MOLE	CAL / DEG MOLE	CAL / DEG MOLE	CAL / MOLE	CAL / DEG MOLE	CAL / MOLE
0.00	0.000	0.000	0.000	0.000	0.000	0.000
5.00	0.001	0.002	0.003	0.012	0.010	0.004
10.00	0.007	0.020	0.027	0.199	0.080	0.066
15.00	0.022	0.067	0.090	1.007	0.267	0.336
20.00	0.053	0.157	0.210	3.142	0.616	1.058
25.00	0.102	0.298	0.400	7.450	1.135	2.553
30.00	0.173	0.491	0.664	14.725	1.794	5.182
35.00	0.266	0.730	0.996	25.546	2.547	9.303
40.00	0.381	1.007	1.388	40.286	3.354	15.240
45.00	0.517	1.314	1.831	59.116	4.178	23.269
50.00	0.672	1.641	2.313	82.046	4.990	33.614
55.00	0.845	1.981	2.826	108.98	5.781	46.451
60.00	1.032	2.331	3.363	139.86	6.571	61.914
65.00	1.233	2.688	3.920	174.71	7.372	80.114
70.00	1.445	3.051	4.496	213.58	8.172	101.15
75.00	1.668	3.419	5.087	256.40	8.955	125.10
80.00	1.900	3.789	5.689	303.08	9.713	152.03
85.00	2.141	4.159	6.300	353.50	10.450	182.00
90.00	2.389	4.528	6.918	407.56	11.171	215.05
95.00	2.644	4.897	7.541	465.19	11.879	251.19
100.00	2.905	5.263	8.168	526.32	12.571	290.46
105.00	3.170	5.627	8.798	590.86	13.244	332.87
110.00	3.440	5.988	9.429	658.73	13.897	378.44
115.00	3.714	6.346	10.061	729.80	14.527	427.16
120.00	3.992	6.700	10.692	803.96	15.134	479.04
125.00	4.273	7.049	11.321	881.09	15.717	534.08
130.00	4.556	7.393	11.949	961.09	16.278	592.25
135.00	4.841	7.732	12.573	1043.8	16.816	653.56
140.00	5.128	8.066	13.194	1129.2	17.334	717.98
145.00	5.417	8.394	13.811	1217.1	17.833	785.50
150.00	5.707	8.717	14.424	1307.5	18.314	856.09
155.00	5.998	9.034	15.032	1400.3	18.776	929.73
160.00	6.290	9.345	15.635	1495.3	19.221	1006.4
165.00	6.582	9.651	16.233	1592.4	19.647	1086.1
170.00	6.875	9.951	16.826	1691.7	20.056	1168.7
175.00	7.168	10.246	17.413	1793.0	20.449	1254.3
180.00	7.460	10.534	17.994	1896.2	20.826	1342.8
185.00	7.753	10.817	18.570	2001.2	21.189	1434.3
190.00	8.045	11.095	19.140	2108.0	21.540	1528.5
195.00	8.337	11.367	19.704	2216.6	21.881	1625.6
200.00	8.628	11.634	20.262	2326.8	22.213	1725.6
205.00	8.918	11.896	20.814	2438.7	22.537	1828.3
210.00	9.208	12.153	21.361	2552.2	22.852	1933.7
215.00	9.497	12.406	21.903	2667.2	23.161	2041.9
220.00	9.785	12.654	22.439	2783.8	23.461	2152.7
225.00	10.072	12.897	22.969	2901.8	23.754	2266.2
230.00	10.358	13.136	23.494	3021.3	24.040	2382.4
235.00	10.643	13.371	24.014	3142.2	24.317	2501.2
240.00	10.927	13.602	24.529	3264.5	24.587	2622.5
245.00	11.210	13.829	25.039	3388.1	24.849	2746.5
250.00	11.492	14.052	25.543	3512.9	25.104	2872.9
255.00	11.772	14.271	26.043	3639.1	25.353	3001.9
260.00	12.051	14.486	26.538	3766.5	25.596	3133.3
265.00	12.329	14.698	27.028	3895.0	25.834	3267.2
270.00	12.606	14.907	27.513	4024.8	26.068	3403.6
273.15	12.780	15.036	27.816	4107.1	26.213	3490.7
275.00	12.881	15.112	27.993	4155.7	26.297	3542.4
280.00	13.155	15.313	28.469	4287.8	26.523	3683.5
285.00	13.428	15.512	28.940	4420.9	26.745	3827.0
290.00	13.700	15.708	29.407	4555.2	26.965	3972.9
295.00	13.970	15.900	29.870	4690.6	27.181	4121.1
298.15	14.139	16.020	30.160	4776.4	27.316	4215.7
300.00	14.239	16.090	30.329	4827.0	27.395	4271.6

H^C_0 AND S^C_0 APPLY TO THE REFERENCE STATE OF THE SOLID AT ZERO DEG K

TABLE B-171

THERMODYNAMIC FUNCTIONS FOR POTASSIUM HYDROGEN FLUORIDE (KHF_2)
SOLID AND LIQUID PHASES

GRAM MOLECULAR WT.= 78.10677 GRAMS   1 CAL=4.1840 JOULES

T DEG K = 273.15 + T DEG C

T	$-(G^0_T-H^C_0)/T$	$(H^0_T-H^C_0)/T$	$(S_T-S^C_0)$	$(H^0_T-H^C_0)$	C^0_P	$-(G^0_T-H^C_0)$
DEG K	CAL/DEG MOLE	CAL/DEG MOLE	CAL/DEG MOLE	CAL/MOLE	CAL/DEG MOLE	CAL/MOLE
			SOLID PHASE (ALPHA)			
0.00	0.000	0.000	0.000	0.000	0.000	0.000
5.00	0.001	0.002	0.002	0.009	0.007	0.003
10.00	0.005	0.014	0.019	0.145	0.059	0.047
15.00	0.016	0.051	0.067	0.761	0.209	0.247
20.00	0.040	0.125	0.165	2.500	0.519	0.802
25.00	0.081	0.253	0.334	6.331	1.053	2.016
30.00	0.143	0.444	0.587	13.313	1.759	4.282
35.00	0.229	0.690	0.919	24.149	2.604	8.013
40.00	0.340	0.989	1.329	39.560	3.568	13.602
45.00	0.476	1.330	1.805	59.832	4.538	21.414
50.00	0.635	1.698	2.333	84.908	5.488	31.742
55.00	0.815	2.084	2.899	114.63	6.390	44.808
60.00	1.013	2.478	3.491	148.68	7.217	60.774
65.00	1.227	2.872	4.099	186.68	7.970	79.743
70.00	1.454	3.261	4.715	228.28	8.662	101.78
75.00	1.692	3.643	5.335	273.20	9.297	126.90
80.00	1.939	4.014	5.953	321.15	9.873	155.12
85.00	2.193	4.375	6.568	371.84	10.392	186.43
90.00	2.453	4.722	7.175	424.99	10.862	220.79
95.00	2.718	5.057	7.774	480.39	11.291	258.17
100.00	2.985	5.378	8.364	537.84	11.685	298.51
105.00	3.255	5.688	8.943	597.19	12.050	341.78
110.00	3.527	5.985	9.511	658.30	12.389	387.92
115.00	3.799	6.270	10.069	721.05	12.706	436.88
120.00	4.072	6.544	10.616	785.33	13.004	488.59
125.00	4.344	6.808	11.153	851.06	13.284	543.02
130.00	4.616	7.063	11.679	918.14	13.546	600.10
135.00	4.887	7.307	12.195	986.49	13.791	659.79
140.00	5.157	7.543	12.700	1056.0	14.020	722.03
145.00	5.426	7.770	13.196	1126.7	14.232	786.78
150.00	5.693	7.989	13.682	1198.3	14.430	853.98
155.00	5.959	8.200	14.158	1270.9	14.614	923.58
160.00	6.222	8.403	14.625	1344.5	14.789	995.54
165.00	6.484	8.599	15.083	1418.8	14.956	1069.8
170.00	6.743	8.788	15.531	1494.0	15.116	1146.4
175.00	7.001	8.971	15.972	1570.0	15.273	1225.1
180.00	7.256	9.148	16.404	1646.7	15.426	1306.1
185.00	7.509	9.320	16.829	1724.2	15.576	1389.1
190.00	7.760	9.487	17.246	1802.5	15.724	1474.3
195.00	8.008	9.648	17.657	1881.5	15.868	1561.6
200.00	8.254	9.806	18.060	1961.2	16.010	1650.9
205.00	8.498	9.959	18.457	2041.6	16.149	1742.2
210.00	8.740	10.108	18.848	2122.6	16.285	1835.5
215.00	8.980	10.253	19.233	2204.4	16.419	1930.7
220.00	9.217	10.395	19.612	2286.8	16.550	2027.8
225.00	9.452	10.533	19.985	2369.9	16.679	2126.8
230.00	9.685	10.668	20.353	2453.6	16.806	2227.6
235.00	9.916	10.800	20.716	2537.9	16.930	2330.3
240.00	10.145	10.929	21.074	2622.9	17.054	2434.8
245.00	10.372	11.055	21.427	2708.5	17.175	2541.0
250.00	10.596	11.179	21.775	2794.7	17.295	2649.0
255.00	10.819	11.300	22.118	2881.4	17.413	2758.8
260.00	11.039	11.418	22.458	2968.8	17.530	2870.2
265.00	11.258	11.535	22.793	3056.7	17.645	2983.3
270.00	11.475	11.649	23.124	3145.2	17.758	3098.1
273.15	11.610	11.720	23.330	3201.3	17.829	3171.3
275.00	11.689	11.761	23.450	3234.3	17.870	3214.6
280.00	11.902	11.871	23.773	3323.9	17.981	3332.6
285.00	12.113	11.979	24.093	3414.1	18.091	3452.3
290.00	12.323	12.086	24.408	3504.8	18.199	3573.5
295.00	12.530	12.190	24.720	3596.1	18.307	3696.4
298.15	12.660	12.255	24.915	3653.9	18.374	3774.5
300.00	12.736	12.293	25.029	3687.9	18.414	3820.7

H^C_0 AND S^C_0 APPLY TO THE REFERENCE STATE OF THE SOLID AT ZERO DEG K

TABLE B-171 (CONT.)

THERMODYNAMIC FUNCTIONS FOR POTASSIUM HYDROGEN FLUORIDE (K H F_2)
SOLID AND LIQUID PHASES

GRAM MOLECULAR WT.= 78.10677 GRAMS 1 CAL=4.1840 JOULES

T DEG K = 273.15 + T DEG C

T	$-(G^0_T-H^C_0)/T$	$(H^0_T-H^C_0)/T$	$(S_T-S^C_0)$	$(H^0_T-H^C_0)$	C^0_P	$-(G^0_T-H^C_0)$
DEG K	CAL/DEG MOLE	CAL/DEG MOLE	CAL/DEG MOLE	CAL/MOLE	CAL/DEG MOLE	CAL/MOLE
			SOLID PHASE (ALPHA)			
300.00	12.736	12.293	25.029	3687.9	18.414	3820.7
310.00	13.142	12.494	25.636	3873.1	18.626	4074.1
320.00	13.542	12.689	26.231	4060.4	18.837	4333.4
330.00	13.935	12.878	26.814	4249.9	19.049	4598.6
340.00	14.323	13.063	27.385	4441.4	19.262	4869.7
350.00	14.704	13.243	27.947	4635.1	19.477	5146.3
360.00	15.079	13.419	28.499	4831.0	19.695	5428.6
370.00	15.449	13.592	29.041	5029.0	19.916	5716.3
373.15	15.565	13.646	29.210	5091.8	19.986	5808.0
380.00	15.814	13.761	29.575	5229.3	20.140	6009.4
390.00	16.174	13.928	30.101	5431.8	20.367	6307.7
400.00	16.528	14.092	30.620	5636.6	20.597	6611.4
425.00	17.395	14.491	31.886	6158.8	21.179	7392.8
450.00	18.234	14.879	33.113	6695.6	21.761	8205.3
469.20	18.862	15.170	34.031	7117.6	22.194	8850.0
			SOLID PHASE (BETA)			
469.20	18.862	20.837	39.698	9776.6	23.960	8850.0
475.00	19.118	20.875	39.993	9915.5	23.960	9081.1
500.00	20.193	21.029	41.222	10515.	23.960	10096.
511.90	20.688	21.098	41.785	10800.	23.960	10590.
			LIQUID PHASE			
511.90	20.688	24.175	44.863	12375.0	25.000	10590.
530.00	21.530	24.202	45.732	12827.	25.000	11411.

H^C_0 AND S^C_0 APPLY TO THE REFERENCE STATE OF THE SOLID AT ZERO DEG K

TABLE B-172

THERMODYNAMIC FUNCTIONS FOR PHOSPHORUS PENTOXIDE (P_4O_{10})
SOLID PHASE

GRAM MOLECULAR WT.= 283.8892 GRAMS 1 CAL=4.1840 JOULES

T DEG K = 273.15 + T DEG C

T	$-(G^0_T-H^C_0)/T$	$(H^0_T-H^C_0)/T$	$(S_T-S^C_0)$	$(H^0_T-H^C_0)$	C^0_P	$-(G^0_T-H^C_0)$
DEG K	CAL/DEG MOLE	CAL/DEG MOLE	CAL/DEG MOLE	CAL/MOLE	CAL/DEG MOLE	CAL/MOLE
0.00	0.000	0.000	0.000	0.000	0.000	0.000
5.00	0.012	0.037	0.049	0.184	0.147	0.062
10.00	0.096	0.281	0.377	2.809	1.073	0.964
15.00	0.304	0.822	1.126	12.331	2.805	4.553
20.00	0.636	1.541	2.178	30.827	4.554	12.727
25.00	1.062	2.299	3.361	57.471	6.060	26.542
30.00	1.546	3.030	4.577	90.914	7.259	46.386
35.00	2.065	3.706	5.771	129.70	8.223	72.269
40.00	2.600	4.320	6.921	172.81	8.992	104.02
45.00	3.142	4.877	8.019	219.45	9.658	141.39
50.00	3.683	5.388	9.070	269.38	10.314	184.13
55.00	4.219	5.866	10.085	322.63	10.990	232.03
60.00	4.749	6.322	11.071	379.31	11.684	284.93
65.00	5.272	6.762	12.034	439.52	12.407	342.70
70.00	5.789	7.192	12.981	503.46	13.177	405.24
75.00	6.300	7.618	13.918	571.38	13.997	472.49
80.00	6.805	8.044	14.849	643.49	14.855	544.41
85.00	7.306	8.470	15.776	719.97	15.743	620.98
90.00	7.802	8.900	16.702	800.97	16.660	702.17
95.00	8.295	9.333	17.627	886.61	17.602	787.99
100.00	8.784	9.770	18.555	977.02	18.565	878.45
105.00	9.272	10.212	19.484	1072.3	19.542	973.54
110.00	9.757	10.659	20.416	1172.5	20.526	1073.3
115.00	10.241	11.109	21.350	1277.6	21.514	1177.7
120.00	10.723	11.563	22.287	1387.6	22.504	1286.8
125.00	11.205	12.021	23.225	1502.6	23.495	1400.6
130.00	11.685	12.481	24.166	1622.5	24.482	1519.1
135.00	12.165	12.944	25.108	1747.4	25.462	1642.2
140.00	12.644	13.408	26.052	1877.1	26.432	1770.1
145.00	13.122	13.874	26.996	2011.7	27.388	1902.8
150.00	13.601	14.340	27.941	2151.0	28.331	2040.1
155.00	14.078	14.806	28.885	2295.0	29.260	2182.2
160.00	14.556	15.272	29.828	2443.6	30.175	2328.9
165.00	15.033	15.738	30.771	2596.7	31.075	2480.4
170.00	15.510	16.202	31.712	2754.3	31.962	2636.7
175.00	15.986	16.665	32.651	2916.3	32.832	2797.6
180.00	16.462	17.126	33.588	3082.6	33.686	2963.2
185.00	16.937	17.584	34.522	3253.1	34.524	3133.4
190.00	17.412	18.041	35.454	3427.8	35.345	3308.4
195.00	17.887	18.495	36.382	3606.6	36.152	3488.0
200.00	18.361	18.947	37.307	3789.3	36.945	3672.2
205.00	18.834	19.395	38.229	3976.0	37.728	3861.0
210.00	19.307	19.841	39.148	4166.6	38.502	4054.5
215.00	19.779	20.284	40.063	4361.0	39.268	4252.5
220.00	20.250	20.724	40.974	4559.2	40.028	4455.1
225.00	20.721	21.161	41.882	4761.3	40.783	4662.2
230.00	21.191	21.596	42.787	4967.1	41.533	4873.9
235.00	21.660	22.028	43.688	5176.6	42.276	5090.1
240.00	22.128	22.458	44.586	5389.8	43.012	5310.8
245.00	22.596	22.884	45.480	5606.7	43.740	5536.0
250.00	23.062	23.309	46.371	5827.2	44.457	5765.6
255.00	23.528	23.730	47.258	6051.2	45.163	5999.7
260.00	23.993	24.149	48.142	6278.8	45.855	6238.2
265.00	24.457	24.565	49.022	6509.8	46.534	6481.1
270.00	24.920	24.978	49.898	6744.1	47.198	6728.4
273.15	25.211	25.237	50.448	6893.4	47.609	6886.4
275.00	25.382	25.388	50.770	6981.7	47.848	6980.0
280.00	25.843	25.795	51.638	7222.6	48.482	7236.1
285.00	26.303	26.198	52.502	7466.5	49.101	7496.4
290.00	26.762	26.598	53.361	7713.6	49.706	7761.1
295.00	27.220	26.995	54.216	7963.6	50.298	8030.0
298.15	27.508	27.243	54.752	8122.6	50.663	8201.6
300.00	27.677	27.388	55.066	8216.5	50.875	8303.2
310.00	28.588	28.164	56.752	8730.9	51.993	8862.3
320.00	29.494	28.926	58.420	9256.2	53.064	9438.2
330.00	30.396	29.673	60.069	9792.0	54.089	10031.

H^C_0 AND S^C_0 APPLY TO THE REFERENCE STATE OF THE SOLID AT ZERO DEG K

USCOMM-NBS-DC

Security Classification

DOCUMENT CONTROL DATA - R&D

(Security classification of title, body of abstract and indexing annotation must be entered when the overall report is classified)

1. ORIGINATING ACTIVITY *(Corporate author)* National Bureau of Standards Physics Building Washington, D. C. 20234	2a. REPORT SECURITY CLASSIFICATION UNCLASSIFIED 2b. GROUP

3. REPORT TITLE

PRELIMINARY REPORT ON THE THERMODYNAMIC PROPERTIES OF SELECTED LIGHT-ELEMENT AND SOME RELATED COMPOUNDS

4. DESCRIPTIVE NOTES *(Type of report and inclusive dates)*

Scientific Interim

5. AUTHOR(S) *(Last name, first name, initial)*

Charles W. Beckett
Thomas B. Douglas

6. REPORT DATE	7a. TOTAL NO. OF PAGES	7b. NO. OF REFS
1 July 1966	269	387

8a. CONTRACT OR GRANT NO. ISSA-65-8 (ARPA) b. PROJECT NO. 9713-02 c. d. 681308	9a. ORIGINATOR'S REPORT NUMBER(S) NBS Report 9389 9b. OTHER REPORT NO(S) *(Any other numbers that may be assigned this report)* AFOSR 66-1938

10. AVAILABILITY/LIMITATION NOTICES

1. Distribution of this document is unlimited

11. SUPPLEMENTARY NOTES	12. SPONSORING MILITARY ACTIVITY
	AF Office of Scientific Research (SREP) 1400 Wilson Boulevard Arlington, Virginia 22209

13. ABSTRACT

Thermodynamic and related properties of substances important in current high-temperature research and development activities are being investigated under contract with the U. S. Air Force (USAF Order No. OAR ISSA 65-8) and the Advanced Research Projects Agency (ARPA Order No. 20). This research program is a direct contribution to the Interagency Chemical Rocket Propulsion Group: Working Group on Thermochemistry and, often simultaneously, to other organizations oriented toward acquiring the basic information needed to solve not only the technical problems in propulsion but also those associated with ballistics, reentry, and high-strength high-temperature materials. For given substances this needed basic information comprises an ensemble of closely related properties being determined by a rather extensive array of experimental and theoretical techniques. Some of those techniques, by relating thermodynamic properties to molecular or crystal structure, make it possible to tabulate these properties over far wider ranges of temperature and pressure than those actually employed in the basic investigations. This report describes in detail a variety of recent NBS experimental results and their interpretation. The vibrational spectra of different isotopic varieties of MgF_2, $MgCl_2$, CaF_2, SrF_2, and BaF_2 molecules trapped in solid rare-gas matrices were determined and analyzed; this technique particularly defines the bending vibrations, heretofore unreliable but a major factor in the thermodynamic properties of such gases. Preliminary microwave studies of the CsOH molecule indicate it to be linear and with highly anharmonic bending vibrations; these pioneering results have important implications for the spectroscopically little investigated hydroxides of all the elements of Groups I, II, and III.

DD FORM 1473 1 JAN 64

Security Classification

DD FORM 1473, 1 Jan 64

13 ABSTRACT (CONTINUED)

Further infrared studies of the borohydrides of aluminum and beryllium show, between the solid and gaseous forms of the beryllium compound, a great difference which is tentatively interpreted. Spectroscopic time histories of aluminum wires exploding in vacuum and controlled atmospheres of nitrogen and oxygen were obtained. Measured calorimetrically were the heats of formation of the perchlorates of hydrazine ($N_2H_4 \cdot 2HC\ell O_4$), sodium, potassium, and silver, as well as the high-temperature heat capacity, heat of transition, and transition temperature of crystalline $A\ell F_3$. The heats of combustion in fluorine of refractory substances (especially graphite, boron, boron carbide, and aluminum borides, measured for the Air Force Aero Propulsion Laboratory), are here summarized and analyzed. The heat of vaporization of liquid $A\ell_2O_3$ has been remeasured with more reliable temperature determination, and new mass-spectrometric data on several compositions of the BeO-$A\ell_2O_3$ system give a consistent value for the heat of formation of the new high-temperature molecule $BeOA\ell$.

Several literature reviews with critical data analysis are included. The present status of the heats of formation of CF_4 and selected fluorides of nitrogen, carbon, chlorine, and oxygen is described, with a report of recent NBS flame calorimetry on OF_2. Thermochemical properties of compounds of cadmium, zinc, and copper (recently evaluated critically as part of a revision of NBS Circular 500) are tabulated. On the basis of a critical data analysis of published condensed-phase heat-capacity and enthalpy data on $BeSO_4$, SrF_2, $SrC\ell_2$, TiF_4, ZrF_4, ZrB_2, P_4O_{10}, KHF_2, and 13 mixed oxides, new tables of their thermodynamic properties are given. Analyses of the infrared spectra of fluorides of seven elements of Groups IV, V, and VI gave Coriolis zeta constants of the degenerate vibrational modes and certain unique harmonic force fields. The high-temperature thermodynamics of the BeO-H_2O system was reviewed, with estimations of the possible effect of postulated higher hydrates on the volatility of BeO in water vapor up to 4000°K. The published data on the vaporization equilibria of the nitrides and carbides of aluminum, beryllium, magnesium, and titanium were reviewed and compared with the values calculated thermodynamically from the available up-to-date thermal data. A comprehensive review is presented of the theory of the equation of state of solid hydrogen and the calculation of properties of the as yet unobserved form metallic hydrogen. This form of hydrogen probably occurs on the planet Jupiter at pressures above one million atmospheres.

Security Classification

14. KEY WORDS	LINK A		LINK B		LINK C	
	ROLE	WT	ROLE	WT	ROLE	WT
Experimental Research Literature Reviews and Critical Data Analysis Thermodynamic Properties Light-element Compounds Propulsion-combustion Products Calorimetry, Equilibrium Studies and Spectroscopy High Temperatures and Fast Measurements Tables of Thermodynamic Functions						

INSTRUCTIONS

1. ORIGINATING ACTIVITY: Enter the name and address of the contractor, subcontractor, grantee, Department of Defense activity or other organization (*corporate author*) issuing the report.

2*a*. REPORT SECURITY CLASSIFICATION: Enter the overall security classification of the report. Indicate whether "Restricted Data" is included. Marking is to be in accordance with appropriate security regulations.

2*b*. GROUP: Automatic downgrading is specified in DoD Directive 5200.10 and Armed Forces Industrial Manual. Enter the group number. Also, when applicable, show that optional markings have been used for Group 3 and Group 4 as authorized.

3. REPORT TITLE: Enter the complete report title in all capital letters. Titles in all cases should be unclassified. If a meaningful title cannot be selected without classification, show title classification in all capitals in parenthesis immediately following the title.

4. DESCRIPTIVE NOTES: If appropriate, enter the type of report, e.g., interim, progress, summary, annual, or final. Give the inclusive dates when a specific reporting period is covered.

5. AUTHOR(S): Enter the name(s) of author(s) as shown on or in the report. Enter last name, first name, middle initial. If military, show rank and branch of service. The name of the principal author is an absolute minimum requirement.

6. REPORT DATE: Enter the date of the report as day, month, year; or month, year. If more than one date appears on the report, use date of publication.

7*a*. TOTAL NUMBER OF PAGES: The total page count should follow normal pagination procedures, i.e., enter the number of pages containing information.

7*b*. NUMBER OF REFERENCES: Enter the total number of references cited in the report.

8*a*. CONTRACT OR GRANT NUMBER: If appropriate, enter the applicable number of the contract or grant under which the report was written.

8*b*, 8*c*, & 8*d*. PROJECT NUMBER: Enter the appropriate military department identification, such as project number, subproject number, system numbers, task number, etc.

9*a*. ORIGINATOR'S REPORT NUMBER(S): Enter the official report number by which the document will be identified and controlled by the originating activity. This number must be unique to this report.

9*b*. OTHER REPORT NUMBER(S): If the report has been assigned any other report numbers (*either by the originator or by the sponsor*), also enter this number(s).

10. AVAILABILITY/LIMITATION NOTICES: Enter any limitations on further dissemination of the report, other than those imposed by security classification, using standard statements such as:

(1) "Qualified requesters may obtain copies of this report from DDC."

(2) "Foreign announcement and dissemination of this report by DDC is not authorized."

(3) "U. S. Government agencies may obtain copies of this report directly from DDC. Other qualified DDC users shall request through
________________________."

(4) "U. S. military agencies may obtain copies of this report directly from DDC. Other qualified users shall request through
________________________."

(5) "All distribution of this report is controlled. Qualified DDC users shall request through
________________________."

If the report has been furnished to the Office of Technical Services, Department of Commerce, for sale to the public, indicate this fact and enter the price, if known.

11. SUPPLEMENTARY NOTES: Use for additional explanatory notes.

12. SPONSORING MILITARY ACTIVITY: Enter the name of the departmental project office or laboratory sponsoring (*paying for*) the research and development. Include address.

13. ABSTRACT: Enter an abstract giving a brief and factual summary of the document indicative of the report, even though it may also appear elsewhere in the body of the technical report. If additional space is required, a continuation sheet shall be attached.

It is highly desirable that the abstract of classified reports be unclassified. Each paragraph of the abstract shall end with an indication of the military security classification of the information in the paragraph, represented as *(TS)*, *(S)*, *(C)*, or *(U)*.

There is no limitation on the length of the abstract. However, the suggested length is from 150 to 225 words.

14. KEY WORDS: Key words are technically meaningful terms or short phrases that characterize a report and may be used as index entries for cataloging the report. Key words must be selected so that no security classification is required. Identifiers, such as equipment model designation, trade name, military project code name, geographic location, may be used as key words but will be followed by an indication of technical context. The assignment of links, rules, and weights is optional.

☆ U. S. GOVERNMENT PRINTING OFFICE : 1966 O - 236-350

DEPARTMENT OF COMMERCE
NATIONAL BUREAU OF STANDARDS